

**Rab GTPases as mediators of neuronal robustness in *Drosophila***

**Inaugural-Dissertation**

to obtain the academic degree

Doctor rerum naturalium (Dr. rer. nat.)

submitted to the Department of Biology, Chemistry, Pharmacy  
of Freie Universität Berlin

by

**Friederike Elisabeth Kohrs**

born in Hamburg, Germany

Berlin 2021

The majority of experiments presented in this dissertation were conducted from February 2017 to March 2021 at the Division of Neurobiology of the Institute of Biology of Freie Universität Berlin under the supervision of Prof. Dr. P. Robin Hiesinger. While the remainder of experiments have been performed in collaboration with Bojana Pavlović at the DKFZ in Heidelberg under the supervision of Prof. Dr. Michael Boutros.

**1<sup>st</sup> reviewer: Prof. Dr. P. Robin Hiesinger**

Division of Neurobiology, Freie Universität Berlin

**2<sup>nd</sup> reviewer: Prof. Dr. Mathias F. Wernet**

Division of Neurobiology, Freie Universität Berlin

**Date of defense: 14.01.2022**

## **Acknowledgement**

I would like to thank my supervisor, Prof Dr. P. Robin Hiesinger, for his support and guidance, for challenging and encouraging me, during each step of my doctoral work.

Special thanks to Prof. Dr. Mathias F. Wernet for his educational feedback and freely given support during these last few years.

Furthermore, I would like to express my appreciation and gratitude to all past and present members of the Hiesinger, Wernet and Hassan groups for making the lab such a friendly, productive, as well as supportive environment and where colleagues can become friends.

Also, I would like to thank my family, near and far, from the bottom of my heart for their love and support, for their encouragement and patience!

Last but not in the very least, Stephan, thank you! For standing by me, for going through thick and thin with me, for your love. You are the best and it would not have been possible without you. We did it!

These last few years, conducting my doctoral research, have been demanding, challenging, sometimes infuriating, but also rewarding, exciting, and fun. I am grateful for everyone who has made this such an extraordinary and special time in my life.

## Table of Contents

Acknowledgement .....	3
Table of Contents .....	4
1. General Introduction.....	6
1.1 Small Rab GTPases as key regulators of intracellular membrane trafficking.....	7
1.1.1 Rab GTPases act as molecular switches in membrane trafficking.....	8
1.1.2 Essential steps in the intracellular vesicle-mediated membrane trafficking....	9
1.1.3 The expression patterns and subcellular localization of <i>Drosophila</i> Rab GTPases.....	10
1.2 Rab-mediated membrane trafficking in neurons.....	11
1.2.1 Rab-mediated membrane trafficking during neuronal development.....	12
1.2.2 Rab-mediated membrane trafficking during neuronal function .....	14
1.2.3 Rab-mediated membrane trafficking during neuronal maintenance .....	16
1.3. <i>Drosophila melanogaster</i> as a model system .....	18
1.3.1 The <i>Drosophila</i> visual system: a model to study intracellular protein trafficking in neurons.....	19
2. Aim .....	24
3. Manuscript 1 .....	26
Rab GTPases and Membrane Trafficking in Neurodegeneration .....	26
Author contributions .....	26
4. Manuscript 2 .....	43
Systematic functional analysis of rab GTPases reveals limits of neuronal robustness to environmental challenges in flies .....	43
Author contributions .....	43
Manuscript .....	44
Supplementary information .....	81
5. Manuscript 3 .....	161
The RUSH System in <i>Drosophila</i> – A transgenic toolbox to study intracellular localization dynamics of Rab GTPases.....	161
Author contributions .....	161
Manuscript .....	162
Supplementary information .....	179

6. General discussion.....	190
6.1 The associations between Rab GTPases and neurodegenerative diseases are more correlative than causative.....	191
6.2 Nervous system-enriched Rab GTPases serve modulatory roles in membrane trafficking, differentially affecting robust development and function.....	192
6.3 The nervous system-enriched Rab26 functions in stimulus-dependent, synapse-specific receptor trafficking in <i>Drosophila</i> .....	196
6.4 Localization dynamics of Rab GTPases revealed by the RUSH system.....	198
7. Concluding remarks and future directions.....	202
8. Summary.....	205
9. Zusammenfassung .....	207
10. References .....	209
11. Declaration of independence .....	218

# 1. General Introduction

Cells are the building blocks of life. The communication of the cell within itself, as well as with its surrounding environment is crucial for tissue function and ultimately, the survival of the organism. A high variety of cell types with differing morphologies and functions exist in multicellular organisms. However, one major defining feature of basically all eukaryotic cells is the intracellular compartmentalization, where various membrane-bound organelles, such as ER, Golgi apparatus, and different types of endosomal compartments are localized to distinct regions inside the cell (Brighouse et al., 2010; Elias et al., 2012; Schlacht et al., 2014). The evolutionary transition to increased subcellular complexity provides an opportunity to efficiently separate cell functions. While at the same time, it presents an organizational challenge for the cell to ensure coordinated transport of cargo-loaded vesicles between these different intracellular compartments. Here, accurate trafficking is dependent on the correct identification of specific small GTPases and lipid species, foremost phosphoinositides, which are present on the organelles (Behnia and Munro, 2005; Dacks and Field, 2007; Elias et al., 2012; Klopper et al., 2012; Tokarev, 2000-2013). These opportunities and challenges of coordinated membrane trafficking are further exacerbated in cell types with highly specialized functions and complex morphologies, as present in neurons. Neurons are highly polarized cells often with a complex morphology. Membrane trafficking needs to be coordinated between distant axonal and dendritic extensions as well as with the cell body, meeting all of their functional requirements. Additionally, unlike other cell types, neurons are long-lived cells, with the ability to exist for the lifetime of an organism, as they are almost exclusively exempt from cellular turnover (Bentley and Banker, 2016; Bezprozvanny and Hiesinger, 2013; Sender and Milo, 2021; Wang et al., 2013). Intracellular trafficking is involved in all steps in the development, function as well as maintenance of neurons and consequently even in their degeneration (Jin et al., 2018a; Kiral et al., 2018; Wang et al., 2013). Rab GTPases are key regulators of intracellular membrane trafficking (Pfeffer, 2017; Stenmark, 2009). Therefore, studying this family of small GTPases provides an opportunity to identify possible neuron-specific Rab-mediated pathways and to learn more about the specific requirements of neurons for membrane trafficking in order to develop into functional cells and to maintain their functionality and health over long periods of time.

## 1.1 Small Rab GTPases as key regulators of intracellular membrane trafficking

Initially discovered in budding yeast in the early 1980s (Gallwitz et al., 1983), the first mammalian Rab GTPases were described by the lab of Armand Tavittian in 1987, where the first four Rab family members were identified from a rat brain cDNA library, hence the name *rab* (*ras* gene from rat *brain*) (Touchot et al., 1987). Within the Ras superfamily of small GTPases, which includes five families (Ras, Rho, Arf/Sar, Ran, and Rab), Rab GTPases constitute the largest family branch (Rojas et al., 2012). They are highly evolutionary conserved across eukaryotic lineages with multiple paralogous family members (Elias et al., 2012; Klopper et al., 2012), with 66 *rab* genes in the human genome (Gillingham et al., 2014), 26 protein-coding *rab* genes in *Drosophila melanogaster* (Chan et al., 2011; Jin et al., 2012), and 11 Rab-related *ypt* genes in the unicellular budding yeast *Saccharomyces cerevisiae* (Grosshans et al., 2006; Pfeffer, 2013). During the evolution from unicellular to multicellular eukaryotes, two great Rab expansions can be observed and it has been proposed that the greater evolutionary plasticity of membrane trafficking determinants, foremost Rab GTPases, is one of the driving forces of membrane trafficking complexity and multicellularity observed in higher eukaryotes (Brighouse et al., 2010; Diekmann et al., 2011; Klopper et al., 2012).

Over the last decades, Rab GTPases have been extensively studied and are now well established as essential regulators of intracellular membrane trafficking processes in eukaryotic cells ensuring that cargo-loaded vesicles are being delivered to their correct acceptor membrane. It is therefore not surprising, that Rab GTPases participate in processes like vesicle formation and movement and the docking and fusion of vesicles with their target compartments (Brighouse et al., 2010; Cai et al., 2007; Pfeffer, 2001, 2017; Stenmark, 2009). In the past, several Rab GTPases have been used as compartment markers conveying specific organelle identities, some even have become ‘gold-standard markers’ such as Rab5 for early endosomes, Rab7 for late endosomes and multivesicular bodies, and Rab11 for recycling endosomes (Barr, 2013; Behnia and Munro, 2005; Pfeffer, 2013; Zerial and McBride, 2001). However, the complete functional repertoire of most if not all Rab GTPases is still unknown, as is the identity of many directly interacting proteins, such as Rab effectors, which will be the subject of further investigations.

### 1.1.1 Rab GTPases act as molecular switches in membrane trafficking

Like other small GTPases, Rab GTPases function as molecular switches as they cycle between two conformational states: a guanosine triphosphate (GTP)-bound active state and a guanosine diphosphate (GDP)-bound inactive state (Figure 1). The cycle itself is tightly controlled by guanine nucleotide exchange factors (GEFs) and GTPase activating proteins (GAPs). GEFs regulate the activation of Rab GTPases by the exchange of bound GDP with GTP, while GAPs inactivate the membrane-bound Rab protein by facilitating the hydrolysis of GTP to GDP. Subsequently, the inactivated, GDP-bound Rab GTPase is removed from the membrane due to the interaction with a GDP dissociation inhibitor (GDI), replenishing the pool of inactive Rab proteins in the cytosol, so a new cycle can begin (Barr and Lambright, 2010; Muller and Goody, 2018; Stenmark, 2009).

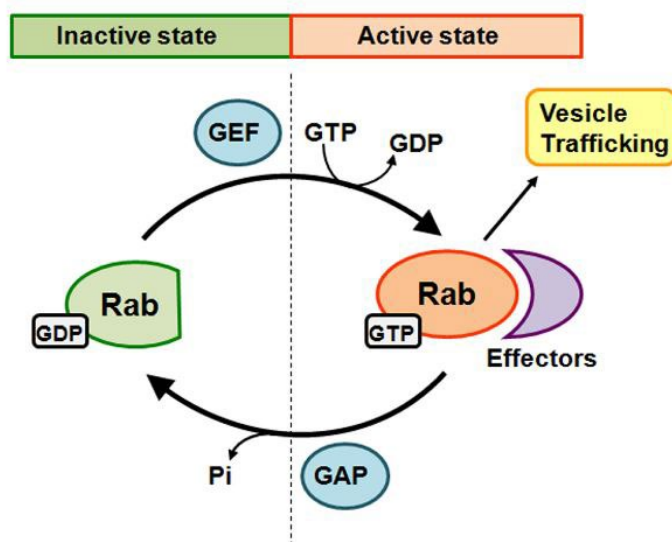


**Figure 1: Schematic illustration of the Rab GTPase cycle**

Rab GTPases cycle between two conformational states, a GDP-bound inactive state and a GTP-bound active state. A guanine nucleotide exchange factor (GEF) facilitates the activation of Rab proteins, as it catalyzes the conversion from the GDP-bound form to the GTP-bound one. Rab GTPases in their active state bind to effectors promoting intracellular vesicle trafficking. A GTPase-activating protein (GAP) facilitates GTP hydrolysis, converting the GTP-bound to the GDP-bound form. This leads to the inactivation of the Rab GTPase and subsequent dissociation of the effector protein. The GDP dissociation inhibitor (GDI), which binds to the GDP-bound Rab protein is not shown here. Adapted from (Wang et al., 2017).

With the binding of the Rab protein to its target membrane, a set of well-orchestrated events is initiated: the binding to and subsequent activation by a specific GEF leads to a change in conformation, allowing for the binding of distinct Rab effectors. These downstream effectors are themselves quite diverse and can be tethering complexes, coiled-coil proteins, protein kinases, phosphatases, or motor linkers. Their recruitment to membranes is spatio-temporally controlled, where active membrane-bound Rab GTPases serve as a form of recognition landmarks. Single Rab GTPases have the ability to interact with a variety of different partner proteins and *vice versa*, thereby achieving the great functional diversity of the Rab family (Gillingham et al., 2014; Grosshans et al., 2006; Hutagalung and Novick, 2011; Kjos et al., 2018; Zhen and Stenmark, 2015). To ensure the specificity and directionality of cargo transport, Rab GTPases form cascading pathway through the recruitment of subsequent downstream Rab proteins. Thereby, Rab cascades coordinate the switch of membrane identities which is needed for the successive transfer of cargo through membranous compartments. The sequential recruitment of individual Rab GTPases can be achieved by the binding of Rab effectors acting simultaneously as GAPs for the previous Rab or as GEFs for the next Rab in the cascade. For example, during the maturation of early-to-late endosomes, Rab5 recruits the Mon1-Ccz1 complex, which in turn acts as a GEF for Rab7. Overall, membrane maturation and cargo routing through Rab cascades has been established for both the endosomal as well as the exocytic pathway (Grosshans et al., 2006; Hutagalung and Novick, 2011; Jean and Kiger, 2012; Muller and Goody, 2018; Pfeffer, 2017).

### 1.1.2 Essential steps in the intracellular vesicle-mediated membrane trafficking

Generally, independent of the cell-type, four essential steps mediate the vesicle-mediated trafficking inside the cell. First, coat and adaptor proteins, such as clathrin, COPI, COPII, and AP1, are recruited to the membrane of the donor compartment, where they function in the selection of to-be-transported cargo and are required to form cargo-loaded transport vesicles (budding step). Second, the loaded vesicles are transported to their correct target membrane, either actively along the cytoskeleton via motor proteins, such as dynein, kinesin, or myosin, or passively via diffusion (movement/transport step). Third, specific coiled-coil proteins and multi-subunit complexes, including HOPS, CORVET, TRAPPI, and TRAPP II, ensure the tethering to the acceptor membrane (tethering step). And last, the tethered, cargo-loaded vesicles fuse with the membrane through the interaction of different SNARE proteins

(v-SNAREs and t-SNAREs), delivering their cargo (fusion step) (Bonifacino and Glick, 2004; Cai et al., 2007; Dacks and Field, 2007; Tokarev, 2000-2013). Members of the small Rab GTPase family are involved in all four of these trafficking steps through their direct interaction with a variety of effectors, such as motor proteins and tethers, as well as through their indirect regulation of SNARE function via effector-interacting proteins (Cai et al., 2007; Gillingham et al., 2014; Grosshans et al., 2006; Pfeffer, 2001).

### 1.1.3 The expression patterns and subcellular localization of *Drosophila* Rab GTPases

In humans, 24 Rab GTPases, roughly one-third of the Rab proteins that are encoded in the genome, are enriched in or specific to the central nervous system and are implicated to play a role there (D'Adamo et al., 2014; Gillingham et al., 2014). In *Drosophila*, an even higher neuronal localization can be observed. Recent large-scale profiling efforts examining cellular expression patterns and subcellular protein localizations of Rab GTPases in various tissues of *Drosophila*, revealed localization restrictions to specific tissues or even single cell types for several Rabs (Chan et al., 2011; Dunst et al., 2015; Jin et al., 2012; Kohrs et al., 2021; Zhang et al., 2007). Roughly one-third of the 26 *Drosophila* Rabs are ubiquitously expressed, present in all analyzed cells and tissues. The most prominent and extensively characterized examples being Rab5 (early endosomes), Rab7 (late endosomes) and Rab11 (recycling endosomes). While all Rab GTPases are expressed somewhere in the developing and adult nervous system, surprisingly, half of them are enriched or even strongly enriched there – with Rab3, X4, 27, and 26 being the most nervous system-enriched ones. Closely examining the subcellular distribution of all nervous system-enriched Rabs, it is evident that they predominantly localize to the synaptic domain or are strongly synapse-enriched. At the synapse itself, neuronal Rab GTPases colocalize mostly with the recycling endosomal marker Rab11 or with the synaptic vesicle marker CSP. In contrast, more ubiquitously expressed Rab GTPases can be found in other subcellular domains inside the neuron as well (Chan et al., 2011; Dunst et al., 2015; Jin et al., 2012).

The family of small Rab GTPases has gained more and more attention in their function as key regulators of intracellular membrane trafficking. Especially their great abundance in nervous systems across various species makes them an interesting and valuable choice for close examination of membrane trafficking pathways in neurons.

## 1.2 Rab-mediated membrane trafficking in neurons

The endomembrane system, consisting of the secretory and endosomal system, is classically made up of the endoplasmic reticulum (ER), the Golgi apparatus with outposts in the dendritic extensions of neurons, the *trans*-Golgi network (TGN), various endosomal and lysosomal compartments and finally, the plasma membrane. However, recently organelles like the nucleus, peroxisomes, and mitochondria have been implicated in the endomembrane trafficking system as well (Hanus and Ehlers, 2008; Lasiecka and Winckler, 2011; Schlacht et al., 2014). Neurons, with their longevity, complex morphology, and specialized function, critically depend on a correctly operating trafficking system. Consequently, specific Rab-mediated membrane trafficking processes have been proposed to be required to maintain neuronal function and health (Jin et al., 2018a; Jin et al., 2018b). Neuron-specific Rabs appear to functionally complement the ubiquitously expressed, cell-type unspecific Rab GTPases to execute neuron-specific roles in transport, including the regulated exocytosis for synaptic transmission, the distribution and insertion of surface receptors into the plasma membrane, as well as the coordinated organelle and protein delivery to axons and dendrites ensuring their correct functional composition (Figure 2) (Binotti et al., 2016; Kiral et al., 2018; Lasiecka and Winckler, 2011; Mignogna and D'Adamo, 2018; Winkle and Gupton, 2016).

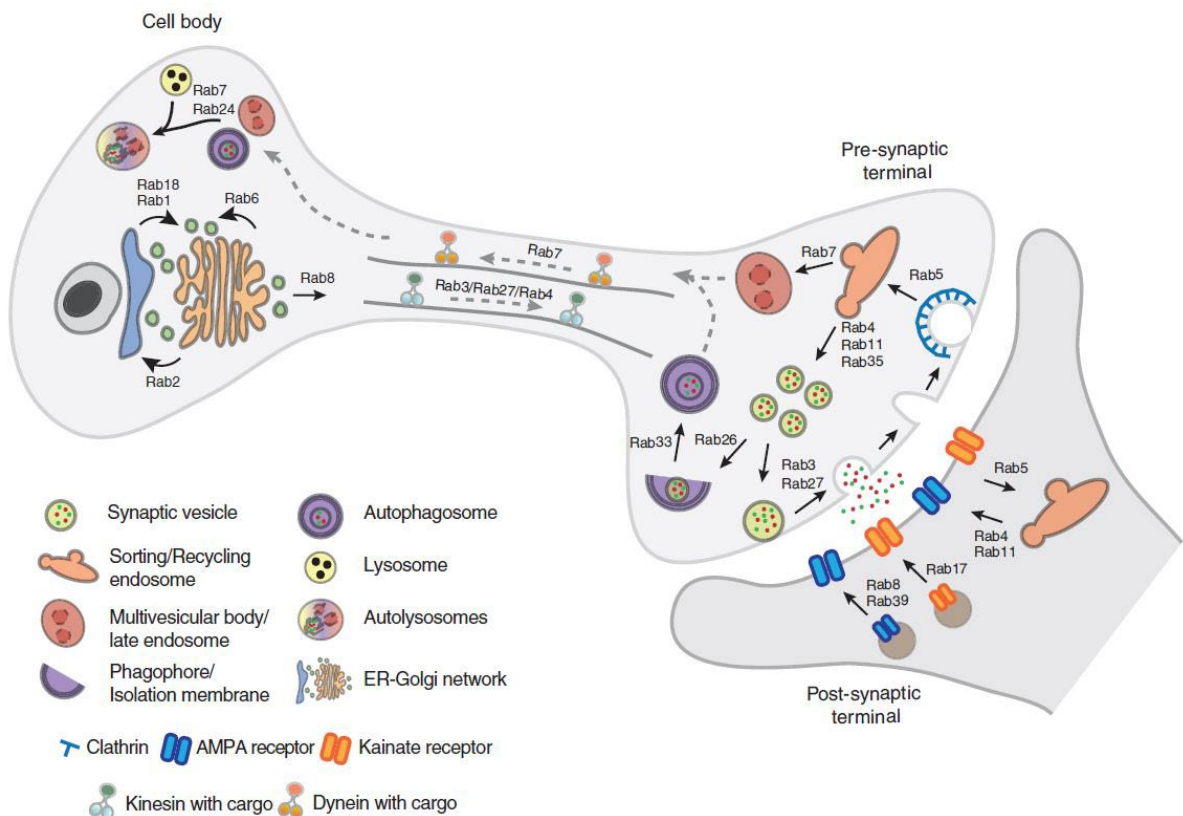


*Figure 2 is on the previous page*

## **Figure 2: Illustration of Rab GTPases in synaptically connected wild type neurons**

Shown here is a schematic representation of a neuronal cell body (left), axon (middle), as well as pre- and postsynaptic terminal (right). The presynaptic neuron is colored in light grey, while the postsynaptic one in dark grey. Individual mammalian and *Drosophila* Rab GTPases have been depicted next to membrane compartments for which their function has been investigated or proposed in wild type neurons. The directionality of the Rab-regulated transport is highlighted with black arrows. Adapted from (Kiral et al., 2018).

Rab GTPases with functions in the regulation of intracellular membrane trafficking during development, function, and maintenance in neurons have been reviewed in detail elsewhere (Binotti et al., 2016; D'Adamo et al., 2014; Kiral et al., 2018; Mignogna and D'Adamo, 2018; Ng and Tang, 2008; Parker et al., 2018; Villarroel-Campos et al., 2016). Here, I will only highlight some examples of ubiquitous and nervous system-enriched Rabs involved in these processes.

### 1.2.1 Rab-mediated membrane trafficking during neuronal development

Especially neurons depend on a functioning membrane trafficking machinery during development to establish their complex polarized morphology as well as asymmetric specialized membrane domains, such as dendrites and axons. A continuous supply of membrane components is required for the elongation of neurites and later of dendrites and the axon. Further, the asymmetric distribution of cell surface receptors, adhesion molecules, and intracellular mediators of axon formation, amongst others, is needed in the differentiating neuron. Mostly, through work on various neuronal cell lines, several Rab proteins have been implicated in neuritogenesis, the first step towards neuronal polarity, neurite pruning, axon and dendrite maturation as well as assembly of presynaptic release machinery components (Cheng and Poo, 2012; Futerman and Banker, 1996; Gotz et al., 2021; Graf et al., 2009; Kramer et al., 2019; Mignogna and D'Adamo, 2018; Parker et al., 2018).

The ubiquitous Rab 5, 6, 7, 8, 11, 13, and 35, as well as the more restrictively expressed Rab14 and Rab21 are involved in the formation and outgrowth of neurites (Parker

et al., 2018; Villarroel-Campos et al., 2016). For instance, mammalian Rab7, with its recently identified effector protrudin, participates in the formation of contact sites between late endosomes and the ER, linking the endocytic to the secretory pathway. Motor protein kinesin-1 is transferred through these contacts onto late endosomes, leading to their microtubule-dependent translocation and subsequent fusion with the plasma membrane promoting neurite outgrowth (Raiborg et al., 2015). Rab8 regulates the anterograde vesicular trafficking of membrane precursors from the TGN to the plasma membrane, while downregulation of *rab8* inhibits the transport of exocytic vesicles terminating neurite outgrowth in hippocampal neurons (Huber et al., 1995). Interestingly, Rabin8, a Rab8 GEF, functions as a Rab11 effector during nerve growth factor-induced neurite outgrowth in PC12 cells. Rab11, the key recycling endosomal Rab GTPase, is implicated in the transport of  $\beta 1$  integrins to the neurite tips. Recycling endosomes themselves act as sources of membrane supply and can serve as intermediates in the secretory pathway. Together this highlights a Rab cascade where Rab11, together with Rabin8, acts functionally upstream of Rab8 on recycling endosomes during neurite outgrowth (Ang et al., 2004; Eva et al., 2010; Homma and Fukuda, 2016).

Polarized trafficking is crucial for the establishment of distinct asymmetric axonal and dendritic domains which in turn is essential for the proper functioning of the neuron. Selective sorting and transport of proteins and lipids, as well as the coordinated reorganization of cytoskeletal components are at the basis of establishing and maintaining neuronal polarity (Bentley and Banker, 2016; Parker et al., 2018; Takano et al., 2015). For axonal outgrowth, various Rab GTPases have been implicated: Rab 4, 5, 7, 10, 11, 27b, and 33a (Mignogna and D'Adamo, 2018; Parker et al., 2018). For example, in the developing axon, Rab27b and Rab7 participate in the anterograde and retrograde trafficking of the Trk neurotrophin receptors respectively, thereby influencing axonal growth (Arimura et al., 2009; Deinhardt et al., 2006; Saxena et al., 2005). While mammalian Rab33a, specifically expressed in the brain and immune system, is involved in the anterograde trafficking of post-Golgi synaptophysin-positive vesicles towards the axonal growth cone. There, synaptophysin is incorporated into the plasma membrane for extension contributing to the growth of the axon. RNAi-mediated downregulation of Rab33a leads to an inhibition of axon outgrowth of hippocampal neurons, whereas the expression of the constitutively active variant causes a multi-axonic phenotype (Nakazawa et al., 2012).

In contrast to axonal growth and maturation, mainly other Rab proteins are regulating trafficking during dendritic outgrowth: Rab 1, 8, 11, 17, and 21 (Mignogna and D'Adamo, 2018; Parker et al., 2018). The small GTPase Rab1 mediates the anterograde transport from ER to Golgi and Golgi outposts, which are exclusively localized to dendrites and contribute to dendritic growth dynamics by acting as a source of membrane supply. Additionally, the *dendritic arbor reduction* mutant *dar6*, encoding *Drosophila* Rab1, displays normal axonal growth but a significant reduction in dendritic arbors of developing neurons (Ye et al., 2007). Ultimately, the correct establishment of neuronal polarization is in turn crucial for the accurate synaptic activity of neurons.

### 1.2.2 Rab-mediated membrane trafficking during neuronal function

Neurons are sophisticated cells that receive, integrate, and transfer signals through synaptic connections, which is at the basis of neuronal connectivity. During neuronal development a polarized structure with specialized subcellular domains, such as the pre- and postsynapse, is established (Parker et al., 2018; Villarroel-Campos et al., 2016). Synapses are characterized by a high membrane turnover during chemical neurotransmission as synaptic vesicles undergo coordinated trafficking cycles of exo- and endocytosis (Sudhof, 2004). Although, the exact roles of many Rab GTPases in mature neurons are not well established, some have been functionally characterized for their involvement in synaptic transmission. In the presynaptic terminal, neuronal Rab3 and Rab27 (Rab27b in mammals) regulate the exocytosis of synaptic vesicles and the subsequent neurotransmitter release into the synaptic cleft. Rab3a, a member of the mammalian Rab3 subfamily, forms a tripartite complex together with the active zone proteins Munc13 and  $\alpha$ -RIM, which in turn function as Rab3 effectors to facilitate the priming of synaptic vesicles. Rab27b is proposed to function to some extent redundantly to Rab3a in synaptic vesicle docking and priming, as both share downstream effectors, such as Rabphilin, RIM, and Munc13 (Binotti et al., 2016; Dulubova et al., 2005; Fischer von Mollard et al., 1991; Guadagno and Progida, 2019; Pavlos and Jahn, 2011; Schluter et al., 2002; Schluter et al., 2004). While in *Drosophila*, Rab3 additionally functions in the distribution of crucial active zone components, such as Bruchpilot, to the larval neuromuscular junction (NMJ) thus controlling the correct active zone development (Chen et al., 2015; Graf et al., 2009).

Clathrin-mediated endocytosis acts as a major pathway in the synaptic vesicle retrieval from the presynaptic plasma membrane. Here, ubiquitously expressed Rab5, a key

early endosomal Rab GTPase, is involved in the endocytic retrieval of synaptic vesicle components and participates in endosome maturation (Binotti et al., 2016; McLauchlan et al., 1998; Semerdjieva et al., 2008). An analysis of Rab5 in *Drosophila* neuromuscular synapses shows that a functional impairment of Rab5 negatively affects the size of the synaptic vesicle pool, as well as the probability of neurotransmitter release and that Rab5 is required for endosome integrity at the synapse (Wucherpfennig et al., 2003). Rab4 and Rab11, associated with early and recycling endosomes respectively, are likely to function in the synaptic vesicle recycling process via endosomal intermediates, as these Rab proteins have been found to localize to synaptic vesicles purified from rat brains (Pavlos et al., 2010). Moreover, expression of mammalian dominant negative Rab4 inhibits the formation of synaptic-like vesicles from endocytic intermediates in neuroendocrine cells (de Wit et al., 2001). However, their precise function in the recycling of synaptic vesicle components in neurons remains unclear. Additionally, Rab35 together with its GAP Skywalker (Sky) has been shown to participate in the regeneration of synaptic vesicles through endosomal intermediates as sorting stations in *Drosophila*. Expression of the constitutively active Rab35 variant or functional loss of *sky* leads to an increase in neurotransmitter release and an enlarged readily releasable pool of synaptic vesicles was observed in the *sky* mutant. Further, it has been proposed that Rab35 and its GAP Sky participate in the turnover of synaptic vesicle proteins, as the degradation of neuronal Synaptobrevin (n-Syb), a synaptic vesicle protein, is increased in the *sky* mutant. Therefore, Rab35 and Sky seem to regulate neurotransmission levels by linking synaptic vesicle recycling and degradation (Fernandes et al., 2014; Uytterhoeven et al., 2011).

Rab-mediated membrane trafficking is not only crucial for the synaptic vesicle trafficking cycle in the presynapse, but also at the postsynaptic site to regulate the correct distribution of transmembrane receptors to transmit synaptic input (Mignogna and D'Adamo, 2018). Independent of cell type, the ubiquitously expressed Rab8 participates in the anterograde trafficking of post-Golgi secretory vesicles towards the plasma membrane (Huber et al., 1993). In neurons, Rab8 exhibits a specialized function, as it is required for the transport of GluA1 AMPA receptor subunit from the ER to the Golgi, as well as for its delivery to postsynaptic sites of excitatory synapses in mammals (Brown et al., 2007; Gerges et al., 2004). While neuronal Rab39b, together with its downstream effector PICK1, coordinates the secretory trafficking of GluA2/GluA3 AMPA receptor subunits from the ER to Golgi for maturation necessary for a correct surface composition of AMPA receptors

(Mignogna et al., 2015). Rab17 is not involved in the surface distribution of AMPA receptors, but regulates the dendritic surface insertion of the GluK2 kainate receptor subunit in developing rat hippocampal neurons by interacting with the t-SNARE Syntaxin 4 (Mori et al., 2014). Most recently, neuronal Rab26 was implicated in the stimulus-dependent trafficking of the D $\alpha$ 4 acetylcholine receptor subunit at cholinergic synapses of outer photoreceptors in *Drosophila* (Kohrs et al., 2021).

Overall, the correct composition and distribution of proteins and lipids need to be maintained to preserve the cell morphology and to ensure synaptic function throughout the entire lifespan of the neuron.

### 1.2.3 Rab-mediated membrane trafficking during neuronal maintenance

Neuronal maintenance mechanisms and their integrity are crucial for the health and function of neurons. Synaptic connections, once established, need to be kept intact throughout the lifespan of the neurons, which are almost exclusively exempt from cellular turnover. Especially, the high rate of membrane turnover at the synapse during chemical neurotransmission represents a major challenge for maintenance mechanisms. Not surprisingly, loss of synaptic integrity has been recognized as an early hallmark of various neurodegenerative diseases, such as Alzheimer's Disease. Furthermore, the complex morphology and spatial segregation between neuronal subdomains, such as synapse and cell body, represents another challenge, possibly requiring specialized cellular maintenance mechanisms. All of these aspects cumulate in the neuronal or synaptic maintenance problem (Bezprozvanny and Hiesinger, 2013; Henstridge et al., 2019; Sender and Milo, 2021; Sudhof, 2004). Endomembrane recycling, along with various membrane protein degradation pathways constitute the neuronal maintenance machinery. So far, only a few involved Rab GTPases have been identified and examined more closely.

The canonical endolysosomal degradation pathway is part of the maintenance machinery and requires the delivery of to-be-degraded membrane proteins to late endosomes/multivesicular bodies and their subsequent fusion with degradative lysosomes (Jin et al., 2018a; Luzio et al., 2007; Piper and Katzmann, 2007). Rab7, the key late endosomal Rab GTPase, functions in the maturation from early to late endosomes and regulates the fusion with lysosomes (Guerra and Bucci, 2016). Although ubiquitously expressed, mutations in the *rab7* gene locus primarily affect the nervous system causing the

neuropathy Charcot-Marie-Tooth 2B (Cherry et al., 2013; Spinosa et al., 2008; Verhoeven et al., 2003). Furthermore, in *Drosophila*, partial loss of Rab7 function leads to a stimulation-dependent loss of synaptic function and progressive neurodegeneration without affecting neuronal development itself or the development and function of other tissues. This highlights the sensitivity of neurons and in particular synapses towards dosage-dependent membrane degradation mediated by Rab7 (Cherry et al., 2013). Moreover, the sorting of plasma membrane proteins into degradative compartments at axon terminals requires the function of Rab7, while the sorting of synaptic vesicle membrane proteins is Rab7-independent and was shown to be performed via a neuron-specific ‘sort-and-degrade’ mechanism. So far, no Rab GTPase has been identified to be involved in this cell type-specific endomembrane degradation pathway, which requires the function of synaptic vesicle proteins n-Syb and vesicular ATPase component V100 (Haberman et al., 2012; Jin et al., 2018b; Williamson et al., 2010). It is highly unlikely that no Rab protein should be involved, given their abundance in neurons and their role as key regulators of intracellular membrane trafficking.

Another major degradative pathway contributing to the maintenance of neuronal and synaptic homeostasis is macroautophagy (hereafter autophagy). This intracellular pathway regulates the effective turnover of cytoplasmic components, like protein aggregates and even entire dysfunctional organelles, such as mitochondria in case of mitophagy, a form of selective autophagy (Mizushima, 2007; Stavoe and Holzbaur, 2019). Impairment of the basal autophagic machinery in neurons, through loss of essential autophagy genes *atg5* or *atg7*, leads to an accumulation and aggregation of intracellular proteins and eventually to late-onset neurodegeneration (Hara et al., 2006; Komatsu et al., 2006). Autophagosomes, containing to-be-degraded cargo, preferentially and continuously form at the tip of the axon before they are retrogradely transported along the axon during which they mature and gradually acidify due to the fusion with lysosomes (Maday and Holzbaur, 2014; Maday et al., 2012; Wong and Holzbaur, 2015). Several Rab GTPases have been identified to be involved in various trafficking steps during autophagy. However, available information comes almost exclusively from investigations in non-neuronal cell types. Among those Rab GTPases are Rab 1, 4a, 6, and 11 (trafficking to the phagophore assembly site), Rab5 (phagophore nucleation), Rab33b and Rab37 (phagophore formation and elongation), as well as Rab7 and Rab24 (fusion of autophagosomes with lysosomes) (Jain and Ganesh, 2016; Kiral et al., 2018; Lu et al., 2021). It remains to be shown, if the same Rab proteins

or different, more neuron-specific ones fulfill the same functions in neurons. So far, only few Rab proteins have been associated with neuronal autophagy: Rab7, together with its effector RILP, functions in the transport of mature autophagosomes to perinuclear lysosomes in cultured Purkinje neurons (Bains et al., 2011). While the downregulation of Rab39b in mouse neuroblastoma cells reduces the formation of autophagolysosomes, thus directly affecting the autophagic flux (Niu et al., 2020). Recently, neuronal Rab26 has been proposed to link synaptic vesicle recycling to autophagy by interacting with the autophagosomal marker Atg16L in mice hippocampal neurons and *Drosophila* NMJs. However, using the *rab26* null mutant in *Drosophila* NMJs and photoreceptor neurons, no direct link to autophagy could be established (Binotti et al., 2015; Kohrs et al., 2021). Several of the Rab functions described in the last three sections (1.2.1 – 1.2.3) were inferred from constitutively active or dominant negative Rab variant phenotypes and not based on RNAi knockdown approaches or even mutant analyses. Thus, the exact functions of nervous-system enriched Rab GTPases and the membrane trafficking these mediate in the development, function, and maintenance of neurons is subject to further investigation.

### **1.3. *Drosophila melanogaster* as a model system**

Model organisms like *Drosophila melanogaster* are widely used for the functional study of intricate systems, such as the human nervous system, as they allow for an analysis in a more simplified manner. Besides obvious features, such as a short generation time and lifetime, a high number of offspring, and no overly costly maintenance, the model organism *Drosophila* provides several more advantages for the research of the development and function of neurons. Many genes, molecular mechanisms, and cellular, as well as electrophysiological properties of the nervous system have been conserved between humans and *Drosophila* through evolution. This is exemplified and highlighted by 75% of disease-causing genes in humans, which have functional equivalents in the fruit fly. Still, *Drosophila* exhibits a reduced complexity, in the number of genes (~25,000 genes in total in humans versus ~13,600 in *Drosophila*, more specifically, 66 protein-encoding *rab* genes in humans versus 26 in the fly), as well as in the number of neurons. Despite the fruit fly's simplicity, its nervous system is complex enough to reliably investigate aspects of neuronal development, function, and maintenance, including intricate membrane trafficking networks. To be able to study this more closely, fortunately, a variety of powerful genetic tools are available in *Drosophila*, which allow for instance the generation of loss-of-function mutations, targeted

expression of genes or endogenous protein tagging (Chan et al., 2011; Colley, 2012; Dunst et al., 2015; Gillingham et al., 2014; Jackson, 2008; Jennings, 2011; Jin et al., 2012; Ugur et al., 2016). Thus, making *Drosophila* a formidable model organism for the close examination of components and mechanistic basics of Rab-mediated membrane trafficking pathways in neurons. The developing and adult fly visual system served as the primary model for the main experimental work of my doctoral thesis presented here.

### 1.3.1 The *Drosophila* visual system: a model to study intracellular protein trafficking in neurons

The *Drosophila* visual system is a well-established model used to examine components and mechanisms of intracellular trafficking pathways involved in the development, function, and maintenance of neurons. Especially photoreceptors with their highly polarized morphology, are well-suited to study polarized membrane trafficking (Iwanami et al., 2016; Schopf and Huber, 2017). Furthermore, the eye itself can be easily stimulated and allows for perturbation experiments without affecting the viability or survival of the organism under controlled laboratory conditions (Wang and Montell, 2007; Zhu, 2013). Anatomically, the visual system is composed of the retina, detecting visual input, and four neuropils in each optic lobe, namely the lamina, the medulla, the lobula, and the lobula plate, which process the visual information. Roughly 150,000 neurons and glia cells are part of the visual system and the optic lobes comprise ~60% of the neurons in the brain (Fischbach and Dittrich, 1989; Neric and Desplan, 2016).

The adult *Drosophila* compound eye is a reiteration of approximately 800 single repetitive unit eyes called ommatidia. Each hexagonally shaped ommatidium contains eight photoreceptors (R cells), with six outer (R1-R6) and two centrally located (R7 and R8) cells, as well as four lens secreting cone cells and two primary pigment cells. Six secondary and three tertiary pigment cells, in addition to three mechano-sensory bristle cells are being shared between neighboring ommatidia (Kumar, 2012; Montell, 2012). Photoreceptors can be divided into two functional groups, outer and inner photoreceptors, based on their position, axonal projections, spectral properties, and specific functional involvement. Outer photoreceptors R1-R6, expressing the major visual pigment molecule Rhodopsin 1 (Rh1), are specialized in motion detection, thus acting as functional equivalents of rods in the vertebrate retina. Their axons are projecting into the first optic neuropil, the lamina, where they form synaptic connections mainly with lamina monopolar cells (Figure 3) (Katz and

Minke, 2009; Meinertzhagen and O'Neil, 1991; Montell, 2012; Rivera-Alba et al., 2011; Sanes and Zipursky, 2010). Inner photoreceptors R7 and R8, located on top of each other in the ommatidium, differ in their spectral sensitivities due to the expression of distinct Rhodopsin molecules and mediate mainly color vision, making them functionally equivalent to cone cells in the vertebrate retina. R7 cells, expressing Rhodopsin 3 or Rhodopsin 4, are UV-sensitive and involved in the detection of polarized light, while R8 cells express blue-sensitive Rhodopsin 5 or green-sensitive Rhodopsin 6. Axons of R7 and R8 target the M6 and M3 layer of the medulla respectively, where they synaptically connect with various types of medulla neurons (Figure 3) (Fischbach and Dittrich, 1989; Morante and Desplan, 2008; Sanes and Zipursky, 2010; Takemura et al., 2015; Wernet et al., 2006; Yamaguchi et al., 2010).

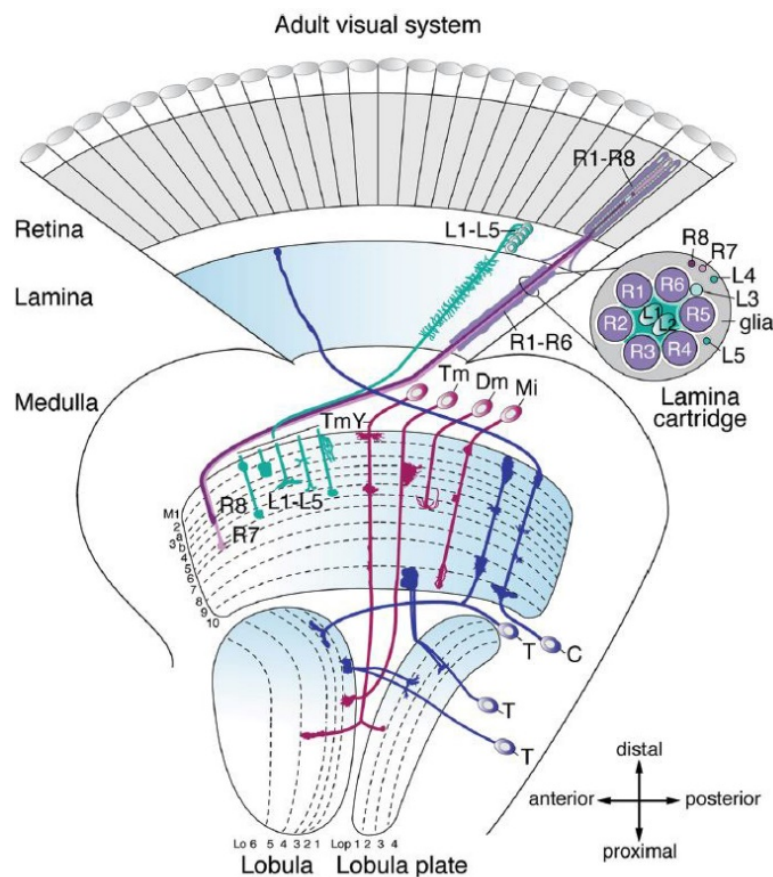


**Figure 3: Schematic illustration of the adult *Drosophila* visual system**

The optic lobe is proximally located to the fly retina and consist of four neuropils, the lamina, medulla, lobula and lobula plate. A subset of neurons and their respective axonal projections are shown here. Outer photoreceptors, R1-R6, project from the retina into the lamina where they form synaptic connections with lamina monopolar neurons in cartridges. Inner photoreceptors, R7 and R8, as well as lamina neurons, L1-L5, extend their axons into one or more of the ten layers in the

*Figure 3 continued*

medulla neuropil (M1-M10). Distal medulla neurons, Dm cells, form lateral branches innervating multiple columns in the distal medulla region, while medulla intrinsic neurons, Mi cells, link distal and proximal layers of the medulla. C neurons extend their axons into the medulla and lamina. Transmedullary neurons, Tm and TmY, project into the lobula (Lo) and lobula plate (Lop), where they innervate subsets of six and four neuropil layers, respectively. T neurons either connect lobula and medulla, lobula plate and medulla or lobula and lobula plate. Adapted from (Apitz and Salecker, 2014).

Photoreceptors are highly polarized, light-activated neurons, each with a specialized compartment known as the rhabdomere, which consists of a stack of tightly packed microvilli housing the signaling proteins of the phototransduction machinery (Katz and Minke, 2009; Montell, 2012). Very briefly, focusing on the phototransduction cascade in R1-R6 photoreceptors, absorption of blue light photons (~480 nm) converts Rh1 into its active form metaRh1. The photoactivated metaRh1 sets off a well-orchestrated cascade of events, ultimately leading to the opening of two Ca<sup>2+</sup>-permeable cation channels, transient receptor potential (TRP) and TRP-like (TRPL), and the depolarization of the photoreceptors. Thermally stable metaRh1 is phosphorylated by rhodopsin kinase and binds to arrestin 1 or 2, which either promotes the endocytosis or the inactivation of metaRh1 respectively. The endocytosed photopigment can either be recycled back to the rhabdomere or degraded mainly through the endolysosomal pathway. As arrestin 2, comprising 85% of the total amount of available arrestin, constitutes the more prevalent isoform, the metaRh1 is primarily inactivated. The calcium/calmodulin-dependent protein kinase 2 (CaMKII) phosphorylates the bound arrestin, facilitating its release. Upon absorption of orange light photons (~580 nm), phosphorylated metaRh1 converts back into its inactive state, triggering the dissociation of phosphorylated arrestin from Rh1. Subsequently, retinal degeneration C phosphatase dephosphorylates Rh1 (Hardie, 2012; Montell, 2012; Schopf and Huber, 2017; Wang and Montell, 2007; Xiong and Bellen, 2013).

Photoreceptor function can be readily analyzed by electroretinogram (ERG) recordings, which are extracellular voltage recordings of a neuronal signal from an entire fly eye in response to a given light stimulus. In addition to functional analysis via electrophysiology, (fluorescent) light or electron microscopy can be used to examine defective trafficking. Especially neuronal degeneration in the fly eye, associated with

impaired maintenance mechanisms, can be morphologically assessed. Hallmarks of retinal degeneration are initial reduction in rhabdomere integrity, complete loss of single rhabdomeres, actual holes in the retina, ultimately followed by the death of photoreceptor cell bodies (Belusic, 2011; Milligan et al., 1997; Shieh, 2011; Wang and Montell, 2007). Moreover, photoreceptors can be easily stimulated with light, to identify and examine activity-dependent cellular mechanisms of neuronal function and maintenance in distinction to stimulus-independent ones. During light-induced activation, photoreceptors are characterized by a high rate of membrane trafficking of rhodopsin and other phototransduction components such as TRPL ion channels. Furthermore, it is well-established that almost every mutation in a gene involved in the photoresponse ultimately leads to retinal defects and degeneration. Many of those protein-encoding genes are involved in Rh1 biosynthesis and maturation, as well as internalization and degradation of its activated form metaRh1 (Belusic, 2011; Colley, 2012; Oberegelsbacher et al., 2011; Schopf and Huber, 2017; Wang and Montell, 2007; Xiong and Bellen, 2013). Not surprisingly, retinal degeneration phenotypes identified thus far are often light-dependent. As such, continuous stimulation of *Drosophila* photoreceptor neurons is an established model to identify mutants affecting intracellular signaling pathways, synaptic transmission, and neuronal maintenance, which ultimately leads to retinal degeneration (Chinchore et al., 2009; Jaiswal et al., 2015; Jaiswal et al., 2012; Wang and Montell, 2007).

Additionally, using *Drosophila* photoreceptors as a model to study basic neuronal function led to the discovery of several key components of intracellular membrane trafficking pathways. At axon terminals, synaptic vesicle SNARE n-Syb and V100 were identified as regulators of a neuron-specific endolysosomal sort-and-degrade pathway, independent of their roles in neurotransmission. Recently, it was shown that synaptic vesicle proteins are sorted and degraded in a cargo-specific manner by this neuronal degradation mechanism, which operates independently of the canonical Rab7-dependent pathway. Furthermore, photoreceptor-specific loss of function of synaptic proteins n-Syb and V100 causes degradation defects downstream of endocytosis, ultimately leading to slow adult-onset neurodegeneration (Haberman et al., 2012; Jin et al., 2018b; Williamson et al., 2010).

More importantly, based on recent cellular expression and subcellular protein localization analyses, half of all *Drosophila* Rab GTPases are enriched or strongly enriched in the nervous system, the majority of these located in the developing and functional fly visual system with unknown functions (Chan et al., 2011; Jin et al., 2012; Kohrs et al., 2021).

Evolutionary conserved functions of already extensively characterized Rab GTPases could be verified in the antero- and retrograde trafficking of Rh1 in adult photoreceptors. Anterogradely, Rh1 is transported from the ER to the Golgi, requiring Rab1 function. Rab6 has been implicated in the exiting of Rh1 from the Golgi, from where Rab11 mediates the transport to the rhabdomere. In the retrograde trafficking pathway, Rab5 and Rab7 are implicated to function in the endocytosis of activated rhodopsin, while Rab11 together with its GEF Crag and the retromer complex are required for the recycling of rhodopsin back to the rhabdomere (Iwanami et al., 2016; Oberegelsbacher et al., 2011; Schopf and Huber, 2017; Xiong et al., 2012). Furthermore, impairment of the canonical degradation pathway in photoreceptors due to loss of *rab7* leads to stimulus-dependent progressive degeneration, initially indicated by an impairment in synaptic transmission (Cherry et al., 2013). Additionally, photoreceptor-specific roles for Rab26 and *Drosophila*-specific RabX4, both highly nervous system-enriched Rabs, could recently be identified. RabX4 has been implicated in the stimulus-dependent vesicular internalization of the ion channel TRPL into the photoreceptor cell body, functioning here in a similar, but non-redundant fashion to the ubiquitously expressed Rab5 (Oberegelsbacher et al., 2011). While Rab26 functions in the receptor trafficking at specific cholinergic synapses in a stimulus-dependent manner (Kohrs et al., 2021). This highlights the value of photoreceptors as a model to study Rab-mediated membrane trafficking components and mechanisms in neurons.

## 2. Aim

Neurons are postmitotic, long-lived, specialized cells with a highly polarized morphology, where axonal and dendritic extensions are spatially separated from each other and the cell body. To ensure robust development, function, and maintenance, neurons have special demands on intracellular membrane trafficking networks. The family of small Rab GTPases provides a great opportunity to closely examine these. In their function as key regulators of vesicular trafficking in the endomembrane system, Rab GTPases mediate essential steps in these intracellular pathways, such as vesicle formation, vesicle motility, as well as docking and fusion of transport vesicles with their target membrane.

Based on the observation that half of all *Drosophila* Rab GTPases are nervous system-enriched with a predominant synaptic localization and that these, as mutants, are viable in homozygosity under laboratory conditions, we formed several ‘Rab-centric’ questions: Why does such a high number of nervous system-enriched Rab GTPases exist? What might be their specific functions? Do nervous system-enriched Rabs perform more context-specific, specialized roles to ensure the robust development and function of the nervous system, as they are not essential for the viability of the organism? When do these roles become apparent - maybe under more environmentally variable and challenging conditions? To address these questions experimentally, unbiased systematic *rab* mutant analyses were carried out with a special focus on viable, nervous system-enriched *rabs*. First, we generated a complete null mutant collection. Then, different functional assays were performed under specifically challenging conditions to determine which Rabs are required for robust development, as well as neuronal function and maintenance. This functional analysis was extended by our newly generated transgenic fly collection for the selective retention and release of tagged Rab proteins in intact multicellular tissues in *Drosophila*. Here, we report proof-of-principle of this assay, which allows the study of intracellular localization dynamics in a spatiotemporally controlled manner. The experimental work was further corroborated by an extensive literature review on Rab-mediated membrane trafficking in neurons. Moreover, this was set in relation to the pathology of neurodegenerative diseases as Rab GTPases in the nervous system have been repeatedly associated with maintenance and neurodegeneration.

Ultimately, functional *rab* analyses will surely help to answer bigger, more ‘neuron-centric’ questions in the field, such as: How is membrane trafficking specifically regulated

in neurons? Do different neuron-specific pathways exist and with what kind of cargo specificity? What are the molecular machineries behind this? And how do neurons, and in particular their synaptic contacts, ultimately stay healthy and functional over long periods of time? Knowing more about Rab-mediated membrane trafficking steps in neurons will surely play a part in solving the neuronal maintenance problem. Furthermore, this will help to elucidate causal and correlative relations between Rab-mediated trafficking and pathologies of neurodegenerative diseases and advance our understanding of these human diseases.

This doctoral work provides a first approach to a systematic and comparative functional analysis of Rab GTPases in the multicellular organism *Drosophila* focusing on molecularly defined *rab* null mutants and a transgenic fly collection for the acute and synchronous release of tagged Rab proteins.

### **3. Manuscript 1**

#### **Rab GTPases and Membrane Trafficking in Neurodegeneration**

Kiral, F. K. \*, Kohrs, F. E. \*, Jin, E. J., and Hiesinger, P. R.

\* These authors contributed equally to this work

Current Biology, 28(8): R471-R486, April 23, 2018

DOI: 10.1016/j.cub.2018.02.010

#### **Author contributions**

The literature research was done by me, Ferdi Ridvan Kiral, and Eugene Jennifer Jin. The review paper was conceptualized and written by me, Ferdi Ridvan Kiral, Eugene Jennifer Jin, and Prof. Dr. P. Robin Hiesinger.

The original article is included on the following pages of this thesis and is available online:

<https://doi.org/10.1016/j.cub.2018.02.010>

## 4. Manuscript 2

### **Systematic functional analysis of rab GTPases reveals limits of neuronal robustness to environmental challenges in flies**

Kohrs, F. E.\* , Daumann, I.-M.\* , Pavlović, B., Jin, E. J., Kiral, F. R., Lin, S.-C., Port, F., Wolfenberg, H., Mathejczyk, T. F., Linneweber, G. A., Chan, C.-C., Boutros, M., Hiesinger, P. R.

\* These authors contributed equally to this work

eLife 2021;10:e59594

DOI: 10.7554/eLife.59594

#### **Author contributions**

Most major experiments in this manuscript were designed, performed, and analyzed with equal contributions from myself and Ilsa-Maria Daumann under the supervision of Prof. Dr. P. Robin Hiesinger. Wing experiments were designed, performed, and analyzed by Bojana Pavlović under the supervision of Dr. Phillip Port and Prof. Dr. Michael Boutros. Eugene Jennifer Jin contributed to the verification of the *rab* null mutants by PCR as well as to the design, performance, and analyses of ERG and adult retina-lamina experiments. Ferdi Ridvan Kiral contributed to the design, performance, and analyses of several experiments in the Rab26 section. Heike Wolfenberg helped with the experiments performed in the Hiesinger lab. Shih-Ching Lin generated the *rab18* null mutant under the supervision of Chih-Chiang Chan, PhD. Thomas F. Mathejczyk helped with the design and construction of both lightboxes, while Dr. Gerit A. Linneweber substantially helped with the statistical analysis and representation of the experimental data as well as with the conceptualization of the backcrossing required for the manuscript revision. The manuscript was written by me, Ilsa-Maria Daumann, Bojana Pavlović, Dr. Filip Port, Chih-Chiang-Chan, Prof. Michael Boutros, and Prof. Dr. P. Robin Hiesinger.

The original article with its supplementary files is included on the following pages of this thesis and is available online: <https://www.doi.org/10.7554/eLife.59594>

# Systematic functional analysis of rab GTPases reveals limits of neuronal robustness to environmental challenges in flies

Friederike E Kohrs<sup>1†</sup>, Ilsa-Maria Daumann<sup>1†</sup>, Bojana Pavlovic<sup>2</sup>, Eugene Jennifer Jin<sup>1‡</sup>, F Ridvan Kiral<sup>1§</sup>, Shih-Ching Lin<sup>3</sup>, Filip Port<sup>2</sup>, Heike Wolfenberg<sup>1</sup>, Thomas F Mathejczyk<sup>1</sup>, Gerit A Linneweber<sup>1</sup>, Chih-Chiang Chan<sup>3</sup>, Michael Boutros<sup>2</sup>, P Robin Hiesinger<sup>1\*</sup>

<sup>1</sup>Division of Neurobiology, Institute for Biology, Freie Universität Berlin, Berlin, Germany; <sup>2</sup>German Cancer Research Center (DKFZ), Division of Signaling and Functional Genomics and Heidelberg University, Heidelberg, Germany; <sup>3</sup>National Taiwan University, Taipei, Taiwan

**Abstract** Rab GTPases are molecular switches that regulate membrane trafficking in all cells. Neurons have particular demands on membrane trafficking and express numerous Rab GTPases of unknown function. Here, we report the generation and characterization of molecularly defined null mutants for all 26 *rab* genes in *Drosophila*. In flies, all *rab* genes are expressed in the nervous system where at least half exhibit particularly high levels compared to other tissues. Surprisingly, loss of any of these 13 nervous system-enriched Rabs yielded viable and fertile flies without obvious morphological defects. However, all 13 mutants differentially affected development when challenged with different temperatures, or neuronal function when challenged with continuous stimulation. We identified a synaptic maintenance defect following continuous stimulation for six mutants, including an autophagy-independent role of *rab26*. The complete mutant collection generated in this study provides a basis for further comprehensive studies of Rab GTPases during development and function in vivo.

\*For correspondence: prh@zedat.fu-berlin.de

†These authors contributed equally to this work

Present address: <sup>‡</sup>University of California, San Diego, La Jolla, United States; <sup>§</sup> Yale University, New Haven, United States

Competing interest: See page 32

Funding: See page 32

Received: 02 June 2020

Accepted: 04 March 2021

Published: 05 March 2021

Reviewing editor: Mani Ramaswami, Trinity College Dublin, Ireland

© Copyright Kohrs et al. This article is distributed under the terms of the [Creative Commons Attribution License](https://creativecommons.org/licenses/by/4.0/), which permits unrestricted use and redistribution provided that the original author and source are credited.

## Introduction

Rab GTPases have been named for their initial discovery in brain tissue (*Ras*-like proteins from rat brain), where their abundance and diversity reflect neuronal adaptations and specialized membrane trafficking (Kiral et al., 2018; Touchot et al., 1987). Yet, Rabs are found in all eukaryotic cells, where they function as key regulators of membrane trafficking between various membrane compartments (Pfeffer, 2017; Zhen and Stenmark, 2015). Consequently, Rab GTPases are commonly used as markers, and some have become gold standard identifiers of various organelles and vesicles in endocytic and secretory systems (Pfeffer, 2017; Zerial and McBride, 2001).

Over the years, Rab GTPases have repeatedly been analyzed as a gene family to gain insight into membrane trafficking networks (Best and Leptin, 2020; Chan et al., 2011; Dunst et al., 2015; Gillingham et al., 2014; Gurkan et al., 2005; Harris and Littleton, 2011; Jin et al., 2012; Pfeffer, 1994; Stenmark, 2009; Zerial and McBride, 2001). Nonetheless, a complete and comparative null mutant analysis of all family members is currently not available for any multicellular organism. The *Drosophila* genome contains 31 potential *rab* or *rab*-related genes, of which 26 have been confirmed to encode protein-coding genes (Chan et al., 2011; Dunst et al., 2015; Jin et al., 2012), compared to 66 *rab* genes in humans (Gillingham et al., 2014) and 11 Rab-related *ypt* genes in

yeast (*Grosshans et al., 2006; Pfeffer, 2013*). Of the 26 *Drosophila rab* genes, 23 have direct orthologs in humans that are at least 50% identical at the protein level, indicating high evolutionary conservation (*Chan et al., 2011; Zhang et al., 2007*).

In the nervous system, Rab GTPases have been predominantly associated with functional maintenance and neurodegeneration (*Kiral et al., 2018; Veleri et al., 2018*). For example, mutations in *rab7* cause the neuropathy CMT2B (*Cherry et al., 2013; Spinosa et al., 2008; Verhoeven et al., 2003*), Rab10 and other Rabs are phosphorylation targets of the Parkinson's Disease-associated kinase LRRK2 (*Dhekne et al., 2018; Steger et al., 2017*), and Rab26 and Rab35 have been implicated in synaptic vesicle recycling (*Binotti et al., 2015; Sheehan et al., 2016; Uytterhoeven et al., 2011*). Neuronal longevity and morphological complexity have been suggested to require specific Rab-mediated membrane trafficking (*Jin et al., 2018a; Jin et al., 2018b*).

We have previously developed a transgenic *Drosophila rab*-Gal4 collection based on large genomic fragments and a design for subsequent homologous recombination to generate molecularly defined null mutants (*Chan et al., 2011; Jin et al., 2012*). Analyses of the cellular expression patterns and subcellular localization based on YFP-Rab expression under endogenous regulatory elements by us and others (*Dunst et al., 2015*) have revealed numerous neuronal Rabs with synaptic localization (*Chan et al., 2011*). We originally found that all 26 *Drosophila* Rab GTPases are expressed somewhere in the nervous system and half of all Rabs are enriched or strongly enriched in neurons (*Chan et al., 2011; Jin et al., 2012*). A more recent collection of endogenous knock-ins identified more varied expression patterns when more tissues were analyzed, but also validated the widespread neuronal and synaptic expression (*Dunst et al., 2015*). The function of most Rabs with high expression in the nervous system is still unknown.

Here, we provide the first comparative null mutant analysis of all *rab* genes in a multicellular organism. We find that viability, development, and neuronal function are highly dependent on environmental conditions in these mutants. Under laboratory conditions, with minimal selection pressure, seven mutants are lethal, one semi-lethal with few male escapers, two are infertile and six are unhealthy based on progeny counts. Remarkably, all 13 nervous system-enriched *rabs* are viable under laboratory conditions. However, all 13 exhibit distinct developmental or functional defects depending on environmental challenges. Our survey of the complete mutant fly collection provides a basis to systematically elucidate Rab-dependent membrane trafficking underlying development and function of all tissues in a multicellular organism.

## Results

### Generation of the *rab* GTPase null mutant collection

Our earlier observation of a synaptic localization of all nervous system-enriched Rabs led us to speculate that many Rab GTPases may serve roles related to neuron-specific development or function (*Chan et al., 2011*). To test this idea, we set out to generate a complete null mutant collection. We have previously published molecularly defined null mutants of *rab27* (*Chan et al., 2011*) and *rab7* (*Cherry et al., 2013*) as Gal4 knock-ins using a BAC recombineering/homologous recombination approach (*Chan et al., 2011*). Seven additional molecularly defined null mutants have previously been reported: *rab1* (*Thibault et al., 2004*), *rab3* (*Graf et al., 2009*), *rab5* (*Wucherpennig et al., 2003*), *rab6* (*Purcell and Artavanis-Tsakonas, 1999*), *rab8* (*Giagtoglou et al., 2012*), *rab11* (*Bellen et al., 2004*), and *rab32* (*Ma et al., 2004*). For the remaining 17 *rab* genes, we generated six null mutants as Gal4 knock-ins that replace the endogenous open-reading frames, or the ATG start codon, using homologous recombination; these include *rab2*, *rab4*, *rab19*, *rab30*, *rabX1*, and *rabX6* (*Figure 1A; Figure 1—figure supplement 1A–B*). The remaining 11 null mutants were generated using CRISPR/Cas9, including *rab9*, *rab10*, *rab14*, *rab18*, *rab21*, *rab23*, *rab26*, *rab35*, *rab39*, *rab40*, and *rabX4* (*Figure 1A; Figure 1—figure supplement 1C–D*). All mutants were molecularly validated as described in the Materials and methods section.

### All nervous system-enriched *rab* mutants are viable under laboratory conditions

All mutant chromosomes were tested for adult lethality in homozygosity. Of the 26 null mutants, seven are homozygous lethal (*rab 1, 2, 5, 6, 7, 8, 11*) and one, *rab35*, is homozygous semi-lethal with

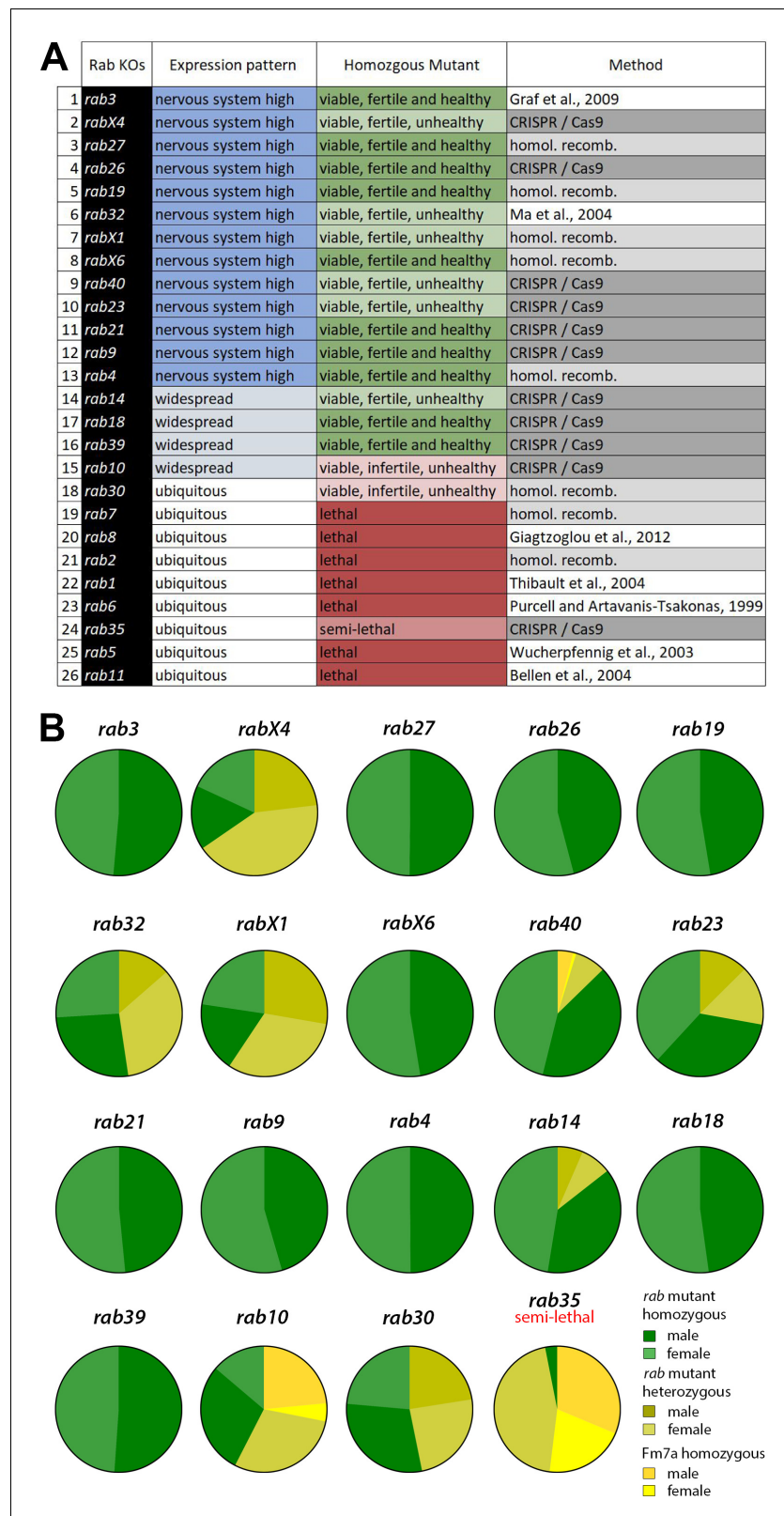


**Figure 1.** Generation and viability analysis of the *rab* null mutant collection. (A) List of all 26 *Drosophila rab* null mutants, sorted by expression pattern from 'nervous system-enriched' to ubiquitous based on [Chan et al., 2011](#); [Jin et al., 2012](#). Two-thirds of the *rab* mutants are homozygous viable and fertile. Eight *rab* mutants are lethal in homozygosity. The origin of the mutants is indicated in the third column. (B) Pie charts showing the ratios of

Figure 1 continued on next page

Figure 1 continued

homozygous versus balanced flies after ten generations. Ten of the 18 viable or semi-lethal *rab* mutants are fully homozygous, while the others still retain their balancer chromosome (shades of yellow) to varying degrees. At least 1000 flies per *rab* mutant were counted.

The online version of this article includes the following figure supplement(s) for figure 1:

**Figure supplement 1.** Design of newly generated *rab* mutants.

**Figure supplement 2.** Pupal expression patterns of nervous system-enriched Rabs based on endogenously tagged Rabs generated by [Dunst et al., 2015](#).

**Figure supplement 3.** Adult expression patterns of nervous system-enriched Rabs based on endogenously tagged Rabs generated by [Dunst et al., 2015](#).

---

few male escapers; 18 of the *rab* null mutants are viable as homozygous adults under laboratory conditions (**Figure 1A**).

All mutants were initially generated with the null mutant chromosome in heterozygosity over a balancer chromosome. Balancers contain multiple genetic aberrations, rendering them generally less healthy than wild type chromosomes; balancer chromosomes are therefore outcompeted in healthy stocks after a few generations. However, after 10 generations, only 10 of the 18 viable lines lost the balancer, indicating that eight *rab* mutant chromosomes confer a competitive disadvantage (**Figure 1B**). For five *rab* mutant chromosomes (*rab14*, *rab23*, *rab30*, *rab32*, and *rab40*) a minority of balanced flies remained in the viable stocks, suggesting that the mutant chromosomes in homozygosity are associated with only mildly reduced viability. By contrast, for *rab10*, *rabX1*, and *rabX4* we found balanced mutant flies in the majority, indicating substantially disadvantageous mutant chromosomes (**Figure 1B**). Sibling crosses between unbalanced homozygous mutant flies revealed an inability to lay eggs for *rab10* mutant flies. In addition, *rab30* mutant males are sterile and crosses of homozygous flies only yield non-developing eggs, a phenotype that was rescued by Rab30 overexpression with the *rab30-Gal4* line (see Materials and methods). In all other cases, homozygous mutant eggs developed, albeit in some cases at significantly lower numbers or at altered developmental speeds, as discussed in detail below. These observations suggest a range of mutant effects that may affect development or function, yet remain sub-threshold for lethality under laboratory conditions.

Remarkably, all lethal mutants are in *Drosophila rab* genes that are ubiquitously expressed, while all 13 Rab GTPases that we previously reported to be enriched in the nervous system are viable and fertile (**Figure 1A**). This surprisingly binary categorization once again puts a spotlight on the question of specialized Rab GTPase functions in the nervous system. The development and maintenance of the nervous system require robustness to variable and challenging conditions. Endogenous expression patterns based on available knock-ins ([Dunst et al., 2015](#)) revealed that all 13 nervous-system Rabs are expressed in different patterns in the developing brain (**Figure 1—figure supplement 2, Supplementary file 1A**) and in the adult brain (**Figure 1—figure supplement 3, Supplementary file 1B**). A comparison of Rab expression in flies with mammalian systems based on published data revealed a high degree of conservation across species, as detailed for each Rab in **Supplementary file 2**. In addition, a comprehensive comparison of functional analyses across species revealed both similarities but also species-specific features of individual Rabs with respect to viability and subcellular localization; this information is presented in detail for each Rab in **Supplementary file 3**. Based on our fly data and these comparisons across species, we hypothesized that many Rabs may provide context-specific neuronal roles that ensure robust development and function that are not apparent under laboratory rearing conditions. To test this hypothesis, we devised a series of assays to test all viable and fertile *Drosophila rab* null mutants for development, function, and maintenance under controlled challenging conditions.

### The majority of viable *rab* mutants affect developmental timing and robustness to different temperatures

First, we analyzed developmental robustness to temperatures at 18°C, 25°C, and 29°C (**Figure 2A–C**). We collected embryos after a 24 hours egg-laying period and measured hatching times of the first 1st instar larvae (**Figure 2D–F**), the first larvae transitioning to pupae (**Figure 2G–I**), and the first adults to eclose (**Figure 2J–L**) at all three temperatures. The 16 homozygous viable and fertile

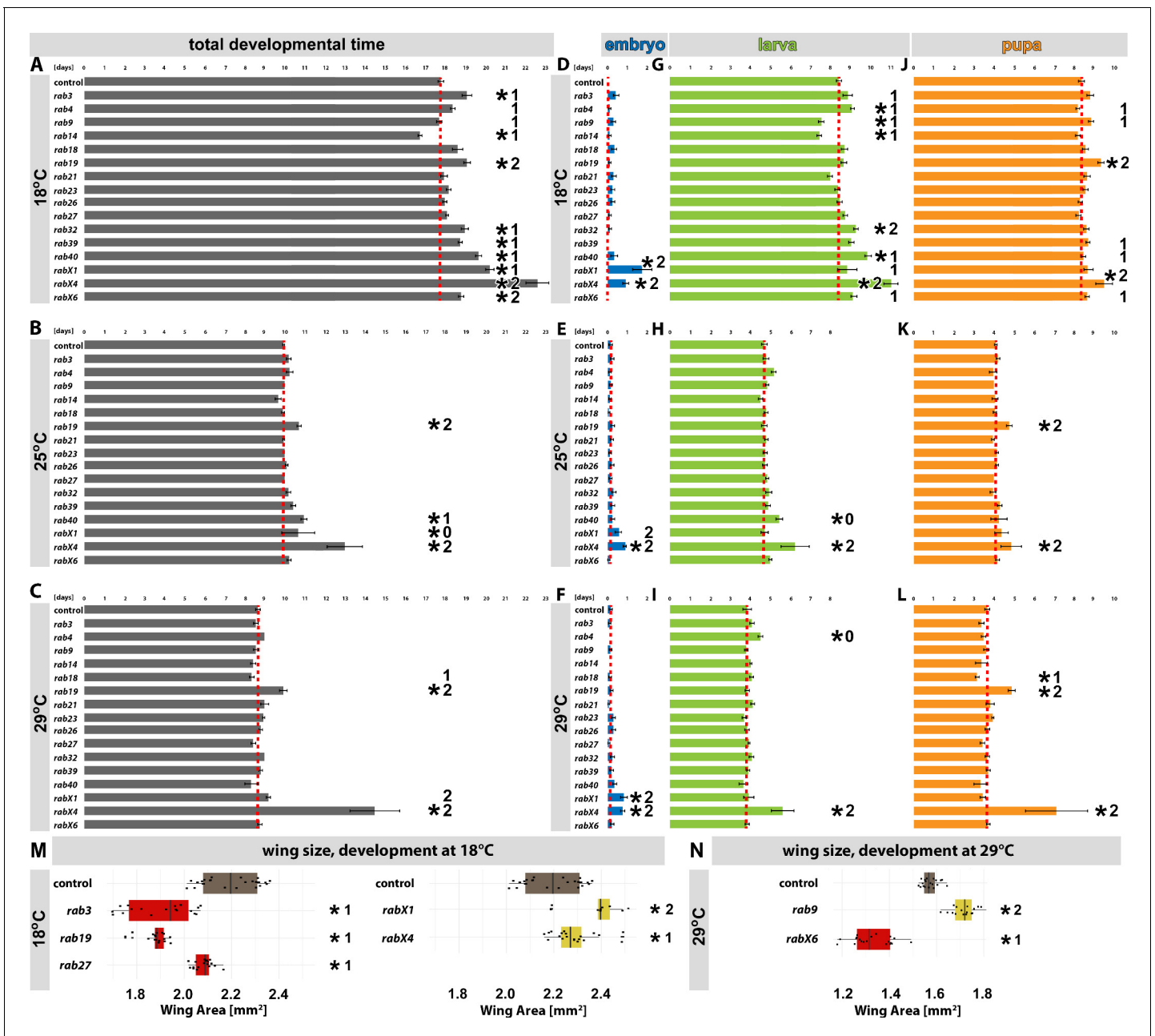


**Figure 2.** Developmental analyses of all viable *rab* mutants at different temperatures. (A–C) Developmental time from embryogenesis to adults at 18°C (A), 25°C (B), and 29°C (C) for all homozygous viable *rab* mutants. (D, G, and J) Developmental time at 18°C for all homozygous viable *rab* mutants, separated into embryonal (blue, D), larval (green, G) and pupal (orange, J) phases. (E, H, and K) Developmental time at 25°C for all homozygous viable *rab* mutants, separated into embryonal (blue, E), larval (green, H) and pupal (orange, K) phases. (F, I, and L) Developmental time at 29°C for all homozygous viable *rab* mutants, separated into embryonal (blue, F), larval (green, I) and pupal (orange, L) phases. (A–L) Dashed red line = mean of control. Mean  $\pm$  SEM; \* $p < 0.05$  (for the specific statistical values see **Figure 2—figure supplement 1**); 0, 1, or 2 indicate if the specific phenotype could not be validated (0), could be validated by either backcrossing or mutant over deficiency (1) or could be validated by both (2); Unpaired non-parametric Kolmogorov-Smirnov test. (M–N) Wing surface area measurement for validated homozygous viable *rab* mutants at 18°C (M) and 29°C (N). Wild type (brown) and *rab* mutant with significantly reduced (red) and increased wing sizes (yellow) compared to control. Boxplot with horizontal line representing the median; individual data points are represented as dots. Fifteen to 22 wings per genotype were quantified; \* $p < 0.05$  (for the specific statistical values see **Figure 2—figure supplement 2**); 0, 1, or 2 indicate if the specific phenotype could not be validated (0), could be validated by either backcrossing or mutant over deficiency (1) or could be validated by both (2); ordinary one-way ANOVA with pair-wise comparison. The online version of this article includes the following figure supplement(s) for figure 2:

**Figure supplement 1.** Validation of developmental timing phenotypes of viable *rab* mutants at different temperatures.

**Figure supplement 2.** Wing surface area measurement for all homozygous viable *rab* mutants at 18°C and 29°C.

Figure 2 continued on next page

Figure 2 continued

**Figure supplement 3.** Examples of wing defects after development at different temperatures.

mutants include all 13 nervous system-enriched *rabs* plus *rab14*, *rab18*, and *rab39*. To control for genetic background effects, we further tested all mutants with developmental phenotypes in two additional genetic backgrounds: first, the mutant chromosome in heterozygosity over a genomic deficiency uncovering the respective mutation; second, we backcrossed the mutants for three generations to control flies, thereby making the genetic background >80% identical to the control stock (see Materials and methods). We only considered phenotypes that were validated in at least one of the two additional genetic backgrounds; the number of validations are indicated as a number next to the asterisks marking significant differences in **Figure 2** as well as in detail in **Figure 2—figure supplement 1** and in **Supplementary file 4**.

Of the 16 homozygous viable and fertile mutants, 12 exhibited specific defects in developmental timing and an additional two mutants exhibited defects in wing development as described below. No developmental defects were observed only for *rab21* and *rab26*. The 12 mutants with developmental timing phenotypes exhibited the following phenotypes (in order of severity): *rabX4* exhibited the longest overall developmental delay, including delays of embryo, larval and pupal stages at all three developmental temperatures. *rabX4* mutant flies exhibited normal egg-laying behavior, but most eggs did not develop; only few *rabX4* adult escapers developed with 2–4 days developmental delay (**Figure 2A–L**; **Figure 2—figure supplement 1A–C**; **Supplementary file 4**). *rabX1* was the only mutant that exhibited selective delays of embryo development at all three temperatures, but normal timing of larval and pupal development (**Figure 2D–L**). *rabX1* mutant flies laid very few eggs, with only a subset of these developing to adulthood (20% of control; **Supplementary file 4**). *rab19* was the only mutant that exhibited selective delays of pupal development (but normal embryo and larval development) at all temperatures (**Figure 2D–L**). In addition, *rab19* exhibited a 50–80% rate of late pupal lethality specifically at 29°C, that was not observed at lower temperatures. All *rab19* adults raised at 29°C died within a few days. *rab32* exhibited increased late pupal lethality specifically at 29°C, while survivors exhibited normal eclosion timing. At 18°C, *rab32* mutants exhibited a mild overall developmental delay due to delayed larval development (**Figure 2A,G**). *rab40* exhibited a developmental delay at 18°C (**Figure 2A,G**) that was validated in both alternate genetic backgrounds (**Figure 2—figure supplement 1D,G**), a mild developmental delay at 25°C (**Figure 2B,H**) that was validated in a backcrossed background (**Figure 2—figure supplement 1E**), and no developmental delay at 29°C (**Figure 2C**). *rabX6* exhibited a mild developmental delay only at 18°C (**Figure 2A**) which could be validated in both alternate genetic backgrounds (**Figure 2—figure supplement 1D**). Similarly, *rab39* and *rab3* both exhibited a mild overall developmental delay at 18°C (**Figure 2A**) that were both validated in a backcrossed background (**Figure 2—figure supplement 1D**). *rab4* exhibited mildly delayed overall development at 18°C (**Figure 2A,G**) that was validated in a backcrossed background (**Figure 2—figure supplement 1D,G**). *rab9* and *rab14* were the only mutants with a shorter larval development at 18°C (**Figure 2G**) that was validated over deficiencies in both cases (**Figure 2—figure supplement 1G**). Finally, *rab18* was the only mutant that exhibited shortened pupal development specifically at 29°C (**Figure 2L**) that was validated in a backcrossed background (**Figure 2—figure supplement 1I**).

Taken together, these 12 mutants uncover developmental sensitivities of different developmental stages and with varying temperature-dependencies. Development at 18°C revealed increased variability of developmental timing in the majority of mutants that resulted from variability of larval development which in turn depends on larval behavior (**Figure 2A,G**). In contrast to larval development, pupae did not exhibit an increased variability of developmental timing. Developmental timing at higher temperatures was significantly less variable for all developmental stages. While some prominent developmental delays occurred at all temperatures (*rabX4* and *rabX1*), other mutants were selectively sensitive to development at higher temperatures (*rab18*, *rab19*, *rab32*) or lower temperatures (*rab4*, *rab40*).

Temperature is known to affect organ development through changes in cell size (Azevedo et al., 2002). For example, the *Drosophila* wing in control flies is 25–45% larger after development at 18°C compared to development at 29°C (**Figure 2M,N**). As with developmental timing, specific *rab*

mutants exhibited opposite developmental defects either only at lower or higher developmental temperatures. At 18°C we observed significantly smaller wings for *rab3*, *rab19*, and *rab27* and significantly larger wings for *rabX1* and *rabX4*, the two mutants with the longest developmental delay at 18°C (**Figure 2A,M**). At 29°C, we found significantly smaller wings in the *rabX6* mutant and significantly larger wings in the *rab9* mutant compared to controls at the same developmental temperature (**Figure 2N**). We only scored phenotypes that were validated in at least one additional genetic background (backcrossed or over deficiency, **Figure 2—figure supplement 2**). Finally, the *rab23* null mutant exhibited a planar cell polarity phenotype of wing bristles reported previously (**Dunst et al., 2015; Pataki et al., 2010**). In addition, we observed a previously not reported highly penetrant transversal p-cv vein shortening (in 90% of the wings studied) at 18°C, which was ameliorated at 29°C (12% penetrance) in the *rab23* mutant (**Figure 2—figure supplement 3**). In summary, 14 of the 16 viable and fertile null mutants exhibit specific developmental defects, most of which only occurred (or were significantly exacerbated) at high (29°C) or low (18°C) developmental temperatures.

### A subset of *rab* mutants affect the maintenance of stimulus-dependent synaptic function

To challenge neuronal function and maintenance, we tested the effect of continuous light stimulation on photoreceptor neurons, a widely used model to identify mutants affecting neuronal maintenance and degeneration in *Drosophila* (**Jaiswal et al., 2012**). Electroretinograms (ERGs) are extracellular recordings that reveal two aspects of photoreceptor function: first, the depolarization measures the ability of photoreceptor neurons to convert a light stimulus into an electrical signal; reduced depolarization can be the result of a reduced ability to perceive light (phototransduction), reduced electrical properties of individual cells, or loss of neurons. Second, the ERG 'on' transient indicates the ability to transmit the presynaptic signal to the postsynaptic interneurons. Loss of the 'on' transient can result from defective neurotransmission or degeneration that starts at the synapse, as shown for the *rab7* mutant previously (**Cherry et al., 2013**). The ERG is mostly used as a qualitative method, because both depolarization and 'on' transient intensities are highly sensitive to differences in genetic background, eye pigmentation, intensity of the light stimulus and other recording variables. To identify a sensitive period during which mild alterations of neuronal function and maintenance should be measurable, we established sensitization curves over several days of stimulation. In control flies, continuous stimulation leads to a gradual decline of the 'on' transient amplitude (**Figure 3A**) and depolarization (**Figure 3B**) over a 7-day period. Two days light stimulation represent a highly sensitized period with a dynamic range for improvement or worsening of potential defects for both the 'on' transient (**Figure 3A**) and depolarization (**Figure 3B**).

For all 16 viable and fertile *rabs* plus the two infertile mutants *rab10* and *rab30*, we tested mutants in a *white minus* background (white-eyed flies). First, we performed ERG recordings of newly hatched flies to assess neuronal function immediately after development ('0 day'; **Figure 3C–D**). None of the mutants exhibited significant reductions of their 'on' transient (**Figure 3C**) or depolarization (**Figure 3D**) immediately after hatching (0 day). Next, we used continuous light stimulation to measure changes in function after continuous stimulation (**Figure 3E–F**) and dark-rearing to assess aging in the absence of stimulation (**Figure 3G–H**). After 2 days of light stimulation, six *rab* mutants exhibited significantly reduced neurotransmission compared to control based on their 'on' transients: *rab3*, *rab14*, *rab19*, *rab26*, *rab30* and *rabX6*. For five of these six, the defect was specific to synaptic function without significant effects on depolarization (*rab3*, *rab19*, *rab26*, *rab30*, and *rabX6*, all with nervous system-enriched expression). By contrast, one mutant (*rab14*, with widespread expression) additionally exhibited a significantly decreased depolarization, indicating more generally reduced cellular function. Hence, neuron-enriched expression and synaptic localization of several Rab GTPases correlate with robustness of synaptic function under continuous stimulation.

To test whether these maintenance defects were strictly stimulus-dependent, we tested dark-reared flies. None of the five *rabs* with specific synaptic defects (*rab3*, *rab19*, *rab26*, *rab30* and *rabX6*) exhibited reduced neurotransmission in the absence of a light stimulus. By contrast, *rab14* and additionally *rab27*, exhibited both reduced transmission and depolarization after 4 days in the dark, suggesting stimulus-independent and aging-related defects. These findings indicate that the synaptic defects of *rab3*, *rab19*, *rab26*, *rab30*, and *rabX6* are stimulus-dependent, and the defects of *rab14* and *rab27* aging-dependent functional maintenance defects. A role for *rab27* in neuronal aging has recently been reported (**Lien et al., 2020**).

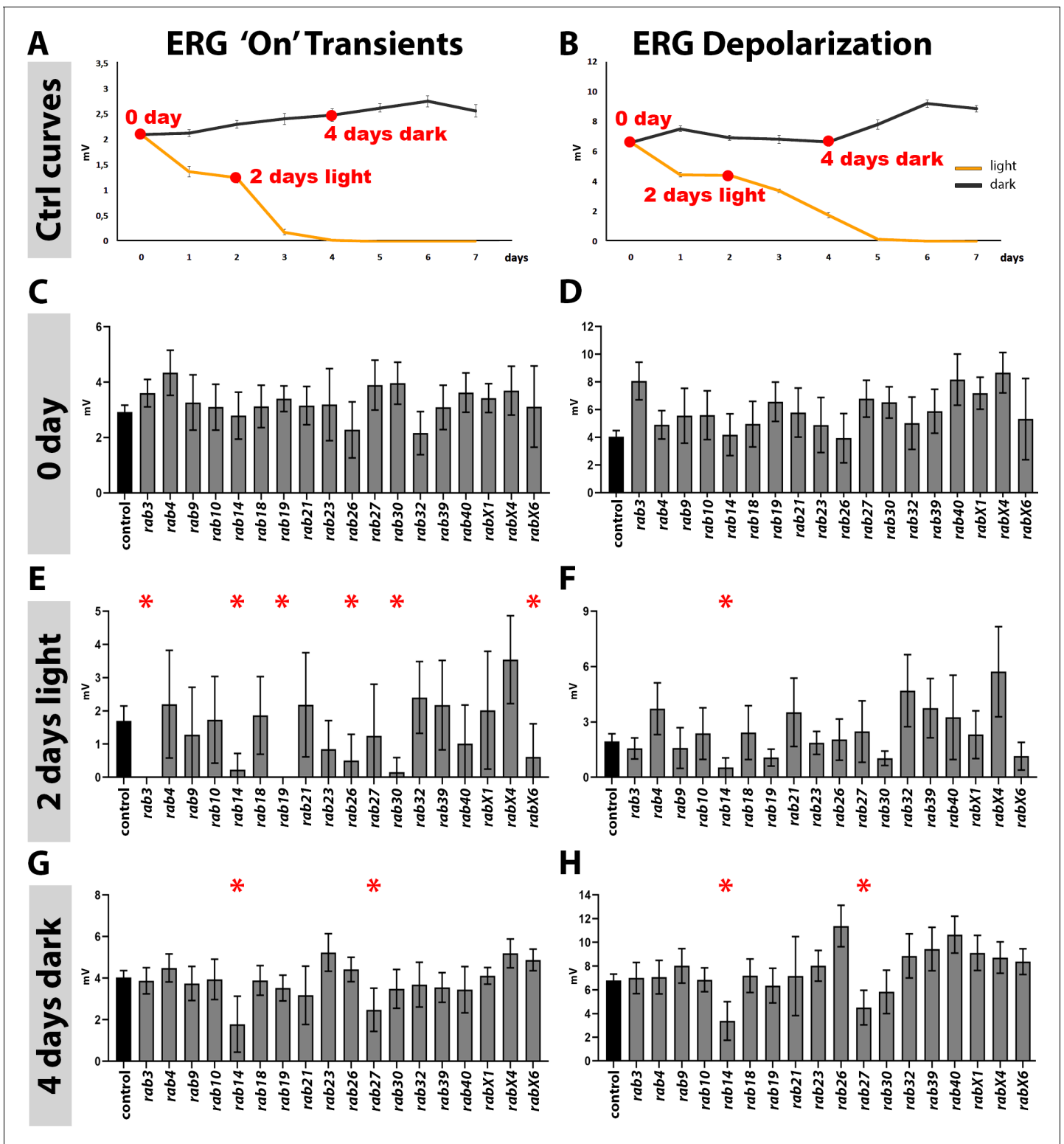


**Figure 3.** Analysis of neuronal function and maintenance based on electroretinograms. (A–B) Sensitization curves for light stimulated (orange curve) and dark-reared (black curve) wild type flies generated by electroretinogram (ERG) recordings. ‘on’ transient signal is lost after 4 days of light stimulation. Complete loss of depolarization signal after 5 days of light stimulation. 0 day, 2 days light stimulation and 4 days dark-rearing are highlighted in red. Mean ± SEM; 25–30 flies were recorded for each day (0–7 days) and each condition (light and dark); Ordinary one-way ANOVA with pair-wise comparison. (C–D) ‘on’ transient and depolarization of newly hatched (0 day) flies. Wild type control in black, all homozygous viable *rab* mutants in grey. (E–F) ‘on’ transient and depolarization of wild type (black) and homozygous viable *rab* mutants (grey) after 2 days of light stimulation. (G–H) ‘on’ transient and depolarization of wild type (black) and homozygous viable *rab* mutants (grey) after 4 days of dark-rearing. *rab* mutants with significant differences from control are marked with red asterisks (\*).

Figure 3 continued

transient and depolarization of wild type (black) and homozygous viable *rab* mutants (grey) after 4 days of dark-rearing. (C–H) Mean  $\pm$  SD; \* $p < 0.05$ ; 25–30 flies were recorded for each genotype and condition; ordinary one-way ANOVA with group-wise comparison.

### **A subset of *rab* mutants affect in a stimulus-dependent manner the maintenance of rhabdomeres, a high-turnover membrane compartment harboring the phototransduction machinery**

During the sensitive period after 2 days of light stimulation, both 'on' transients (Figure 3E) and depolarization (Figure 3F) exhibited higher variability amongst individuals than before stimulation (Figure 3C,D) or after 4 days in the dark (Figure 3G,H). This variability after 2 days of light stimulation could be a consequence either of functional differences amongst individuals or of progressive cell death, which is known to be induced by prolonged stimulation of photoreceptor neurons (Kiselev et al., 2000; Xiong and Bellen, 2013). We tested for programmed cell death using cleaved *Drosophila* death caspase-1 (DCP-1) as an apoptotic marker. None of the 18 viable *rab* mutants exhibited elevated levels of DCP-1 before or after 2 days of light stimulation (Figure 4A–B; Figure 4—figure supplement 1). As a positive control, we used DCP-1 to visualize retinal degeneration in the *rdgC<sup>306</sup>* mutant (Steele and O'Tousa, 1990; Figure 4C). Hence, increased phenotypic variability during this sensitized period likely reflects individual differences of functional and maintenance defects compared to control. Indeed, the co-labeling of rhabdomeres in these experiments revealed highly variable structural defects in *rab* mutant eyes after 2 days of light stimulation. The rhabdomeres are densely stacked membranes that are characterized by large-scale, light-dependent membrane trafficking of rhodopsin and other phototransduction proteins (Frechter and Minke, 2006; Schopf and Huber, 2017; Xiong and Bellen, 2013). We found no rhabdomere defects in any of the 16 viable plus viable but infertile *rab* mutants before stimulation, consistent with the absence of functional defects after development but prior to a functional challenge (Figure 4A,E; Figure 4—figure supplement 1). By contrast, after 2 days of light stimulation rhabdomere structures exhibited highly increased variability (Figure 4B,D,F). In control, rhabdomere area increased on average ~30% after 2 days of stimulation, while seven *rab* mutants exhibited a significant decrease in area greater than the control variability indicated by its standard deviation (*rab4*, *rab18*, *rab21*, *rab27*, *rab30*, *rab32*, *rab40*; Figure 4D). In addition, rhabdomere shapes exhibited similarly increased variability and significant changes in three additional *rab* mutants (*rab19*, *rab23*, and *rab26*; Figure 4E–F). We conclude that at least 10 of the 18 viable *rab* mutants affect membrane turnover in rhabdomeres when challenged with continuous stimulation.

### **Synaptic maintenance defects in viable *rab* mutants do not coincide with defective autophagy or Rab11-dependent endosomal recycling**

Next, we analyzed the morphology of photoreceptor axon projections after light stimulation compared to newly hatched flies using an antibody against the photoreceptor membrane protein Chaoptin. All 13 nervous system-enriched *rab* mutants exhibited axonal projections that were indistinguishable from control in newly hatched flies (Figure 5—figure supplement 1). We found no obvious developmental defects amongst newly hatched flies. All except one mutant looked indistinguishable from control; *rabX1* exhibited normal axonal projections, but unusual accumulations of Chaoptin in non-photoreceptor cell bodies surrounding the neuropils (arrowheads in Figure 5A), a phenotype previously observed for endomembrane degradation mutants including *rab7* (Cherry et al., 2013) and the v-ATPase *v100* (Williamson et al., 2010).

After 2 days of light stimulation, two mutants exhibited alterations of their axon terminal morphology. Mutants for *rab26*, and to a lesser extent *rab19*, exhibited distinct membrane accumulations at the distal tips of R1–R6 photoreceptor axon terminals (arrows in Figure 5A). Both *rab19* and *rab26* are amongst the five neuronal *rabs* exhibiting stimulus-dependent specific transmission maintenance defects. We next tested whether these membrane accumulations are associated with defects in autophagosome formation or clearance. In wild type flies, Atg8/LC3-positive autophagosomes were relatively infrequent given the number of axon terminals in the lamina both before and after light stimulation (Figure 5B). Notably, none of the five neuronal *rab* mutants with synaptic maintenance defects exhibited significantly altered Atg8 labeling. By contrast, in the *rabX1* mutant,

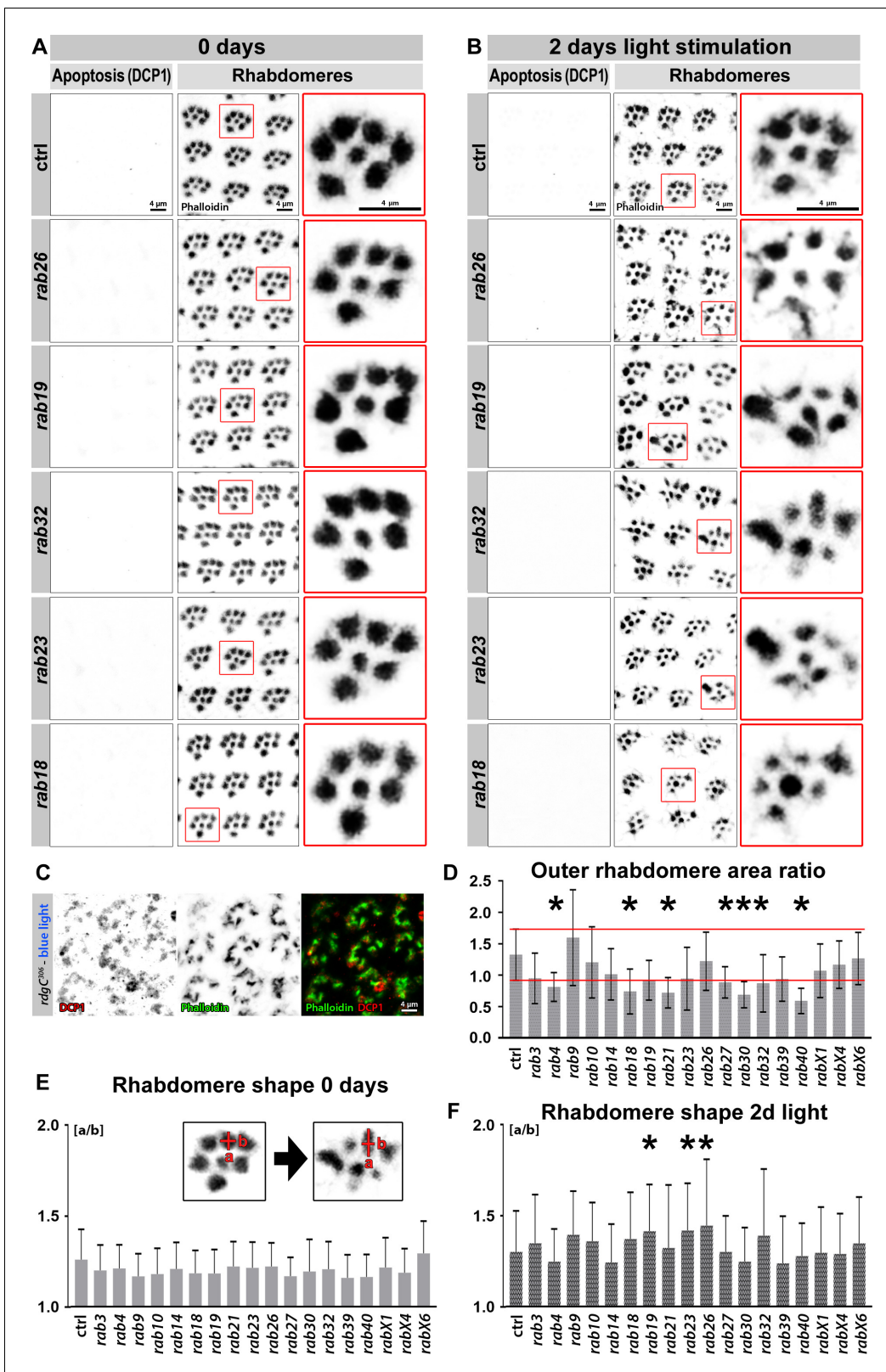


**Figure 4.** Viable *rab* mutants show no apoptosis based on DCP-1 immunolabeling but display morphological changes in rhabdomeres after continuous light stimulation. (A–B) Examples of *rab* mutant retinas which show rhabdomere changes and no increased levels in the apoptotic marker DCP-1 after 2 days of light stimulation compared to control (B) and newly hatched flies (A). Zoom-ins of single ommatidia are highlighted by red boxes. Scale bar = 4  $\mu$ m; number of retinas  $n = 5\text{--}7$  from different animals per antibody staining. (C) *rdgC<sup>306</sup>* mutant ommatidia show high levels of DCP-1 (red) after light stimulation. Figure 4 continued on next page

Figure 4 continued

continuous blue light stimulation. Labeling with phalloidin (green) reveals highly disrupted rhabdomere morphology. Scale bar = 4  $\mu\text{m}$ ; number of retinas  $n = 4$  per antibody staining. (D) Area ratio of outer rhabdomeres R1-R6. The standard deviation range of wild type control is highlighted by red lines. Outer rhabdomere area ratio was calculated as described in Materials and methods. Mean  $\pm$  SD; \* $p < 0.05$  (only significances outside SD range are marked); number of outer rhabdomeres counted  $n = 150$  from three to six animals. Ordinary one-way ANOVA with group-wise comparison. (E–F) After 2 days of light stimulation outer rhabdomere shape exhibited increased variability (F) compared to newly eclosed flies (E). Outer rhabdomere shape was calculated as described in Materials and methods and examples of single ommatidia (left: 0 day, right: 2 days of light stimulation) are shown in the zoom-ins (E). Mean  $\pm$  SD; \* $p < 0.05$ ; number of outer rhabdomeres counted  $n = 150$  from three to six animals. Ordinary one-way ANOVA with group-wise comparison.

The online version of this article includes the following figure supplement(s) for figure 4:

**Figure supplement 1.** No viable *rab* mutants show apoptosis based on DCP-1 immunolabeling, some display morphological changes in rhabdomeres after 2 days of continuous light stimulation.

Atg8 levels were increased in cell bodies distal of axon terminals already prior to stimulation (arrowheads in **Figure 5B**). Stimulus-dependent increased numbers of Atg8-positive compartments in axon terminals were observed for *rab23*, *rab27*, *rab32*, and as prominent clusters for *rabX1*, none of which exhibited stimulus-dependent synaptic maintenance defects (**Figure 5B**). These observations do not support a link between synaptic maintenance and autophagy based on viable, neuron-enriched Rabs.

We previously showed that most nervous system-enriched Rabs, including Rab19 and Rab26, encode proteins that colocalize with the recycling endosome marker Rab11 at photoreceptor axon terminals (**Chan et al., 2011**). Using the same 2 days light stimulation assay, we found that in wild type, Rab11 is strongly upregulated in the synaptic terminals after stimulation, indicating increased membrane trafficking. Surprisingly, we found the same stimulus-dependent increase of Rab11 as in control in all mutants except *rabX1*, consistent with a recent characterization of RabX1's endolysosomal function (**Laiouar et al., 2020; Woichansky et al., 2016, Figure 5C**). In summary, all Rabs implicated in synaptic functional maintenance exhibited Atg8 and Rab11 levels similar to control after light stimulation; our analyses therefore suggest that these Rabs employ mechanisms distinct from canonical Rab11-dependent endomembrane recycling and Atg8-dependent autophagy at synapses.

### Loss of *rab26* does not discernibly affect membrane trafficking associated with synaptic vesicles or autophagy in the adult brain

Rab26 has been proposed to link synaptic vesicle recycling to autophagy based on experiments in mammalian cell culture and *Drosophila* using overexpression of GTP-locked and GDP-locked variants (**Binotti et al., 2015**). Here, we provide an analysis of the *rab26* null mutant. In support of a role of autophagy in synaptic vesicle turnover, we found that *rab26* is one of the *rab* null mutants that exhibit reduced stimulus-dependent functional maintenance (**Figure 3E**), while being one of only two mutants without any developmental defect in our assays (**Figure 2**). In addition, *rab26* null mutant axon terminals exhibited pronounced membrane accumulations after continuous light stimulation (**Figure 5A**). However, we found no significant changes of the autophagosomal marker Atg8/LC3 (**Figure 5B**). These findings prompted us to probe putative roles of Rab26 at synaptic terminals in more detail.

Expression of GTP-locked Rab26 in adult photoreceptor neurons led to a complete loss of neurotransmission, while neither complete loss of *rab26* function nor expression of GDP-locked Rab26 significantly affected neurotransmission in newly hatched flies (**Figure 6A**). GTP-locked Rab26 protein formed enlarged accumulations as observed in the earlier study. Compartments and accumulations marked by YFP-tagged WT or GTP-locked Rab26 largely exclude synaptic markers (Syt1 and CSP; **Figure 6B–C**) as well as the autophagosome marker Atg8 (**Figure 6D–E**). By contrast, the recycling endosomal markers Rab11 (**Figure 6D–E**) and the endosomal markers Hrs and Syx7 (**Figure 6F–G**) all exhibit elevated levels in axon terminals expressing GTP-locked Rab26. These findings suggest an endosomal role at synaptic terminals that may not be directly linked to synaptic vesicles and autophagy.

Next, we compared the findings from GTP-locked Rab26 overexpression to the *rab26* null mutant. Adult brains mutant for *rab26* did not exhibit obvious changes of Atg8 or Syt1 (**Figure 6H–K**). The null mutant brains appeared morphologically normal and exhibited no difference for any of

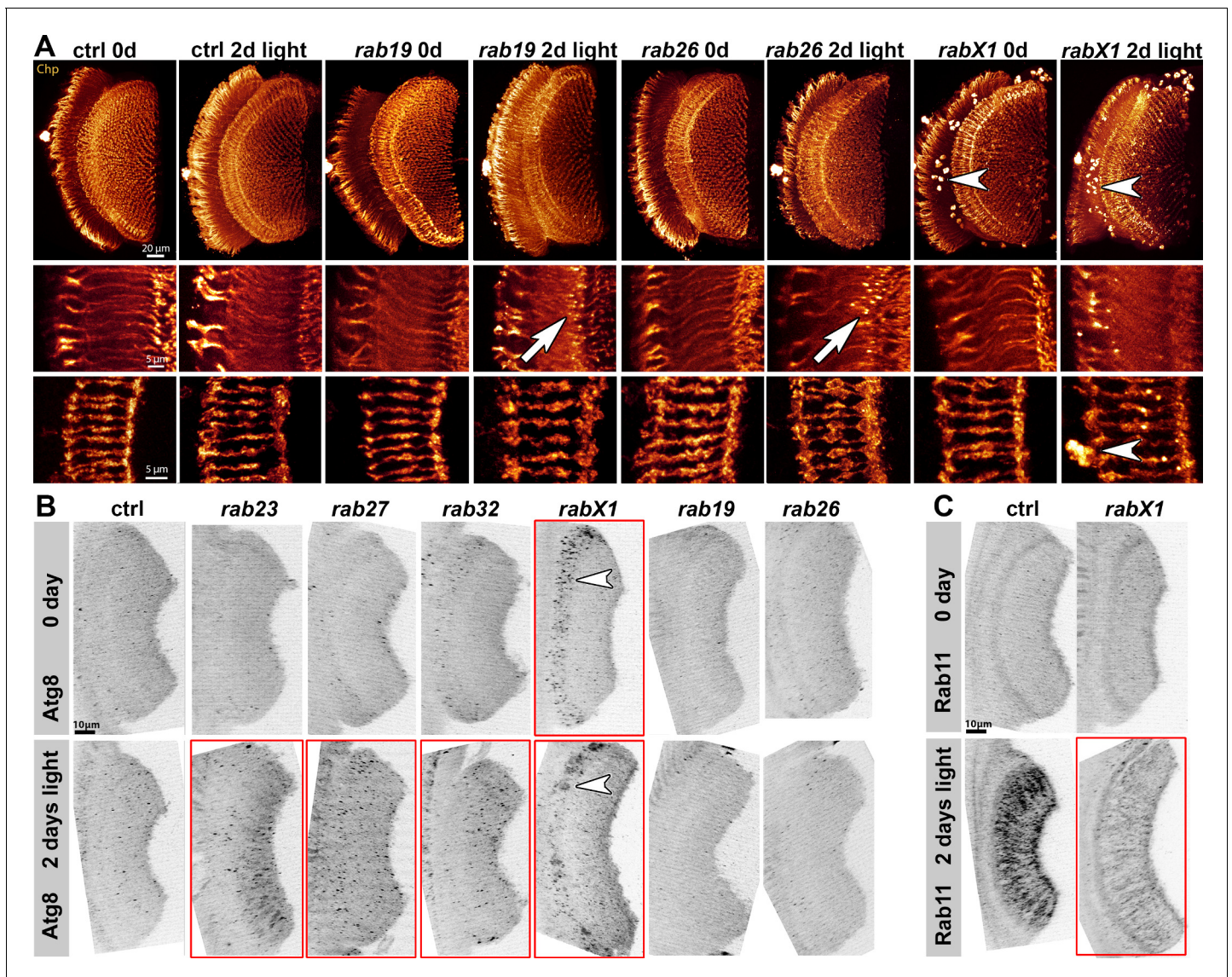


**Figure 5.** Analyses of morphology, recycling endosomal function (Rab11) and autophagy (Atg8) at photoreceptor axon terminals after continuous light stimulation. (A) Examples of Chaoptin-labeling (Chp) of 0 day and 2 days light stimulated wild type and *rab* mutant photoreceptor projections (overview top panel, R1-R6 middle panel, R7-R8 bottom panel). The *rabX1* mutant exhibits Chaoptin accumulations in non-photoreceptor cell bodies independent of stimulation (arrowheads). After 2 days of light stimulation, *rab26* and *rab19* mutants display membrane accumulations in their axon terminals (arrows). Scale bar = 20  $\mu\text{m}$  (top panel), 5  $\mu\text{m}$  (middle and bottom panel); number of brains  $n = 3\text{--}5$  per antibody staining. (B) Examples of Atg8 labeling of photoreceptor projections in retina-lamina preparations of newly hatched and 2 days light stimulated wild type flies and six *rab* mutants. Only *rab23*, *rab27*, and *rab32* show significant increases in Atg8-positive compartments after 2 days of light stimulation (highlighted by red boxes). *rabX1* flies exhibit Atg8-positive compartments in cell bodies (arrowheads). Scale bar = 10  $\mu\text{m}$ ; number of retina-lamina preparations  $n = 3$  for each condition and staining. (C) Examples of Rab11 labeling of photoreceptor projections in retina-lamina preparations of newly hatched and 2 days light stimulated wild type and *rabX1* flies. Increase in Rab11 levels is suppressed in *rabX1* mutants after 2 days of light stimulation (highlighted by red box). Scale bar = 10  $\mu\text{m}$ ; number of retina-lamina preparations  $n = 3$  for each condition and staining.

The online version of this article includes the following figure supplement(s) for figure 5:

**Figure supplement 1.** Systematic analysis of photoreceptor axon morphology of newly eclosed adults and after 2 days of continuous light stimulation.

the markers analyzed above. These findings do not support a strict requirement for any essential endomembrane trafficking process during development and initial function.

*Binotti et al., 2015* focused their *Drosophila* analyses on the larval neuromuscular junction (NMJ), we also investigated *rab26* loss-of-function in presynaptic boutons of these motoneurons and their postsynaptic muscle. We further generated a polyclonal antibody against the cytosolic N-terminus of

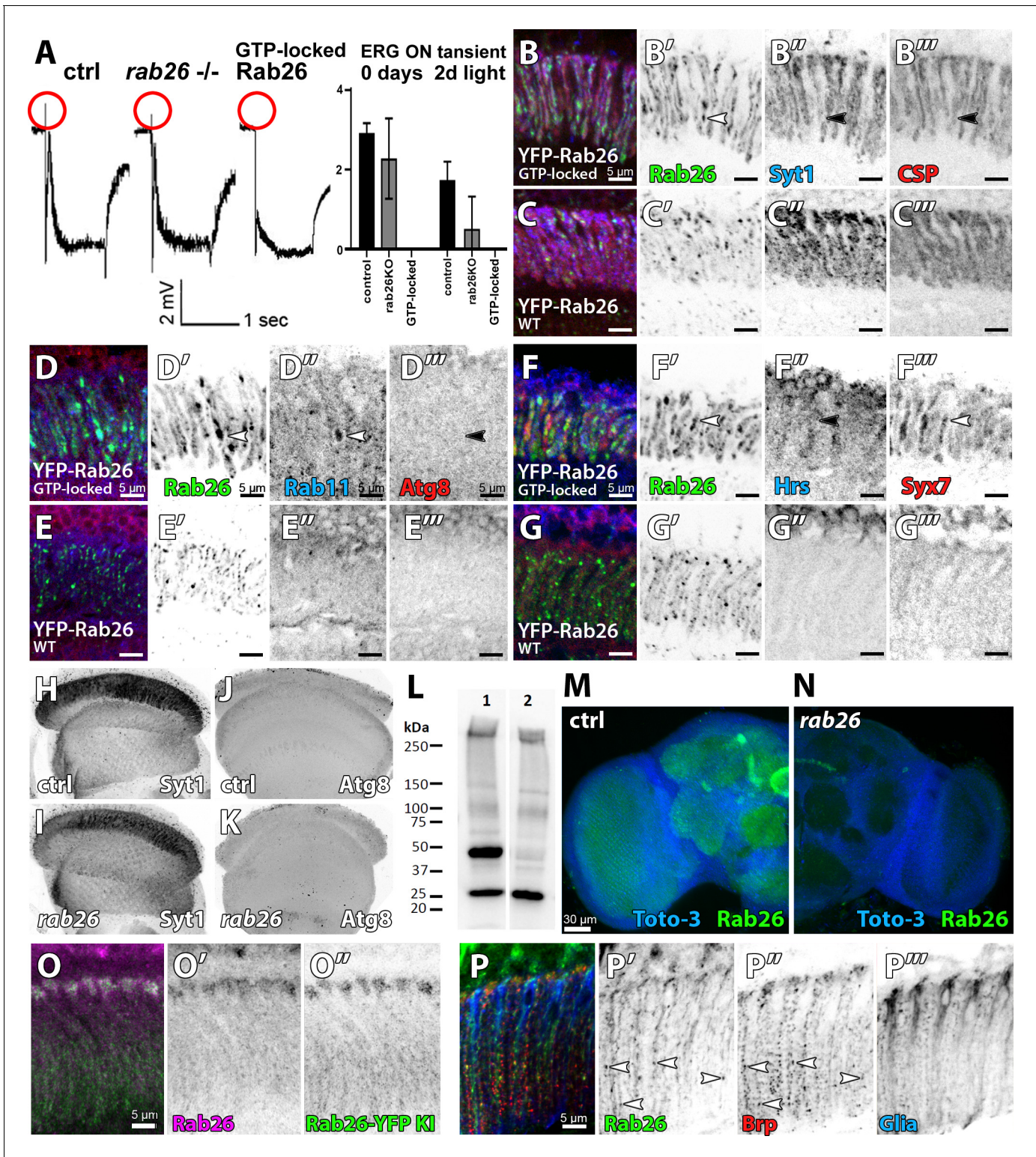


**Figure 6.** Loss of *rab26* does not discernibly affect markers for synaptic vesicles or autophagy in the adult brain. (A) Representative ERG traces of recordings of 2 days light stimulated wild type, *rab26* mutant, and Rab26 GTP-locked overexpression flies. Only the Rab26 GTP-locked flies show a complete loss of 'on' transient (highlighted in red). Quantification of the 'on' transient is shown right. (B–G) Labeling of lamina cross-sections of Rab26 GTP-locked (B, D, and F) and YFP-tagged Rab26WT (C, E, and G) against Syt1 and CSP (B and C), Rab11 and ATG8 (D and E), and Hrs and Syx7/ Avalanche (F and G). GTP-locked Rab26 shows colocalization with Rab11 and Syx7/Avalanche (white arrowheads), but not with Syt1, CSP, Atg8 nor Hrs (black arrowheads). Scale bar = 5 μm; number of brains n = 3–5 per antibody staining. (H–K) Intensity comparison of optic lobes of newly hatched wild type and *rab26* mutant flies. (L) Western blot analysis of Rab26 protein levels in control and *rab26* mutant flies. (M–N) Whole-brain immunofluorescence analysis of Rab26 localization in control (M) and *rab26* mutant (N) flies. (O–P) High-magnification immunofluorescence (O) and electron microscopy (P) analysis of Rab26 localization in control (O', P') and *rab26* mutant (O'', P'') flies. Scale bar = 5 μm; number of brains n = 3–5 per antibody staining.

Figure 6 continued

type and *rab26* mutant flies, stained against Syt1 (H and I) and Atg8 (J and K). Number of brains  $n = 3\text{--}5$  per antibody staining. (L) Validation of the *rab26* null mutant by Western Blot with the newly generated Rab26 antibody. Wild type control shows the Rab26 band at around 45 kDa (1), which is lost in the *rab26* mutant (2). (M and N) Validation of the *rab26* null mutant by immunohistochemistry with the newly generated Rab26 antibody. The Rab26 antibody labels synaptic neuropil in different regions of wild type brains (green, M), which is lost in the *rab26* null mutant (N). Labeling of nuclei/cell bodies with Toto-3 (blue). Scale bar = 30  $\mu\text{m}$ ; number of brains  $n = 3$  per antibody staining. (O) Immunolabeling of Rab26 (red) shows high colocalization with the endogenously YFP-tagged Rab26 (green). Lamina cross-section of newly hatched flies. Scale bar = 5  $\mu\text{m}$ ; number of brains  $n = 3\text{--}5$  per antibody staining. (P) Co-labeling of wild type lamina with Rab26 (green), Brp (synaptic marker, red), and ebony (glia marker, blue) reveals few synapses, positive for Rab26 and Brp in the proximal region of the lamina (white arrowheads, P' and P''). No colocalization between Rab26 and ebony could be observed (P'''). Scale bar = 5  $\mu\text{m}$ ; number of brains  $n = 3\text{--}5$  per antibody staining.

The online version of this article includes the following figure supplement(s) for figure 6:

**Figure supplement 1.** Rab26 colocalizes with synaptic vesicle and endosomal markers at larval neuromuscular junction (NMJ) boutons.

Rab26 (see Materials and methods). In western blots of whole-brain homogenate, the Rab26 antibody labeled a 45 kDa band, consistent with a predicted molecular weight between 41 kDa and 45 kDa, that is lost in the null mutant (Figure 6L). Additionally, immunolabeling of Rab26 in the adult brain (Figure 6M–N) and at the larval NMJ (Figure 6—figure supplement 1A) is not detectable in the null mutant. At the NMJ, Rab26 is present at presynaptic boutons, but not in the postsynaptic muscle (Figure 6—figure supplement 1A,B). Rab26 immunolabeling colocalizes partially with Rab11, the synaptic vesicle markers CSP and Syt1 and the endosomal marker Syx7. However, none of these markers were discernibly affected in the *rab26* null mutant (Figure 6—figure supplement 1B). Similarly, overexpressed YFP-tagged Rab26, GDP-locked Rab26 and GTP-locked Rab26 exhibited varying levels of colocalization with synaptic vesicle and endosomal markers, but no obvious disruption of their localization or levels (Figure 6—figure supplement 1C,E,F). Finally, we found no effect of the *rab26* null mutant or overexpression of the three YFP-tagged Rab26 variants on the autophagosomal marker Atg8 (Figure 6—figure supplement 1D). We hypothesize that, as in photoreceptor neurons, Rab26 is not required for the formation of functional synapses.

In the adult brain, Rab26 immunolabeling revealed synaptic neuropils at varying levels in different regions (Figure 6M) and colocalized well with an endogenously tagged Rab26 (Figure 6O). In the lamina, Rab26 immunolabeling revealed a punctate pattern across the photoreceptor axon terminals and a row of cells just distal of the lamina (Figure 6O,P). Co-labeling with the glia marker ebony did not mark these cells and revealed a largely complementary pattern to Rab26 in the lamina; the synaptic marker Brp revealed a small subset of colocalizing synapses selectively in the proximal regions of the axon terminals (arrowheads in Figure 6P), that is in the region where continuous stimulation led to protein accumulations (comp. Figure 5A). These observations raise the question whether Rab26 functions specifically in a certain type of neuron or synapse.

### Rab26 is required for stimulus-dependent membrane receptor turnover associated with cholinergic synapses

So far, our *rab26* null mutant analyses have revealed a stimulus-dependent role in functional maintenance (Figure 3E) associated with membrane protein accumulations at the proximal end of photoreceptor synaptic terminals (Figure 5A). These mutant accumulations of the photoreceptor membrane protein Chaoptin became more pronounced with further increased (4 days light) stimulation (Figure 7A–B). This phenotype was mimicked by photoreceptor-specific Rab26 RNAi (Figure 7—figure supplement 1A–E) and rescued by photoreceptor-specific expression of Rab26 in null mutant flies (Figure 7C–D). These findings indicate that the stimulus-dependent membrane accumulations are a cell-autonomous phenotype in photoreceptor neurons.

To characterize the nature of these presynaptic protein accumulations, we tested a panel of markers for membrane-associated proteins (Figure 7E–M). Amongst these markers, in addition to Chaoptin, the protein accumulations were specifically enriched for the synaptic transmembrane cell adhesion molecule N-Cadherin (CadN) (Figure 7E–G). By contrast, neither the autophagosomal marker Atg8, the synaptic vesicle marker Syt1 (Figure 7J–M), nor the endosomal markers Rab5 and Rab7 were associated with the accumulations (Figure 7E). Of the endosomal markers, only Syx7 was significantly increased (Figure 7E,H–I). We conclude that continuous stimulation leads to the

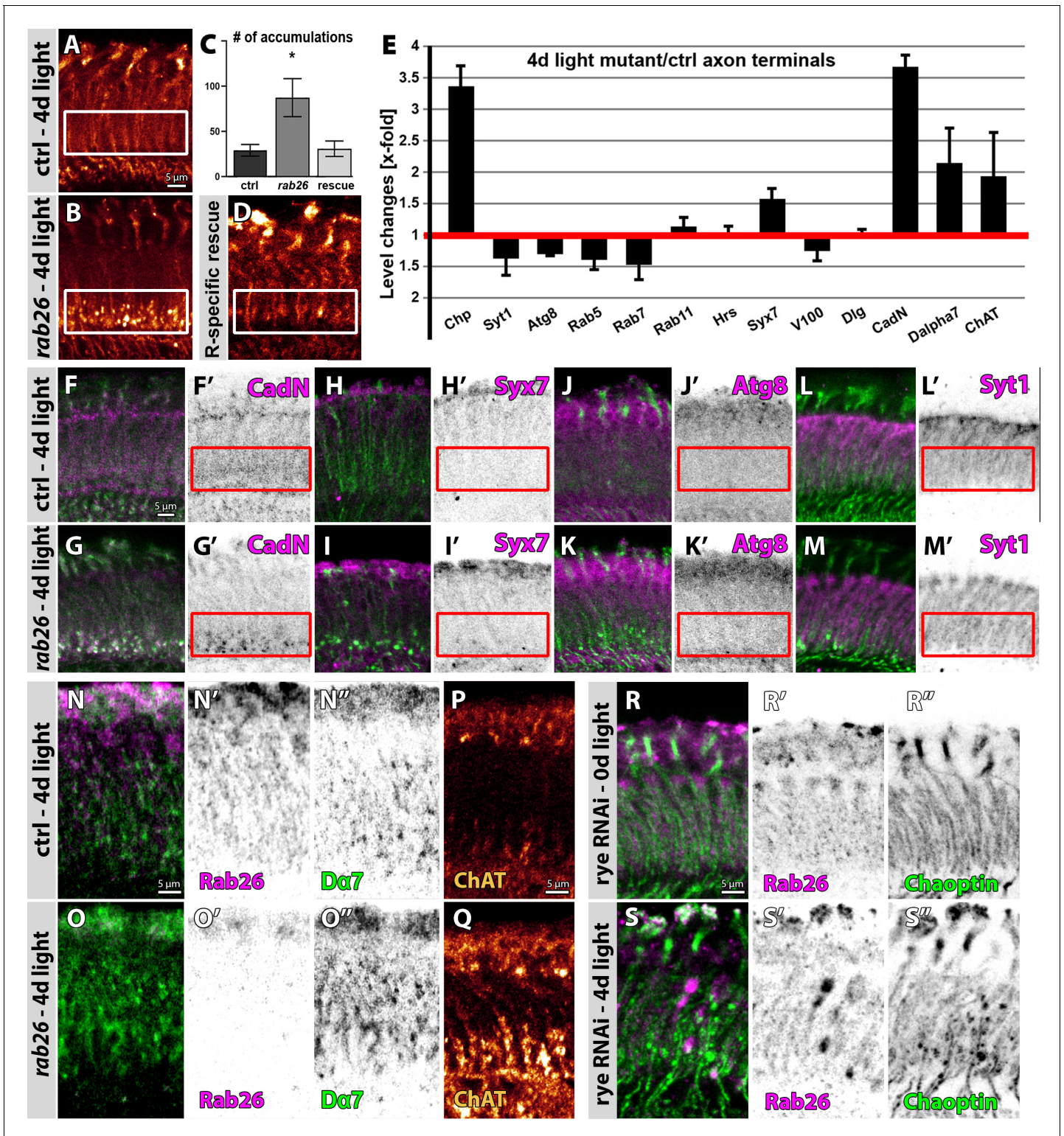


**Figure 7.** Rab26 is required for membrane receptor turnover associated with cholinergic synapses. (A–D) *rab26* mutant R1–R6 photoreceptor terminals (B) exhibit Chaoptin-positive accumulations in the proximal lamina after 4 days of light stimulation (highlighted with white boxes), which are rescued by photoreceptor-specific Rab26 expression (C and D). (C) Quantification. Mean  $\pm$  SEM; \* $p < 0.05$ ; number of lamina per genotype  $n = 8$ ; ordinary one-way ANOVA with pair-wise comparison. Scale bar = 5  $\mu$ m; number of brains  $n = 5$ . (E) Quantification of level changes of 13 membrane-associated proteins in the *rab26* mutant axon terminals after 4 days of light stimulation. (F–M) Examples of lamina cross-sections of wild type (F, H, J and L) and *rab26* mutant (G, I, K and M) after 4 days of light stimulation, showing proteins that are upregulated in R1–R6 terminals (CadN, (F–G); Syx7 (H–I) and proteins Figure 7 continued on next page

Figure 7 continued

that are unaffected (Atg8, (J–K); Syt1, (L–M)). The proximal lamina region is highlighted by red boxes. Scale bar = 5  $\mu$ m; number of brains  $n = 3$ –5 per antibody staining. (N–O) The *rab26* mutant exhibits an increase of D $\alpha$ 7 (green) across the lamina compared to wild type after 4 days of light stimulation. Shown are lamina cross-sections. Scale bar = 5  $\mu$ m; number of brains  $n = 3$ –5 per antibody staining. (P–Q) The *rab26* mutant shows an increase of ChAT in the proximal lamina compared to wild type after 4 days of light stimulation. Scale bar = 5  $\mu$ m; number of brains  $n = 3$ –5 per antibody staining. (R–S) Photoreceptor-specific knock down of rye leads to an increase of Chaoptin and Rab26 in the lamina after 4 days of light stimulation (S) compared to newly hatched flies (R). Rab26 accumulates throughout the lamina (S'), whereas Chaoptin accumulates in the proximal lamina (S''). Scale bar = 5  $\mu$ m; number of brains  $n = 3$ –5 per antibody staining.

The online version of this article includes the following figure supplement(s) for figure 7:

**Figure supplement 1.** Rab26 RNAi recapitulates the null mutant lamina phenotype.

selective accumulation of presynaptic transmembrane receptors, including Chaoptin and CadN, specifically in the most proximal part of photoreceptor terminals.

Amongst lamina neurons, only L4 specifically forms synapses at the most proximal end of photoreceptor axon terminals (Fischbach and Dittrich, 1989; Lüthy et al., 2014; Rivera-Alba et al., 2011; Tadros et al., 2016). L4 neurons function in the detection of progressive motion (Tuthill et al., 2013) and are cholinergic based on the expression of the vesicular acetylcholine transporter and choline acetyltransferase (ChAT) (Davis et al., 2020; Kolodziejczyk et al., 2008). Immunolabeling of presynaptic ChAT and the postsynaptic cholinergic receptor D $\alpha$ 7 (Fayyazuddin et al., 2006) revealed increased levels of both proteins after 4 days of light stimulation, with ChAT increases specific to the proximal lamina, while D $\alpha$ 7 appears across the entire lamina (Figure 7N–Q). Across the optic lobe, the endogenous Rab26 knock-in exhibits an expression pattern similar to ChAT (Figure 7—figure supplement 1F). However, photoreceptors that terminate in the lamina are not known to be cholinergic, and they neither express ChAT nor the D $\alpha$ 7 receptor based on a recent systematic transcriptome analysis (Davis et al., 2020).

Amongst lamina neurons, L4 and lamina wide-field feedback (Lawf) neurons have been shown to be both cholinergic and provide synaptic input to R1–R6 photoreceptor axon terminals (Davis et al., 2020; Rivera-Alba et al., 2011). Co-labeling of these neurons with Rab26 and ChAT (Figure 7—figure supplement 1G–I) revealed that the Rab26-positive cells distal of the lamina were Lawf2 neurons (Figure 7—figure supplement 1H–I), while the ChAT-positive labeling in the proximal lamina colocalized with L4 (Figure 7—figure supplement 1G); Rab26 labeling was complementary to the ChAT-positive L4 collaterals (Figure 7—figure supplement 1G).

In addition to receiving input from cholinergic L4 neurons (Rivera-Alba et al., 2011), photoreceptors are predicted to express a single acetylcholine receptor subunit, D $\alpha$ 4 (Davis et al., 2020). D $\alpha$ 4, also called redeye (rye), was previously found to promote sleep in Shi et al., 2014. We therefore used an RNAi approach established in the sleep study to knock down D $\alpha$ 4 specifically in photoreceptor neurons. D $\alpha$ 4 RNAi exhibited no obvious defects prior to stimulation (Figure 7R). By contrast, after 4 days of light stimulation, photoreceptor-specific D $\alpha$ 4 RNAi led to both Rab26-positive accumulations in the lamina as well as the proximal Chaoptin accumulations characteristic for the *rab26* mutant after stimulation (Figure 7—figure supplement 1). Hence, loss of *rab26* in photoreceptors has a stimulus-dependent effect similar to decreased cholinergic input onto photoreceptor axon terminals, that function as postsynaptic partners in this case. These findings suggest a specialized role of Rab26 in stimulus-dependent, synapse-specific receptor trafficking.

## Discussion

In this study, we generated a complete *rab* null mutant collection and provide comparative functional analyses of those that are viable under laboratory conditions. Surprisingly, all previously described nervous system-enriched Rab GTPases fall into this category. However, challenging development with temperature or challenging function with continuous stimulation revealed distinct requirements for all homozygous viable *rabs*. Our findings suggest that the majority of Rab GTPases modulate membrane trafficking in neurons and other tissues to maintain robust development and function under challenging environmental conditions.

## A functional *rab* family profile

Since the identification of Ypt1 (Rab1) in yeast, the Rab GTPase family has been well characterized as an evolutionarily conserved group of proteins involved in the regulation of membrane trafficking in all eukaryotes (*Hutagalung and Novick, 2011; Klöpper et al., 2012; Lipatova et al., 2015; Pfeffer, 2017*). Rab GTPases have been analyzed in several comparative studies in order to gain a systematic view of membrane trafficking in cells (*Best and Leptin, 2020; Chan et al., 2011; Dunst et al., 2015; Gillingham et al., 2014; Gurkan et al., 2005; Harris and Littleton, 2011; Jin et al., 2012; Pfeffer, 1994; Stenmark, 2009; Zerial and McBride, 2001*). All comparative studies to date have been based on expression profiling, the expression of GDP- and GTP-locked Rabs or RNAi. As a cautionary note, we have previously described differences between loss of gene function and the expression of GDP-locked (often called dominant negative) variants (*Chan et al., 2011; Cherry et al., 2013*). The complete mutant collection allows the comparison of molecularly defined null mutants with other functional perturbation approaches for all 26 *Drosophila rab* genes.

The *Drosophila rab* null mutant collection and comparative characterization of all viable *rabs* provides an opportunity for a comprehensive comparison of the Rab family between *Drosophila* and other species. We have therefore assembled available information on viability, function, subcellular localization and expression patterns for all Rabs in several mammalian species, flies and yeast. **Supplementary file 3** provides a comparison of functional and subcellular localization data for Rabs in different mammals, *D. melanogaster* and *S. cerevisiae*. Amongst a wealth of information in phenotypic homologies, these data also show that the majority of Rab family members yield viable organisms under laboratory conditions when mutated. **Supplementary file 2** provides a comparison of differential tissue expression in multicellular animal species. These data reveal numerous parallels especially with respect to enrichment in the nervous system. Rabs are listed according to lineage tracing and homology pairing, as comprehensively reported previously (*Hutagalung and Novick, 2011; Klöpper et al., 2012; Pereira-Leal and Seabra, 2000; Pereira-Leal and Seabra, 2001; Zhang et al., 2007*).

Our mutant analyses highlight that viability vs lethality is not a binary distinction of the null mutants, but represents a continuous range of context-dependent phenotypes (*Hiesinger, 2021*). Of the 26 null mutants, only seven are fully lethal under laboratory conditions in our study (*rab1, rab2, rab5, rab6, rab7, rab8, rab11*), while an eighth mutant is 'semi-lethal' based on few adult escapers (*rab35*). Two more lines are viable, but infertile as homozygous adults (*rab10, rab30*). Several others are highly sensitive to rearing conditions and may appear lethal depending on for example temperature, including *rabX1, rabX4, rab19*, and *rab32*. In addition, several mutants exhibit reduced numbers of offspring or developmental or neuronal functional impairments depending on environmental conditions. Similar sensitivities and reduced viability have been found for several mammalian *rabs* (**Supplementary file 3**).

Based on an analysis of endogenously tagged Rabs (*Dunst et al., 2015*), all 13 nervous system Rabs are expressed in varying patterns in the nervous system with predominant protein localization to synaptic neuropils (**Figure 1—figure supplements 2–3; Supplementary file 1**), consistent with our previous analyses of tagged Rabs in the larval nervous system (*Chan et al., 2011; Jin et al., 2012*). All mutants with stimulus-dependent functional maintenance defects exhibit strong adult synaptic localization (**Table 1**). These observations support the idea that the majority of Rabs with adult synaptic localization serve modulatory functions that become apparent under light challenging conditions, namely Rab3, Rab26, Rab19, RabX6, Rab30, and RabX4. By contrast, Rab27, Rab32, Rab23, and Rab9 are more likely to serve cell-specific functions, consistent with previous observations for each of the four in *Drosophila* (*Chan et al., 2011; Dong et al., 2013; Gillingham et al., 2014; Lien et al., 2020; Ma et al., 2004*).

## Neuronal maintenance, membrane trafficking, and the role of *rab26*

Our previous systematic analysis was based on expression profiling and suggested that the nervous system exhibits particularly pronounced expression of all Rab GTPases in *Drosophila* (*Chan et al., 2011; Jin et al., 2012*). We were surprised to find that all Rabs identified to be particularly enriched in the nervous system proved to be viable under laboratory conditions. However, laboratory conditions avoid environmental challenges while nervous system development and function have evolved robustness to variable conditions (*Hiesinger and Hassan, 2018*).

**Table 1.** Summary of functional analyses.

	Viability and development				Temp. sens.		Neuronal function								
	Viability	Total dev.	Embryo	Larva	Pupa	Lethal	Wing	Syn 2d	Depol 2d	Syn dark	Depol dark	Rhabd. 2d	Axon morph	Rab11	Atg8
Rab3		only 18°C		only 18°C			18°C								
RabX4	Reduced					18°C	18°C								
Rab27							18°C					Area			
Rab26												Shape			
Rab19						29°C						Shape			
Rab32	Reduced	only 18°C		only 18°C		29°C						Area			
RabX1	Reduced						18°C								
RabX6		only 18°C					29°C								
Rab40	Reduced			only 18°C								Area			
Rab23	Reduced											Shape			
Rab21												Area			
Rab9							29°C								
Rab4				only 18°C	only 18°C							Area			
Rab14	Reduced														
Rab39		only 18°C													
Rab18												Area			
Rab10	Infertile						18°C								
Rab30	Infertile											Area			
Rab7	Lethal														
Rab8	Lethal														
Rab2	Lethal														
Rab1	Lethal														
Rab6	Lethal														
Rab35	Semi-lethal														
Rab5	Lethal														
Rab11	Lethal														

Overview of analyses ('Viability and Development', 'Temperature sensitivity' and 'Neuronal Function') done in this study for the indicated Rab GTPases. Abbreviations: bc = backcrossed *rab* mutants, depol = depolarization, dev. = development, Df = deficiency, morph = morphology, Rhabdom = rhabdome, sens = sensitivity, syn = synaptic, temp = temperature, 2d = 2 days.

Color code: green denotes no difference to control; grey through yellow and orange denotes increasing deviation from controls in functional analyses.

It is likely that key roles of Rab-dependent functions are executed by the lethal mutants not analyzed here. For example, *rab7* is a ubiquitously expressed gene, but disease-associated mutations primarily affect the nervous system and cause the neuropathy CMT2B (Cherry et al., 2013; Verhoeven et al., 2003). In axon terminals, local *rab7*-dependent degradation is required for turnover of membrane receptors, but not synaptic vesicles (Jin et al., 2018b). While null mutants for *rab7* are lethal, haploinsufficiency revealed neuronal sensitivity to reduced membrane degradation (Cherry et al., 2013). Similar to heterozygous *rab7*, our analyses of viable lines suggest that such evolutionarily selected functional properties may 'hide' in mutants that are characterized as viable under laboratory conditions.

Neurons require compartment-specific membrane trafficking in both axon terminals and dendrites (Jin et al., 2018a; Jin et al., 2018b). At presynaptic axon terminals, Rabs have been implicated in synaptic vesicle recycling, synaptic development and maintenance (Binotti et al., 2015; Graf et al., 2009; Sheehan et al., 2016; Uytterhoeven et al., 2011). We previously found that several neuron-enriched Rabs at axon terminals were positive for the recycling endosome marker Rab11

(Chan et al., 2011), including Rab26. Rab26 was subsequently identified as a possible link between autophagy and synaptic vesicle recycling (Binotti et al., 2015). Here, we describe that *rab26* mutants indeed exhibited neuronal functional defects when challenged with continuous stimulation. However, we did not find obvious changes to autophagosomal and synaptic vesicle markers in the null mutant. Instead, the null mutant revealed stimulation-dependent increases of selected membrane proteins, including the presynaptic choline acetyltransferase (ChAT) and the postsynaptic alpha7 acetylcholine receptor. Correspondingly, the Rab26 protein is highly enriched in cholinergic neurons in the fly visual system. Interestingly, R1-R6 photoreceptors are not cholinergic, but are predicted to express the acetylcholine receptor alpha4 (Davis et al., 2020). Our findings support an unusual postsynaptic role of the R1-R6 axon terminals for cholinergic, Rab26-dependent signaling from L4 neurons through feedback synapses (Rivera-Alba et al., 2011). We speculate that these feedback synapses are activated by continuous visual stimulation and lead to Rab26-dependent receptor endocytosis defects in the photoreceptor terminals. Based on this idea, it will be interesting to test the role of Rab26 at other cholinergic synapses and test its requirement in an activity-dependent manner. We conclude that the study of *rab* mutants that are viable under laboratory conditions may help to elucidate an understanding of evolutionarily selected functional requirements of the nervous system under varying environmental conditions. The complete collection of null mutants provides a resource designed to facilitate such further studies.

## Materials and methods

### Key resources table

Reagent type (species) or resource	Designation	Source or reference	Identifiers	Additional information
Gene ( <i>D. melanogaster</i> )	Rab2		FlyBase ID:FBgn0014009	Sequence location: 2R:6,696,739.6,699,469 [+]
Gene ( <i>D. melanogaster</i> )	Rab4		FlyBase ID:FBgn0016701	Sequence location: 2R:17,573,462.17,574,979 [+]
Gene ( <i>D. melanogaster</i> )	Rab9		FlyBase ID:FBgn0032782	Sequence location: 2L:19,432,574.19,435,841 [+]
Gene ( <i>D. melanogaster</i> )	Rab10		FlyBase ID:FBgn0015789	Sequence location: X:20,251,338.20,254,691 [+]
Gene ( <i>D. melanogaster</i> )	Rab14		FlyBase ID:FBgn0015791	Sequence location: 2L:14,355,145.14,358,764 [+]
Gene ( <i>D. melanogaster</i> )	Rab18		FlyBase ID:FBgn0015794	Sequence location: X:5,670,827.5,671,812 [-]
Gene ( <i>D. melanogaster</i> )	Rab19		FlyBase ID:FBgn0015793	Sequence location: 3L:8,297,018.8,298,506 [+]
Gene ( <i>D. melanogaster</i> )	Rab21		FlyBase ID:FBgn0039966	Sequence location: X:23,012,140.23,013,409 [-]
Gene ( <i>D. melanogaster</i> )	Rab23		FlyBase ID:FBgn0037364	Sequence location: 3R:5,680,054.5,685,434 [-]
Gene ( <i>D. melanogaster</i> )	Rab26		FlyBase ID:FBgn0086913	Sequence location: 3L:21,318,774.21,335,027 [+]
Gene ( <i>D. melanogaster</i> )	Rab30		FlyBase ID:FBgn0031882	Sequence location: 2L:7,030,493.7,032,606 [-]
Gene ( <i>D. melanogaster</i> )	Rab35		FlyBase ID:FBgn0031090	Sequence location: X:20,155,766.20,159,872 [-]
Gene ( <i>D. melanogaster</i> )	Rab39		FlyBase ID:FBgn0029959	Sequence location: X:7,734,923.7,736,756 [+]
Gene ( <i>D. melanogaster</i> )	Rab40		FlyBase ID:FBgn0030391	Sequence location: X:12,459,796.12,463,112 [-]
Gene ( <i>D. melanogaster</i> )	RabX1		FlyBase ID:FBgn0015372	Sequence location: 2R:23,519,839.23,523,613 [-]

Continued on next page

Continued

Reagent type (species) or resource	Designation	Source or reference	Identifiers	Additional information
Gene ( <i>D. melanogaster</i> )	RabX4		FlyBase ID:FBgn0051118	Sequence location: 3R:24,826,665.24,828,409 [-]
Gene ( <i>D. melanogaster</i> )	RabX6		FlyBase ID: FBgn0035155	Sequence location: 3L:690,517.691,951 [+]
Strain, strain background ( <i>D. melanogaster</i> )	yw			yw;;
Strain, strain background ( <i>D. melanogaster</i> )	w <sup>1118</sup>			w <sup>1118</sup> ;;
Genetic reagent ( <i>D. melanogaster</i> )	<i>rab30</i> <sup>Gal4-KI</sup> , UAS-YFP-Rab30WT	Hiesinger lab stock		
Genetic reagent ( <i>D. melanogaster</i> )	<i>rab3</i> -Df	Bloomington <i>Drosophila</i> Stock Center (BDSC)	BDSC:8909	Deficiency line for <i>rab3</i>
Genetic reagent ( <i>D. melanogaster</i> )	<i>rab4</i> -Df	Bloomington <i>Drosophila</i> Stock Center	BDSC:38465	Deficiency line for <i>rab4</i>
Genetic reagent ( <i>D. melanogaster</i> )	<i>rab9</i> -Df	Bloomington <i>Drosophila</i> Stock Center	BDSC:7849	Deficiency line for <i>rab9</i>
Genetic reagent ( <i>D. melanogaster</i> )	<i>rab10</i> -Df	Bloomington <i>Drosophila</i> Stock Center	BDSC:29995	Deficiency line for <i>rab10</i>
Genetic reagent ( <i>D. melanogaster</i> )	<i>rab14</i> -Df	Bloomington <i>Drosophila</i> Stock Center	BDSC:7518	Deficiency line for <i>rab14</i>
Genetic reagent ( <i>D. melanogaster</i> )	<i>rab19</i> -Df	Bloomington <i>Drosophila</i> Stock Center	BDSC:7591	Deficiency line for <i>rab19</i>
Genetic reagent ( <i>D. melanogaster</i> )	<i>rab32</i> -Df	Bloomington <i>Drosophila</i> Stock Center	BDSC:23664	Deficiency line for <i>rab32</i>
Genetic reagent ( <i>D. melanogaster</i> )	<i>rab39</i> -Df	Bloomington <i>Drosophila</i> Stock Center	BDSC:26563	Deficiency line for <i>rab39</i>
Genetic reagent ( <i>D. melanogaster</i> )	<i>rab40</i> -Df	Bloomington <i>Drosophila</i> Stock Center	BDSC:26578	Deficiency line for <i>rab40</i>
Genetic reagent ( <i>D. melanogaster</i> )	<i>rabX1</i> -Df	Bloomington <i>Drosophila</i> Stock Center	BDSC:26513	Deficiency line for <i>rabX1</i>
Genetic reagent ( <i>D. melanogaster</i> )	<i>rabX4</i> -Df	Bloomington <i>Drosophila</i> Stock Center	BDSC:25024	Deficiency line for <i>rabX4</i>
Genetic reagent ( <i>D. melanogaster</i> )	<i>rabX6</i> -Df	Bloomington <i>Drosophila</i> Stock Center	BDSC:8048	Deficiency line for <i>rabX6</i>
Genetic reagent ( <i>D. melanogaster</i> )	EYFP-Rab3	<b>Dunst et al., 2015</b>	FlyBase ID:FBst0062541; BDSC:62541	FlyBase Genotype: w <sup>1118</sup> ; Tl{Tl}Rab3 <sup>EYFP</sup>
Genetic reagent ( <i>D. melanogaster</i> )	EYFP-Rab4	<b>Dunst et al., 2015</b>	FlyBase ID:FBst0062542; BDSC:62542	FlyBase Genotype: y <sup>1</sup> w <sup>1118</sup> ; Tl{Tl}Rab4 <sup>EYFP</sup>
Genetic reagent ( <i>D. melanogaster</i> )	EYFP-Rab9	<b>Dunst et al., 2015</b>	FlyBase ID:FBst0062547; BDSC:62547	FlyBase Genotype: w <sup>1118</sup> ; Tl{Tl}Rab9 <sup>EYFP</sup>
Genetic reagent ( <i>D. melanogaster</i> )	EYFP-Rab19	<b>Dunst et al., 2015</b>	FlyBase ID:FBst0062552; BDSC:62552	FlyBase Genotype: w <sup>1118</sup> ; Tl{Tl}Rab19 <sup>EYFP</sup>

Continued on next page

Continued

Reagent type (species) or resource	Designation	Source or reference	Identifiers	Additional information
Genetic reagent ( <i>D. melanogaster</i> )	EYFP-Rab21	<b>Dunst et al., 2015</b>	FlyBase ID:FBst0062553; BDSC:62553	FlyBase Genotype: $y^1 w^{1118} Tl\{Ti\}Rab21^{EYFP}$
Genetic reagent ( <i>D. melanogaster</i> )	EYFP-Rab23	<b>Dunst et al., 2015</b>	FlyBase ID:FBst0062554; BDSC:62554	FlyBase Genotype: $y^1 w^{1118}; Tl\{Ti\}Rab23^{EYFP}$
Genetic reagent ( <i>D. melanogaster</i> )	EYFP-Rab26	<b>Dunst et al., 2015</b>	FlyBase ID:FBst0062555; BDSC:62555	FlyBase Genotype: $y^1 w^{1118}; Tl\{Ti\}Rab26^{EYFP}$
Genetic reagent ( <i>D. melanogaster</i> )	EYFP-Rab27	<b>Dunst et al., 2015</b>	FlyBase ID:FBst0062556; BDSC:62556	FlyBase Genotype: $y^1 Tl\{Ti\}Rab27^{EYFP} w^{1118}$
Genetic reagent ( <i>D. melanogaster</i> )	EYFP-Rab32	<b>Dunst et al., 2015</b>	FlyBase ID:FBst0062558; BDSC:62558	FlyBase Genotype: $w^{1118}; Tl\{Ti\}Rab32^{EYFP}$
Genetic reagent ( <i>D. melanogaster</i> )	EYFP-Rab40	<b>Dunst et al., 2015</b>	FlyBase ID:FBst0062561; BDSC:62561	FlyBase Genotype: $y^1 w^{1118} Tl\{Ti\}Rab40^{EYFP}$
Genetic reagent ( <i>D. melanogaster</i> )	EYFP-RabX1	<b>Dunst et al., 2015</b>	FlyBase ID:FBst0062562; BDSC:62562	FlyBase Genotype: $w^{1118}; Tl\{Ti\}RabX1^{EYFP}$
Genetic reagent ( <i>D. melanogaster</i> )	EYFP-RabX4	<b>Dunst et al., 2015</b>	FlyBase ID:FBst0062563; BDSC:62563	Heterozygous flies used; FlyBase Genotype: $w^{1118}; Tl\{Ti\}RabX4^{EYFP}$
Genetic reagent ( <i>D. melanogaster</i> )	EYFP-RabX6	<b>Dunst et al., 2015</b>	FlyBase ID:FBst0062565; BDSC:62565	FlyBase Genotype: $w^{1118}; Tl\{Ti\}RabX6^{EYFP}$
Genetic reagent ( <i>D. melanogaster</i> )	<i>rab2</i>	This paper		Fly stock maintained in Hiesinger lab; see Materials and methods
Genetic reagent ( <i>D. melanogaster</i> )	<i>rab4</i>	This paper		Fly stock maintained in Hiesinger lab; see Materials and methods
Genetic reagent ( <i>D. melanogaster</i> )	<i>rab9</i>	This paper		Fly stock maintained in Hiesinger lab; see Materials and methods
Genetic reagent ( <i>D. melanogaster</i> )	<i>rab10</i>	This paper		Fly stock maintained in Hiesinger lab; see Materials and methods
Genetic reagent ( <i>D. melanogaster</i> )	<i>rab14</i>	This paper		Fly stock maintained in Hiesinger lab; see Materials and methods
Genetic reagent ( <i>D. melanogaster</i> )	<i>rab18</i>	This paper		Fly stock maintained in Hiesinger lab; see Materials and methods
Genetic reagent ( <i>D. melanogaster</i> )	<i>rab19</i>	This paper		Fly stock maintained in Hiesinger lab; see Materials and methods
Genetic reagent ( <i>D. melanogaster</i> )	<i>rab21</i>	This paper		Fly stock maintained in Hiesinger lab; see Materials and methods
Genetic reagent ( <i>D. melanogaster</i> )	<i>rab23</i>	This paper		Fly stock maintained in Hiesinger lab; see Materials and methods
Genetic reagent ( <i>D. melanogaster</i> )	<i>rab26</i>	This paper		Fly stock maintained in Hiesinger lab; see Materials and methods
Genetic reagent ( <i>D. melanogaster</i> )	<i>rab30</i>	This paper		Fly stock maintained in Hiesinger lab; see Materials and methods

Continued on next page

Continued

Reagent type (species) or resource	Designation	Source or reference	Identifiers	Additional information
Genetic reagent ( <i>D. melanogaster</i> )	<i>rab35</i>	This paper		Fly stock maintained in Hiesinger lab; see Materials and methods
Genetic reagent ( <i>D. melanogaster</i> )	<i>rab39</i>	This paper		Fly stock maintained in Hiesinger lab; see Materials and methods
Genetic reagent ( <i>D. melanogaster</i> )	<i>rab40</i>	This paper		Fly stock maintained in Hiesinger lab; see Materials and methods
Genetic reagent ( <i>D. melanogaster</i> )	<i>rabX1</i>	This paper		Fly stock maintained in Hiesinger lab; see Materials and methods
Genetic reagent ( <i>D. melanogaster</i> )	<i>rabX4</i>	This paper		Fly stock maintained in Hiesinger lab; see Materials and methods
genetic reagent ( <i>D. melanogaster</i> )	<i>rabX6</i>	This paper		Fly stock maintained in Hiesinger lab; see Materials and methods
Genetic reagent ( <i>D. melanogaster</i> )	<i>rab1</i>	<b>Thibault et al., 2004</b>	FlyBase ID:FBst0017936; BDSC:17936	FlyBase Genotype: w <sup>1118</sup> ; PBac{RB}Rab1 <sup>e01287</sup> /TM6B, Tb <sup>1</sup>
Genetic reagent ( <i>D. melanogaster</i> )	<i>rab3</i>	<b>Graf et al., 2009</b>	FlyBase ID:FBst0078045; BDSC:78045	FlyBase Genotype: w; Rab3 <sup>rup</sup>
Genetic reagent ( <i>D. melanogaster</i> )	<i>rab5</i>	<b>Wucherpennig et al., 2003</b>	FlyBase ID:FBal0182047	w; Rab5 <sup>2</sup> P{neoFRT}40A/CyO;
Genetic reagent ( <i>D. melanogaster</i> )	<i>rab6</i>	<b>Purcell and Artavanis-Tsakonas, 1999</b>	FlyBase ID: FBst0005821; BDSC:5821	FlyBase Genotype: w*; Rab6 <sup>D23D</sup> /CyO; ry <sup>506</sup>
Genetic reagent ( <i>D. melanogaster</i> )	<i>rab7</i>	<b>Cherry et al., 2013</b>	FlyBase ID:FBal0294205	Fly stock maintained in Hiesinger lab; ";Sp/CyO; P{neoFRT}82B, Rab7 <sup>Gal4-KO</sup> /TM3'
Genetic reagent ( <i>D. melanogaster</i> )	<i>rab8</i>	<b>Giagtzoglou et al., 2012</b>	FlyBase ID:FBst0026173; BDSC:26173	FlyBase Genotype: Rab8 <sup>1</sup> red <sup>1</sup> e <sup>4</sup> /TM6B, Sb <sup>1</sup> Tb <sup>1</sup> ca <sup>1</sup>
Genetic reagent ( <i>D. melanogaster</i> )	<i>rab11</i>	<b>Bellen et al., 2004</b>	FlyBase ID:FBst0042708; BDSC:42708	FlyBase Genotype: w; P{EP}Rab11 <sup>EP3017</sup> /TM6B, Tb <sup>1</sup>
Genetic reagent ( <i>D. melanogaster</i> )	<i>rab27</i>	<b>Chan et al., 2011</b>		Fly stock maintained in Hiesinger lab; rab27 <sup>Gal4-KO</sup> ;;
Genetic reagent ( <i>D. melanogaster</i> )	<i>rab32</i>	<b>Ma et al., 2004</b>	FlyBase ID:FBst0000338; BDSC:338	FlyBase Genotype: Rab32 <sup>1</sup>
Genetic reagent ( <i>D. melanogaster</i> )	IGMR-Gal4, UAS-white RNAi	Hiesinger lab stock		Fly stock maintained in Hiesinger lab; long version of GMR
Genetic reagent ( <i>D. melanogaster</i> )	UAS-YFP-Rab26WT	<b>Zhang et al., 2007</b>	BDSC:23245	YFP-tagged, wild type form of Rab26
Genetic reagent ( <i>D. melanogaster</i> )	UAS-YFP-Rab26CA	<b>Zhang et al., 2007</b>	BDSC:9809	YFP-tagged, constitutively active form of Rab26
Genetic reagent ( <i>D. melanogaster</i> )	UAS-YFP-Rab26DN	<b>Zhang et al., 2007</b>	BDSC:9807	YFP-tagged, dominant negative form of Rab26
Genetic reagent ( <i>D. melanogaster</i> )	elav-Gal4	Bloomington <i>Drosophila</i> Stock Center	FlyBase ID:FBst0008765; BDSC:8765	FlyBase Genotype: P{GAL4-elav.L}2/CyO
Genetic reagent ( <i>D. melanogaster</i> )	sGMR-Gal4	Bloomington <i>Drosophila</i> Stock Center	FlyBase ID:FBst0001104; BDSC:1104	FlyBase Genotype: w; P{GAL4-ninaE.GMR}12

Continued on next page

Continued

Reagent type (species) or resource	Designation	Source or reference	Identifiers	Additional information
Genetic reagent ( <i>D. melanogaster</i> )	UAS-Rab26 RNAi	Vienna <i>Drosophila</i> Resource Center (VDRC)	VDRC:101330	Rab26 RNAi line KK107584
Genetic reagent ( <i>D. melanogaster</i> )	<i>rab26<sup>exon1</sup></i> -Gal4	<b>Chan et al., 2011</b>		Fly stock is maintained in Hiesinger lab
Genetic reagent ( <i>D. melanogaster</i> )	UAS-CD4-tdGFP	Bloomington <i>Drosophila</i> Stock Center	FlyBase ID:FBst0035839; BDSC:35839	FlyBase Genotype: <i>y</i> <sup>1</sup> <i>w</i> <sup>+</sup> ; P{UAS-CD4-tdGFP}8 M2
Genetic reagent ( <i>D. melanogaster</i> )	31C06-Gal4 (L4-Gal4)	Bloomington <i>Drosophila</i> Stock Center	FlyBase ID:FBst0049883; BDSC:49883	FlyBase Genotype: <i>w</i> <sup>1118</sup> ; P{GMR31C06-GAL4}attP2
Genetic reagent ( <i>D. melanogaster</i> )	Lawf1-Split-Gal	<b>Tuthill et al., 2013</b>		R11G01AD attP40; R17C11DBD attP2; 'SS00772'
Genetic reagent ( <i>D. melanogaster</i> )	Lawf2-Split-Gal	<b>Tuthill et al., 2013</b>		R11D03AD attP40; R19C10DBD attP2; 'SS00698'
Genetic reagent ( <i>D. melanogaster</i> )	UAS-rye RNAi; UAS-Dicer2	Gift from Amita Sehgal		D $\alpha$ 4 receptor subunit RNAi line
Genetic reagent ( <i>D. melanogaster</i> )	<i>rdgC<sup>306</sup></i>	Bloomington <i>Drosophila</i> Stock Center	FlyBase ID:FBst0003601; BDSC:3601	FlyBase Genotype: <i>w</i> <sup>1118</sup> ; <i>rdgC<sup>306</sup></i> <i>kar</i> <sup>1</sup> <i>ry</i> <sup>1</sup> /TM3, <i>Sb</i> <sup>1</sup> <i>Ser</i> <sup>1</sup>
Antibody	Anti-Rab5 (Rabbit polyclonal)	Abcam (Cambridge, UK)	Cat #: ab31261; RRID: <a href="#">AB_882240</a>	IHC (1:1000)
Antibody	Anti-Rab7 (Rabbit polyclonal)	Gift from Patrick Dolph		IHC (1:1000)
Antibody	Anti-Rab11 (Mouse monoclonal)	BD Biosciences (San Jose, CA, USA)	clone47; RRID: <a href="#">AB_397983</a>	IHC (1:500)
Antibody	Anti-Rab26 (Guinea pig polyclonal)	This paper		See Materials and methods; IHC (1:2000); WB (1:1000)
Antibody	Anti-Syt1 (Mouse monoclonal)	Developmental Studies Hybridoma Bank (DSHB) (Iowa City, IA, USA)	3H2 2D7; RRID: <a href="#">AB_528483</a>	IHC (1:500)
Antibody	Anti-GABARAP+ GABARAPL1+ GABARAPL2 (Atg8) (Rabbit monoclonal)	Abcam (Cambridge, UK)	Cat #: ab109364; RRID: <a href="#">AB_10861928</a>	IHC (1:100)
Antibody	Anti-Syx7/Avalanche (Rabbit polyclonal)	Gift from Helmut Kramer		IHC (1:1000)
Antibody	Anti-Hrs (Guinea pig polyclonal)	Gift from Hugo Bellen		IHC (1:300)
Antibody	Anti-HRP (Rabbit polyclonal)	Jackson Immuno Research Laboratories (West Grove, PA, USA)	RRID: <a href="#">AB_2314648</a>	IHC (1:500)
Antibody	Anti-DPAK (Rabbit polyclonal)			IHC (1:2000)
Antibody	Anti-D $\alpha$ 7 (Rat polyclonal)	Gift from Hugo Bellen		IHC (1:2000)
Antibody	Anti-nCadherin (Rat monoclonal)	Developmental Studies Hybridoma Bank (DSHB) (Iowa City, IA, USA)	DN-Ex #8; RRID: <a href="#">AB_528121</a>	IHC (1:100)
Antibody	Anti-V100 (Guinea pig polyclonal)	<b>Hiesinger et al., 2005</b>		IHC (1:1000)

Continued on next page

Continued

Reagent type (species) or resource	Designation	Source or reference	Identifiers	Additional information
Antibody	Anti-CSP (Mouse monoclonal)	Developmental Studies Hybridoma Bank (DSHB) (Iowa City, IA, USA)	DCSP-2 (6D6); RRID:AB_528183	IHC (1:50)
Antibody	Anti-ChAT (Mouse monoclonal)	Developmental Studies Hybridoma Bank (DSHB) (Iowa City, IA, USA)	ChAT4B1; RRID:AB_528122	IHC (1:100)
Antibody	Anti-nc82 (Mouse monoclonal)	Developmental Studies Hybridoma Bank (DSHB) (Iowa City, IA, USA)	RRID: AB_2314866	IHC (1:20)
Antibody	Anti-ebony (Rabbit polyclonal)			IHC (1:200)
Antibody	Anti-Chaoptin (Mouse monoclonal)	Developmental Studies Hybridoma Bank (DSHB) (Iowa City, IA, USA)	24B10; RRID: AB_528161	IHC (1:50)
Antibody	Anti-DCP-1 (Rabbit polyclonal)	Cell Signaling Technology (Danvers, MA, USA)	Asp216; Cat#: 9578; RRID:AB_2721060	IHC (1:100)
Antibody	DyLight 405 AffiniPure Donkey Anti-Mouse IgG (H+L)	Jackson Immuno Research (West Grove, PA, USA)	715-475-150; RRID:AB_2340839	IHC (1:500)
Antibody	Alexa Fluor 488 AffiniPure Goat Anti-Mouse IgG (H+L)	Jackson Immuno Research (West Grove, PA, USA)	115-545-003; RRID: AB_2338840	IHC (1:500)
Antibody	Alexa Fluor 488 AffiniPure Goat Anti-Mouse IgG (H+L)	Jackson Immuno Research (West Grove, PA, USA)	115-545-166; RRID: AB_2338852	Minimal cross-reactive; IHC (1:500)
Antibody	Alexa Fluor 488 AffiniPure Goat Anti-Rat IgG (H+L)	Jackson Immuno Research (West Grove, PA, USA)	112-545-167; RRID: AB_2338362	Minimal cross-reactive; IHC (1:500)
Antibody	Alexa Fluor 488 AffiniPure Goat Anti-Guinea Pig IgG (H+L)	Jackson Immuno Research (West Grove, PA, USA)	106-545-003; RRID: AB_2337438	IHC (1:500)
Antibody	Cy3 AffiniPure Goat Anti-Rabbit IgG (H+L)	Jackson Immuno Research (West Grove, PA, USA)	111-165-003; RRID: AB_2338000	IHC (1:500)
Antibody	Alexa Fluor 647 AffiniPure Goat Anti-Rabbit IgG (H+L)	Jackson Immuno Research (West Grove, PA, USA)	111-605-045; RRID: AB_2338075	IHC (1:500)
Antibody	Alexa Fluor 647 AffiniPure Goat Anti-Rat IgG (H+L)	Jackson Immuno Research (West Grove, PA, USA)	112-605-003; RRID: AB_2338393	IHC (1:500)
Antibody	Goat Anti-Guinea pig IgG H&L (Cy5)	Abcam (Cambridge, UK)	Cat. #: ab102372; RRID: AB_10710629	IHC (1:500)
Antibody	Cy5 AffiniPure Goat Anti-Mouse IgG (H+L)	Jackson Immuno Research (West Grove, PA, USA)	115-175-166; RRID: AB_2338714	Minimal cross-reactive; IHC (1:500)
Antibody	Cy5 AffiniPure Goat Anti-Rat IgG (H+L)	Jackson Immuno Research (West Grove, PA, USA)	112-175-167; RRID: AB_2338264	Minimal cross-reactive; IHC (1:500)

Continued on next page

Continued

Reagent type (species) or resource	Designation	Source or reference	Identifiers	Additional information
Antibody	Peroxidase AffiniPure Goat Anti-Guinea Pig IgG (H+L)	Jackson Immuno Research (West Grove, PA, USA)	106-035-003; RRID: <a href="https://doi.org/10.1093/ab/2337402">AB_2337402</a>	WB (1:5000)
Sequence-based reagent	<i>rab2</i>	This paper	PCR primers	Fwd: 5'-TGGCCCACTGTGCG TAGCC; Rev: 5'-CGCCTCCTCTACG TTGGCAG
Sequence-based reagent	<i>rab3</i>	This paper	PCR primers	Fwd: 5'-ACACTGAGGCGAGC TTACGC; Rev: 5'-CTACTACCGAGGAGC-GATGGG
Sequence-based reagent	<i>rab4</i>	This paper	PCR primers	Fwd: 5'-GGTTTTGATCGTGTCC TGCG; Rev: 5'-AGACAACTCTTACCGC TGCC
Sequence-based reagent	<i>rab9</i>	This paper	PCR primers	Fwd: 5'-GGCACTATGACGAACA TGCGG; Rev: 5'-ttgcagcactggaaatccg
Sequence-based reagent	<i>rab10</i>	This paper	PCR primers	Fwd: 5'-atatcttctgtcacctgccc; Rev: 5'-cgaccaccatccatcgtcgg
Sequence-based reagent	<i>rab14</i>	This paper	PCR primers	Fwd: 5'-gggGCCAG TTCGAGAAAGGG; Rev: 5'-CACGAGCACTGATCC TTGGC
Sequence-based reagent	<i>rab18</i>	This paper	PCR primers	Fwd: 5'-AAACAAAGCAGCAAGGTGGC; Rev: 5'-CTCCTCGTCGATCTTG TTGCC
Sequence-based reagent	<i>rab19</i>	This paper	PCR primers	Fwd: 5'-CCAG TTAACGGCCAGAACGG; Rev: 5'-TTGCCTCTCTGAGCA TTGCC
Sequence-based reagent	<i>rab21</i>	This paper	PCR primers	Fwd: 5'-CAATGGGAACGGC TAAATGCC; Rev: 5'-caacatttaTCGCC-GAGTGCC
Sequence-based reagent	<i>rab23</i>	This paper	PCR primers	Fwd: 5'-CACCTGCCGGCTTAGA TGCG; Rev: 5'-GAGATA TCGGAACCGGCCCG
Sequence-based reagent	<i>rab26</i>	This paper	PCR primers	Fwd: 5'-CGATGAAGTGGACA TGCAACC; Rev: 5'-tgcacttgaacttactgccc
Sequence-based reagent	<i>rab30</i>	This paper	PCR primers	Fwd: 5'-ACCCAGCGAC TCAAAAACCC; Rev: 5'-GCTGCACAGTTCCAGA TCCG
Sequence-based reagent	<i>rab32</i>	This paper	PCR primers	Fwd: 5'-GTAGACACGGGTCATG TTGCC; Rev: 5'-accagcaaatctcagtgcgg
Sequence-based reagent	<i>rab35</i>	This paper	PCR primers	Fwd: 5'-CGAATCG TAAGCCAAGAACCC; Rev: 5'-ACTAATGGTGACGCAC TGCC
Sequence-based reagent	<i>rab39</i>	This paper	PCR primers	Fwd: 5'-TAACAACCACCAGCGACAGCC ; Rev: 5'-CGTATACCTCGTG TGA CTGGC

Continued on next page

Continued

Reagent type (species) or resource	Designation	Source or reference	Identifiers	Additional information
Sequence-based reagent	<i>rab40</i>	This paper	PCR primers	Fwd: 5'- caatgagtaaaccctagcgg; Rev: 5'-TGGGTATGGGTATGGTA TGGG
Sequence-based reagent	<i>rabX1</i>	This paper	PCR primers	Fwd: 5'- GTGCCCAAGAAA TCAGACGC; Rev: 5'-AGTCAGATGGGCTTA- GAGCG
Sequence-based reagent	<i>rabX4</i>	This paper	PCR primers	Fwd: 5'- CTGTAACCGAAAACC TCCGC; Rev: 5'-CAACTTGCTCAGGTTC TGCG
Sequence-based reagent	<i>rabX6</i>	This paper	PCR primers	Fwd: 5'- GTCGCACTGTTGTTG TCGCC; Rev: 5'-CTCTGCGTGAGCA TTGAGCC
Sequence-based reagent	Reverse primer in Gal4-region	This paper	PCR primers	5'-CGGTGAGTGACGA TAGGGC
Sequence-based reagent	Second reverse primer in Gal4-region	This paper	PCR primers	5'-CAATGGCACAGG TGAAGCC
Sequence-based reagent	Reverse primer in RFP-region	This paper	PCR primers	5'- GCTGCACAGGCTTCTTTGCC
Sequence-based reagent	Second reverse primer in RFP-region	This paper	PCR primers	5'- ACAATCGCATGC TTGACGGC
Sequence-based reagent	Forward primer in RFP-region	This paper	PCR primers	5'- GGCTCTGAAGC TGAAAGACGG
Sequence-based reagent	Forward primer in dsRed-region	This paper	PCR primers	5'- ATGGTTACAAATAAGCAA TAGCATC
Sequence-based reagent	Reverse primer behind right-arm of inserted dsRed-cassette	This paper	PCR primers	5'-AAACCACAGCCCATAGACG
Commercial assay or kit	SapphireAmp Fast PCR Master Mix	Takara Bio Group	Cat. #: RR350A	
Commercial assay or kit	Phusion High-Fidelity PCR kit	Thermo Fisher Scientific Inc (Waltham, MA, USA)	Cat. #: F553S	
Commercial assay or kit	NucleoSpin Gel and PCR Clean-up	Macherey-Nagel (Düren, Germany)	Cat. #: 740609.50	Mini kit for gel extraction and PCR clean-up
Software, algorithm	ImageJ	National Institutes of Health (NIH)	<a href="https://imagej.nih.gov/ij/">https://imagej.nih.gov/ij/</a>	
Software, algorithm	Imaris	Bitplane (Zurich, Switzerland)	<a href="https://imaris.oxinst.com/packages">https://imaris.oxinst.com/packages</a>	
Software, algorithm	Amira	Thermo Fisher Scientific Inc (Waltham, MA, USA)	<a href="https://www.thermofisher.com/de/de/home/industrial/electron-microscopy/electron-microscopy-instruments-workflow-solutions/3d-visualization-analysis-software.html">https://www.thermofisher.com/de/de/home/industrial/electron-microscopy/electron-microscopy-instruments-workflow-solutions/3d-visualization-analysis-software.html</a>	
Software, algorithm	Adobe Photoshop	Adobe Inc (San Jose, CA, USA)	<a href="https://www.adobe.com/products/photoshop.html">https://www.adobe.com/products/photoshop.html</a>	
Software, algorithm	Adobe Illustrator	Adobe Inc (San Jose, CA, USA)	<a href="https://www.adobe.com/products/illustrator.html">https://www.adobe.com/products/illustrator.html</a>	
Software, algorithm	RStudio	RStudio Inc (Boston, MA, USA)	<a href="https://rstudio.com/products/rstudio/">https://rstudio.com/products/rstudio/</a>	
Software, algorithm	GraphPad Prism	GraphPad Software Inc (San Diego, CA, USA)	<a href="https://www.graphpad.com/scientific-software/prism/">https://www.graphpad.com/scientific-software/prism/</a>	
Software, algorithm	AxoScope	Molecular Devices LLC. (San Jose, CA, USA)	<a href="https://www.moleculardevices.com/">https://www.moleculardevices.com/</a>	

Continued on next page

Continued

Reagent type (species) or resource	Designation	Source or reference	Identifiers	Additional information
Software, algorithm	SnapGene	GSL Biotech LLC (Chicago, IL, USA)	<a href="https://www.snapgene.com/">https://www.snapgene.com/</a>	
Other	Toto-3 stain	Thermo Fisher Scientific Inc (Waltham, MA, USA)	Cat. #: T3604	TOTO-3 Iodide (642/660); IHC (1:1000)
Other	Phalloidin stain	Abcam (Cambridge, UK)	Cat. #: ab176752	Phalloidin-iFluor 405; IHC (1:250)
Other	SDS-polyacrylamide Gel	Bio-Rad Laboratories, Inc (Hercules, CA, USA)	Cat. #: 4561083	4–15% Mini-PROTEAN TGX Precast Gels
Other	PVDF membrane	Bio-Rad Laboratories, Inc (Hercules, CA, USA)	Cat. #: 162–0177	
Other	Clarity Western ECL Substrate	Bio-Rad Laboratories, Inc (Hercules, CA, USA)	Cat. #: 170–5060	
Other	Insect needles	Entomoravia (Slavkov u Brna, Czech Republic)	<a href="https://entomoravia.eu/">https://entomoravia.eu/</a>	Austerlitz insect needles; ø 0.1 mm

## Fly husbandry and genetics

Flies were raised on molasses formulation food. Stocks were kept at room temperature (22–23°C) in non-crowded conditions, which we defined as ‘normal laboratory conditions’. Flies were mostly raised at 25°C or 18°C and 29°C (developmental timing assay).

For the rescue of *rab30* infertility we used: *rab30<sup>Gal4-KI</sup>*, UAS-YFP-Rab30WT.

For the developmental assays, the following deficiency lines were used: *rab3-Df* (Bloomington stock #8909), *rab4-Df* (Bloomington stock #38465), *rab9-Df* (Bloomington stock #7849), *rab10-Df* (Bloomington stock #29995), *rab14-Df* (Bloomington stock #7518), *rab19-Df* (Bloomington stock #7591), *rab32-Df* (Bloomington stock #23664), *rab39-Df* (Bloomington stock #26563), *rab40-Df* (Bloomington stock #26578), *rabX1-Df* (Bloomington stock #26513), *rabX4-Df* (Bloomington stock #25024), and *rabX6-Df* (Bloomington stock #8048). *yw* was used as wild type control.

For the analysis of the expression pattern of endogenously tagged Rab GTPases in pupae and 1 day-old adults, the following homozygous *Drosophila* lines were used: EYFP-Rab3, EYFP-Rab4, EYFP-Rab9, EYFP-Rab19, EYFP-Rab21, EYFP-Rab23, EYFP-Rab26, EYFP-Rab27, EYFP-Rab32, EYFP-Rab40, EYFP-RabX1, EYFP-RabX4 (EYFP-RabX4/TM6B for adult brain analysis), and EYFP-RabX6 (Dunst et al., 2015).

For the analysis of the identity of the Choptin-positive accumulations in *rab26* lamina after 4 days of light stimulation, following *Drosophila* lines were used: *rab26* and *yw* as wild type control. For the rescue of the Choptin-accumulation phenotype, following *Drosophila* lines were used: ;UAS-YFP-Rab26WT/+; *rab26*, IGMR-Gal4, UAS-white RNAi/*rab26* as well as ;;IGMR-Gal4, UAS-white RNAi and ;;*rab26*, IGMR-Gal4, UAS-white RNAi/*rab26* as negative and positive control, respectively. To test the efficiency of the Rab26 RNAi line KK107584 (VDRC stock ID: 101330) the following fly lines were used: UAS-Rab26 RNAi/+; *elav-Gal4/+* and UAS-YFP-Rab26WT/UAS-Rab26 RNAi; IGMR-Gal4, UAS-white RNAi/+. To reproduce the *rab26* mutant phenotype, the following *Drosophila* line was used: UAS-Rab26 RNAi/+; IGMR-Gal4, UAS-white RNAi. For the analysis of possible colocalization between Rab26-positive compartments and synaptic vesicle markers as well as endomembrane trafficking markers, following *Drosophila* lines were used: ;*elav-Gal4/UAS-YFP-Rab26WT*; ;*elav-Gal4/UAS-YFP-Rab26CA*; ;*elav-Gal4/UAS-YFP-Rab26DN*; ;*sGMR-Gal4/UAS-YFP-Rab26WT*; and ;*sGMR-Gal4/UAS-YFP-Rab26CA*; . For the comparison of the anti-Rab26 antibody labeling with the YFP-knock in line, the following *Drosophila* line was used: ;UAS-YFP-Rab26WT/+; *rab26<sup>exon1</sup>-Gal4/+*. For the Rab26 lamina localization analysis, the 31C06-Gal4 (L4-Gal4) as well as Split-Gal4 Lawf1 (SS00772) and Lawf2 (SS00698) lines were crossed to ;UAS-CD4-tdGFP;. For the photoreceptor-specific knock down of Dα4 receptor subunit the following fly line was used: ;UAS-rye RNAi; UAS-Dicer2/IGMR-Gal4,UAS-white-RNAi. The ;UAS-rye RNAi; UAS-Dicer2 stock was a gift from the Amita Sehgal lab.

## Generation of null mutant flies

All CRISPR/Cas9-mediated *rab* mutants, except *rab18* and *rab26*, were generated by WellGenetics Inc (Taipei, Taiwan), by homology-dependent repair (HDR) using two guide RNAs and a dsDNA plasmid donor (Kondo and Ueda, 2013). Briefly, upstream and downstream gRNA sequences were cloned into a U6 promoter plasmid. For repair, a cassette, containing two loxP-sites flanking a 3xP3-RFP with two homology arms was cloned into a donor template (pUC57-Kan). A control strain (*w*<sup>1118</sup>) was injected with the donor template as well as specific *rab*-targeting gRNAs and hs-Cas9. F1 progeny positive for the positive selection marker, 3xP3-RFP, were further validated by genomic PCR and sequencing. The CRISPR null mutants were validated as described in the next section. gRNA sequences as well as specifics on the different CRISPR mutants are as follows:

- ***rab9***: Replacement of 2446 bp region, +98 bp relative to ATG to +111 bp relative to the first bp of *rab9* stop codon, by floxable cassette. Upstream gRNA sequence: GTTGTTCCTCG TAGCGAT, downstream gRNA sequence: ATTCCAGTCCGCGGAGGGGC.
- ***rab10***: Replacement of 1644 bp region, +57 bp relative to ATG to +70 bp relative to the first bp of *rab10* stop codon, by cassette, which contains three stop codons upstream of floxable 3xP3-RFP. Upstream gRNA sequence: CTGATCGGTGATTCAGGAGT, downstream gRNA sequence: GAACGGGGCGTGGTTTGCC.
- ***rab14***: Replacement of 930 bp region, –17 bp relative to ATG of *rab14-RB* isoform to –61 bp relative to the first bp of *rab14* stop codon, by floxable cassette. Upstream gRNA sequence: GATGAGCAAAGTGCGCAGCG, downstream gRNA sequence: GAAG TTCGCGACGGCTGCCA.
- ***rab21***: Replacement of 608 bp region, +12 bp relative to ATG of *rab21-RD* isoform to –109 bp relative to first bp of *rab21* stop codon, by floxable cassette. Upstream gRNA sequence: CAATGAGCTCGAGCAGAACG, downstream gRNA sequence: GACTCGCA TCCGGTTGCCGT.
- ***rab23***: Replacement of 1700 bp region, –35 bp relative to ATG to +173 bp relative to the first bp of *rab23* stop codon, by floxable cassette. Upstream gRNA sequence: CAATCAAACACC TGGGCGAG, downstream gRNA sequence: CATGTCTGAACCACATCACG.
- ***rab35***: Replacement of 816 bp region, –24 bp relative to ATG of *rab35-RC* isoform to +20 bp relative to the first bp of *rab35* stop codon, by floxable cassette. Upstream gRNA sequence: CAGCAATGTCATATGCCGAA, downstream gRNA sequence: AGGTGAAAGCGGC TCCGGCA.
- ***rab39***: Replacement of 898 bp region, +92 bp relative to ATG to –93 bp relative to the first bp of *rab39* stop codon, by floxable cassette. Upstream gRNA sequence: CACAGACGGCAAATTCGCCG, downstream gRNA sequence: TCGATCCGGCGAA TATAAGG.
- ***rab40***: Replacement of 1407 bp region, +2 bp relative to ATG to –93 bp to the first bp of *rab40* stop codon, by floxable cassette. Upstream gRNA sequence: CCTTGGTCATGG TTCCCATG, downstream gRNA sequence: TTGAGCGTCTGACTTCACCGA.
- ***rabX4***: Replacement of 962 bp, –2 bp relative to ATG to –61 bp to first bp of *rabx4* stop codon, by floxable cassette. This results in the deletion of the entire coding sequence. Upstream gRNA sequence: CTCCGCCAGCTCCGTCAACA, downstream gRNA sequence: AAGAAATCACCCGGCTCCAA.
- ***rab18***: For the generation of the *rab18* null mutant, first a *rab18* sgRNA-expressing plasmid (pBFv-U6.2-*rab18*-sgRNA) was generated. For this, *rab18* sgRNA sequence 5'-GGTGA TCGGGAAAGCGGCG (directly after the *rab18* start codon) was cloned into BbsI-digested pBFv-U6.2 plasmid. Second, a pCR8-*rab18*-3xP3-RFP plasmid was generated by soeing PCR and restriction enzyme digestion. For this, two 500 bp homology arms (HA) around the *rab18* sgRNA targeting site were amplified, using the following primers: left HA fwd: TCC TAAATTTATGATATTTTATAATTATTT; left HA rev: CTGGACTTGCCTCGAGTTTTTTAGATCTG TGTGGTTTGAGCTCCGCTT; right HA fwd: CAAACCACACAGATCTAAAAAACTCGAGG-CAAGTCCAGGTGCAGTCCC; right HA rev: CGAACTGATCGCATTTGGCT. The resulting PCR product was then cloned into pCR8 vector (pCR8-*rab18*LA+RA). The 3xP3-RFP cassette, containing three stop codons upstream of the RFP, was cloned into pCR8-*rab18*LA+RA by *Bgl*II and *Xho*I double digestion to get the final pCR8-*rab18*-3xP3RFP plasmid. *Nanos*-Cas9 fly embryos were co-injected with the two plasmids pBFv-U6.2-*rab18*-sgRNA and pCR8-*rab18*-3xP3RFP. F1 progeny positive for the selection marker, 3xP3-RFP, were further validated by genomic PCR.

- **rab26:** Replacement of 9760 bp region, - 125 bp relative to ATG to +1310 bp to the end of coding exon 2, by positive selection marker 3xP3-dsRed flanked by loxP-sites. This leads to the complete deletion of ATG1 (exon 1) and ATG2 (exon 2) of *rab26* gene. Briefly, a *rab26* sgRNA-expressing plasmid was generated by cloning the *rab26* sgRNA 5'-GACAG TTTCGGAGTTAATTA into a BbsI-digested U6-BbsI-chiRNA plasmid (Addgene, plasmid #45946, donated by Kate O'Connor-Giles lab). *Nanos-Cas9* fly embryos were co-injected with the *rab26* sgRNA containing U6-chiRNA plasmid and the pHD-DsRed-attP plasmid (donated by Kate O'Connor-Giles lab). F1 progeny positive for the selection marker, 3xP3-dsRed, were further validated by genomic PCR.

In addition, six *rab* mutants (*rab2*, *rab4*, *rab19*, *rab30*, *rabX1*, and *rabX6*) were generated by ends-out homologous recombination based on previously generated Gal4 knock-ins in large genomic fragments (Chan et al., 2011). All *rab* mutants generated by ends-out homologous recombination are 'ORF knock-ins' (replacing the entire open reading frame), except for *rab4*, which is an 'ATG knock-in' (replacing the first exon including the start codon). The methods used for the replacements in the endogenous loci have been described previously in detail (Chan et al., 2012; Chan et al., 2011).

### Verification of *rab* null mutants by PCR

The newly generated *rab* null mutants were confirmed by genomic PCR, either using Phusion High-Fidelity PCR Kit (Thermo Fisher Scientific) (majority of *rab* mutants) or the SapphireAmp Fast PCR Master Mix (TaKaRa) (*rab26*). The following primer pairs, flanking the gene or inserted cassette, were used for the validation: *rab2* (Fwd: 5'-TGGCCACACTGTCGCTAGCC and Rev: 5'-CGCCTCCTC TACGTTGGCAG), *rab4* (Fwd: 5'-GGTTTTGATCGTGCCTGCG and Rev: 5'-AGACAACCTC TTACCGCTGCC), *rab9* (Fwd: 5'-GGCACTATGACGAACATGCGG and Rev: 5'-TTTGCAGCAC TGGGAAATCCG), *rab10* (Fwd: 5'-ATATCTCTTGTACCTGCGCC and Rev: 5'-CGACCACCATCCA TCGTTCCGG), *rab14* (Fwd: 5'-gggGCCAGTTTCGAGAAAGGG and Rev: 5'-CACGAGCACTGATCC TTGGC), *rab18* (Fwd: 5'-AAACAAAGCAGCAAGGTGGC and Rev: 5'-CTCCTCGTCGATCTTG TTGCC), *rab19* (Fwd: 5'-CCAGTTAACGGCCAGAACGG and Rev: 5'-TTGCCTCTCTGAGCATTGCC ), *rab21* (Fwd: 5'-CAATGGGAACGGCTAAATGCC and Rev: 5'-CAACATTTATCGCCGAGTGCC), *rab23* (Fwd: 5'-CACCTGCCGGCTTAGATGCG and Rev: 5'-GAGATATCGGAACCGGCC), *rab26* (Fwd: 5'-CGATGAAGTGGACATGCACCC and Rev: 5'-TGCCTTGAACCTCACTGGCG), *rab30* (Fwd: 5'-ACCCAGCGACTCAAAAACCC and Rev: 5'-GCTGCACAGTTCCAGATCCG), *rab35* (Fwd: 5'-CGAATCGTAAGCCAAGAACCC and Rev: 5'-ACTAATGGTGACGCACTGGC), *rab39* (Fwd: 5'-TAACAACCACCAGCGACAGCC and Rev: 5'-CGTATACCTCGTGTGACTGGC), *rab40* (Fwd: 5'-caat-gagtaaaccctagcgg and Rev: 5'-TGGGTATGGGTATGGTATGGG), *rabX1* (Fwd: 5'-GTGCCAA-GAAATCAGACGC and Rev: 5'-AGTCAGATGGGCTTAGAGCG), *rabX4* (Fwd: 5'-CTG TAACCGAAAACCTCCGC and Rev: 5'-CAACTTGCTCAGTTCTGCG), and *rabX6* (Fwd: 5'-G TCGCACTGTTGTTGTCGCC and Rev: 5'-CTCTGCGTGAGCATTGAGCC). For the validation of the mutants generated by homologous recombination, the following cassette-specific primers were used: Reverse primer in Gal4-region: 5'-CGGTGAGTGCACGATAGGGC (*rab2*, *rab4*, *rabX1*), second reverse primer in Gal4-region: 5'-CAATGGCACAGGTGAAGGCC (*rab19*, *rab30*, *rabX6*). The following cassette specific primers were used for the validation of CRISPR-generated null mutants: Reverse primer in RFP-region: 5'-GCTGCACAGGCTTCTTTGCC (*rab9*, *rab10*, *rab14*, *rab18*, *rab39*, *rabX4*), second reverse primer in RFP-region: 5'-ACAATCGCATGCTTGACGGC (*rab21*, *rab35*, *rab40*), forward primer in RFP-region: 5'-GGCTCTGAAGCTGAAAGACGG (*rab23*), forward primer in dsRed-region: 5'-ATGGTTACAAATAAAGCAATAGCATC (*rab26*) and reverse primer behind right-arm of inserted dsRed-cassette: 5'-AAACCACAGCCCATAGACG (*rab26*). The CRISPR null mutants were independently validated in our lab and by WellGenetics Inc (Taipei, Taiwan). All primers were designed with SnapGene (GSL Biotech LLC).

### Immunohistochemistry

Pupal and adult eye-brain complexes were dissected and collected in ice-cold PBS. The tissues were fixed in PBS with 4% paraformaldehyde for 30 min and washed in PBST (PBS + 1% Triton X-100). Wandering L3 larvae were immobilized at their abdomen and mouth hooks on a Sylgard-filled dissection dish, using insect needles (ø0.1 mm, Austerlitz insect pins). Larvae were dissected, from the dorsal side, in ice-cold 1x Schneider's *Drosophila* Medium (Thermo Fisher Scientific) and immediately

fixed in PBS with 4% paraformaldehyde for 10 min. After fixation, the gut and main trachea were carefully removed and the larval filets washed in PBS-Tween (PBS + 0.1% Tween).

The following primary antibodies were used: rabbit anti-Rab5 (1:1000, Abcam), rabbit anti-Rab7 (1:1000, gift from P. Dolph), mouse anti-Rab11 (1:500, BD Transduction Laboratories), guinea pig anti-Rab26 (1:2000 (IHC), 1:1000 (WB), made for this study), mouse anti-Syt1 (1:1000, DSHB), rabbit anti GABARAP+GABARAPL1+GABARAPL2 (Atg8) (1:100, Abcam), rabbit anti-Syx7/Avalanche (1:1000, gift from H. Krämer), guinea pig anti-Hrs (1:300, gift from H. Bellen), rabbit anti-HRP (1:500, Jackson ImmunoResearch Laboratories), rabbit anti-DPAK (1:2000), rat anti-D $\alpha$ 7 (1:2000, gift from H. Bellen), rat anti-nCadherin (1:100, DSHB), guinea pig anti-V100 (1:1000, *Hiesinger et al., 2005*), mouse anti-CSP (1:50, DSHB), mouse anti-ChAT (1:100, DSHB), mouse anti-nc82 (1:20, DSHB), rabbit anti-ebony (1:200), mouse anti-Chaoptin (24B10) (1:50, DSHB) and rabbit anti-DCP-1 (1:100; Cell Signaling Technology). Secondary antibodies used were Donkey anti-mouse DyLight 405, Goat anti-mouse Alexa 488, Goat anti-guinea pig Alexa 488, Goat anti-rat Alexa 488, Goat anti-rabbit Cy3, Goat anti-rabbit Alexa 647, Goat anti-rat Alexa 647, Goat anti-mouse Cy5, Goat anti-rat Cy5 (1:500; Jackson ImmunoResearch Laboratories), Goat anti-guinea pig HRP-linked (1:5000, Jackson ImmunoResearch Laboratories), Goat anti-guinea pig Cy5 (1:500, Abcam), Phalloidin-iFluor 405 (1:250; Abcam) and Toto-3 (1:1000; Thermo Fisher Scientific).

All samples were mounted in Vectashield mounting medium (Vector Laboratories). Larval filet preparations were incubated in Vectashield for at least 30 min at 4°C prior to mounting. To fully expose lamina photoreceptor terminals, pupal brains were mounted with their dorsal side up.

### Generation of rab26 antibody

The cDNA sequence corresponding to amino acids 1–192 of *rab26* was amplified by PCR and cloned into the pET28a (Invitrogen) vector for protein expression. Guinea pig antibodies against this domain were raised by Cocalico Biomedicals, Inc using the purified recombinant protein.

### Confocal microscopy, image processing, and quantification

All microscopy was performed using a Leica TCS SP8 X (white laser) with 20x and 63x Glycerol objectives (NA = 1.3). Leica image files were visualized and processed using Imaris (Bitplane) and Amira (Thermo Fisher Scientific). Postprocessing was performed using ImageJ (National Institute of Health), and Photoshop (CS6, Adobe Inc). Data was plotted using Illustrator (CS6, Adobe Inc), Photoshop (CS6, Adobe Inc) and GraphPad Prism 8.3.0 (GraphPad Software Inc).

For Chaoptin-accumulation and rhabdomere morphology experiments, all quantification was performed manually on single slices and only individually discernible compartments or rhabdomeres were counted. Only Chaoptin-accumulations in the central region of the lamina (length 115  $\mu$ m and depth 27  $\mu$ m) were quantified. For the rhabdomere analysis, the measurement tool from ImageJ was used. For Rhabdomere quantifications, 150 outer rhabdomeres were analyzed the following way: The longest (a) as well as the shortest (b) rhabdomere diameter was measured using the ImageJ measurement tool. For the shape analysis, the longest diameter was divided by the shortest (shape = a/b). For the area analysis, the following mathematical formula was used:  $area = pi * \left(\frac{a}{2}\right) * \left(\frac{b}{2}\right)$ .

The rhabdomere area ratio was calculated by dividing the area of newly hatched flies by the area of flies after 2 days of light stimulation. Area is more variable than shape in wild type and only significant changes outside the standard deviation range of the wild type control were scored. The statistical analyses were performed using RStudio (RStudio Inc) and GraphPad Prism 8.3.0 (GraphPad Software Inc), and the specific statistical tests used as well as sample numbers for experiments are indicated in the respective figure legends.

### Biochemistry

Proteins were extracted from 20 adult fly brains per genotype in RIPA buffer containing 150 mM NaCl, 0.1% Triton X-100 (Sigma), 0.1% SDS (Amresco), 50 mM Tris-HCL and 1x complete protease inhibitors (Sigma), pH 8. Samples were incubated on ice for 20 min and centrifuged at 16,000 RCF, 10 min at 4°C to remove cell debris. Laemmli buffer (Bio-Rad Laboratories) was added to the supernatant. After incubation for 5 min at 95°C, the samples were loaded on a 4–15% SDS-polyacrylamide gel (Bio Rad Laboratories) and then transferred to PVDF membrane (Bio-Rad Laboratories). Primary

antibody used was guinea pig anti-Rab26 (1:1000) and corresponding secondary was used 1:5000 (Abcam). The signals were detected with Clarity Western ECL (Bio-Rad Laboratories).

### Backcrossing of *rab* mutant flies

Serial backcrossing to a wild type (*yw*) background was performed for three consecutive generations. The single *rab* mutants as well as the respective balancer chromosomes, used to generate the final stocks, were backcrossed to the same genetic background. All mutant alleles, except *rab3* and *rab32*, could be traced by their red fluorescent marker. Where direct tracing was not possible, backcrossing was performed 'blindly' and after three generations roughly 100 separate single (*fe*-)male stocks were generated and subsequently sequenced to identify the backcrossed *rab3* and *rab32* mutants.

The genomic DNA was amplified using the Phusion High-Fidelity PCR Kit (Thermo Fisher Scientific) with the following primers for *rab3* (Fwd: 5'-ACACTGAGGCGAGCTTACGC and Rev: 5'-CTACTACCGAGGAGCGATGGG) and *rab32* (Fwd: 5'-GTAGACACGGGTCATGTTGCC and Rev: 5'-accagcaaatctcagtgcgg). The amplified DNA was extracted from agarose gel, cleaned using the Nucleo-Spin Gel and PCR Clean-up kit (Macherey-Nagel) and send for sequencing to Microsynth Seqlab GmbH (Göttingen, Germany). Sequencing results were visualized using SnapGene (GSL Biotech LLC). All primers were designed with SnapGene (GSL Biotech LLC).

### Developmental assays

For the analysis of developmental timing of homozygous, viable *rab* mutants, three crosses with equal number of flies (ratio female to male ~2:1) and same genotype were set up a few days prior to the start of the experiment, to ensure good egg laying. Of each of those, again three equal groups were formed and egg laying was allowed for 24 hr at room temperature. Egg containing vials were then shifted to the respective temperatures (18°C, 25°C, or 29°C), while the parental flies remained at room temperature for the duration of the experiment. The shifting of egg containing vials was repeated six more times, leading to a total of 21 'experimental' vials per temperature per genotype. Developing flies were kept at the respective temperatures until three days after they hatched, and the total number of hatched offspring was counted.

To study the effect of temperature stress on fly wing development, *rab* null mutants were reared at 18°C and 29°C. All mutant lines were set up with 10 females and three males and kept in their vials for 48 hr of egg laying, so as to prevent overcrowding in the vials. Adult female flies were collected not earlier than 24 hr after eclosion and placed in a 1:1 solution of glycerol:ethanol for a minimum of several hours, after which the wings were removed at the joint and mounted in the same solution. Wings were imaged with a Zeiss Cell Observer microscope and their size measured in ImageJ (National Institute of Health).

To validate the phenotypes of the developmental assay, backcrossed mutants as well as transheterozygotes of mutant chromosomes over deficiency chromosomes were used. All deficiency chromosomes were placed over a fluorescent balancer prior to the assay, to allow for identification. We did not succeed in identifying and validating a deficiency line for *rab18*. Homozygous backcrossed *rab32* females are lethal at 29°C, therefore no wing surface area measurements are available. All conditions, like temperature and number of parental flies, were kept same.

### Neuronal stimulation with white light and electroretinogram (ERG) recordings

Newly eclosed adults were either placed in a box for constant white light stimulation or placed in light-sealed vials (in the same box) for constant darkness. The lightbox contains two opposing high-intensity warm white light LED-stripe panels, each emitting ~1600 lumen (beam angle = 120°, distance between light source and vials = 16 cm). Temperature (22°C) and humidity (59%) inside the box were kept constant. Flies were kept inside the box for up to 7 days (wild type sensitization curve) or for 2 and 4 days (function and maintenance experiments).

For the ERG recordings, the flies were anesthetized and reversibly glued on microscope slides using non-toxic school glue. The recording and reference electrodes were filled with 2 M NaCl and placed on the retina and inside the thorax. Flies were exposed to a series of 1 s light/dark pulses provided by a computer-controlled white light-emitting diode system (MC1500; Schott) as previously

reported (Cherry *et al.*, 2013). Two different light stimulus intensities, dim ( $5.29 \times 10^{13}$  photons/cm<sup>2</sup>/s) and bright ( $1.31 \times 10^{16}$  photons/cm<sup>2</sup>/s), were used. Retinal responses were amplified by a Digidata 1440A, filtered through a Warner IE-210, and recorded using AxoScope 10.6 by Molecular Devices. All ERG recordings were performed in non-pigmented, white-eyed flies, which are more sensitive to light stimulation than pigmented ones. A total of 25–30 flies were examined for each genotype, condition, and time point.

For the quantification of the ERG data AxoScope 10.6 by Molecular Devices was used. First, the 'on' transient was quantified, by measuring the difference between the averaged baseline, prior to the onset of the light stimulus, and the peak value of the 'on' transient itself. Second, the depolarization was quantified, by measuring the difference between the baseline prior to stimulation and the depolarization when the signal has reached its plateau in the second half of the 1 s light stimulus prior to the end of the stimulus and repolarization.

## Neuronal stimulation with blue light

Newly eclosed *rdgC*<sup>306</sup> mutant flies (Bloomington stock #3601) were placed in an illuminated aluminum tube for constant, high-intensity, pure blue light stimulation. The aluminum tube has an outer diameter of 45 mm and a wall thickness of 2.5 mm. It contains one high-intensity blue light LED-stripe, covering the complete inside of the tube and emitting 155 lumen (beam angle = 120°, distance between light source and vials = ~1 cm). Temperature (22°C) and humidity (59%) inside the tube were kept constant. Flies were kept under constant blue light stimulation for 4 consecutive days and afterwards immediately placed in the dark for 2 days.

## Acknowledgements

We would like to thank members of the Boutros, Hiesinger, Wernet and Hassan labs for their support and helpful discussions. We thank Hugo Bellen, Helmut Krämer, Amita Sehgal and the Developmental Hybridoma Bank for flies and reagents. This work was supported by grants from the NIH (RO1EY018884), the German Research Foundation (DFG, SFB/TRR186) to PRH and the German Research Foundation (DFG, SFB/TRR186) to MB.

## Additional information

### Competing interests

P Robin Hiesinger: Reviewing editor, *eLife*. The other authors declare that no competing interests exist.

### Funding

Funder	Grant reference number	Author
National Institutes of Health	RO1EY018884	P Robin Hiesinger
Deutsche Forschungsgemeinschaft	SFB/TRR186	P Robin Hiesinger
Deutsche Forschungsgemeinschaft	SFB/TRR186	Michael Boutros

The funders had no role in study design, data collection and interpretation, or the decision to submit the work for publication.

### Author contributions

Friederike E Kohrs, Ilsa-Maria Daumann, Bojana Pavlovic, Filip Port, Formal analysis, Investigation, Methodology, Writing - original draft, Writing - review and editing; Eugene Jennifer Jin, Conceptualization, Formal analysis, Investigation, Methodology; F Ridvan Kiral, Formal analysis, Investigation, Methodology; Shih-Ching Lin, Heike Wolfenberg, Thomas F Mathejczyk, Methodology; Gerit A Linneweber, Formal analysis, Validation, Methodology; Gerit Linneweber was added as an author during the revision with the approval of all authors regarding inclusion and position in the author list,

because he substantially helped with the backcrossing required for the revision and all data analyses associated with the new developmental data in Figure 2 plus supplements; Chih-Chiang Chan, Conceptualization, Supervision, Funding acquisition, Investigation, Methodology, Writing - original draft, Writing - review and editing; Michael Boutros, P Robin Hiesinger, Conceptualization, Formal analysis, Supervision, Funding acquisition, Writing - original draft, Project administration, Writing - review and editing

#### Author ORCIDs

Shih-Ching Lin [id](http://orcid.org/0000-0003-2960-5348) <http://orcid.org/0000-0003-2960-5348>

Filip Port [id](http://orcid.org/0000-0002-5157-4835) <http://orcid.org/0000-0002-5157-4835>

Chih-Chiang Chan [id](http://orcid.org/0000-0003-2626-3805) <http://orcid.org/0000-0003-2626-3805>

Michael Boutros [id](http://orcid.org/0000-0002-9458-817X) <http://orcid.org/0000-0002-9458-817X>

P Robin Hiesinger [id](https://orcid.org/0000-0003-4698-3527) <https://orcid.org/0000-0003-4698-3527>

#### Decision letter and Author response

Decision letter <https://doi.org/10.7554/eLife.59594.sa1>

Author response <https://doi.org/10.7554/eLife.59594.sa2>

---

## Additional files

### Supplementary files

- Supplementary file 1. Notes on pupal and adult expression patterns of nervous system-enriched Rabs based on endogenously tagged Rabs generated by *Dunst et al., 2015*. (A) Expression notes on optic lobe expression at 40% pupal development. (B) Expression notes on adult brains. The expression patterns are shown in **Figure 1—figure supplements 2–3**.
- Supplementary file 2. Tissue localization of Rab proteins in humans, rodents (*mus musculus*, *rattus norvegicus*, white New Zealand rabbits (*Oryctolagus cuniculus*)) and *Drosophila melanogaster* based on RNA- and protein-level expression. For the human protein atlas ([www.proteinatlas.org](http://www.proteinatlas.org) based on Fagerberg et al., 2014) 27 tissues were analyzed. The data was summarized in the following way: “ubiquitous” (detected in all tissue/region/cell types), “widespread” (detected in at least a third but not all tissue/region/cell types), “restricted” (detected in more than one but less than one third of tissue/region/cell types). The classifications “tissue specific”, “tissue enriched”, “group enriched” and “uncertain” were used as described in the human protein atlas. Regarding the data of the mouse embryo (E 14.5) transcriptome atlas ([www.eurexpress.org](http://www.eurexpress.org) based on Diez-Roux et al., 2011) the original classifications were adopted: “regional signal” (signal detected in a limited number of discrete locations), “no regional signal” (in all tissues or not detectable) or “not detected”. Out of the analyzed tissues “brain, spinal cord, CNS nerves, peripheral nervous system, ganglia” were grouped as nervous system and “gut, stomach, liver, pancreas” as intestines. For the flyatlas2 ([www.flyatlas.gla.ac.uk](http://www.flyatlas.gla.ac.uk), see also based on Leader et al., 2018) only data of female adults were considered. “Head, brain and thoracoabdominal ganglion” were grouped as “nervous system high”. The following abbreviations were used: human (H), rodent (R), *Drosophila melanogaster* (Dm), embryo (E), larva (L), adult (A), *Mus musculus* (Mm), *Rattus norvegicus* (Rn), *Oryctolagus cuniculus* (Oc), cell culture (CC). Asterisks indicate if the Rab is specific to Hominidae (\*), specific to primates (\*\*), or specific to primates and dolphins (\*\*\*).
- Supplementary file 3. Function, subcellular localization, and mutant viability of Rab GTPases in mammals, *Saccharomyces cerevisiae* and *Drosophila melanogaster*. Mouse knockout models were listed for the mammalian rab GTPase mutants. Among primary publications, the International Mouse Phenotype Consortium (<https://www.mousephenotype.org/>) was used for information on the viability of mouse knockout models. Information on *Drosophila* mutant viability is based on this study, if not stated otherwise in the table. Only viability / lethality for homozygous mutants was listed. The following abbreviations were used: *Drosophila melanogaster* (Dm), endoplasmic reticulum (ER), glucose transporter type 4 (GLUT4), insulin-producing cells (IPCs), Jun-N-terminal kinase (JNK), knockout (KO), mammals (M), matrix metalloproteinases (MMP), multivesicular bodies (MVBs), neuromuscular junction (NMJ), planar cell polarity (PCP), plasma membrane (PM), *Saccharomyces cerevisiae* (Sc),

trans-Golgi network (TGN), 37tyrosinase-related protein-1 (Typr-1), ventral nerve cord (VNC). Asterisks indicate if the Rab is specific to Hominidae (\*), specific to primates (\*\*), or specific to primates and dolphins (\*\*\*).

- Supplementary file 4. Quantitative analysis of the developmental timing assay at different temperatures. (A) Summary of developmental time for wild type and all fertile, homozygous viable *rab* mutants at 18°C, 25°C, and 29°C. Listed are number of days (after 24 hr of egg collection) until first 1st instar larvae, pupae, or adults appear, as well as total number of adults hatched and number of adults per vial. Days are given in mean ± SEM. (B) Summary of developmental time for wild type and tested backcrossed *rab* mutants at 18°C, 25°C, and 29°C. Listed are number of days (after 24 hr of egg collection) until first 1st instar larvae, pupae, or adults appear, as well as total number of adults hatched and number of adults per vial. Days are given in mean ± SEM. (C) Summary of developmental time for wild type and tested *rab* mutants over deficiencies at 18°C, 25°C and 29°C. Listed are number of days (after 24 hr of egg collection) until first 1st instar larvae, pupae, or adults appear, as well as total number of adults hatched and number of adults per vial. Days are given in mean ± SEM.
- Transparent reporting form

### Data availability

All data generated or analysed during this study are included in the manuscript and supporting files.

## References

- Azevedo RB**, French V, Partridge L. 2002. Temperature modulates epidermal cell size in *Drosophila melanogaster*. *Journal of Insect Physiology* **48**:231–237. DOI: [https://doi.org/10.1016/S0022-1910\(01\)00168-8](https://doi.org/10.1016/S0022-1910(01)00168-8), PMID: 12770123
- Bellen HJ**, Levis RW, Liao G, He Y, Carlson JW, Tsang G, Evans-Holm M, Hiesinger PR, Schulze KL, Rubin GM, Hoskins RA, Spradling AC. 2004. The BDGP gene disruption project: single transposon insertions associated with 40% of *Drosophila* genes. *Genetics* **167**:761–781. DOI: <https://doi.org/10.1534/genetics.104.026427>, PMID: 15238527
- Best BT**, Leptin M. 2020. Multiple requirements for rab GTPases in the development of *Drosophila* Tracheal Dorsal Branches and Terminal Cells. *G3: Genes, Genomes, Genetics* **10**:1099–1112. DOI: <https://doi.org/10.1534/g3.119.400967>, PMID: 31980432
- Binotti B**, Pavlos NJ, Riedel D, Wenzel D, Vorbrüggen G, Schalk AM, Kühnel K, Boyken J, Erck C, Martens H, Chua JJ, Jahn R. 2015. The GTPase Rab26 links synaptic vesicles to the autophagy pathway. *eLife* **4**:e05597. DOI: <https://doi.org/10.7554/eLife.05597>, PMID: 25643395
- Chan CC**, Scoggin S, Wang D, Cherry S, Dembo T, Greenberg B, Jin EJ, Kuey C, Lopez A, Mehta SQ, Perkins TJ, Brankatschk M, Rothenfluh A, Buszczak M, Hiesinger PR. 2011. Systematic discovery of rab GTPases with synaptic functions in *Drosophila*. *Current Biology* **21**:1704–1715. DOI: <https://doi.org/10.1016/j.cub.2011.08.058>, PMID: 22000105
- Chan CC**, Scoggin S, Hiesinger PR, Buszczak M. 2012. Combining recombineering and ends-out homologous recombination to systematically characterize *Drosophila* gene families: rab GTPases as a case study. *Communicative & Integrative Biology* **5**:179–183. DOI: <https://doi.org/10.4161/cib.18788>, PMID: 22808327
- Cherry S**, Jin EJ, Ozel MN, Lu Z, Agi E, Wang D, Jung WH, Epstein D, Meinertzhagen IA, Chan CC, Hiesinger PR. 2013. Charcot-Marie-Tooth 2B mutations in rab7 cause dosage-dependent neurodegeneration due to partial loss of function. *eLife* **2**:e01064. DOI: <https://doi.org/10.7554/eLife.01064>, PMID: 24327558
- Davis FP**, Nern A, Picard S, Reiser MB, Rubin GM, Eddy SR, Henry GL. 2020. A genetic, genomic, and computational resource for exploring neural circuit function. *eLife* **9**:e50901. DOI: <https://doi.org/10.7554/eLife.50901>, PMID: 31939737
- Dhekne HS**, Yanatori I, Gomez RC, Tonelli F, Diez F, Schüle B, Steger M, Alessi DR, Pfeffer SR. 2018. A pathway for parkinson's Disease LRRK2 kinase to block primary cilia and Sonic hedgehog signaling in the brain. *eLife* **7**:e40202. DOI: <https://doi.org/10.7554/eLife.40202>, PMID: 23322046
- Dong B**, Kakahara K, Otani T, Wada H, Hayashi S. 2013. Rab9 and retromer regulate retrograde trafficking of luminal protein required for epithelial tube length control. *Nature Communications* **4**:1358. DOI: <https://doi.org/10.1038/ncomms2347>, PMID: 23322046
- Dunst S**, Kazimiers T, von Zadow F, Jambor H, Sagner A, Brankatschk B, Mahmoud A, Spann S, Tomancak P, Eaton S, Brankatschk M. 2015. Endogenously tagged rab proteins: a resource to study membrane trafficking in *Drosophila*. *Developmental Cell* **33**:351–365. DOI: <https://doi.org/10.1016/j.devcel.2015.03.022>, PMID: 25942626
- Fayyazuddin A**, Zaheer MA, Hiesinger PR, Bellen HJ. 2006. The nicotinic acetylcholine receptor Dα7 is required for an escape behavior in *Drosophila*. *PLOS Biology* **4**:e63. DOI: <https://doi.org/10.1371/journal.pbio.0040063>, PMID: 16494528

- Fischbach K-F, Ditttrich APM. 1989. The optic lobe of *Drosophila melanogaster*. I. A golgi analysis of wild-type structure. *Cell and Tissue Research* **258**:441–475. DOI: <https://doi.org/10.1007/BF00218858>
- Frechter S, Minke B. 2006. Light-regulated translocation of signaling proteins in *Drosophila* photoreceptors. *Journal of Physiology-Paris* **99**:133–139. DOI: <https://doi.org/10.1016/j.jphysparis.2005.12.010>, PMID: 16458490
- Giagtzoglou N, Yamamoto S, Zitserman D, Graves HK, Schulze KL, Wang H, Klein H, Roegiers F, Bellen HJ. 2012. dEHBP1 controls exocytosis and recycling of Delta during asymmetric divisions. *Journal of Cell Biology* **196**:65–83. DOI: <https://doi.org/10.1083/jcb.201106088>
- Gillingham AK, Sinka R, Torres IL, Lilley KS, Munro S. 2014. Toward a comprehensive map of the effectors of rab GTPases. *Developmental Cell* **31**:358–373. DOI: <https://doi.org/10.1016/j.devcel.2014.10.007>, PMID: 25453831
- Graf ER, Daniels RW, Burgess RW, Schwarz TL, DiAntonio A. 2009. Rab3 dynamically controls protein composition at active zones. *Neuron* **64**:663–677. DOI: <https://doi.org/10.1016/j.neuron.2009.11.002>, PMID: 20005823
- Grosshans BL, Ortiz D, Novick P. 2006. Rabs and their effectors: achieving specificity in membrane traffic. *PNAS* **103**:11821–11827. DOI: <https://doi.org/10.1073/pnas.0601617103>, PMID: 16882731
- Gurkan C, Lapp H, Alory C, Su AI, Hogenesch JB, Balch WE. 2005. Large-scale profiling of rab GTPase trafficking networks: the membrome. *Molecular Biology of the Cell* **16**:3847–3864. DOI: <https://doi.org/10.1091/mbc.e05-01-0062>, PMID: 15944222
- Harris KP, Littleton JT. 2011. Vesicle trafficking: a rab family profile. *Current Biology* **21**:R841–R843. DOI: <https://doi.org/10.1016/j.cub.2011.08.061>, PMID: 22032185
- Hiesinger PR, Fayyazuddin A, Mehta SQ, Rosenmund T, Schulze KL, Zhai RG, Verstreken P, Cao Y, Zhou Y, Kunz J, Bellen HJ. 2005. The v-ATPase V0 subunit a1 is required for a late step in synaptic vesicle exocytosis in *Drosophila*. *Cell* **121**:607–620. DOI: <https://doi.org/10.1016/j.cell.2005.03.012>, PMID: 15907473
- Hiesinger PR. 2021. Brain wiring with composite instructions. *BioEssays* **43**:2000166. DOI: <https://doi.org/10.1002/bies.202000166>
- Hiesinger PR, Hassan BA. 2018. The evolution of variability and robustness in neural development. *Trends in Neurosciences* **41**:577–586. DOI: <https://doi.org/10.1016/j.tins.2018.05.007>, PMID: 29880259
- Hutagalung AH, Novick PJ. 2011. Role of rab GTPases in membrane traffic and cell physiology. *Physiological Reviews* **91**:119–149. DOI: <https://doi.org/10.1152/physrev.00059.2009>, PMID: 21248164
- Jaiswal M, Sandoval H, Zhang K, Bayat V, Bellen HJ. 2012. Probing mechanisms that underlie human neurodegenerative diseases in *Drosophila*. *Annual Review of Genetics* **46**:371–396. DOI: <https://doi.org/10.1146/annurev-genet-110711-155456>, PMID: 22974305
- Jin EJ, Chan CC, Agi E, Cherry S, Hanacik E, Buszczak M, Hiesinger PR. 2012. Similarities of *Drosophila* rab GTPases based on expression profiling: completion and analysis of the rab-Gal4 kit. *PLOS ONE* **7**:e40912. DOI: <https://doi.org/10.1371/journal.pone.0040912>, PMID: 22844416
- Jin EJ, Kiral FR, Hiesinger PR. 2018a. The where, what, and when of membrane protein degradation in neurons. *Developmental Neurobiology* **78**:283–297. DOI: <https://doi.org/10.1002/dneu.22534>, PMID: 28884504
- Jin EJ, Kiral FR, Ozel MN, Burchardt LS, Osterland M, Epstein D, Wolfenbergh H, Prohaska S, Hiesinger PR. 2018b. Live observation of two parallel membrane degradation pathways at axon terminals. *Current Biology* **28**:1027–1038. DOI: <https://doi.org/10.1016/j.cub.2018.02.032>, PMID: 29551411
- Kiral FR, Kohrs FE, Jin EJ, Hiesinger PR. 2018. Rab GTPases and membrane trafficking in Neurodegeneration. *Current Biology* **28**:R471–R486. DOI: <https://doi.org/10.1016/j.cub.2018.02.010>, PMID: 29689231
- Kiselev A, Socolich M, Vinós J, Hardy RW, Zuker CS, Ranganathan R. 2000. A molecular pathway for light-dependent photoreceptor apoptosis in *Drosophila*. *Neuron* **28**:139–152. DOI: [https://doi.org/10.1016/S0896-6273\(00\)00092-1](https://doi.org/10.1016/S0896-6273(00)00092-1), PMID: 11086990
- Klöpffer TH, Kienle N, Fasshauer D, Munro S. 2012. Untangling the evolution of rab G proteins: implications of a comprehensive genomic analysis. *BMC Biology* **10**:71. DOI: <https://doi.org/10.1186/1741-7007-10-71>, PMID: 22873208
- Kolodziejczyk A, Sun X, Meinertzhagen IA, Nässel DR. 2008. Glutamate, GABA and acetylcholine signaling components in the Lamina of the *Drosophila* visual system. *PLOS ONE* **3**:e2110. DOI: <https://doi.org/10.1371/journal.pone.0002110>, PMID: 18464935
- Kondo S, Ueda R. 2013. Highly improved gene targeting by germline-specific Cas9 expression in *Drosophila*. *Genetics* **195**:715–721. DOI: <https://doi.org/10.1534/genetics.113.156737>, PMID: 24002648
- Laiouar S, Berns N, Brech A, Riechmann V. 2020. RabX1 organizes a late endosomal compartment that forms tubular connections to lysosomes consistent with a "Kiss and Run" Mechanism. *Current Biology* **30**:1177–1188. DOI: <https://doi.org/10.1016/j.cub.2020.01.048>, PMID: 32059769
- Lien WY, Chen YT, Li YJ, Wu JK, Huang KL, Lin JR, Lin SC, Hou CC, Wang HD, Wu CL, Huang SY, Chan CC. 2020. Lifespan regulation in  $\alpha/\beta$  posterior neurons of the fly mushroom bodies by Rab27. *Aging Cell* **19**:e13179. DOI: <https://doi.org/10.1111/acer.13179>, PMID: 32627932
- Lipatova Z, Hain AU, Nazarko VY, Segev N. 2015. Ypt/Rab GTPases: principles learned from yeast. *Critical Reviews in Biochemistry and Molecular Biology* **50**:203–211. DOI: <https://doi.org/10.3109/10409238.2015.1014023>, PMID: 25702751
- Lüthy K, Ahrens B, Rawal S, Lu Z, Tarnogorska D, Meinertzhagen IA, Fischbach KF. 2014. The irre cell recognition module (IRM) protein kirre is required to form the reciprocal synaptic network of L4 neurons in the *Drosophila* Lamina. *Journal of Neurogenetics* **28**:291–301. DOI: <https://doi.org/10.3109/01677063.2014.883390>, PMID: 24697410

- Ma J, Plesken H, Treisman JE, Edelman-Novemsky I, Ren M. 2004. Lightoid and claret: a rab GTPase and its putative guanine nucleotide exchange factor in biogenesis of *Drosophila* eye pigment granules. *PNAS* **101**: 11652–11657. DOI: <https://doi.org/10.1073/pnas.0401926101>, PMID: 15289618
- Pataki C, Matussek T, Kurucz E, Andó I, Jenny A, Mihály J. 2010. *Drosophila* Rab23 is involved in the regulation of the number and planar polarization of the adult cuticular hairs. *Genetics* **184**:1051–1065. DOI: <https://doi.org/10.1534/genetics.109.112060>, PMID: 20124028
- Pereira-Leal JB, Seabra MC. 2000. The mammalian rab family of small GTPases: definition of family and subfamily sequence motifs suggests a mechanism for functional specificity in the ras superfamily. *Journal of Molecular Biology* **301**:1077–1087. DOI: <https://doi.org/10.1006/jmbi.2000.4010>, PMID: 10966806
- Pereira-Leal JB, Seabra MC. 2001. Evolution of the rab family of small GTP-binding proteins. *Journal of Molecular Biology* **313**:889–901. DOI: <https://doi.org/10.1006/jmbi.2001.5072>
- Pfeffer SR. 1994. Rab GTPases: master regulators of membrane trafficking. *Current Opinion in Cell Biology* **6**: 522–526. DOI: [https://doi.org/10.1016/0955-0674\(94\)90071-X](https://doi.org/10.1016/0955-0674(94)90071-X), PMID: 7986528
- Pfeffer SR. 2013. Rab GTPase regulation of membrane identity. *Current Opinion in Cell Biology* **25**:414–419. DOI: <https://doi.org/10.1016/j.ceb.2013.04.002>, PMID: 23639309
- Pfeffer SR. 2017. Rab GTPases: master regulators that establish the secretory and endocytic pathways. *Molecular Biology of the Cell* **28**:712–715. DOI: <https://doi.org/10.1091/mbc.e16-10-0737>, PMID: 28292916
- Purcell K, Artavanis-Tsakonas S. 1999. The developmental role of warthog, the notch modifier encoding Drab6. *Journal of Cell Biology* **146**:731–740. DOI: <https://doi.org/10.1083/jcb.146.4.731>
- Rivera-Alba M, Vitaladevuni SN, Mishchenko Y, Mischenko Y, Lu Z, Takemura SY, Scheffer L, Meinertzhagen IA, Chklovskii DB, de Polavieja GG. 2011. Wiring economy and volume exclusion determine neuronal placement in the *Drosophila* brain. *Current Biology* **21**:2000–2005. DOI: <https://doi.org/10.1016/j.cub.2011.10.022>, PMID: 22119527
- Schopf K, Huber A. 2017. Membrane protein trafficking in *Drosophila* photoreceptor cells. *European Journal of Cell Biology* **96**:391–401. DOI: <https://doi.org/10.1016/j.ejcb.2016.11.002>, PMID: 27964885
- Sheehan P, Zhu M, Beskow A, Vollmer C, Waites CL. 2016. Activity-Dependent degradation of synaptic vesicle proteins requires Rab35 and the ESCRT pathway. *The Journal of Neuroscience* **36**:8668–8686. DOI: <https://doi.org/10.1523/JNEUROSCI.0725-16.2016>, PMID: 27535913
- Shi M, Yue Z, Kuryatov A, Lindstrom JM, Sehgal A. 2014. Identification of redeye, a new sleep-regulating protein whose expression is modulated by sleep amount. *eLife* **3**:e01473. DOI: <https://doi.org/10.7554/eLife.01473>, PMID: 24497543
- Spinosa MR, Progida C, De Luca A, Colucci AM, Alifano P, Bucci C. 2008. Functional characterization of Rab7 mutant proteins associated with Charcot-Marie-Tooth type 2B disease. *Journal of Neuroscience* **28**:1640–1648. DOI: <https://doi.org/10.1523/JNEUROSCI.3677-07.2008>, PMID: 18272684
- Steele F, O'Tousa JE. 1990. Rhodopsin activation causes retinal degeneration in *Drosophila* *rdgC* mutant. *Neuron* **4**:883–890. DOI: [https://doi.org/10.1016/0896-6273\(90\)90141-2](https://doi.org/10.1016/0896-6273(90)90141-2), PMID: 2361011
- Steger M, Diez F, Dhekne HS, Lis P, Nirujogi RS, Karayel O, Tonelli F, Martinez TN, Lorentzen E, Pfeffer SR, Alessi DR, Mann M. 2017. Systematic proteomic analysis of LRRK2-mediated rab GTPase phosphorylation establishes a connection to ciliogenesis. *eLife* **6**:e31012. DOI: <https://doi.org/10.7554/eLife.31012>, PMID: 29125462
- Stenmark H. 2009. Rab GTPases as coordinators of vesicle traffic. *Nature Reviews Molecular Cell Biology* **10**: 513–525. DOI: <https://doi.org/10.1038/nrm2728>, PMID: 19603039
- Tadros W, Xu S, Akin O, Yi CH, Shin GJ, Millard SS, Zipursky SL. 2016. Dscam proteins direct dendritic targeting through adhesion. *Neuron* **89**:480–493. DOI: <https://doi.org/10.1016/j.neuron.2015.12.026>, PMID: 26844831
- Thibault ST, Singer MA, Miyazaki WY, Milash B, Dompe NA, Singh CM, Buchholz R, Demsky M, Fawcett R, Francis-Lang HL, Ryner L, Cheung LM, Chong A, Erickson C, Fisher WW, Greer K, Hartouni SR, Howie E, Jakkula L, Joo D, et al. 2004. A complementary transposon tool kit for *Drosophila melanogaster* using P and piggyBac. *Nature Genetics* **36**:283–287. DOI: <https://doi.org/10.1038/ng1314>, PMID: 14981521
- Touchot N, Chardin P, Tavitian A. 1987. Four additional members of the ras gene superfamily isolated by an oligonucleotide strategy: molecular cloning of YPT-related cDNAs from a rat brain library. *PNAS* **84**:8210–8214. DOI: <https://doi.org/10.1073/pnas.84.23.8210>, PMID: 3317403
- Tuthill JC, Nern A, Holtz SL, Rubin GM, Reiser MB. 2013. Contributions of the 12 neuron classes in the fly Lamina to motion vision. *Neuron* **79**:128–140. DOI: <https://doi.org/10.1016/j.neuron.2013.05.024>, PMID: 23849200
- Uytterhoeven V, Kuenen S, Kasprzyk J, Miskiewicz K, Verstreken P. 2011. Loss of Skywalker reveals synaptic endosomes as sorting stations for synaptic vesicle proteins. *Cell* **145**:117–132. DOI: <https://doi.org/10.1016/j.cell.2011.02.039>, PMID: 21458671
- Veleri S, Punnakkal P, Dunbar GL, Maiti P. 2018. Molecular insights into the roles of rab proteins in intracellular dynamics and neurodegenerative diseases. *NeuroMolecular Medicine* **20**:18–36. DOI: <https://doi.org/10.1007/s12017-018-8479-9>, PMID: 29423895
- Verhoeven K, De Jonghe P, Coen K, Verpoorten N, Auer-Grumbach M, Kwon JM, FitzPatrick D, Schmedding E, De Vriendt E, Jacobs A, Van Gerwen V, Wagner K, Hartung HP, Timmerman V. 2003. Mutations in the small GTP-ase late endosomal protein RAB7 cause Charcot-Marie-Tooth type 2B neuropathy. *The American Journal of Human Genetics* **72**:722–727. DOI: <https://doi.org/10.1086/367847>, PMID: 12545426
- Williamson WR, Wang D, Haberman AS, Hiesinger PR. 2010. A dual function of V0-ATPase a1 provides an endolysosomal degradation mechanism in *Drosophila melanogaster* photoreceptors. *Journal of Cell Biology* **189**:885–899. DOI: <https://doi.org/10.1083/jcb.201003062>

- Woichansky I**, Beretta CA, Berns N, Riechmann V. 2016. Three mechanisms control E-cadherin localization to the zonula adherens. *Nature Communications* **7**:10834. DOI: <https://doi.org/10.1038/ncomms10834>, PMID: 26960923
- Wucherpennig T**, Wilsch-Bräuninger M, Gonzalez-Gaitan M. 2003. Role of *Drosophila* Rab5 during endosomal trafficking at the synapse and evoked neurotransmitter release. *Journal of Cell Biology* **161**:609–624. DOI: <https://doi.org/10.1083/jcb.200211087>
- Xiong B**, Bellen HJ. 2013. Rhodopsin homeostasis and retinal degeneration: lessons from the fly. *Trends in Neurosciences* **36**:652–660. DOI: <https://doi.org/10.1016/j.tins.2013.08.003>, PMID: 24012059
- Zerial M**, McBride H. 2001. Rab proteins as membrane organizers. *Nature Reviews Molecular Cell Biology* **2**:107–117. DOI: <https://doi.org/10.1038/35052055>, PMID: 11252952
- Zhang J**, Schulze KL, Hiesinger PR, Suyama K, Wang S, Fish M, Acar M, Hoskins RA, Bellen HJ, Scott MP. 2007. Thirty-one flavors of *Drosophila* rab proteins. *Genetics* **176**:1307–1322. DOI: <https://doi.org/10.1534/genetics.106.066761>, PMID: 17409086
- Zhen Y**, Stenmark H. 2015. Cellular functions of rab GTPases at a glance. *Journal of Cell Science* **128**:3171–3176. DOI: <https://doi.org/10.1242/jcs.166074>, PMID: 26272922

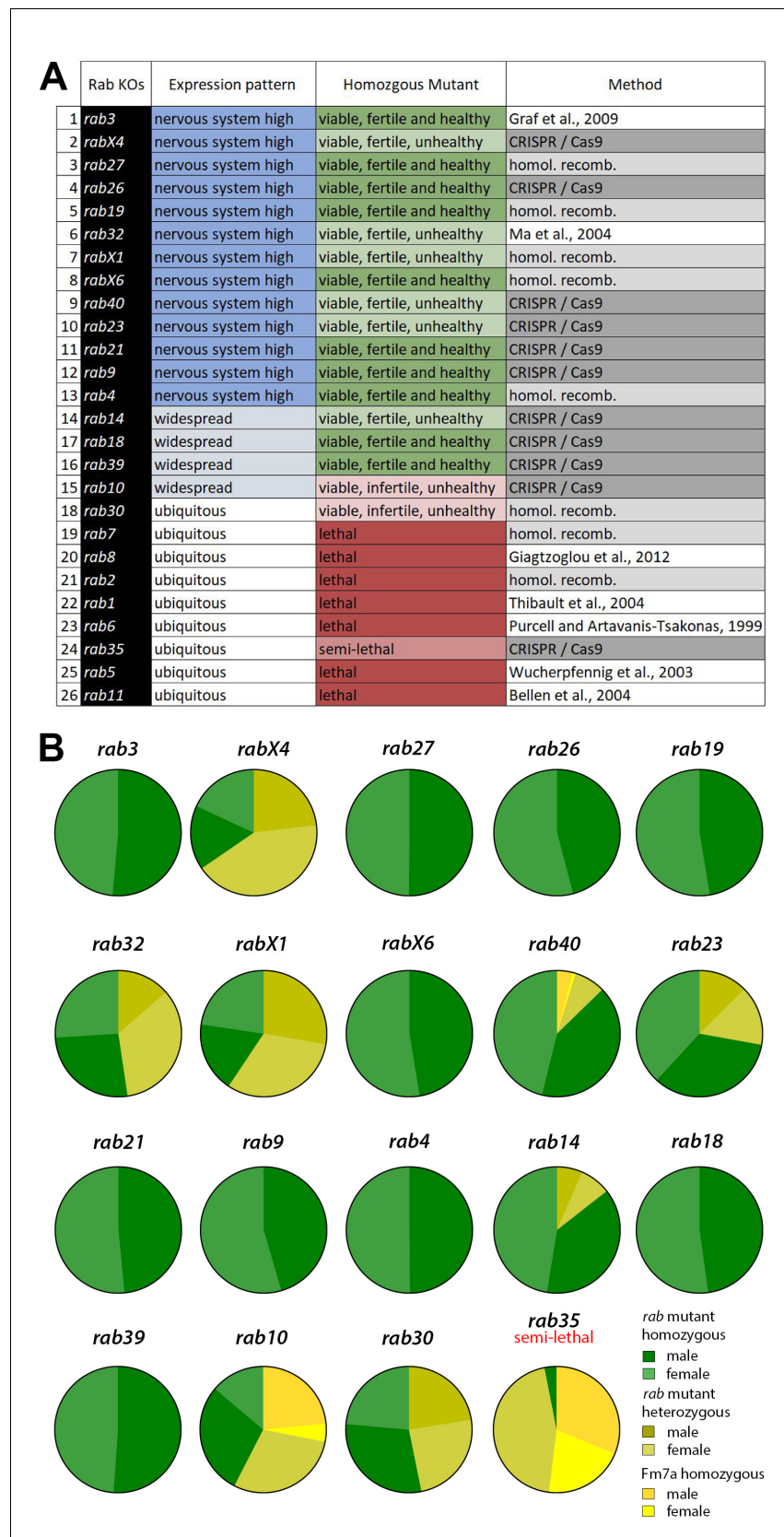


---

## Figures and figure supplements

Systematic functional analysis of rab GTPases reveals limits of neuronal robustness to environmental challenges in flies

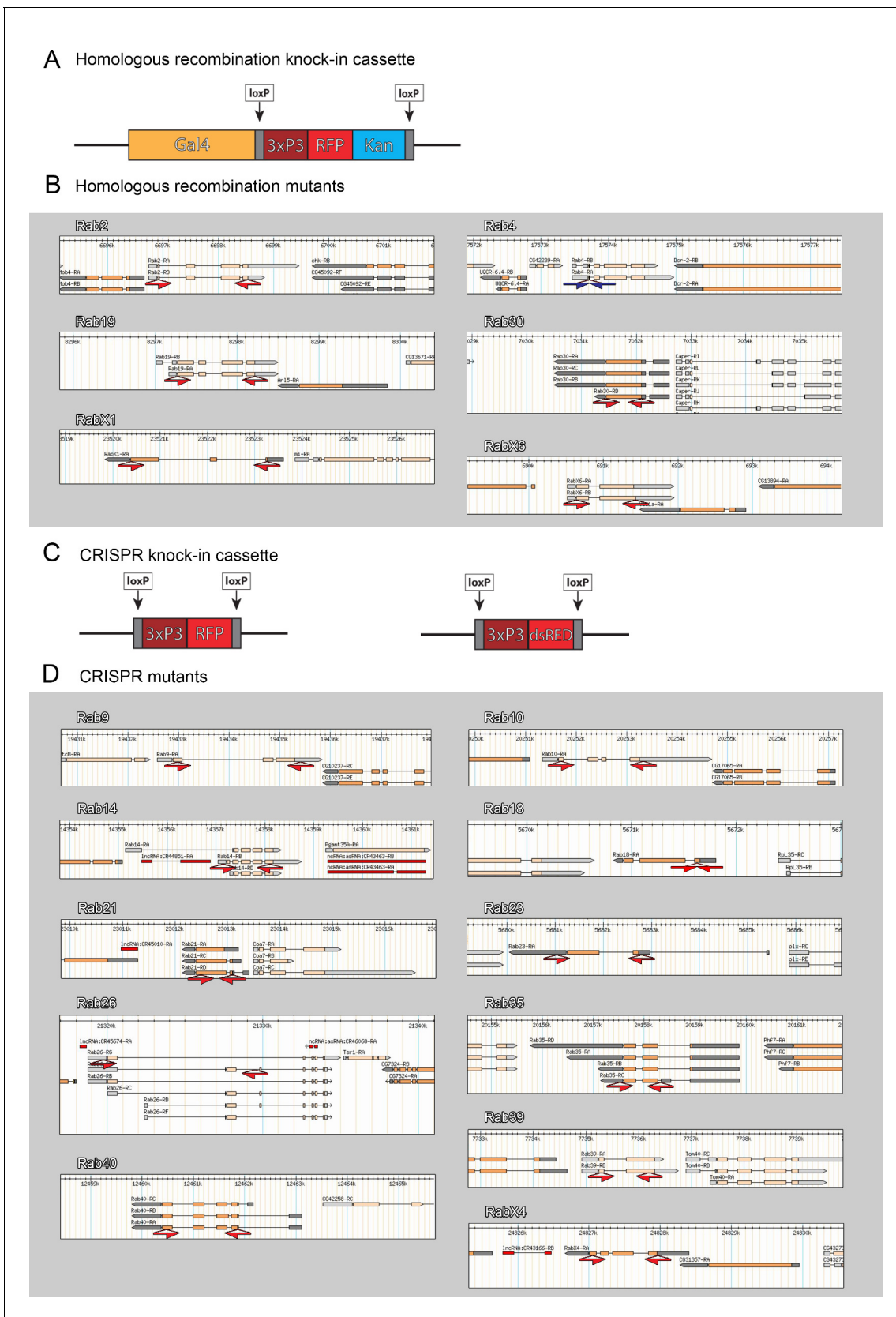
**Friederike E Kohrs et al**



**Figure 1.** Generation and viability analysis of the *rab* null mutant collection. (A) List of all 26 *Drosophila rab* null mutants, sorted by expression pattern from 'nervous system-enriched' to ubiquitous based on Chan et al., 2011; Figure 1 continued on next page

Figure 1 continued

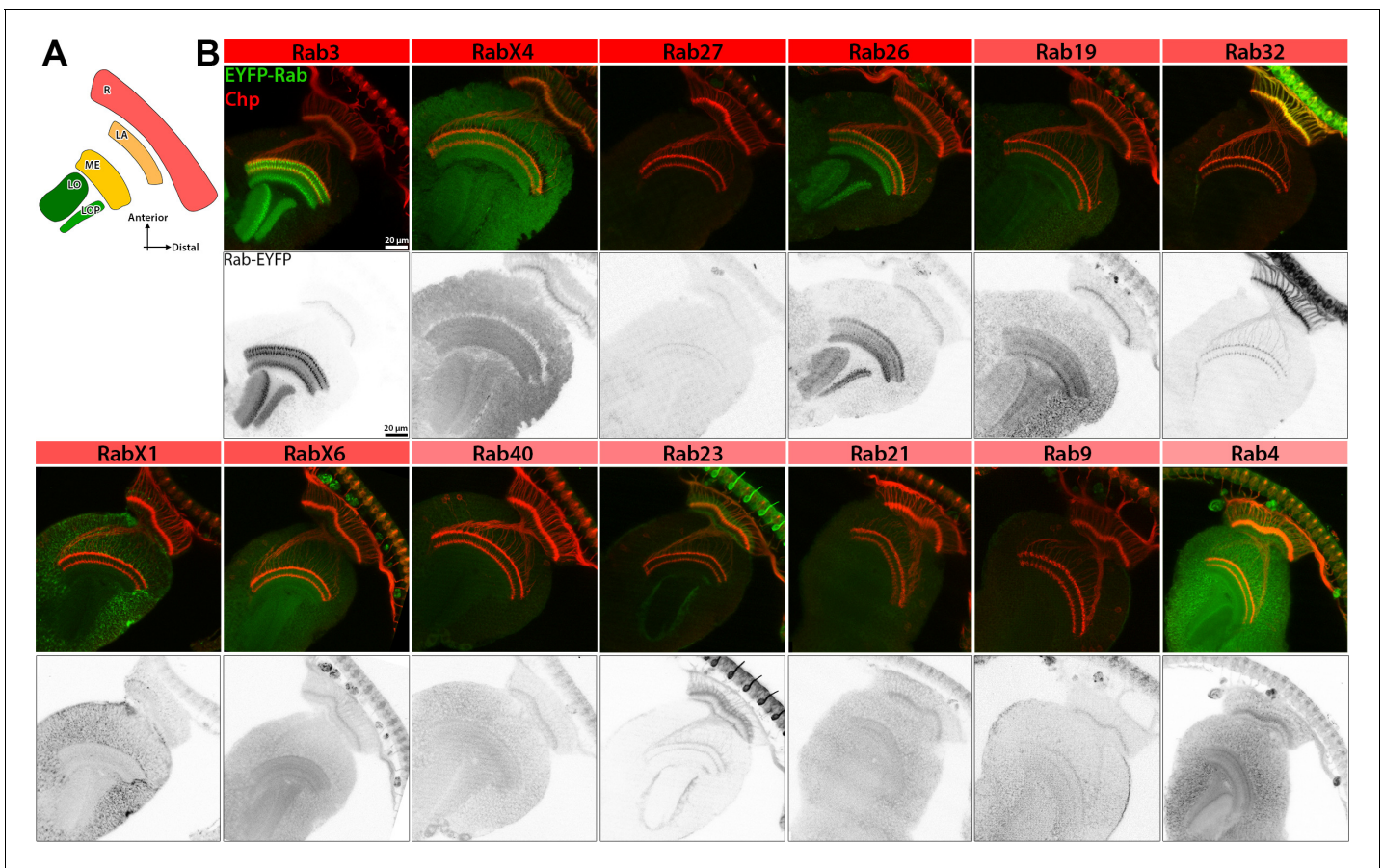
**Jin et al., 2012.** Two-thirds of the *rab* mutants are homozygous viable and fertile. Eight *rab* mutants are lethal in homozygosity. The origin of the mutants is indicated in the third column. **(B)** Pie charts showing the ratios of homozygous versus balanced flies after ten generations. Ten of the 18 viable or semi-lethal *rab* mutants are fully homozygous, while the others still retain their balancer chromosome (shades of yellow) to varying degrees. At least 1000 flies per *rab* mutant were counted.



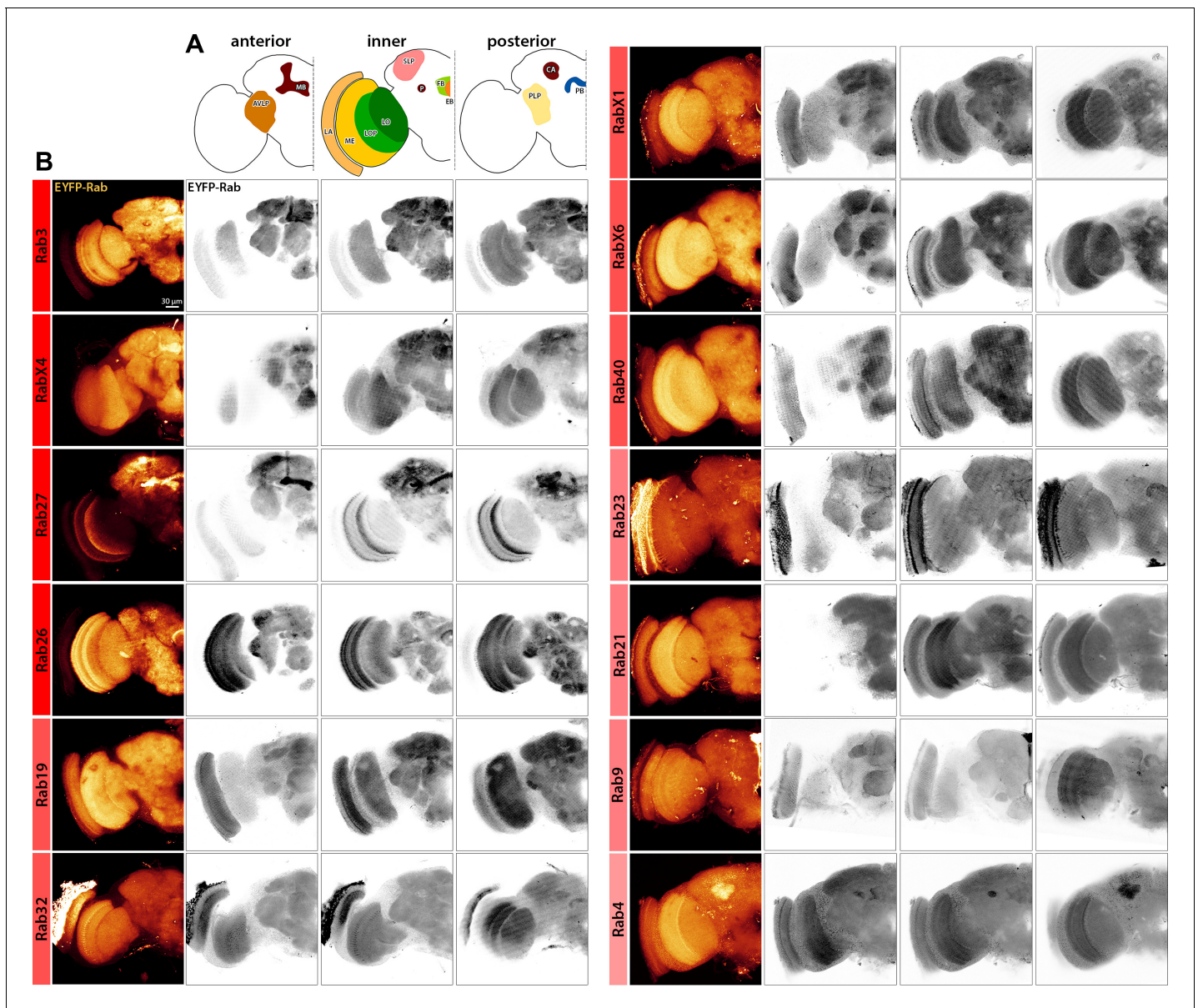
**Figure 1—figure supplement 1.** Design of newly generated *rab* mutants. (A and C) Schematic depiction of the inserted knock-in cassettes. For end-out homologous recombination a Gal4-3xP3-RFP-Kanamycin cassette, with loxP-sites flanking the 3xP3-RFP-Kan region, was inserted. For CRISPR/Cas9-  
*Figure 1—figure supplement 1 continued on next page*

Figure 1—figure supplement 1 continued

mediated mutagenesis a 3xP3-RFP- or 3xP3-dsRed (for *rab26*) cassette, flanked by loxP-sites, was inserted. **(B and D)** Schematics of genomic loci as depicted on FlyBase GBrowse (<https://flybase.org/cgi-bin/gbrowse2/dmel/>). The exon/intron region, with exon as wide orange bars, introns as black lines and 5' UTRs and 3'UTRS as grey wide bars. The red half-arrows highlight regions replaced for 'ORF knock-ins' (**B**) or 'CRISPR knock-ins' (**D**); blue half-arrows highlight regions replaced for 'ATG knock-ins' (*rab4* in **B**).



**Figure 1—figure supplement 2.** Pupal expression patterns of nervous system-enriched Rabs based on endogenously tagged Rabs generated by *Dunst et al., 2015*. (A) Schematic of the main optic neuropils and retina of the developing pupal brain. (B) Expression pattern of EYFP-tagged Rabs (green) in ~P+40% pupal brains. Immunolabeling of pupal photoreceptor projections with Choptin (red). Inverted channel shows expression of EYFP-tag. Scale bar = 20  $\mu$ m; number of brains  $n = 3-6$ . Abbreviations: R = retina, LA = lamina, ME = medulla, LO = lobula and LOP = lobula plate. See *Supplementary file 1* listing regions with EYFP-Rab expression.



**Figure 1—figure supplement 3.** Adult expression patterns of nervous system-enriched Rabs based on endogenously tagged Rabs generated by *Dunst et al., 2015*. *Dunst et al., 2015*. (A) Illustrations of the main anterior, inner and posterior neuropil regions of the adult brain exhibit strong Rab expression (shown in B). (B) Expression pattern of EYFP-tagged Rabs (green) in newly hatched adult brains. Inverted channels show expression of EYFP-tag. Scale bar = 30  $\mu$ m; number of brains  $n = 3-6$ . AVLP = anterior ventrolateral protocerebrum, MB = mushroom body, LA = lamina, ME = medulla, LOP = lobula plate, LO = lobula, P = pedunculus, SLP = superior medial protocerebrum, FB = fan-shaped body, EB = ellipsoid body, PLP = posterior lateral protocerebrum, CA = calyx and PB = protocerebral bridge. See **Supplementary file 1** listing regions with EYFP-Rab expression.

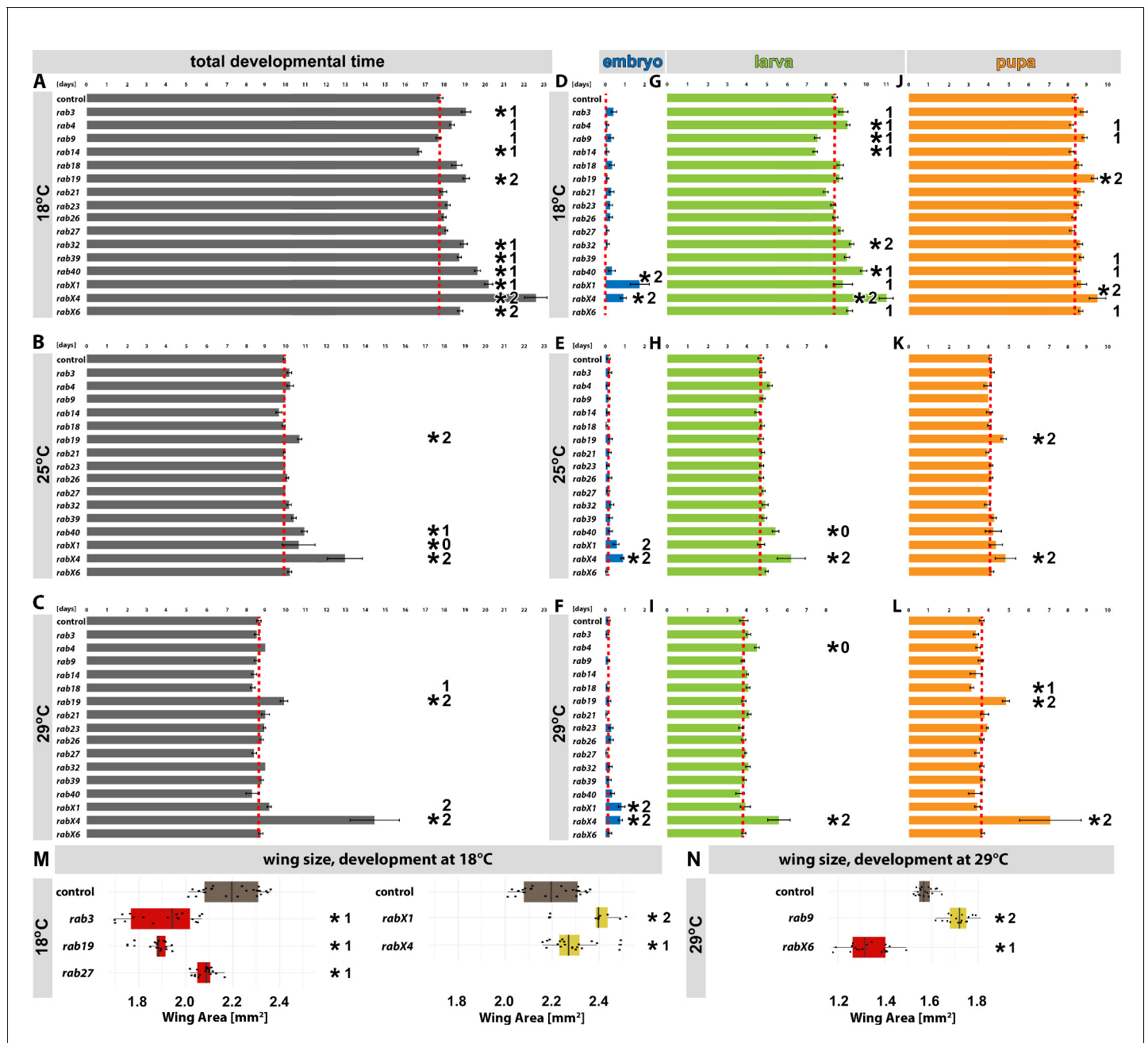


**Figure 2.** Developmental analyses of all viable *rab* mutants at different temperatures. (A–C) Developmental time from embryogenesis to adults at 18°C (A), 25°C (B), and 29°C (C) for all homozygous viable *rab* mutants. (D, G, and J) Developmental time at 18°C for all homozygous viable *rab* mutants, separated into embryonic (blue, D), larval (green, G) and pupal (orange, J) phases. (E, H, and K) Developmental time at 25°C for all homozygous viable *rab* mutants, separated into embryonic (blue, E), larval (green, H) and pupal (orange, K) phases. (F, I, and L) Developmental time at 29°C for all homozygous viable *rab* mutants, separated into embryonic (blue, F), larval (green, I) and pupal (orange, L) phases. (A–L) Dashed red line = mean of control. Mean ± SEM; \**p*<0.05 (for the specific statistical values see **Figure 2—figure supplement 1**); 0, 1, or 2 indicate if the specific phenotype could not be validated (0), could be validated by either backcrossing or mutant over deficiency (1) or could be validated by both (2); Unpaired non-parametric Kolmogorov-Smirnov test. (M–N) Wing surface area measurement for validated homozygous viable *rab* mutants at 18°C (M) and 29°C (N). Wild type (brown) and *rab* mutant with significantly reduced (red) and increased wing sizes (yellow) compared to control. Boxplot with horizontal line representing the median; individual data points are represented as dots. Fifteen to 22 wings per genotype were quantified; \**p*<0.05 (for the specific statistical values see **Figure 2—figure supplement 2**); 0, 1, or 2 indicate if the specific phenotype could not be validated (0), could be validated by either backcrossing or mutant over deficiency (1) or could be validated by both (2); ordinary one-way ANOVA with pair-wise comparison.

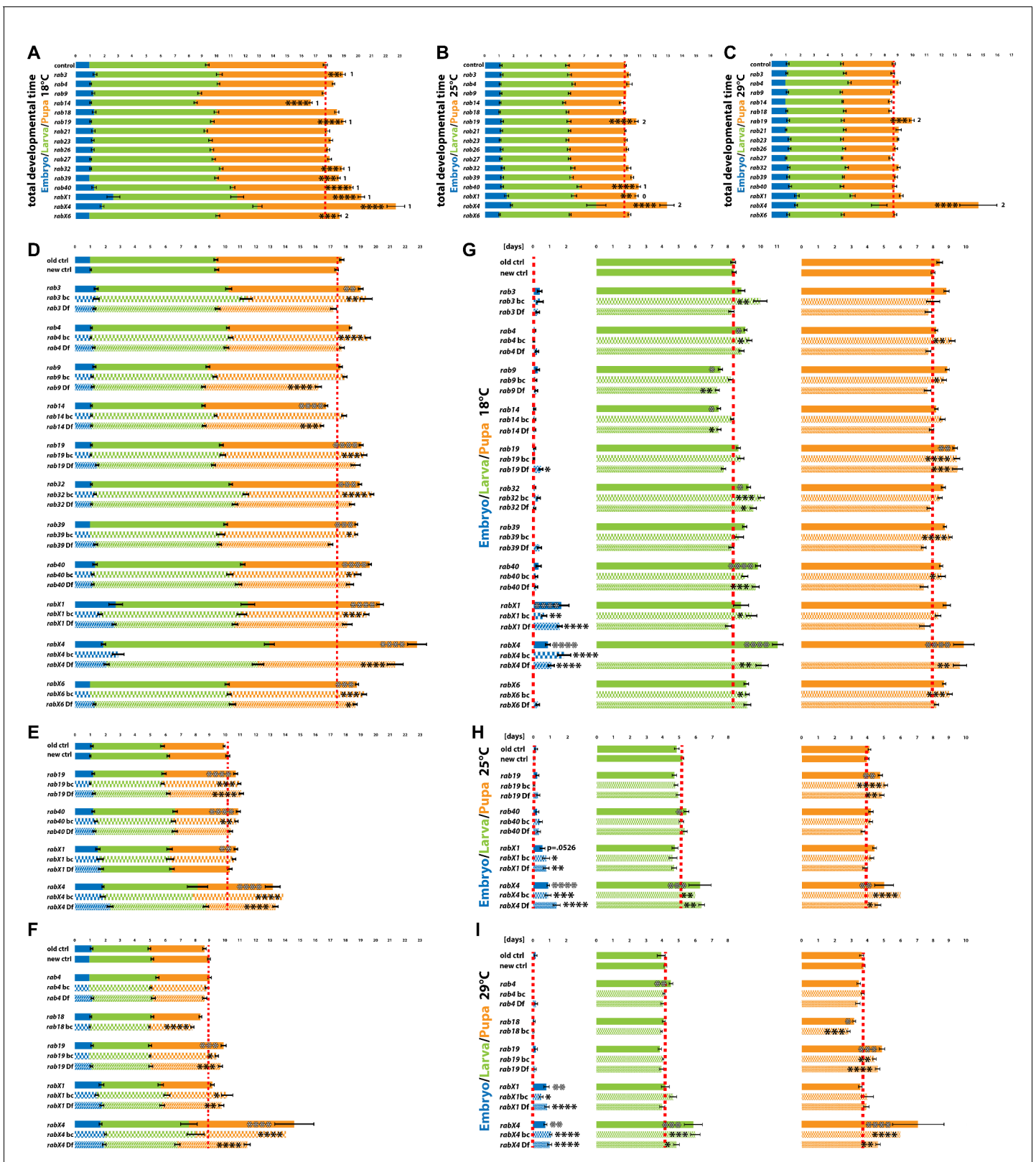


**Figure 2—figure supplement 1.** Validation of developmental timing phenotypes of viable *rab* mutants at different temperatures. (A–C) Total developmental time of control and viable *rab* mutants at 18°C (A), 25°C (B) and 29°C (C). 0, 1, or 2 indicate if the specific phenotype could not be validated (0), could be validated by either backcrossing or mutant over deficiency (1) or could be validated by both (2). (D–I) Validation of *Figure 2—figure supplement 1 continued on next page*

*Figure 2—figure supplement 1 continued*

developmental timing phenotypes with either backcrossed mutants (bc, chequered pattern) or/and *rab* mutant over deficiency (Df, shaded pattern). Shown are total development and the specific developmental stages at 18°C (**D and G**), 25°C (**E and H**), and 29°C (**F and I**). (**A–I**) Dashed red line = mean of control. Developmental stages: embryo (blue), larva (green) and pupa (orange). Mean  $\pm$  SEM; \* $p < 0.05$ , \*\* $p < 0.01$ , \*\*\* $p < 0.001$ , \*\*\*\* $p < 0.0001$ ; Unpaired non-parametric Kolmogorov-Smirnov test.

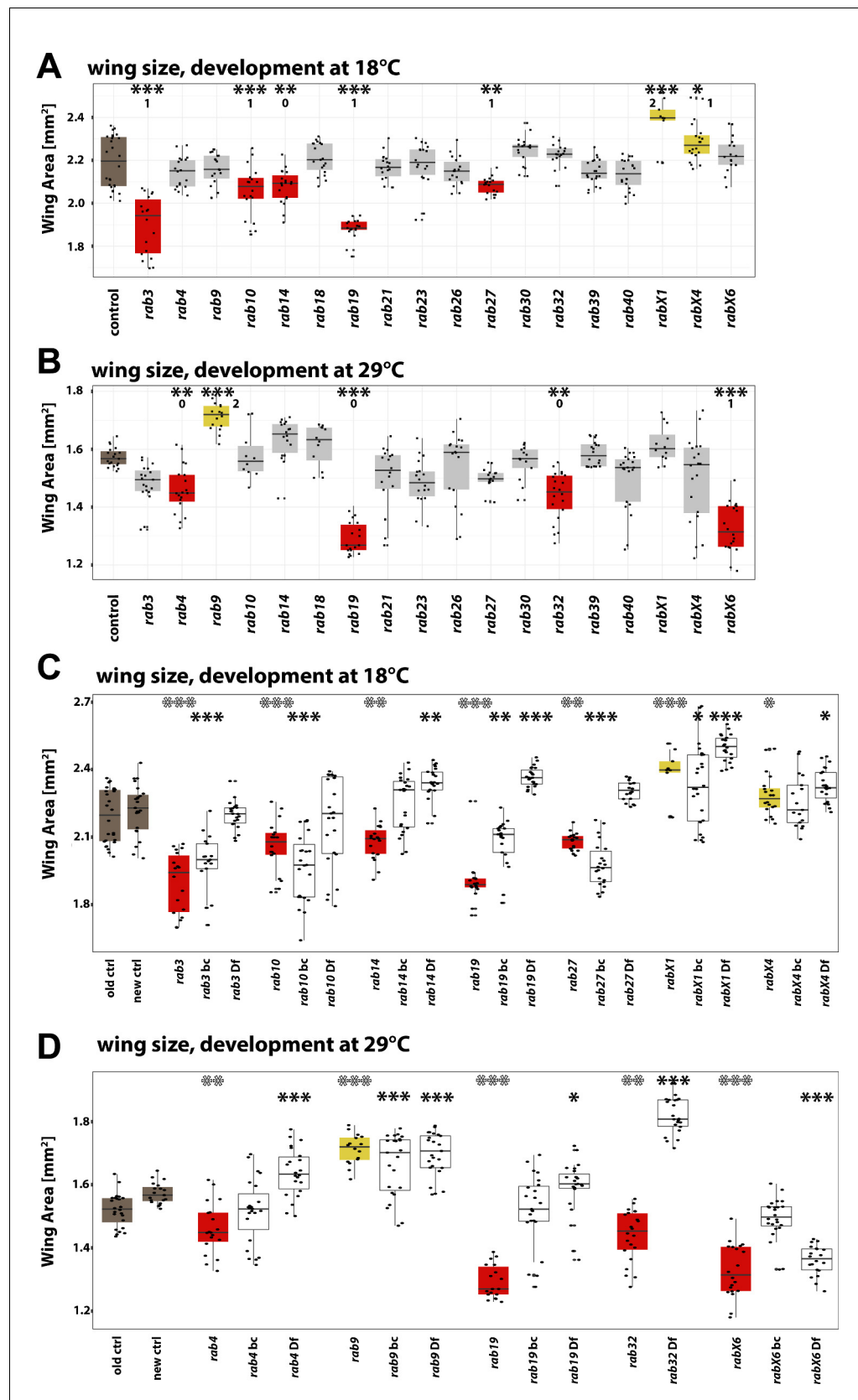


**Figure 2—figure supplement 2.** Wing surface area measurement—for all homozygous viable *rab* mutants at 18°C and 29°C. (A–B) Wing surface area measurement for all homozygous viable *rab* mutants at 18°C (A) and 29°C (B). *Figure 2—figure supplement 2 continued on next page*

*Figure 2—figure supplement 2 continued*

Wild type (brown) and *rab* mutant (gray) wing size. Significantly reduced (red) and increased wing sizes (yellow) compared to control are highlighted. 0, 1, or 2 indicate if the specific phenotype could not be validated (0), could be validated by either backcrossing or mutant over deficiency (1) or could be validated by both (2). (C–D) Wing surface area measurements of either backcrossed mutants (bc) or/and *rab* mutant over deficiency (Df) showing significant altered wing size at 18°C (C) and 29°C (D). *rab* mutants with significantly reduced wing size are highlighted in red and with an increased wing size in yellow. (A–D) Boxplot with horizontal line representing the median; individual data points are represented as dots. Ten to 22 wings per genotype were quantified; \* $p < 0.05$ , \*\* $p < 0.01$ , \*\*\* $p < 0.001$ , \*\*\*\* $p < 0.0001$ ; ordinary one-way ANOVA with pair-wise comparison.

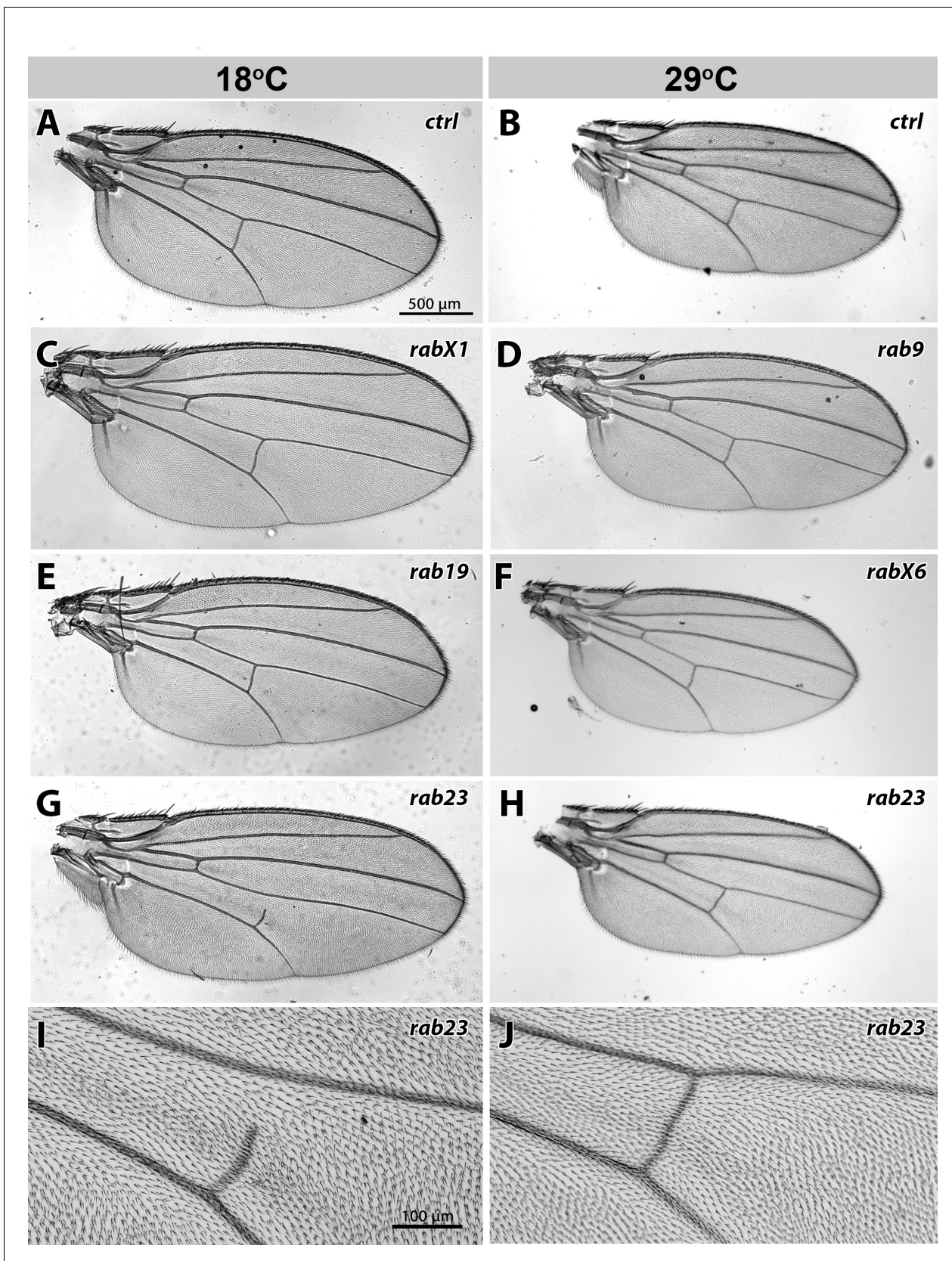


**Figure 2—figure supplement 3.** Examples of wing defects after development at different temperatures. (A–J) Wing sizes of *rab* mutants at 18°C and 29°C. Flies at 29°C have on average 30% smaller wings than flies at 18°C (A–B). At 18°C, *rabX1* has significantly larger wings than control, while *rab19* Figure 2—figure supplement 3 continued on next page

Figure 2—figure supplement 3 continued

has significantly smaller wings than control (C, E). At 29°C, *rab9* has larger wings than control, while *rabX6* has smaller wings than control (D, F). *rab23* shows, in addition to the PCP phenotype that is consistent at both temperatures, a p-cv vein shortening that is present in 90% of cases at 18°C (G, I), but is reduced to 12% at 29°C (H, J). Scale bar = 500 μm (A–H), 100 μm (I–J).

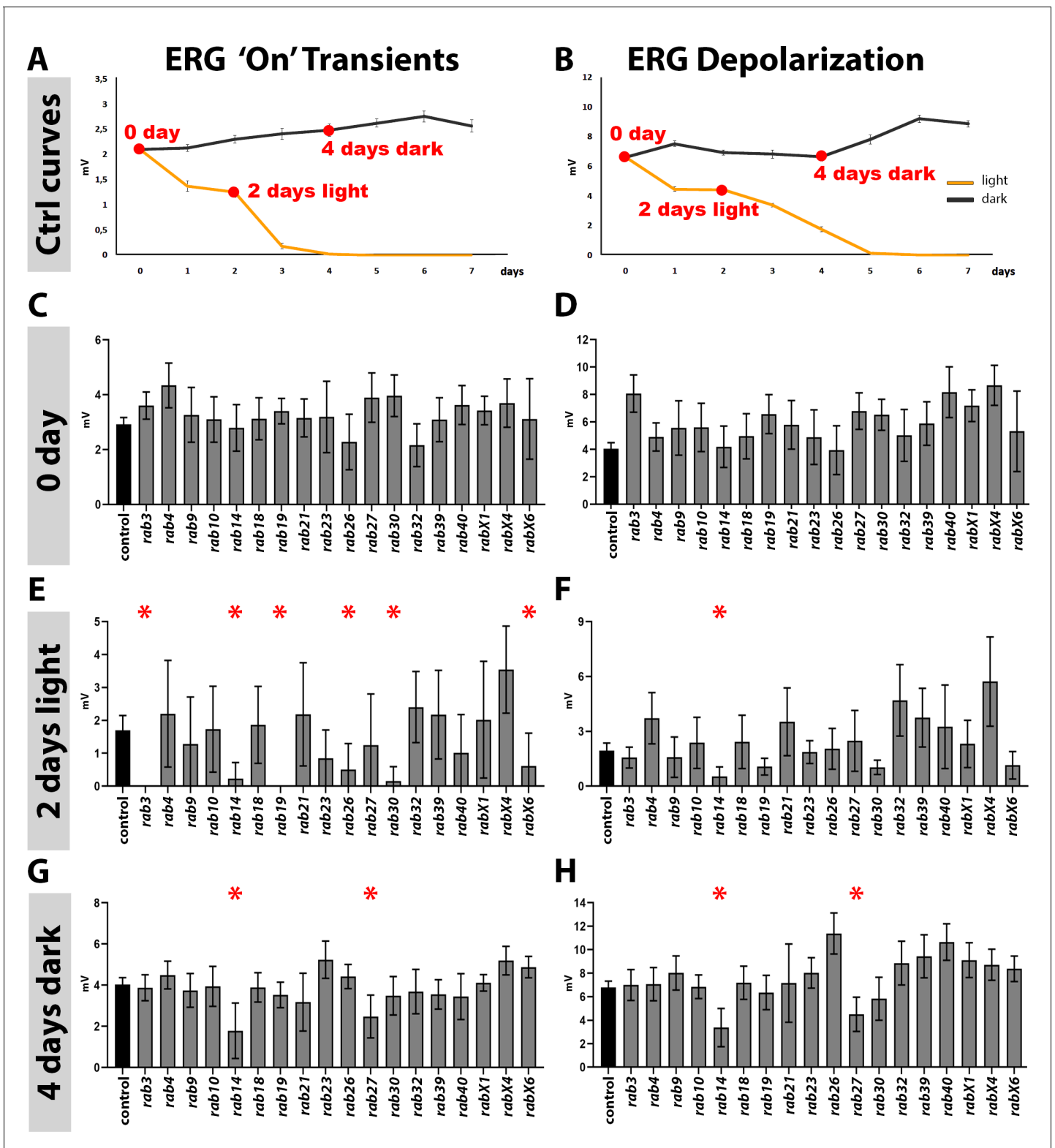


**Figure 3.** Analysis of neuronal function and maintenance based on electroretinograms. (A–B) Sensitization curves for light stimulated (orange curve) and dark-reared (black curve) wild type flies generated by electroretinogram (ERG) recordings. ‘on’ transient signal is lost after 4 days of light stimulation. Complete loss of depolarization signal after 5 days of light stimulation. 0 day, 2 days light stimulation and 4 days dark-rearing are highlighted in red. Mean ± SEM; 25–30 flies were recorded for each day (0–7 days) and each condition (light and dark); Ordinary one-way ANOVA with pair-wise comparison. (C–D) ‘on’ transient and depolarization of newly hatched (0 day) flies. Wild type control in black, all homozygous viable *rab* mutants in Figure 3 continued on next page

Figure 3 continued

grey. (E–F) 'on' transient and depolarization of wild type (black) and homozygous viable *rab* mutants (grey) after 2 days of light stimulation. (G–H) 'on' transient and depolarization of wild type (black) and homozygous viable *rab* mutants (grey) after 4 days of dark-rearing. (C–H) Mean  $\pm$  SD; \* $p < 0.05$ ; 25–30 flies were recorded for each genotype and condition; ordinary one-way ANOVA with group-wise comparison.

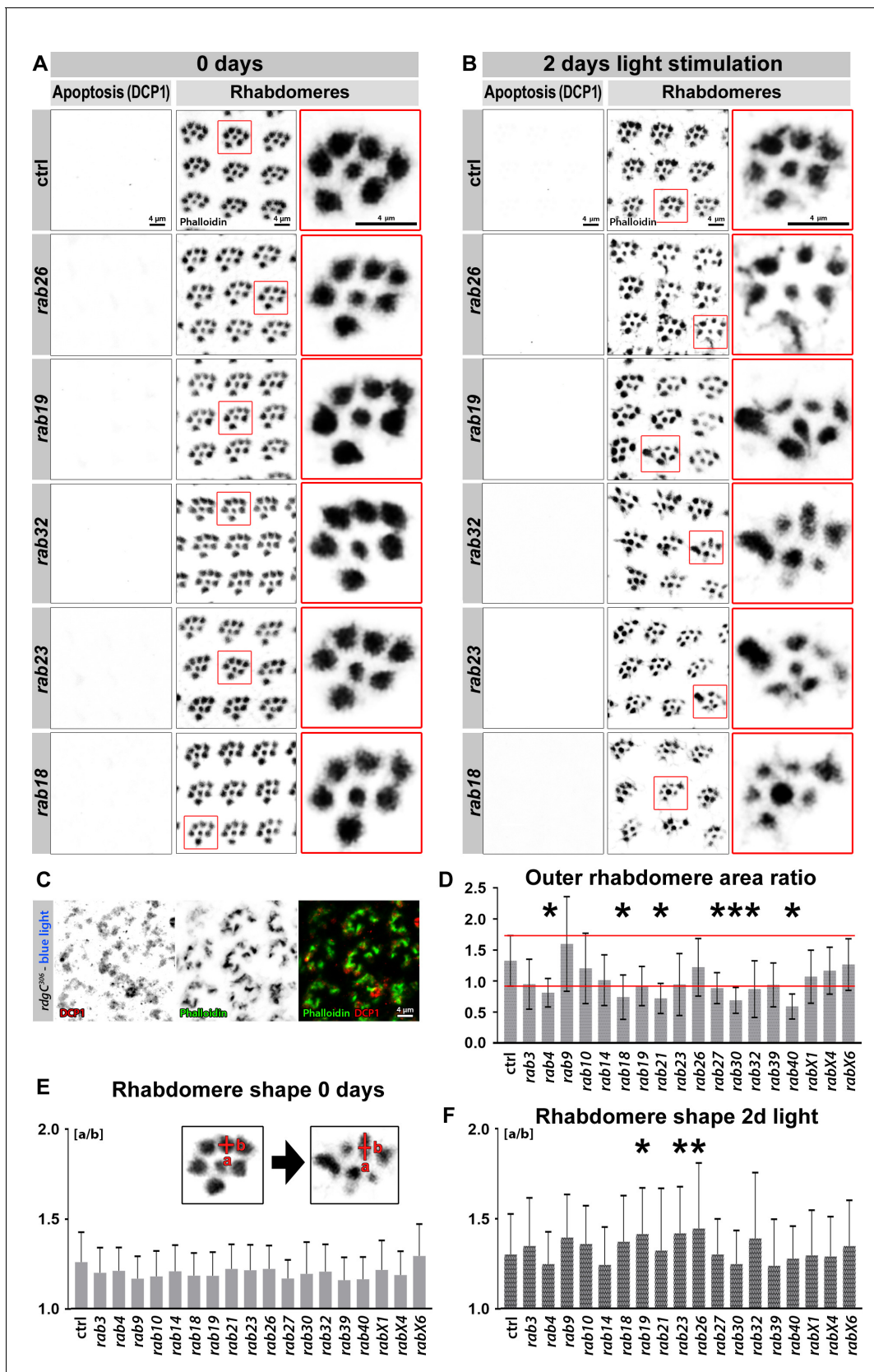


**Figure 4.** Viable *rab* mutants show no apoptosis based on DCP-1 immunolabeling but display morphological changes in rhabdomeres after continuous light stimulation. (A–B) Examples of *rab* mutant retinas which show rhabdomere changes and no increased levels in the apoptotic marker DCP-1 after 2 days of light stimulation. *Figure 4 continued on next page*

## Figure 4 continued

days of light stimulation compared to control (B) and newly hatched flies (A). Zoom-ins of single ommatidia are highlighted by red boxes. Scale bar = 4  $\mu\text{m}$ ; number of retinas  $n = 5-7$  from different animals per antibody staining. (C) *rdgC<sup>306</sup>* mutant ommatidia show high levels of DCP-1 (red) after continuous blue light stimulation. Labeling with phalloidin (green) reveals highly disrupted rhabdomere morphology. Scale bar = 4  $\mu\text{m}$ ; number of retinas  $n = 4$  per antibody staining. (D) Area ratio of outer rhabdomeres R1-R6. The standard deviation range of wild type control is highlighted by red lines. Outer rhabdomere area ratio was calculated as described in Materials and methods. Mean  $\pm$  SD; \* $p < 0.05$  (only significances outside SD range are marked); number of outer rhabdomeres counted  $n = 150$  from three to six animals. Ordinary one-way ANOVA with group-wise comparison. (E-F) After 2 days of light stimulation outer rhabdomere shape exhibited increased variability (F) compared to newly eclosed flies (E). Outer rhabdomere shape was calculated as described in Materials and methods and examples of single ommatidia (left: 0 day, right: 2 days of light stimulation) are shown in the zoom-ins (E). Mean  $\pm$  SD; \* $p < 0.05$ ; number of outer rhabdomeres counted  $n = 150$  from three to six animals. Ordinary one-way ANOVA with group-wise comparison.

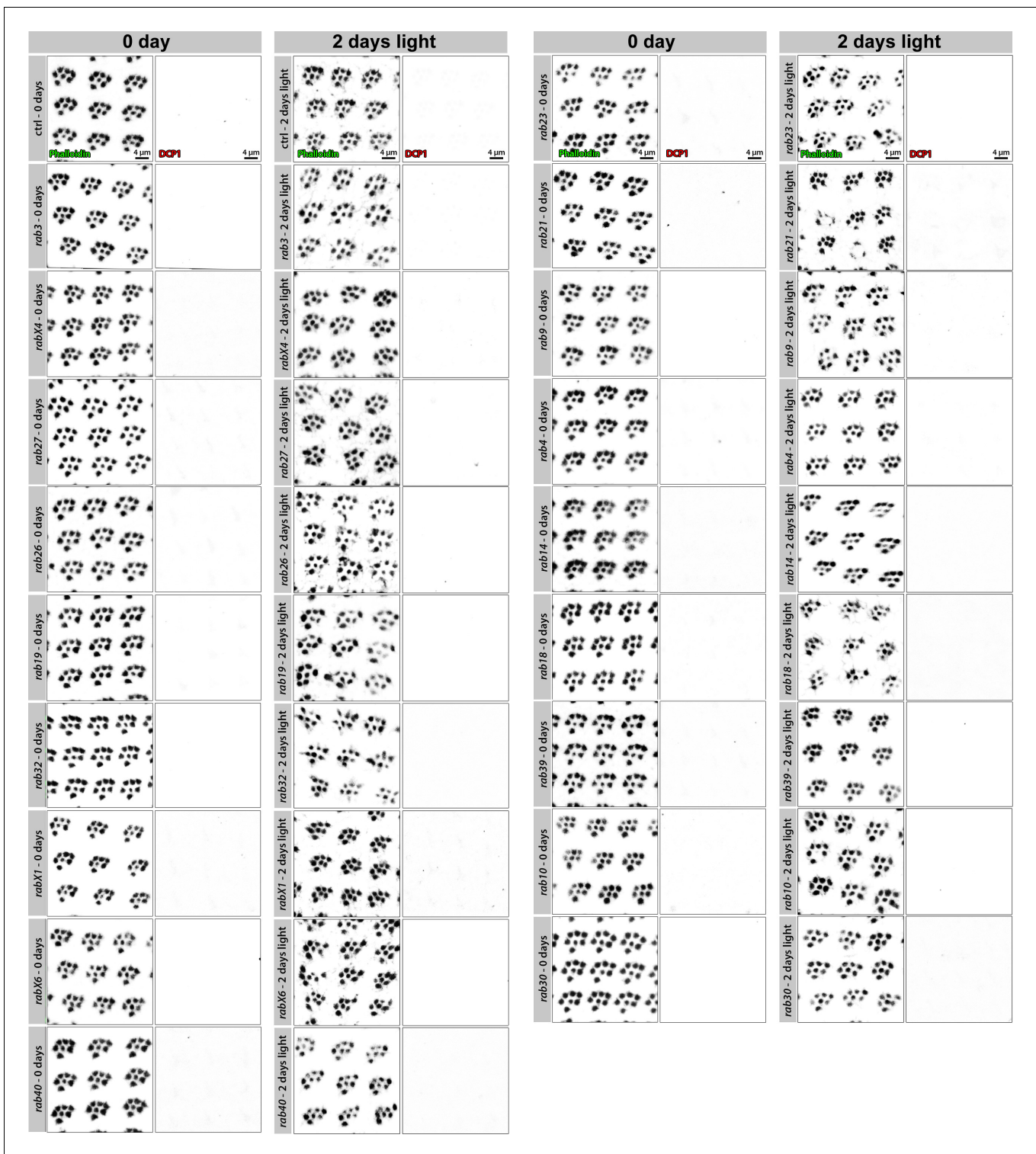


**Figure 4—figure supplement 1.** No viable *rab* mutants show apoptosis based on DCP-1 immunolabeling, some display morphological changes in rhabdomeres after 2 days of continuous light stimulation. Labeling of newly hatched wild type and *rab* mutant retinas with Phalloidin and DCP-1 reveals normal rhabdomere development and no indication of apoptosis. No apoptotic cell death can be observed after 2 days of light stimulation. A number of *rab* mutants reveal morphological changes of the rhabdomeres (for rhabdomere area and shape quantification see **Figure 4**). Shown are representative examples of ommatidia. Scale bar = 4 μm; number of retinas n = 5–7 from different animals per antibody staining.

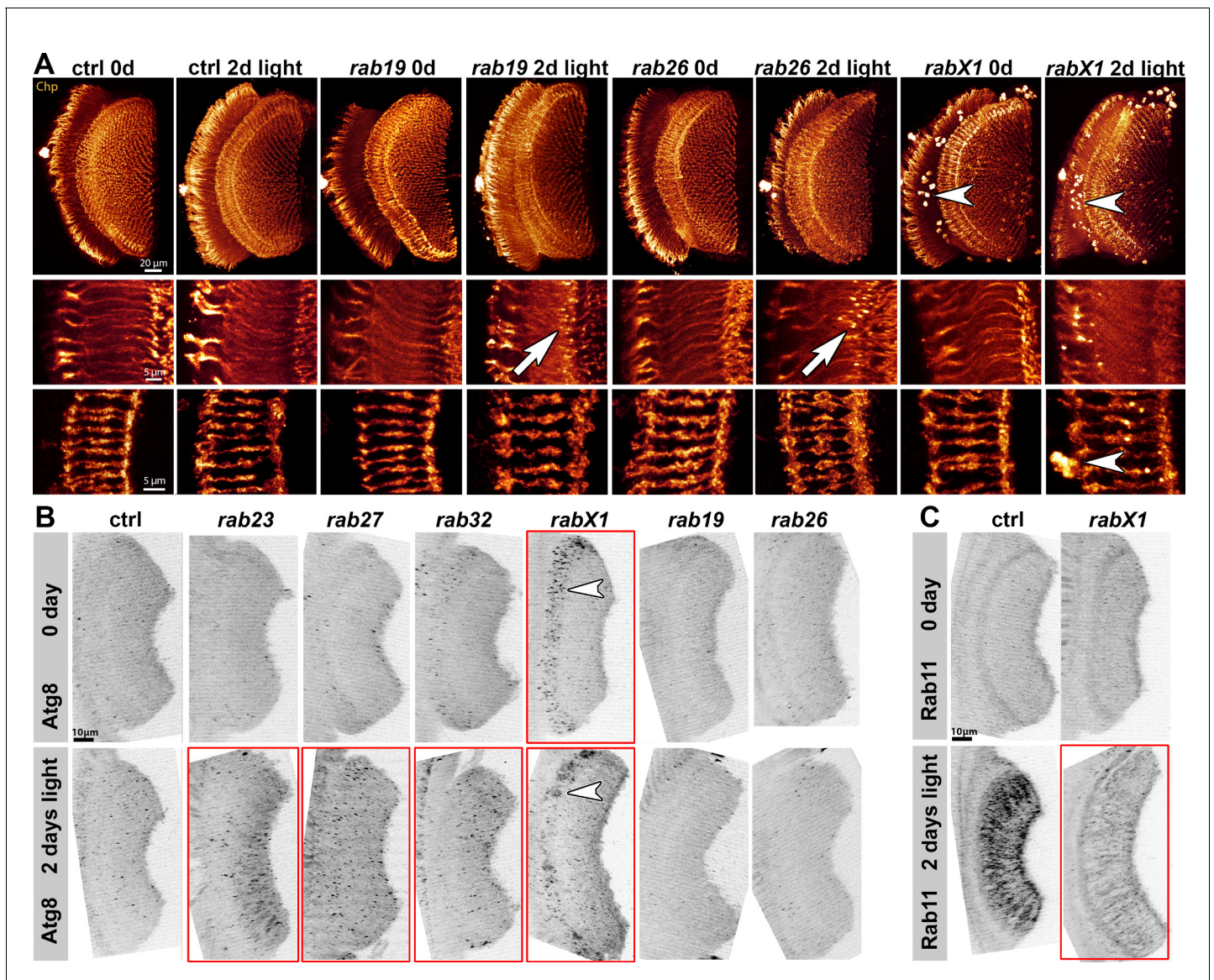


**Figure 5.** Analyses of morphology, recycling endosomal function (Rab11) and autophagy (Atg8) at photoreceptor axon terminals after continuous light stimulation. (A) Examples of Choptin-labeling (Chp) of 0 day and 2 days light stimulated wild type and *rab* mutant photoreceptor projections (overview top panel, R1-R6 middle panel, R7-R8 bottom panel). The *rabX1* mutant exhibits Choptin accumulations in non-photoreceptor cell bodies independent of stimulation (arrowheads). After 2 days of light stimulation, *rab26* and *rab19* mutants display membrane accumulations in their axon terminals (arrows). Scale bar = 20  $\mu$ m (top panel), 5  $\mu$ m (middle and bottom panel); number of brains  $n = 3-5$  per antibody staining. (B) Examples of Atg8 labeling of photoreceptor projections in retina-lamina preparations of newly hatched and 2 days light stimulated wild type flies and six *rab* mutants. Only *rab23*, *rab27*, and *rab32* show significant increases in Atg8-positive compartments after 2 days of light stimulation (highlighted by red boxes). *rabX1* flies exhibit Atg8-positive compartments in cell bodies (arrowheads). Scale bar = 10  $\mu$ m; number of retina-lamina preparations  $n = 3$  for each condition and staining. (C) Examples of Rab11 labeling of photoreceptor projections in retina-lamina preparations of newly hatched and 2 days light stimulated wild type and *rabX1* flies. Increase in Rab11 levels is suppressed in *rabX1* mutants after 2 days of light stimulation (highlighted by red box). Scale bar = 10  $\mu$ m; number of retina-lamina preparations  $n = 3$  for each condition and staining.

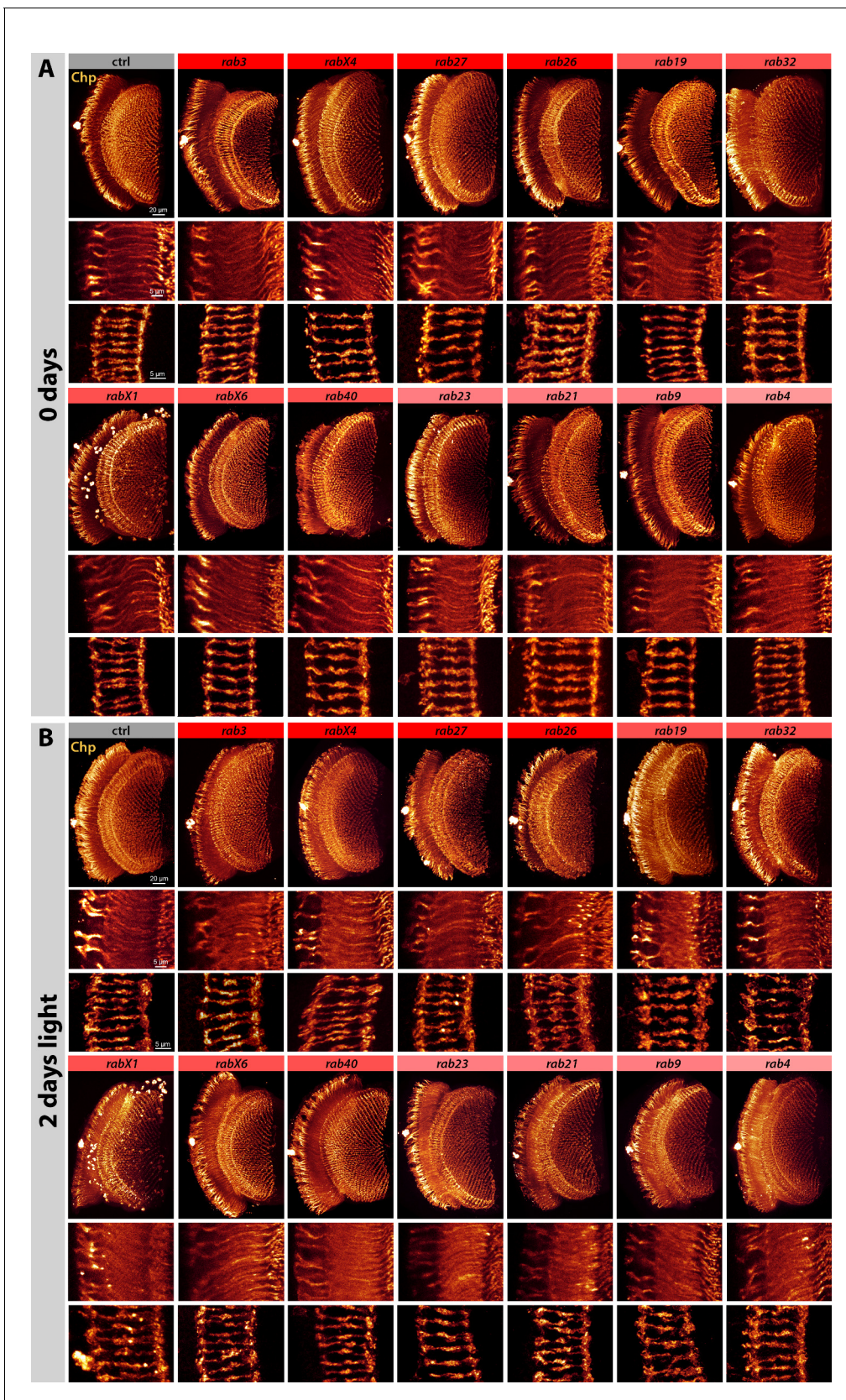


**Figure 5—figure supplement 1.** Systematic analysis of photoreceptor axon morphology of newly eclosed adults and after 2 days of continuous light stimulation. (A) Labeling of newly hatched wild type and mutant photoreceptor projections with Choptin (Chp) reveals no noticeable morphological Figure 5—figure supplement 1 continued on next page

*Figure 5—figure supplement 1 continued*

differences. Chaoptin-positive accumulations in non-photoreceptor cells are visible in *rabX1*. Optic lobe overview (top panel), lamina cross-section with R1-R6 axon terminals (middle panel), and R7-R8 axon terminals (bottom panel). Scale bar top panel = 20  $\mu\text{m}$ , middle and bottom panel = 5  $\mu\text{m}$ ; number of brains  $n = 3\text{--}5$  per antibody staining. **(B)** Labeling of wild type and mutant photoreceptor projections with Chaoptin (Chp) after 2 days of light stimulation. Chaoptin-positive accumulations in non-photoreceptor cells are visible in *rabX1*. Only *rab19* and *rab26* display morphological differences in their photoreceptor projection terminals, showing membrane accumulations in the tips of R1-R6 axon terminals. Optic lobe overview (top panel), lamina cross-section with R1-R6 axon terminals (middle panel), and R7-R8 axon terminals (bottom panel). Scale bar top panel = 20  $\mu\text{m}$ , middle and bottom panel = 5  $\mu\text{m}$ ; number of brains  $n = 3\text{--}5$  per antibody staining.

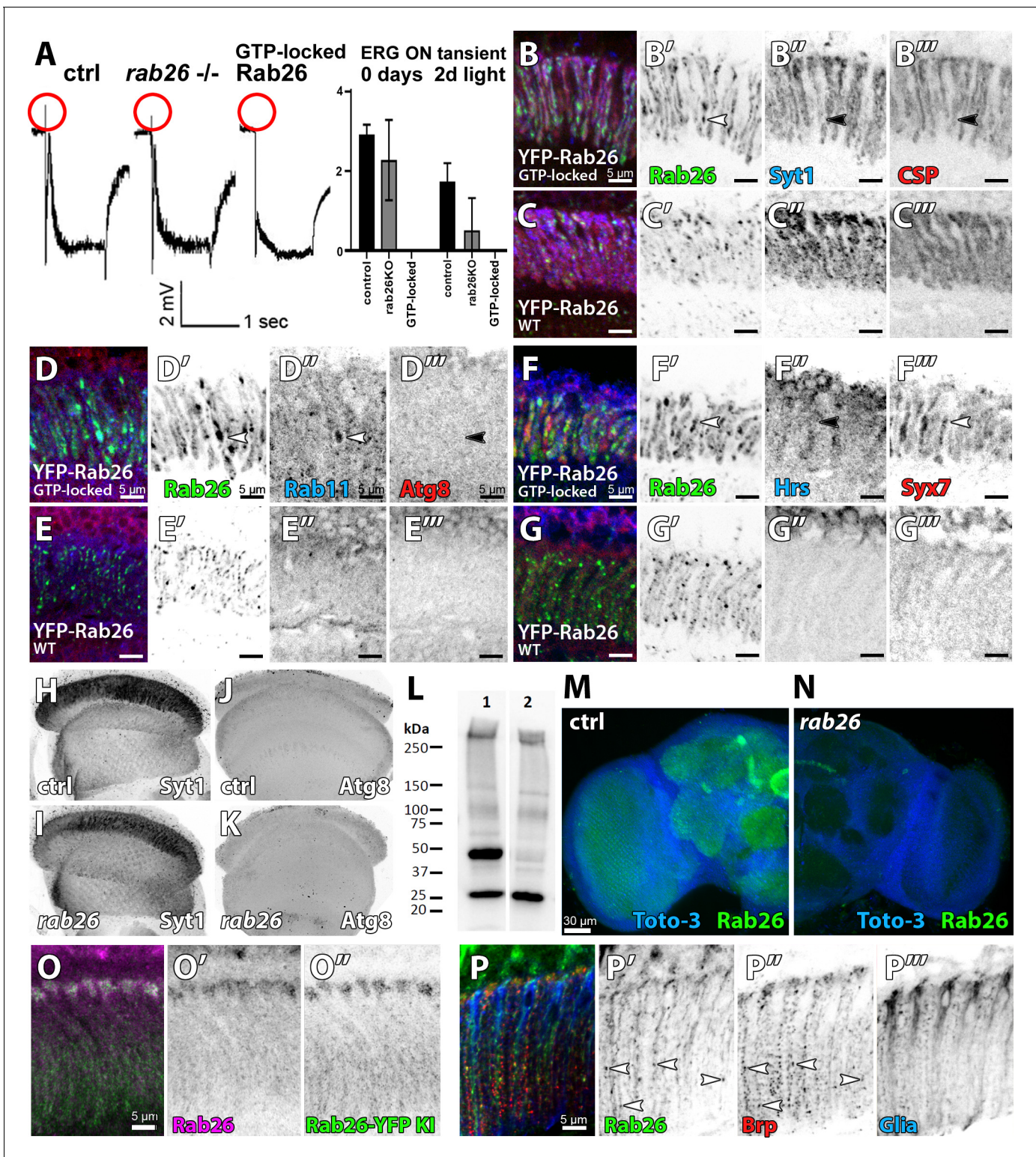


**Figure 6.** Loss of *rab26* does not discernibly affect markers for synaptic vesicles or autophagy in the adult brain. (A) Representative ERG traces of recordings of 2 days light stimulated wild type, *rab26* mutant, and Rab26 GTP-locked overexpression flies. Only the Rab26 GTP-locked flies show a complete loss of 'on' transient (highlighted in red). Quantification of the 'on' transient is shown right. (B–G) Labeling of lamina cross-sections of Rab26 GTP-locked (B, D, and F) and YFP-tagged Rab26WT (C, E, and G) against Syt1 and CSP (B and C), Rab11 and ATG8 (D and E), and Hrs and Syx7/ Avalanche (F and G). GTP-locked Rab26 shows colocalization with Rab11 and Syx7/Avalanche (white arrowheads), but not with Syt1, CSP, Atg8 nor Hrs (black arrowheads). Scale bar = 5 μm; number of brains n = 3–5 per antibody staining. (H–K) Intensity comparison of optic lobes of newly hatched wild type and *rab26* mutant flies. (L) Western blot analysis of Rab26 protein levels in control and *rab26* mutant flies. (M–N) Whole-brain immunofluorescence analysis of Rab26 localization in control (M) and *rab26* mutant (N) flies. (O–P) High-magnification immunofluorescence (O) and electron microscopy (P) analysis of Rab26 localization in control (O) and *rab26* mutant (P) flies. Scale bar = 5 μm.

## Figure 6 continued

type and *rab26* mutant flies, stained against Syt1 (**H and I**) and Atg8 (**J and K**). Number of brains  $n = 3-5$  per antibody staining. (**L**) Validation of the *rab26* null mutant by Western Blot with the newly generated Rab26 antibody. Wild type control shows the Rab26 band at around 45 kDa (1), which is lost in the *rab26* mutant (2). (**M and N**) Validation of the *rab26* null mutant by immunohistochemistry with the newly generated Rab26 antibody. The Rab26 antibody labels synaptic neuropil in different regions of wild type brains (green, **M**), which is lost in the *rab26* null mutant (**N**). Labeling of nuclei/cell bodies with Toto-3 (blue). Scale bar = 30  $\mu\text{m}$ ; number of brains  $n = 3$  per antibody staining. (**O**) Immunolabeling of Rab26 (red) shows high colocalization with the endogenously YFP-tagged Rab26 (green). Lamina cross-section of newly hatched flies. Scale bar = 5  $\mu\text{m}$ ; number of brains  $n = 3-5$  per antibody staining. (**P**) Co-labeling of wild type lamina with Rab26 (green), Brp (synaptic marker, red), and ebony (glia marker, blue) reveals few synapses, positive for Rab26 and Brp in the proximal region of the lamina (white arrowheads, **P'** and **P''**). No colocalization between Rab26 and ebony could be observed (**P'''**). Scale bar = 5  $\mu\text{m}$ ; number of brains  $n = 3-5$  per antibody staining.

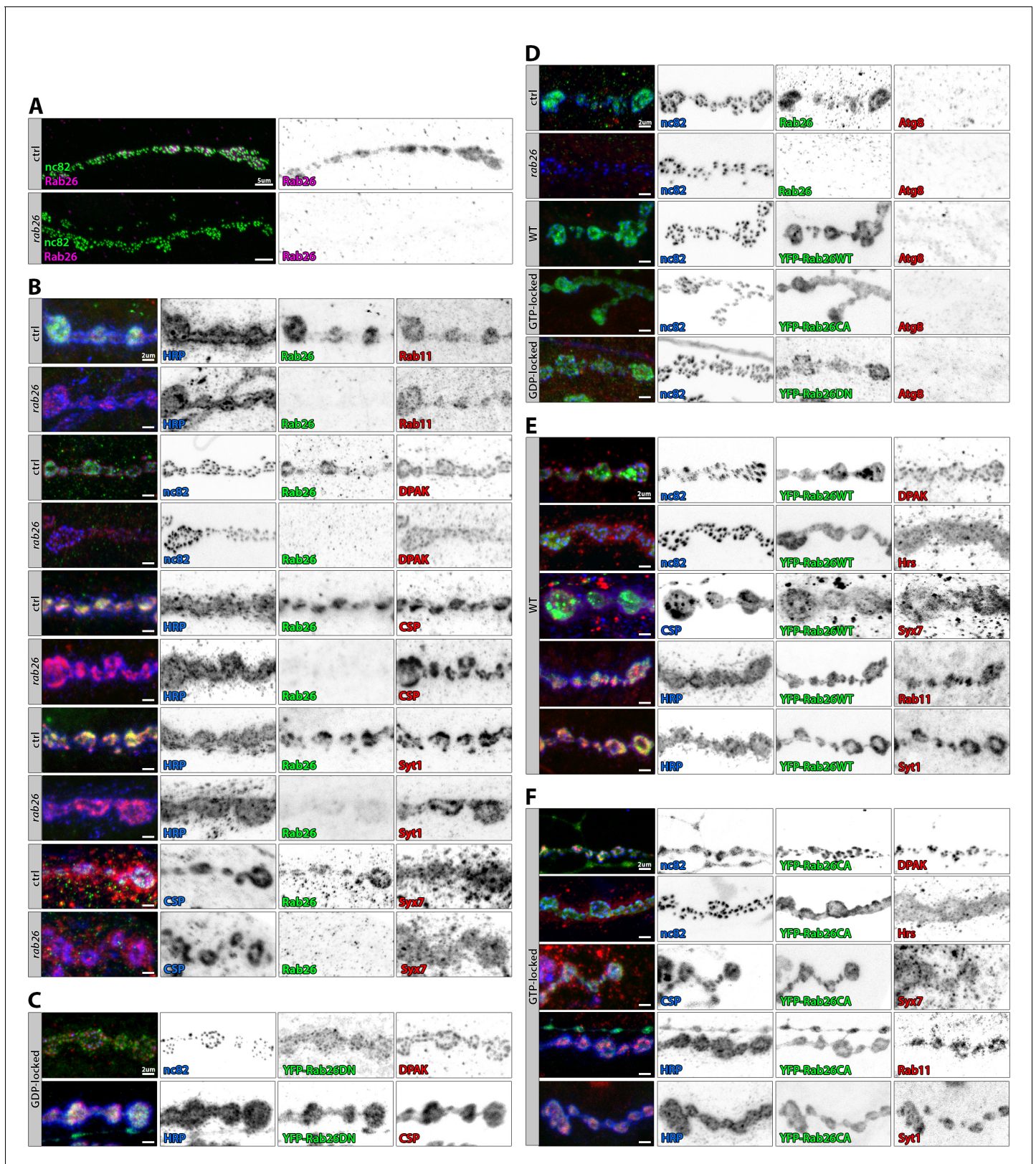


**Figure 6—figure supplement 1.** Rab26 colocalizes with synaptic vesicle and endosomal markers at larval neuromuscular junction (NMJ) boutons. (A) Immunolabeling of Rab26 (magenta) reveals its presence in NMJ boutons labeled by the active zone marker nc82 (green). The loss of Rab26 seems to have no effect on the overall NMJ morphology. Scale bar = 5  $\mu$ m; number of NMJs  $n = 5$ –12 from three to six larvae per antibody staining. (B–F) Figure 6—figure supplement 1 continued on next page

*Figure 6—figure supplement 1 continued*

Colocalization of Rab26 (green) with several markers (red) in larval NMJs which are labeled by nc82, HRP, or CSP (blue). **(B)** Endogenous Rab26 partially colocalizes with synaptic vesicle markers (CSP, Syt1), with endosomal (Syx7) and recycling endosomal (Rab11) markers, but not the postsynaptic marker DPAK. **(C)** GDP-locked Rab26 is more diffusely localized and partially colocalizes with CSP. **(D)** The autophagosomal marker Atg8 is not enriched in larval NMJs and does not colocalize with endogenous or overexpressed Rab26. Rab26 overexpression or the *rab26* mutant do not affect Atg8 immunolabeling. **(E–F)** Overexpressed WT and GTP-locked forms of Rab26 colocalize with Syt1, CSP, Syx7, and Rab11, but not with the postsynaptic marker DPAK. Scale bar = 2  $\mu$ m; number of NMJs n = 5–12 from three to six larvae per antibody staining.

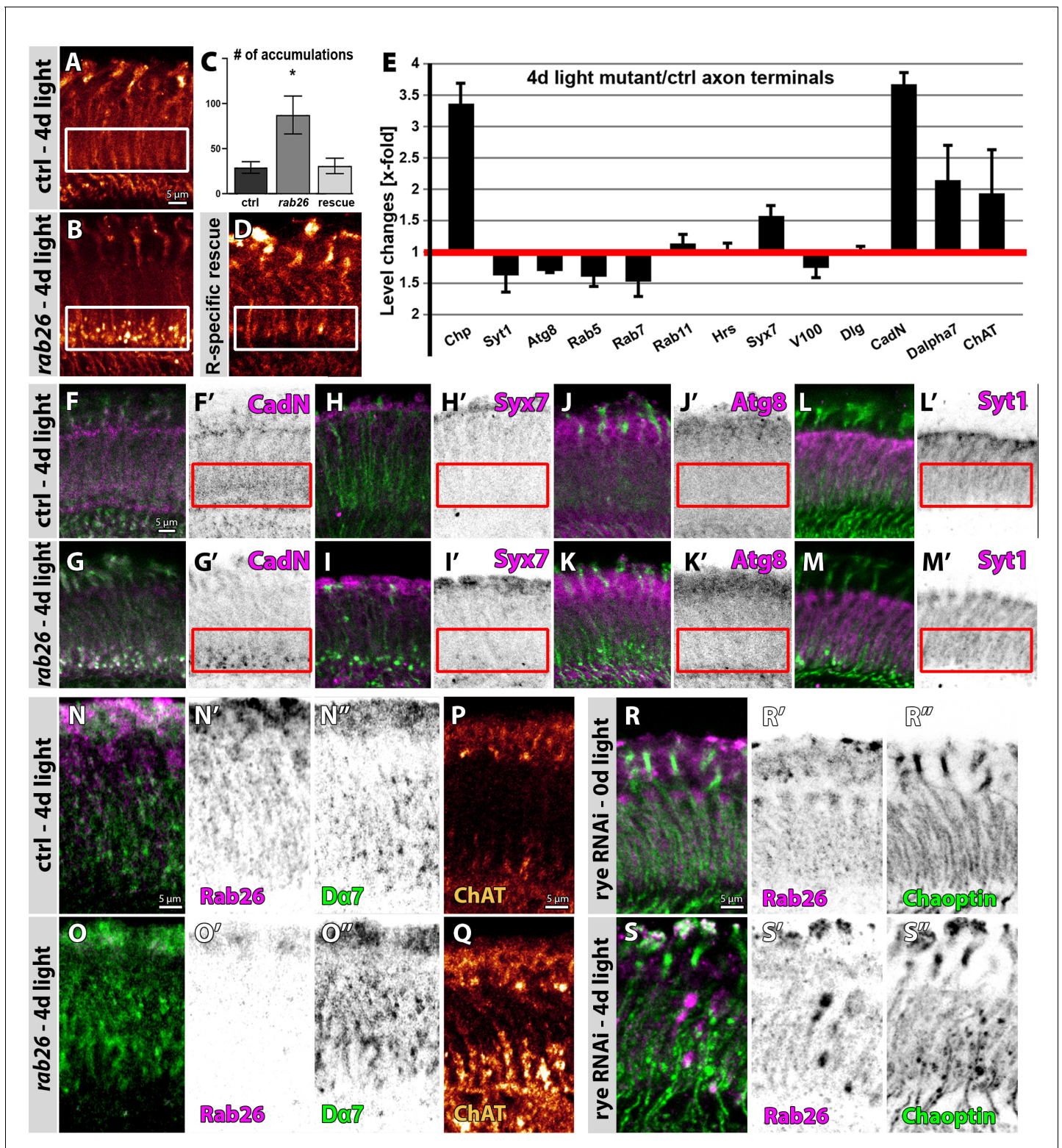


**Figure 7.** Rab26 is required for membrane receptor turnover associated with cholinergic synapses. (A–D) *rab26* mutant R1–R6 photoreceptor terminals (B) exhibit Choptin-positive accumulations in the proximal lamina after 4 days of light stimulation (highlighted with white boxes), which are rescued by photoreceptor-specific Rab26 expression (C and D). (C) Quantification. Mean  $\pm$  SEM; \* $p < 0.05$ ; number of lamina per genotype  $n = 8$ ; ordinary one-way ANOVA with pair-wise comparison. Scale bar = 5  $\mu\text{m}$ ; number of brains  $n = 5$ . (E) Quantification of level changes of 13 membrane-associated proteins in the *rab26* mutant axon terminals after 4 days of light stimulation. (F–M) Examples of lamina cross-sections of wild type (F, H, J and L) and *rab26* (G, I, K and M) after 4 days of light stimulation. (N–Q) Examples of lamina cross-sections of wild type (N, P) and *rab26* (O, Q) after 4 days of light stimulation. (R–S) Examples of lamina cross-sections of wild type (R) and *rab26* (S) after 0 days of light stimulation. Figure 7 continued on next page

## Figure 7 continued

mutant (**G**, **I**, **K** and **M**) after 4 days of light stimulation, showing proteins that are upregulated in R1-R6 terminals (CadN, (**F–G**); Syx7 (**H–I**)) and proteins that are unaffected (Atg8, (**J–K**); Syt1, (**L–M**)). The proximal lamina region is highlighted by red boxes. Scale bar = 5  $\mu\text{m}$ ; number of brains  $n = 3\text{--}5$  per antibody staining. (**N–O**) The *rab26* mutant exhibits an increase of D $\alpha$ 7 (green) across the lamina compared to wild type after 4 days of light stimulation. Shown are lamina cross-sections. Scale bar = 5  $\mu\text{m}$ ; number of brains  $n = 3\text{--}5$  per antibody staining. (**P–Q**) The *rab26* mutant shows an increase of ChAT in the proximal lamina compared to wild type after 4 days of light stimulation. Scale bar = 5  $\mu\text{m}$ ; number of brains  $n = 3\text{--}5$  per antibody staining. (**R–S**) Photoreceptor-specific knock down of rye leads to an increase of Chaoptin and Rab26 in the lamina after 4 days of light stimulation (**S**) compared to newly hatched flies (**R**). Rab26 accumulates throughout the lamina (**S'**), whereas Chaoptin accumulates in the proximal lamina (**S''**). Scale bar = 5  $\mu\text{m}$ ; number of brains  $n = 3\text{--}5$  per antibody staining.

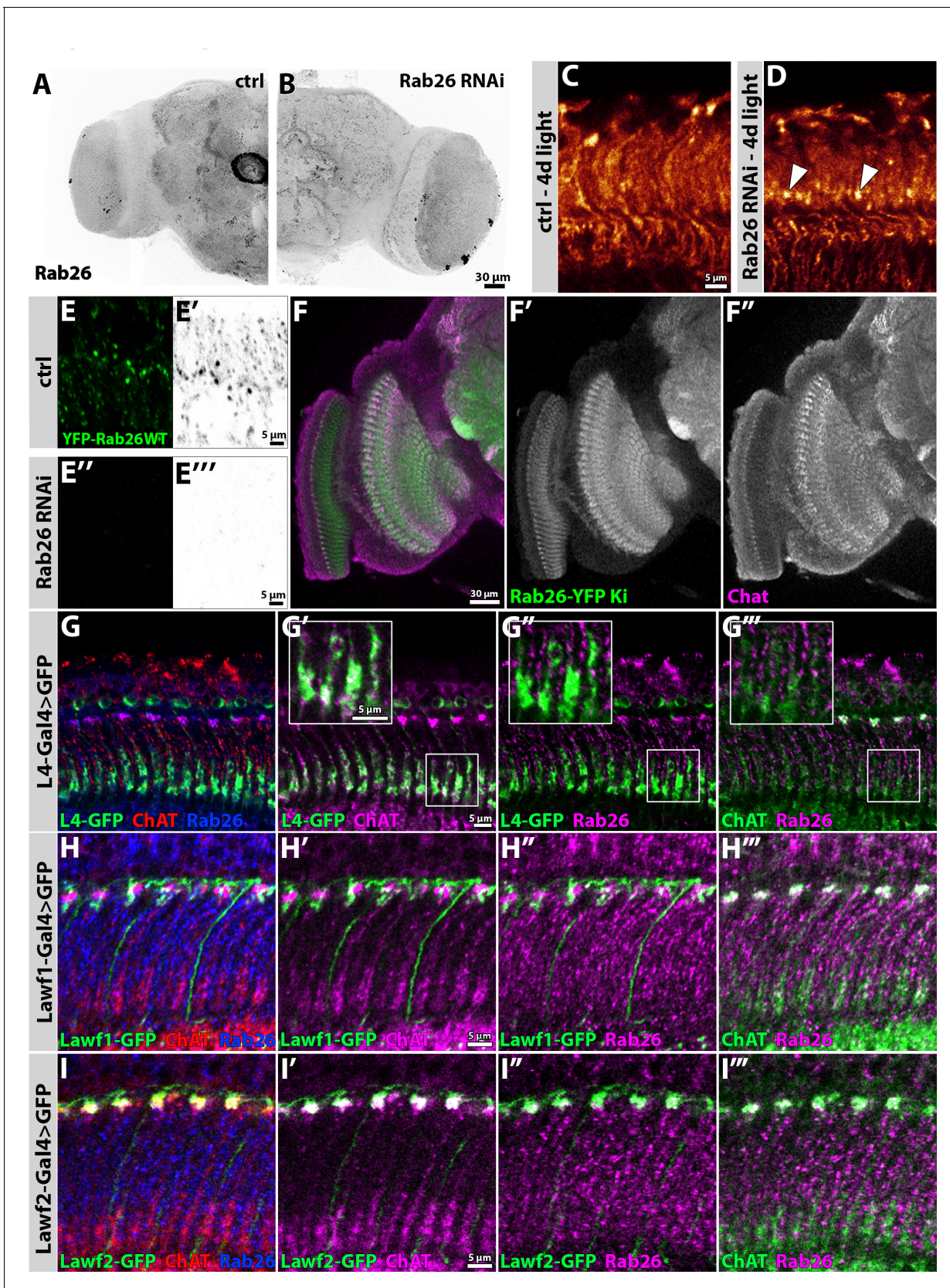


**Figure 7—figure supplement 1.** Rab26 RNAi recapitulates the null mutant lamina phenotype. Endogenous Rab26 protein localizes to Lawf2-neurons in the lamina and strongly colocalizes with choline acetyl transferase throughout the adult brain. (A–B) Rab26 RNAi leads to reduced anti-Rab26

Figure 7—figure supplement 1 continued on next page

## Figure 7—figure supplement 1 continued

immunolabeling when driven by *elav-Gal4* (B). Scale bar = 30  $\mu\text{m}$ ; number of brains  $n = 3\text{--}5$ . (C–D) Photoreceptor-specific expression of Rab26 RNAi leads to Chaoptin-accumulations in the proximal lamina after days of light stimulation (D, white arrowheads) compared to control (C, driver only) mimicking the *rab26* mutant phenotype. Scale bar = 5  $\mu\text{m}$ ; number of brains  $n = 4\text{--}5$  per antibody staining. (E) In flies, expressing both the YFP-tagged wild type form of Rab26 (green (E, E''), gray (E', E''')) and Rab26 RNAi driven by GMR-Gal4 (E''–E'''), the YFP signal is strongly decreased compared to the control (GMR-Gal4 driving only expression of Rab26 WT, E–E'). Scale bar = 5  $\mu\text{m}$ ; number of brains  $n = 3\text{--}5$ . (F) Across the optic lobe, the expression pattern of Rab26 (green) is similar to ChAT immunolabeling (magenta). Ki = knock in; Scale bar = 30  $\mu\text{m}$ ; number of brains  $n = 3\text{--}5$  per antibody staining. (G) Co-labeling of L4 monopolar cells (green) with Rab26 (blue) and ChAT (red) in newly hatched flies. Proximal L4 terminals (green) in the lamina colocalize with ChAT (magenta) (G'), while Rab26 (magenta) labeling is complementary to the L4 terminals (green) (G''). Bulbous processes in the distal lamina are positive for Rab26 (magenta) and ChAT (green) (G'''). Zoom-ins of the L4 terminal region, are indicated by the white boxes. Scale bar = 5  $\mu\text{m}$ ; number of brains  $n = 3\text{--}5$  per antibody staining. (H) Co-labeling of lamina wide-field feedback neurons type 1 (Lawf1, green) with Rab26 (blue) and ChAT (red) in newly hatched flies. Lawf1-processes in the distal lamina only partially colocalize with ChAT (H') and Rab26 (H''). Rab26 and ChAT strongly colocalize in bulbous-like structures in the distal lamina (H'''). Scale bar = 5  $\mu\text{m}$ ; number of brains  $n = 3\text{--}5$  per antibody staining. (I) Co-labeling of lamina wide-field feedback neurons type 2 (Lawf2, green) with Rab26 (blue) and ChAT (red) in newly hatched flies. Lawf2-processes in the distal lamina strongly colocalize with ChAT (I') and Rab26 (I''). Rab26 and ChAT strongly colocalize in bulbous-like structures in the distal lamina (I'''). Scale bar = 5  $\mu\text{m}$ ; number of brains  $n = 3\text{--}5$  per antibody staining.

## Supplementary Table / Supplementary File 1

### A: Expression in the developing optic lobe (P+40%)

EYFP-Rab	Expression notes
Rab3	Strongly enriched in the synaptic neuropils medulla, lobula and lobula plate. Weakly expressed in the lamina. Weak punctate labeling in cellular cortex regions. No discernable expression in the retina.
RabX4	Intermediate levels in both neuropils and cellular cortex regions. Mildly enriched in the lamina. Weak expression in the retina.
Rab27	Very weak expression at this developmental stage.
Rab26	Strongly enriched in the synaptic neuropils medulla, lobula and lobula plate. Weakly expressed in the lamina. Weak punctate labeling in cellular cortex regions. Weak expression in the retina.
Rab19	Strongly expressed in the lamina and specific regions of the medulla, lobula and lobula complex. Strongly expressed in the cell cortex region adjacent to the lobula plate, weaker in all other cellular cortex regions. Intermediate expression in the retina.
Rab32	Strongly expressed only in photoreceptor neurons, including cell bodies in the retina, axons and terminals in the lamina and medulla.
RabX1	Strongly expressed in all cellular cortex regions; largely excluded from synaptic neuropils. Weak expression in the retina.
RabX6	Intermediate enrichment in all synaptic neuropils and relatively weaker expression in cellular cortices. Intermediate to strong expression in the retina.
Rab40	Weak expression throughout all synaptic neuropils, cellular cortices and in the retina.
Rab23	Strongly but sparsely expressed in a few visual neurons, around the lobula, and in the retina, here especially bristle cells.
Rab21	Weakly expressed in both synaptic neuropils and cellular cortices. Slightly enriched in the lamina and retina.
Rab9	Weakly expressed in all cellular cortices with mild enrichment in the outer layer of the brain, the synaptic neuropils and the retina.
Rab4	Strongly expressed in all cell cortices with a particular enrichment in cells near the lobula plate. Mild enrichment in the retina and in specific neuropil layers, including the distal medulla and the lamina.

### B: Adult neuropil expression pattern

EYFP-Rab	Expression notes
Rab3	Strongly expressed in most or all synaptic neuropils, with particular enrichment in the mushroom body, ellipsoid body and other central brain regions. Relatively weaker expression in the lamina. Largely excluded from cell bodies.
RabX4	Strongly and relatively evenly expressed in most or all synaptic neuropils. Relatively weaker expression in the lamina. Weak expression in cell bodies.
Rab27	Strongly expressed in specific medulla layers, mushroom bodies and some central synaptic neuropils. Relatively weaker expression in many other synaptic neuropil regions, including the lamina and lobula complex. Largely excluded from cell bodies.
Rab26	Strongly expressed in specific synaptic neuropil regions, including distal and proximal medulla layers, the outer central domain of the ellipsoid body (EBoc), the posterior lateral protocerebrum, and the calyx of the mushroom body. Relatively weaker expression in the lamina. Largely excluded from cell bodies.
Rab19	Strongly and relatively evenly expressed in synaptic neuropil regions. Relatively weaker expression in cell bodies.
Rab32	Strong expression in the visual system, with relative enrichment in the synaptic neuropils lamina and medulla. Relatively weaker and even expression in central neuropils and relatively weaker expression in cell bodies.

<b>RabX1</b>	Intermediate expression in both cell bodies and most or all synaptic neuropils.
<b>RabX6</b>	Intermediate expression in both cell bodies and most or all synaptic neuropils.
<b>Rab40</b>	Intermediate expression in most or all synaptic neuropils. Relatively weaker expression in cell bodies.
<b>Rab23</b>	Strongly expressed in cells distal and proximal of the lamina and the protocerebral bridge in the central brain. Weak expression in most other neuropils and cell bodies.
<b>Rab21</b>	Intermediate and relatively even expression in most synaptic neuropils. Weakly expressed in cell bodies.
<b>Rab9</b>	Intermediate to weak expression in synaptic neuropils and cell bodies.
<b>Rab4</b>	Strongly expressed in both synaptic neuropils and cell bodies. Particularly enriched in the mushroom body and the medulla.

## Supplementary Table / Supplementary File 2

Mammalian Rabs	Rab tissue localization in human	Rab tissue localization in rodent	<i>D. melanogaster</i> Rabs	Rab tissue localization in <i>D. melanogaster</i>	References
Rab1a	<b>RNA:</b> low tissue specificity - ubiquitous <b>protein:</b> general cytoplasmic expression	<b>RNA:</b> no regional signal (Mm, E)	DmRab1 (omelette)	<b>RNA:</b> ubiquitous (E, A) <b>protein:</b> ubiquitous (L), brain (A), heart (A)	<b>H:</b> The human protein atlas <b>R:</b> Transcriptome Atlas mouse embryo <b>Dm:</b> (Chan et al., 2011; Zhang et al., 2007) (Cammarato et al., 2011), flyatlas2
Rab1b	<b>RNA:</b> Low tissue specificity – ubiquitous <b>protein:</b> general cytoplasmic expression	<b>RNA:</b> no regional signal (Mm, E)			<b>H:</b> The human protein atlas <b>R:</b> Transcriptome Atlas mouse embryo
Rab2a	<b>RNA:</b> Low tissue specificity – ubiquitous <b>protein:</b> general cytoplasmic expression	<b>RNA:</b> no regional signal (Mm, E)	DmRab2	<b>RNA:</b> central nervous system (E), ubiquitous (A) <b>protein:</b> ubiquitous (L), brain (A), heart (A)	<b>H:</b> The human protein atlas <b>R:</b> Transcriptome Atlas mouse embryo <b>Dm:</b> (Cammarato et al., 2011; Chan et al., 2011; Zhang et al., 2007), flyatlas2
Rab2b	<b>RNA:</b> Low tissue specificity – ubiquitous	<b>RNA:</b> weak regional signal in the nervous system (Mm, E)			<b>H:</b> The human protein atlas <b>R:</b> Transcriptome Atlas mouse embryo
Rab3a	<b>RNA:</b> tissue enriched (brain) -widespread in low levels <b>protein:</b> selective expression in CNS, islets of Langerhans and adrenal medulla	<b>RNA:</b> brain (Mm, A and Rn, A)	DmRab3	<b>RNA:</b> central nervous system (E), nervous system high (A) <b>protein:</b> nervous system high (L), brain (A)	<b>H:</b> The human protein atlas <b>R:</b> (Elferink et al., 1992; Sollner et al., 2017) <b>Dm:</b> (Chan et al., 2011; Zhang et al., 2007), flyatlas2
Rab3b	<b>RNA:</b> tissue enhanced (brain, placenta, prostate) - widespread <b>protein:</b> cytoplasmic expression in pancreatic islet cells, glandular cells in prostate and	<b>RNA:</b> No regional signal (Mm, E)			<b>H:</b> The human protein atlas <b>R:</b> Transcriptome Atlas mouse embryo

	enteroendocrine cells of the gastrointestinal tract				
Rab3c	<b>RNA:</b> group enriched (adrenal gland, brain, pituitary gland) - widespread <b>protein:</b> cytoplasmic expression in CNS, adrenal medulla and islets of Langerhans.	<b>RNA:</b> strong regional signal in nervous system and weak in nose (Mm, E)			<b>H:</b> The human protein atlas <b>R:</b> Transcriptome Atlas mouse embryo
Rab3d (Rab16)	<b>RNA:</b> Low tissue specificity – ubiquitous <b>protein:</b> cytoplasmic expression in most tissues.	<b>RNA:</b> moderate regional signal in nervous system and skin (Mm, E)			<b>H:</b> The human protein atlas <b>R:</b> Transcriptome Atlas mouse embryo
Rab4a	<b>RNA:</b> Low tissue specificity – ubiquitous	<b>RNA:</b> moderate regional signal in the nervous system (Mm, E)	DmRab4	<b>RNA:</b> ubiquitous (E, A), enriched in mesoderm and ectoderm (E) <b>protein:</b> nervous system high (L), brain (A), heart (A)	<b>H:</b> The human protein atlas <b>R:</b> Transcriptome Atlas mouse embryo <b>Dm:</b> (Cammarato et al., 2011; Chan et al., 2011; Zhang et al., 2007), flyatlas2
Rab4b	<b>RNA:</b> Low tissue specificity – ubiquitous	<b>RNA:</b> strong regional signal (nose, alimentary system, skeleton) (Mm, E)			<b>H:</b> The human protein atlas <b>R:</b> Transcriptome Atlas mouse embryo
Rab5a	<b>RNA:</b> Low tissue specificity – ubiquitous <b>protein:</b> cytoplasmic expression in all tissues	no data	DmRab5	<b>RNA:</b> ubiquitous (E, A), enriched in garland cells (E) <b>protein:</b> ubiquitous (L), brain (A)	<b>H:</b> The human protein atlas <b>Dm:</b> (Chan et al., 2011; Zhang et al., 2007), flyatlas2
Rab5b	<b>RNA:</b> Low tissue specificity – ubiquitous <b>protein:</b> ubiquitous cytoplasmic expression	no data			<b>H:</b> The human protein atlas

Rab5c	<b>RNA:</b> Low tissue specificity – ubiquitous <b>protein:</b> cytoplasmic expression in several tissues	<b>RNA:</b> not detected (Mm, E)			<b>H:</b> The human protein atlas <b>R:</b> Transcriptome Atlas mouse embryo
Rab6a	<b>RNA:</b> Low tissue specificity – ubiquitous <b>protein:</b> ubiquitous	<b>RNA:</b> strong regional signal in the nervous and alimentary system, eye and nose (Mm, E) <b>protein:</b> ubiquitously expressed (Mm, E)	DmRab6 (warthog)	<b>RNA:</b> ubiquitous (E, A) <b>protein:</b> ubiquitous (L), brain (A)	<b>H:</b> The human protein atlas <b>R:</b> Transcriptome Atlas mouse embryo, (Bardin et al., 2015) <b>Dm:</b> (Chan et al., 2011; Zhang et al., 2007), flyatlas2
Rab6b	<b>RNA:</b> Group enriched (brain, parathyroid gland) – widespread <b>protein:</b> predominantly expressed in the brain	<b>RNA:</b> strong regional signal in the nervous system, eye and nose (Mm, E)			<b>H:</b> The human protein atlas, (Opdam et al., 2000) <b>R:</b> Transcriptome Atlas mouse embryo
Rab6a'	<b>protein:</b> ubiquitous expression	<b>protein:</b> ubiquitously expressed (Mm, E)			<b>H:</b> (Echard et al., 2000) <b>R:</b> (Bardin et al., 2015)
Rab6c*	<b>RNA:</b> tissue enhanced (parathyroid gland) – widespread; fetal and adult brain, prostate, testis, and spinal cord	not in mouse			<b>H:</b> The human protein atlas, (Young et al., 2010)
Rab6d (Rab41)	See Rab41	not in mouse			
Rab7a	<b>RNA:</b> Low tissue specificity – ubiquitous <b>protein:</b> Ubiquitous cytoplasmic expression, high expression in skeletal muscle	<b>RNA:</b> ubiquitous expression, with high levels in liver, heart and kidney (Mm, E)	DmRab7	<b>RNA:</b> ubiquitous (E, A) <b>protein:</b> ubiquitous (L), brain (A), heart (A)	<b>H:</b> The human protein atlas, (Verhoeven et al., 2003) <b>R:</b> Transcriptome Atlas mouse embryo, (Verhoeven et al., 2003) <b>Dm:</b> (Cammarato et al., 2011; Chan et al., 2011; Zhang et al., 2007), flyatlas2
Rab7b	<b>RNA:</b> Tissue enhanced (adipose tissue, skin) – widespread	no data			<b>H:</b> The human protein atlas

Rab8a	<b>RNA:</b> Low tissue specificity – ubiquitous	no data	DmRab8	<b>RNA:</b> ubiquitous (E+A), enriched in mesoderm and ectoderm (E) <b>protein:</b> ubiquitous (L), brain (A)	<b>H:</b> The human protein atlas <b>Dm:</b> (Chan et al., 2011; Zhang et al., 2007), flyatlas2
Rab8b	<b>RNA:</b> Low tissue specificity – ubiquitous	<b>RNA:</b> no regional signal (Mm, E)			<b>H:</b> The human protein atlas <b>R:</b> Transcriptome Atlas mouse embryo
Rab8c (Rab13)	See Rab13	See Rab13			
Rab9a	<b>RNA:</b> Low tissue specificity – ubiquitous <b>protein:</b> Ubiquitous cytoplasmic expression, most abundant in glandular and lymphoid cells	<b>RNA:</b> no regional signal (Mm, E)	DmRab9	<b>RNA:</b> ubiquitous (E+A), enriched in CNS (E) <b>protein:</b> nervous system high (L), brain (A)	<b>H:</b> The human protein atlas <b>R:</b> Transcriptome Atlas mouse embryo <b>Dm:</b> (Chan et al., 2011; Zhang et al., 2007), flyatlas2
Rab9b	<b>RNA:</b> Tissue enhanced (heart muscle) – widespread <b>protein:</b> Membranous and cytoplasmic expression in most tissues, highest expression in intercalated discs of heart myocytes	<b>RNA:</b> no regional signal (Mm, E)			<b>H:</b> The human protein atlas <b>R:</b> Transcriptome Atlas mouse embryo
Rab10	<b>RNA:</b> Low tissue specificity – ubiquitous <b>protein:</b> Ubiquitous cytoplasmic expression	<b>RNA:</b> no regional signal (Mm, E)	DmRab10	<b>RNA:</b> ubiquitous (E+A), enriched in CNS (E) <b>protein:</b> widespread (L), brain (A), heart (A)	<b>H:</b> The human protein atlas <b>R:</b> Transcriptome Atlas mouse embryo <b>Dm:</b> (Cammarato et al., 2011; Chan et al., 2011; Zhang et al., 2007), flyatlas2,
Rab11a	<b>RNA:</b> Low tissue specificity -ubiquitous	<b>RNA:</b> no regional signal (Mm, E)	DmRab11	<b>RNA:</b> ubiquitous (E+A), enriched in gut (E)	<b>H:</b> The human protein atlas <b>R:</b> Transcriptome Atlas mouse embryo

	<b>protein:</b> Ubiquitous cytoplasmic and membranous expression			<b>protein:</b> ubiquitous (L), brain (A), heart (A)	<b>Dm:</b> (Cammarato et al., 2011; Chan et al., 2011; Zhang et al., 2007) flyatlas2
Rab11b	<b>RNA:</b> Low tissue specificity – ubiquitous	<b>RNA:</b> no regional signal (Mm, E)			<b>H:</b> The human protein atlas <b>R:</b> Transcriptome Atlas mouse embryo
Rab11c (Rab25)	See Rab25	See Rab25			
Rab12	<b>RNA:</b> Tissue enhanced (skeletal muscle) – ubiquitous <b>protein:</b> Ubiquitous cytoplasmic expression	<b>RNA:</b> no regional signal (Mm, E)	-	-	<b>H:</b> The human protein atlas <b>R:</b> Transcriptome Atlas mouse embryo
Rab13 (Rab8c)	<b>RNA:</b> Low tissue specificity – ubiquitous <b>protein:</b> Cytoplasmic expression in most tissues	<b>RNA:</b> moderate regional signal brain and spinal cord (Mm, E)	DmRab8	see DmRab8	<b>H:</b> The human protein atlas <b>R:</b> Transcriptome Atlas mouse embryo
Rab14	<b>RNA:</b> Low tissue specificity – ubiquitous <b>protein:</b> General cytoplasmic expression, ubiquitous	<b>RNA:</b> no regional signal (Mm, E) <b>protein:</b> ubiquitous expression with highest levels in brain, kidney, spleen and thymus (Rn)	DmRab14	<b>RNA:</b> ubiquitous (E+A), enriched in salivary gland and CNS (E) <b>protein:</b> widespread(L), brain (A)	<b>H:</b> The human protein atlas, (Junutula et al., 2004) <b>R:</b> Transcriptome Atlas mouse embryo, (Junutula et al., 2004) <b>Dm:</b> (Chan et al., 2011; Zhang et al., 2007), flyatlas2
Rab15	<b>RNA:</b> tissue enhanced (brain) – widespread <b>protein:</b> Cytoplasmic expression in all tissues (uncertain)	<b>RNA:</b> Specifically expressed in brain (Rn)	-	-	<b>H:</b> The human protein atlas <b>R:</b> (Elferink et al., 1992)
Rab16 (Rab3d)	See Rab3d	See Rab3d	See DmRab3		
Rab17	<b>RNA:</b> Tissue enhanced (intestine, liver) – widespread <b>protein:</b> Cytoplasmic and membranous expression in several	<b>RNA:</b> moderate regional signal in nose, alimentary system and salivary gland (Mm, E), specific to epithelial cells, in tissue like	-	-	<b>H:</b> The human protein atlas <b>R:</b> Transcriptome Atlas mouse embryo,(Lutcke et al., 1993)

	different tissue types, including CNS and most glandular cells	kidney, liver and intestine (Mm, A) <b>protein:</b> kidney (basolateral plasma membrane and to apical tubules) (Mm, A)			
Rab18	<b>RNA:</b> low tissue specificity - ubiquitous <b>protein:</b> Ubiquitous cytoplasmic expression (uncertain)	<b>RNA:</b> no regional signal (Mm, E), detected in kidney, liver, intestine, brain, lung, spleen, heart (Mm, A) <b>protein:</b> kidney cortex, tubular structures (Mm)	DmRab18	<b>RNA:</b> ubiquitous (E+A) <b>protein:</b> widespread (L), brain(A), heart (A)	<b>H:</b> The human protein atlas <b>R:</b> Transcriptome Atlas mouse embryo, (Lutcke et al., 1994) <b>Dm:</b> (Cammarato et al., 2011; Chan et al., 2011; Zhang et al., 2007), flyatlas2
Rab19a	<b>RNA:</b> Tissue enhanced (pancreas)- widespread	<b>RNA:</b> not detected in embryo, tissue specifically (Mm, E), intestine lung and spleen, kidney (Mm, A)	DmRab19	<b>RNA:</b> ubiquitous(E+A) <b>protein:</b> nervous system high (L), brain (A)	<b>H:</b> The human protein atlas <b>R:</b> Transcriptome Atlas mouse embryo, (Lutcke et al., 1995) <b>Dm:</b> (Chan et al., 2011; Zhang et al., 2007), flyatlas2, this study
Rab19b (Rab43)	See Rab43	See Rab43			
Rab20	<b>RNA:</b> Low tissue specificity – ubiquitous <b>protein:</b> Cytoplasmic expression in several tissues (uncertain)	<b>RNA:</b> not detected in embryo (Mm, E), in a variety of adult mouse tissue: kidney, liver, lung, spleen, heart but not detected in the brain (Mm, A) <b>protein:</b> kidney (Mm)	-	-	<b>H:</b> The human protein atlas <b>R:</b> Transcriptome Atlas mouse embryo,(Lutcke et al., 1994)
Rab21	<b>RNA:</b> Low tissue specificity – ubiquitous <b>protein:</b> General cytoplasmic expression	<b>RNA:</b> moderate regional signal in nervous, alimentary and haemolymphoid system and eye (Mm, E)	DmRab21	<b>RNA:</b> ubiquitous (E+A), enriched in gut (E) <b>protein:</b> nervous system high (L), brain (A)	<b>H:</b> The human protein atlas <b>R:</b> Transcriptome Atlas mouse embryo <b>Dm:</b> (Chan et al., 2011; Zhang et al., 2007), flyatlas2, this study
Rab22a	<b>RNA:</b> Low tissue specificity – ubiquitous	<b>RNA:</b> no regional signal (Mm, E)	-	-	<b>H:</b> The human protein atlas <b>R:</b> Transcriptome Atlas mouse embryo

	<b>protein:</b> Cytoplasmic expression in most tissues				
Rab22b (Rab31)	<b>RNA:</b> Low tissue specificity – ubiquitous <b>protein:</b> Cytoplasmic expression in most tissues	<b>RNA:</b> moderate regional signal in the nervous and alimentary system, salivary gland, skeletal muscles, and skin (Mm, E) <b>protein:</b> enriched in the brain (Mm, A and Rn, A) spleen, and intestine, in much lower levels in other organs (Rn)	-	-	<b>H:</b> The human protein atlas <b>R:</b> Transcriptome Atlas mouse embryo, (Chua et al., 2014; Ng et al., 2007)
Rab23	<b>RNA:</b> Tissue enhanced (smooth muscle, urinary bladder) – widespread <b>protein:</b> General cytoplasmic and membranous expression	<b>RNA:</b> Predominantly brain-enriched (Mm, A) <b>protein:</b> predominantly brain-enriched, low levels in multiple tissues (Mm, A)	DmRab23	<b>RNA:</b> stripes (E) <b>protein:</b> nervous system high (L), brain (A)	<b>H:</b> The human protein atlas <b>R:</b> (Guo et al., 2006; Olkkonen et al., 1994) <b>Dm:</b> (Chan et al., 2011; Zhang et al., 2007), this study
Rab24	<b>RNA:</b> Low tissue specificity – ubiquitous	<b>RNA:</b> regional signal in peripheral nervous system and skin (Mm, E)	-	-	<b>H:</b> The human protein atlas <b>R:</b> Transcriptome Atlas mouse embryo
Rab25 (Rab11c)	<b>RNA:</b> Tissue enhanced (esophagus) – widespread <b>protein:</b> Membranous expression in most epithelial cells	<b>RNA:</b> moderate regional signal in nose, alimentary system, salivary gland, intestines, renal/urinary system and skin (Mm, E), specifically expressed in epithelial cells (Oc)	See DmRab11		<b>H:</b> The human protein atlas <b>R:</b> Transcriptome Atlas mouse embryo, (Goldenring et al., 1993)
Rab26a	<b>RNA:</b> Tissue enhanced (brain, liver, pancreas, salivary gland) – widespread	<b>protein:</b> parotid gland (Rn, A)	DmRab26	<b>RNA:</b> CNS (E), nervous system high (A) <b>protein:</b> nervous system high (L), brain (A)	<b>H:</b> The human protein atlas,(Jin and Mills, 2014) <b>R:</b> (Yoshie et al., 2000) <b>Dm:</b> (Chan et al., 2011; Zhang et al., 2007), flyatlas2, this study

Rab26b (Rab37)	See Rab37	See Rab37			
Rab27a	<b>RNA:</b> Low tissue specificity – ubiquitous <b>protein:</b> Cytoplasmic expression in most tissues, including immune cells	<b>RNA:</b> strong regional signal in brain, peripheral nervous, haemolymphoid and alimentary system and adrenal gland (Mm, E) <b>protein:</b> broad expression with high levels in large intestine, spleen, eye, lung, stomach, and platelets (Mm)	DmRab27	<b>RNA:</b> ubiquitous (E), nervous system high and ovary (A) <b>protein:</b> nervous system high (L), brain (A)	<b>H:</b> The human protein atlas <b>R:</b> Transcriptome Atlas mouse embryo, (Barral et al., 2002) <b>Dm:</b> (Chan et al., 2011; Zhang et al., 2007), flyatlas2, this study
Rab27b	<b>RNA:</b> Tissue enhanced (brain, stomach) – widespread <b>protein:</b> Cytoplasmic and membranous expression mainly in glandular cells of gastrointestinal tract, breast, salivary gland, prostate, cells in renal tubules and urothelial cells	<b>RNA:</b> strong regional signal in the ear, eye, nose, intestines, nervous, alimentary respiratory renal/urinary, reproductive system and limb (Mm, E) <b>protein:</b> platelets, gastrointestinal tract (Mm), pancreas (Rn and Mm, A), bladder, spleen, and brain (Mm, A)			<b>H:</b> The human protein atlas <b>R:</b> Transcriptome Atlas mouse embryo, (Barral et al., 2002; Chen et al., 2004; Chen et al., 2003b; Zhao et al., 2002)
Rab28	<b>RNA:</b> Low tissue specificity – ubiquitous <b>protein:</b> Cytoplasmic expression in most tissues	<b>RNA:</b> strong regional signal in nose, skeleton, limb (Mm, E)	-	-	<b>H:</b> The human protein atlas <b>R:</b> Transcriptome Atlas mouse embryo
Rab29	<b>RNA:</b> Low tissue specificity, ubiquitous <b>protein:</b> Cytoplasmic expression in most tissues	no data	-	-	<b>H:</b> The human protein atlas

Rab30	<b>RNA:</b> Low tissue specificity – ubiquitous <b>protein:</b> Cytoplasmic expression in most tissues	no data	DmRab30	<b>RNA:</b> ubiquitous (E+A), enriched in CNS (E) <b>protein:</b> ubiquitous (L), brain (A)	<b>H:</b> The human protein atlas <b>R:</b> Transcriptome Atlas mouse embryo <b>Dm:</b> (Jin et al., 2012; Zhang et al., 2007), flyatlas2, this study
Rab31 (Rab22b)	see Rab22b	See Rab22b	-	-	
Rab32a	<b>RNA:</b> Tissue enhanced (bone marrow) – ubiquitous <b>protein:</b> Cytoplasmic expression in most tissues	<b>RNA:</b> Broad expression with high levels in the liver (Mm, E)	DmRab32 (lightoid)	<b>RNA:</b> malpighian tubules(E), ubiquitous and eye enriched (A) <b>protein:</b> nervous system high (L), brain (A)	<b>H:</b> The human protein atlas <b>R:</b> (Cohen-Solal et al., 2003) <b>Dm:</b> (Chan et al., 2011; Zhang et al., 2007), flyatlas2, this study
Rab32b (Rab38)	See Rab38	See Rab38			
Rab33a	<b>RNA:</b> Tissue enhanced (blood, brain) – widespread	<b>RNA:</b> Expression restricted to brain, weak in ovary and thymus (Mm)	-	-	<b>H:</b> The human protein atlas <b>R:</b> (Zheng et al., 1997)
Rab33b	<b>RNA:</b> Low tissue specificity – ubiquitous	<b>RNA:</b> ubiquitous expression (Mm)	-	-	<b>H:</b> The human protein atlas <b>R:</b> (Zheng et al., 1998)
Rab34	<b>RNA:</b> Low tissue specificity – ubiquitous <b>protein:</b> General cytoplasmic expression	<b>RNA:</b> no regional signal (Mm, E)	-	-	<b>H:</b> The human protein atlas <b>R:</b> Transcriptome Atlas mouse embryo
Rab35	<b>RNA:</b> Low tissue specificity – ubiquitous <b>protein:</b> Cytoplasmic expression in most	no data	DmRab35	<b>RNA:</b> ubiquitous (E+A), enriched in CNS (E) <b>protein:</b> ubiquitous (L), brain (A)	<b>H:</b> The human protein atlas <b>Dm:</b> (Chan et al., 2011; Zhang et al., 2007), flyatlas2
Rab36	<b>RNA:</b> Tissue enhanced (fallopian tube) – widespread	<b>RNA:</b> not detected (Mm, E)	-		<b>H:</b> The human protein atlas <b>R:</b> Transcriptome Atlas mouse embryo
Rab37	<b>RNA:</b> Tissue enhanced (blood, brain), widespread	<b>RNA:</b> not detected (Mm, E), bone marrow mast cells (Mm, CC)	DmRab26	See DmRab26	<b>H:</b> The human protein atlas <b>R:</b> Transcriptome Atlas mouse embryo, (Masuda et al., 2000)

Rab38	<b>RNA:</b> Tissue enhanced (retina, tongue)-widespread	<b>RNA:</b> strong regional signal in ear, nose, alimentary and respiratory system, salivary gland, stomach and gut, skeleton and skin (Mm, E)	DmRab32	See DmRab32	<b>H:</b> The human protein atlas <b>R:</b> Transcriptome Atlas mouse embryo
Rab39a	<b>RNA:</b> Tissue enhanced (brain, pituitary gland and epithelial cells) – widespread	<b>RNA:</b> Not detected (Mm, E)	DmRab39	<b>RNA:</b> ubiquitous (E+A) <b>protein:</b> widespread (L), brain (A)	<b>H:</b> The human protein atlas, (Chen et al., 2003a) Chen et al., 2003 <b>R:</b> Transcriptome Atlas mouse embryo <b>Dm:</b> (Chan et al., 2011; Zhang et al., 2007), flyatlas2
Rab39 b	<b>RNA:</b> Tissue enhanced (brain) – widespread <b>protein:</b> Cytoplasmic and membranous expression in several tissues, including cerebral cortex	<b>RNA:</b> strong regional signal in the peripheral nervous system, ganglia (Mm, E), brain specific (Mm, A)			<b>H:</b> The human protein atlas,(Giannandrea et al., 2010) <b>R:</b> Transcriptome Atlas mouse embryo, (Giannandrea et al., 2010)
Rab40a**	<b>RNA:</b> Tissue enhanced (epididymis) – widespread	not in mouse	DmRab40	<b>RNA:</b> ubiquitous (E+A), enriched in CNS (E) <b>protein:</b> nervous system high (L), brain (A)	<b>H:</b> The human protein atlas <b>Dm:</b> (Jin et al., 2012; Zhang et al., 2007), flyatlas2, this study
Rab40b	<b>RNA:</b> Tissue enhanced (brain) - ubiquitous	<b>RNA:</b> brain, inner ear and heart tissues (Mm, E+A)			<b>H:</b> The human protein atlas <b>R:</b> (Bedoyan et al., 2012)
Rab40a1** (RLGP)	<b>RNA:</b> Tissue enhanced (epididymis); human fetal and adult brain and kidney, and adult lung, heart, liver and skeletal muscle	not in mouse			<b>H:</b> The human protein atlas, (Bedoyan et al., 2012)
Rab40c	<b>RNA:</b> Tissue enhanced (pancreas) – ubiquitous	<b>RNA:</b> no regional signal			<b>H:</b> The human protein atlas <b>R:</b> Transcriptome Atlas mouse embryo
Rab41 (Rab6d) ***	<b>RNA:</b> Tissue enhanced (brain, testis) - restricted	not in mouse	DmRab6	See DmRab6	<b>H:</b> The human protein atlas

Rab42 (Rab39c)	<b>RNA:</b> Tissue enhanced (lymphoid tissue) - widespread	no data	DmRab39	See DmRab39	<b>H:</b> The human protein atlas
Rab43 (Rab19b)	<b>RNA:</b> Tissue enriched (liver) – ubiquitous <b>protein:</b> Cytoplasmic expression in several tissues. Strong positivity in colloid in thyroid gland as well	no data	DmRab19	See DmRab19	<b>H:</b> The human protein atlas
Rab44	<b>RNA:</b> Tissue enhanced (blood, bone marrow) – widespread	<b>RNA:</b> highly expressed in the bone marrow and slightly expressed in the epididymis, lung, skin, spleen, thymus, ovary, uterus, and liver (Mm, CC) <b>protein:</b> bone marrow, spleen and thymus (Mm, CC)	--	-	<b>H:</b> The human protein atlas <b>R:</b> (Tokuhsa et al., 2020)
Rab45	<b>RNA:</b> Low tissue specificity – widespread <b>protein:</b> General cytoplasmic expression	no data	-	-	<b>H:</b> The human protein atlas
-	-	-	DmRabX1 (chrowded)	<b>RNA:</b> ubiquitous (A) <b>protein:</b> nervous system high (L), brain (A)	<b>Dm:</b> (Chan et al., 2011), flyatlas2, this study
-	-	-	DmRabX4	<b>RNA:</b> CNS(E), nervous system high (A) <b>protein:</b> nervous system high (L), brain (A)	<b>Dm:</b> (Chan et al., 2011; Zhang et al., 2007), flyatlas2, this study
-	-	-	DmRabX6	<b>RNA:</b> ubiquitous (E+A) <b>protein:</b> nervous system high (L), brain (A)	<b>Dm:</b> (Jin et al., 2012; Zhang et al., 2007), flyatlas2, this study

## References – Supplementary Table 2

- Bardin, S., Miserey-Lenkei, S., Hurbain, I., Garcia-Castillo, D., Raposo, G., and Goud, B. (2015). Phenotypic characterisation of RAB6A knockout mouse embryonic fibroblasts. *Biol Cell* *107*, 427-439.
- Barral, D.C., Ramalho, J.S., Anders, R., Hume, A.N., Knapton, H.J., Tolmachova, T., Collinson, L.M., Goulding, D., Authi, K.S., and Seabra, M.C. (2002). Functional redundancy of Rab27 proteins and the pathogenesis of Griscelli syndrome. *J Clin Invest* *110*, 247-257.
- Bedoyan, J.K., Schaibley, V.M., Peng, W., Bai, Y., Mondal, K., Shetty, A.C., Durham, M., Micucci, J.A., Dhiraaj, A., Skidmore, J.M., *et al.* (2012). Disruption of RAB40AL function leads to Martin--Probst syndrome, a rare X-linked multisystem neurodevelopmental human disorder. *J Med Genet* *49*, 332-340.
- Cammarato, A., Ahrens, C.H., Alayari, N.N., Qeli, E., Rucker, J., Reedy, M.C., Zmasek, C.M., Gucek, M., Cole, R.N., Van Eyk, J.E., *et al.* (2011). A mighty small heart: the cardiac proteome of adult *Drosophila melanogaster*. *PLoS One* *6*, e18497.
- Chan, C.C., Scoggin, S., Wang, D., Cherry, S., Dembo, T., Greenberg, B., Jin, E.J., Kuey, C., Lopez, A., Mehta, S.Q., *et al.* (2011). Systematic discovery of Rab GTPases with synaptic functions in *Drosophila*. *Curr Biol* *21*, 1704-1715.
- Chen, T., Han, Y., Yang, M., Zhang, W., Li, N., Wan, T., Guo, J., and Cao, X. (2003a). Rab39, a novel Golgi-associated Rab GTPase from human dendritic cells involved in cellular endocytosis. *Biochem Biophys Res Commun* *303*, 1114-1120.
- Chen, X., Li, C., Izumi, T., Ernst, S.A., Andrews, P.C., and Williams, J.A. (2004). Rab27b localizes to zymogen granules and regulates pancreatic acinar exocytosis. *Biochem Biophys Res Commun* *323*, 1157-1162.
- Chen, Y., Guo, X., Deng, F.M., Liang, F.X., Sun, W., Ren, M., Izumi, T., Sabatini, D.D., Sun, T.T., and Kreibich, G. (2003b). Rab27b is associated with fusiform vesicles and may be involved in targeting uroplakins to urothelial apical membranes. *Proc Natl Acad Sci U S A* *100*, 14012-14017.
- Chua, C.E., Goh, E.L., and Tang, B.L. (2014). Rab31 is expressed in neural progenitor cells and plays a role in their differentiation. *FEBS Lett* *588*, 3186-3194.
- Cohen-Solal, K.A., Sood, R., Marin, Y., Crespo-Carbone, S.M., Sinsimer, D., Martino, J.J., Robbins, C., Makalowska, I., Trent, J., and Chen, S. (2003). Identification and characterization of mouse Rab32 by mRNA and protein expression analysis. *Biochim Biophys Acta* *1651*, 68-75.
- Echard, A., Opdam, F.J., de Leeuw, H.J., Jollivet, F., Savelkoul, P., Hendriks, W., Voorberg, J., Goud, B., and Fransen, J.A. (2000). Alternative splicing of the human Rab6A gene generates two close but functionally different isoforms. *Mol Biol Cell* *11*, 3819-3833.
- Elferink, L.A., Anzai, K., and Scheller, R.H. (1992). rab15, a novel low molecular weight GTP-binding protein specifically expressed in rat brain. *J Biol Chem* *267*, 22693.
- Giannandrea, M., Bianchi, V., Mignogna, M.L., Sirri, A., Carrabino, S., D'Elia, E., Vecellio, M., Russo, S., Cogliati, F., Larizza, L., *et al.* (2010). Mutations in the small GTPase gene RAB39B are responsible for X-linked mental retardation associated with autism, epilepsy, and macrocephaly. *Am J Hum Genet* *86*, 185-195.
- Goldenring, J.R., Shen, K.R., Vaughan, H.D., and Modlin, I.M. (1993). Identification of a small GTP-binding protein, Rab25, expressed in the gastrointestinal mucosa, kidney, and lung. *J Biol Chem* *268*, 18419-18422.
- Guo, A., Wang, T., Ng, E.L., Aulia, S., Chong, K.H., Teng, F.Y., Wang, Y., and Tang, B.L. (2006). Open brain gene product Rab23: expression pattern in the adult mouse brain and functional characterization. *J Neurosci Res* *83*, 1118-1127.
- Jin, E.J., Chan, C.C., Agi, E., Cherry, S., Hanacik, E., Buszczak, M., and Hiesinger, P.R. (2012). Similarities of *Drosophila* rab GTPases based on expression profiling: completion and analysis of the rab-Gal4 kit. *PLoS One* *7*, e40912.
- Jin, R.U., and Mills, J.C. (2014). RAB26 coordinates lysosome traffic and mitochondrial localization. *J Cell Sci* *127*, 1018-1032.

Junutula, J.R., De Maziere, A.M., Peden, A.A., Ervin, K.E., Advani, R.J., van Dijk, S.M., Klumperman, J., and Scheller, R.H. (2004). Rab14 is involved in membrane trafficking between the Golgi complex and endosomes. *Mol Biol Cell* *15*, 2218-2229.

Lutcke, A., Jansson, S., Parton, R.G., Chavrier, P., Valencia, A., Huber, L.A., Lehtonen, E., and Zerial, M. (1993). Rab17, a novel small GTPase, is specific for epithelial cells and is induced during cell polarization. *J Cell Biol* *121*, 553-564.

Lutcke, A., Olkkonen, V.M., Dupree, P., Lutcke, H., Simons, K., and Zerial, M. (1995). Isolation of a murine cDNA clone encoding Rab19, a novel tissue-specific small GTPase. *Gene* *155*, 257-260.

Lutcke, A., Parton, R.G., Murphy, C., Olkkonen, V.M., Dupree, P., Valencia, A., Simons, K., and Zerial, M. (1994). Cloning and subcellular localization of novel rab proteins reveals polarized and cell type-specific expression. *J Cell Sci* *107 ( Pt 12)*, 3437-3448.

Masuda, E.S., Luo, Y., Young, C., Shen, M., Rossi, A.B., Huang, B.C., Yu, S., Bennett, M.K., Payan, D.G., and Scheller, R.H. (2000). Rab37 is a novel mast cell specific GTPase localized to secretory granules. *FEBS Lett* *470*, 61-64.

Ng, E.L., Wang, Y., and Tang, B.L. (2007). Rab22B's role in trans-Golgi network membrane dynamics. *Biochem Biophys Res Commun* *361*, 751-757.

Olkkonen, V.M., Peterson, J.R., Dupree, P., Lutcke, A., Zerial, M., and Simons, K. (1994). Isolation of a mouse cDNA encoding Rab23, a small novel GTPase expressed predominantly in the brain. *Gene* *138*, 207-211.

Opdam, F.J., Echard, A., Croes, H.J., van den Hurk, J.A., van de Vorstenbosch, R.A., Ginsel, L.A., Goud, B., and Fransen, J.A. (2000). The small GTPase Rab6B, a novel Rab6 subfamily member, is cell-type specifically expressed and localised to the Golgi apparatus. *J Cell Sci* *113 ( Pt 15)*, 2725-2735.

Sollner, J.F., Leparc, G., Hildebrandt, T., Klein, H., Thomas, L., Stupka, E., and Simon, E. (2017). An RNA-Seq atlas of gene expression in mouse and rat normal tissues. *Sci Data* *4*, 170185.

Tokuhisa, M., Kadowaki, T., Ogawa, K., Yamaguchi, Y., Kido, M.A., Gao, W., Umeda, M., and Tsukuba, T. (2020). Expression and localisation of Rab44 in immune-related cells change during cell differentiation and stimulation. *Sci Rep* *10*, 10728.

Verhoeven, K., De Jonghe, P., Coen, K., Verpoorten, N., Auer-Grumbach, M., Kwon, J.M., FitzPatrick, D., Schmedding, E., De Vriendt, E., Jacobs, A., *et al.* (2003). Mutations in the small GTP-ase late endosomal protein RAB7 cause Charcot-Marie-Tooth type 2B neuropathy. *Am J Hum Genet* *72*, 722-727.

Yoshie, S., Imai, A., Nashida, T., and Shimomura, H. (2000). Expression, characterization, and localization of Rab26, a low molecular weight GTP-binding protein, in the rat parotid gland. *Histochem Cell Biol* *113*, 259-263.

Young, J., Menetrey, J., and Goud, B. (2010). RAB6C is a retrogene that encodes a centrosomal protein involved in cell cycle progression. *J Mol Biol* *397*, 69-88.

Zhang, J., Schulze, K.L., Hiesinger, P.R., Suyama, K., Wang, S., Fish, M., Acar, M., Hoskins, R.A., Bellen, H.J., and Scott, M.P. (2007). Thirty-one flavors of *Drosophila* rab proteins. *Genetics* *176*, 1307-1322.

Zhao, S., Torii, S., Yokota-Hashimoto, H., Takeuchi, T., and Izumi, T. (2002). Involvement of Rab27b in the regulated secretion of pituitary hormones. *Endocrinology* *143*, 1817-1824.

Zheng, J.Y., Koda, T., Arimura, Y., Kishi, M., and Kakinuma, M. (1997). Structure and expression of the mouse S10 gene. *Biochim Biophys Acta* *1351*, 47-50.

Zheng, J.Y., Koda, T., Fujiwara, T., Kishi, M., Ikehara, Y., and Kakinuma, M. (1998). A novel Rab GTPase, Rab33B, is ubiquitously expressed and localized to the medial Golgi cisternae. *J Cell Sci* *111 ( Pt 8)*, 1061-1069.

## Supplementary Table / Supplementary File 3

Mammalian Rabs	<i>S. cerevisiae</i> Rabs	<i>D. melanogaster</i> Rabs	Function	Subcellular localization	Mutant viability	References
Rab1a	Ypt1	DmRab1 (omelette)	<p><b>M:</b> anterograde melanosome transport</p> <p><b>Sc:</b> ER-Golgi, intra Golgi and ER-autophagosome transport</p> <p><b>Dm:</b> controls Golgi structure, cytokinesis, ER-to-Golgi transport, modulates insulin-like peptide secretion in IPCs</p>	<p><b>M:</b> ER, Golgi, mature melanosomes</p> <p><b>Sc:</b> ER, Golgi</p> <p><b>Dm:</b> Golgi, ER exit sites</p>	<p><b>M:</b> lethal</p> <p><b>Sc:</b> lethal</p> <p><b>Dm:</b> lethal</p>	<p><b>Function</b></p> <p><b>M:</b> (Ishida et al., 2012)</p> <p><b>Sc:</b> (Jedd et al., 1995; Lipatova et al., 2012; Segev et al., 1988)</p> <p><b>Dm:</b> (Cao et al., 2014; Ke et al., 2018; Sechi et al., 2017)</p> <p><b>Subcellular localization</b></p> <p><b>M:</b> (Ishida et al., 2012; Plutner et al., 1991)</p> <p><b>Sc:</b> (Baker et al., 1990; Segev et al., 1988)</p> <p><b>Dm:</b> (Cao et al., 2014; Ke et al., 2018; Sechi et al., 2017)</p> <p><b>Viability</b></p> <p><b>M:</b> International Mouse Phenotyping Consortium</p> <p><b>Sc:</b> (Giaever et al., 2002)</p> <p><b>Dm:</b> (Thibault et al., 2004)</p>
Rab1b			<p><b>M:</b> vesicular transport ER-Golgi</p>	<p><b>M:</b> Er, Golgi</p>	<p><b>M:</b> no KO model</p>	<p><b>Function and subcellular localization</b></p> <p><b>M:</b> (Plutner et al., 1991)</p>
Rab2a	-	DmRab2	<p><b>M:</b> ER-to-Golgi, maturation of pre-Golgi intermediates</p> <p><b>Dm:</b> ER-to-Golgi transport, endosome-lysosome fusion, endolysosome to autophagosome fusion</p>	<p><b>M:</b> Pre-Golgi intermediates</p> <p><b>Dm:</b> Golgi, late endosomes, lysosomes</p>	<p><b>M:</b> lethal</p> <p><b>Dm:</b> lethal</p>	<p><b>Function</b></p> <p><b>M:</b> (Tisdale and Balch, 1996; Tisdale et al., 1992)</p> <p><b>Dm:</b> (Ke et al., 2018; Lorincz et al., 2017; Lund et al., 2018)</p> <p><b>Subcellular localization</b></p> <p><b>M:</b> (Tisdale and Balch, 1996; Tisdale et al., 1992)</p>

						<b>Dm:</b> (Gillingham et al., 2014; Lund et al., 2018) <b>Viability</b> <b>M:</b> International Mouse Phenotyping Consortium
Rab2b	-		<b>M:</b> ER-to-Golgi, maturation of pre-Golgi intermediates	<b>M:</b> Pre-Golgi intermediates	<b>M:</b> no KO model <b>Dm:</b> lethal	<b>Function and subcellular localization</b> <b>M:</b> (Tisdale and Balch, 1996; Tisdale et al., 1992)
Rab3a	-	DmRab3	<b>M:</b> transport of synaptic vesicles to PM (regulated exocytosis)  <b>Dm:</b> regulation and maintenance of presynaptic active zone structure	<b>M:</b> synaptic and secretory vesicles, chromaffin granules  <b>Dm:</b> presynaptic active zone, synapse	<b>M:</b> viable <b>Dm:</b> viable	<b>Function</b> <b>M:</b> (Fischer von Mollard et al., 1991) <b>Dm:</b> (Ehmann et al., 2014; Graf et al., 2009) <b>Subcellular localization</b> <b>M:</b> (Darchen et al., 1990; Fischer von Mollard et al., 1990; Schluter et al., 2002) <b>Dm:</b> (Chan et al., 2011; Graf et al., 2009) <b>Viability</b> <b>M:</b> (Geppert et al., 1994) <b>Dm:</b> (Graf et al., 2009)
Rab3b	-		<b>M:</b> exocytosis	<b>M:</b> synaptic and secretory vesicles	<b>M:</b> viable	<b>Function and subcellular localization</b> <b>M:</b> (Schluter et al., 2002) <b>Viability</b> <b>M:</b> (Schluter et al., 2004)
Rab3c	-		<b>M:</b> exocytosis	<b>M:</b> synaptic and secretory vesicles	<b>M:</b> viable	<b>Function and subcellular localization</b> <b>M:</b> (Schluter et al., 2002) <b>Viability</b> <b>M:</b> (Schluter et al., 2004)
Rab3d (Rab16)	-		<b>M:</b> exocytosis	<b>M:</b> secretory granules (in mast cells)	<b>M:</b> viable	<b>Function and subcellular localization</b> <b>M:</b> (Tuvim et al., 1999) <b>Viability</b> <b>M:</b> (Riedel et al., 2002)
Rab4a	-	DmRab4	<b>M:</b> controls early sorting event in endocytosis, protein recycling to PM	<b>M:</b> early sorting endosomes, recycling endosomes	<b>M:</b> viable <b>Dm:</b> viable	<b>Function</b> <b>M:</b> (Seachrist et al., 2000; van der Sluijs et al., 1992) <b>Dm:</b> (de Madrid et al., 2015; Dey et al., 2017) <b>Subcellular localization</b>

			<b>Dm:</b> regulation of synapse organization, anterograde vesicle trafficking, trafficking of cell adhesion molecules to cell surface	<b>Dm:</b> fast recycling endosomes, sorting endosomes, axon termini		<b>M:</b> (Trischler et al., 1999; van der Sluijs et al., 1992) <b>Dm:</b> (de Madrid et al., 2015; Dey et al., 2017; West et al., 2015) <b>Viability</b> <b>M:</b> International Mouse Phenotyping Consortium
Rab4b	-		<b>M:</b> controls early sorting event in endocytosis, protein recycling to PM	<b>M:</b> early sorting endosomes, recycling endosomes	<b>M:</b> viable	<b>Function</b> <b>M:</b> (Seachrist et al., 2000; van der Sluijs et al., 1992) <b>Subcellular localization</b> <b>M:</b> (Trischler et al., 1999; van der Sluijs et al., 1992) <b>Viability</b> <b>M:</b> International Mouse Phenotyping Consortium
Rab5a	Ypt51, 52, 53	DmRab5	<b>M:</b> (lateral) early endosomes fusion (endocytosis)  <b>Sc:</b> endocytosis and vacuolar protein sorting, Ypt51 and Ypt52: MVB biogenesis and sorting  <b>Dm:</b> synaptic vesicle recycling, formation of early endosomes, regulation of endocytosis	<b>M:</b> PM, early endosomes  <b>Sc:</b> early endosomes  <b>Dm:</b> early endosomes	<b>M:</b> viable <b>Sc:</b> viable <b>Dm:</b> lethal	<b>Function</b> <b>M:</b> (Bucci et al., 1992; Gorvel et al., 1991) <b>Sc:</b> (Nickerson et al., 2012; Singer-Kruger et al., 1994) <b>Dm:</b> (Compagnon et al., 2009; Wucherpfennig et al., 2003) <b>Subcellular localization</b> <b>M:</b> (Bucci et al., 1992) <b>Sc:</b> (Singer-Kruger et al., 1994) <b>Dm:</b> (Wucherpfennig et al., 2003) <b>Viability</b> <b>M:</b> (Dickinson et al., 2016) <b>Sc:</b> (Singer-Kruger et al., 1994) <b>Dm:</b> (Wucherpfennig et al., 2003)
Rab5b			<b>M:</b> (lateral) early endosomes fusion (endocytosis)	<b>M:</b> PM, early endosomes	<b>M:</b> viable	<b>Function</b> <b>M:</b> (Bucci et al., 1992; Gorvel et al., 1991) <b>Subcellular localization</b> <b>M:</b> (Bucci et al., 1992) <b>Viability</b>

						<b>M:</b> International Mouse Phenotyping Consortium
Rab5c			<b>M:</b> (lateral) early endosomes fusion (endocytosis)	<b>M:</b> PM, early endosomes	<b>M:</b> lethal	<b>Function</b> <b>M:</b> (Bucci et al., 1992; Gorvel et al., 1991) <b>Subcellular localization</b> <b>M:</b> (Bucci et al., 1992) <b>Viability</b> <b>M:</b> International Mouse Phenotyping Consortium
Rab6a	Ypt6	DmRab6 (warthog)	<b>M:</b> Golgi-to-ER recycling <b>Sc:</b> Endosome-Golgi, intra Golgi and retrograde Golgi-ER transport, delivery of Atg9 to phagophore assembly site <b>Dm:</b> regulates autophagy and insulin-TOR signaling, regulation of autolysosomal homeostasis, insulin signaling, axon guidance in R7 photoreceptors, apical transport pathway in photoreceptors	<b>M:</b> trans-Golgi cisternae, TGN <b>Sc:</b> Golgi <b>Dm:</b> Golgi, cytoplasmic vesicles, lysosomes and autophagosomes	<b>M:</b> lethal <b>Sc:</b> viable <b>Dm:</b> lethal	<b>Function</b> <b>M:</b> (Young et al., 2005) <b>Sc:</b> (Kawamura et al., 2014; Luo and Gallwitz, 2003; Suda et al., 2013; Yang and Rosenwald, 2016) <b>Dm:</b> (Ayala et al., 2018; Iwanami et al., 2016; Tong et al., 2011) <b>Subcellular localization</b> <b>M:</b> (Antony et al., 1992; Goud et al., 1990; Sun et al., 2007) <b>Sc:</b> (Kawamura et al., 2014) <b>Dm:</b> (Ayala et al., 2018; Tong et al., 2011) <b>Viability</b> <b>M:</b> (Bardin et al., 2015) <b>Sc:</b> (Giaever et al., 2002) <b>Dm:</b> (Purcell and Artavanis-Tsakonas, 1999)
Rab6a'			<b>M:</b> recycling/retrograde traffic endosome-to-Golgi, Golgi-to-ER recycling	<b>M:</b> trans-Golgi cisternae, TGN	<b>M:</b> lethal	<b>Function</b> <b>M:</b> (Mallard et al., 2002; Young et al., 2005) <b>Subcellular localization</b> <b>M:</b> (Antony et al., 1992; Goud et al., 1990; Sun et al., 2007) <b>Viability</b> <b>M:</b> (Bardin et al., 2015)

Rab6b			<b>M:</b> Golgi-associated membrane trafficking	<b>M:</b> Golgi	<b>M:</b> viable	<b>Function and subcellular localization</b> <b>M:</b> (Opdam et al., 2000) <b>Viability</b> <b>M:</b> (Nyitrai et al., 2020)
Rab6c*			<b>M:</b> cell cycle progression	<b>M:</b> centrosome	<b>M:</b> no KO model	<b>Function and subcellular localization</b> <b>M:</b> (Young et al., 2010)
Rab6d (Rab41)			<b>M:</b> Golgi ribbon formation, ER-to-Golgi trafficking	<b>M:</b> Golgi	<b>M:</b> no KO model	<b>Function</b> <b>M:</b> (Liu et al., 2013; Liu et al., 2016) <b>Subcellular localization</b> <b>M:</b> (Liu et al., 2013)
Rab7a	Ypt7	DmRab7	<b>M:</b> maturation MVBs, fusion MVBs to lysosomes, late endocytic membrane trafficking  <b>Sc:</b> endocytosis, autophagy  <b>Dm:</b> targets endocytic cargo to late endosomes and lysosomes	<b>M:</b> late endosomes, lysosomes  <b>Sc:</b> late endosomes  <b>Dm:</b> late endosomes, maturing endosomes	<b>M:</b> lethal <b>Sc:</b> viable <b>Dm:</b> lethal	<b>Function</b> <b>M:</b> (Guerra and Bucci, 2016; Meresse et al., 1995; Vitelli et al., 1997) <b>Sc:</b> (Kirisako et al., 1999; Schimmoller and Riezman, 1993) <b>Dm:</b> (Entchev et al., 2000) <b>Subcellular localization</b> <b>M:</b> (Meresse et al., 1995; Vitelli et al., 1997) <b>Sc:</b> (Kirisako et al., 1999; Schimmoller and Riezman, 1993) <b>Dm:</b> (Entchev et al., 2000; Yousefian et al., 2013) <b>Viability</b> <b>M:</b> (Kawamura et al., 2012) <b>Sc:</b> (Giaever et al., 2002) <b>Dm:</b> (Cherry et al., 2013)
Rab7b			<b>M:</b> maturation MVBs, fusion MVBs to lysosomes, late endocytic membrane trafficking	<b>M:</b> late endosomes, lysosomes	<b>M:</b> lethal	<b>Function</b> <b>M:</b> (Guerra and Bucci, 2016; Meresse et al., 1995; Vitelli et al., 1997) <b>Subcellular localization</b> <b>M:</b> (Meresse et al., 1995; Vitelli et al., 1997) <b>Viability</b> <b>M:</b> (Kawamura et al., 2012)
Rab8a	Sec4	DmRab8	<b>M:</b> primary cilia formation (ciliogenesis),	<b>M:</b> Golgi, early endosomes, vesicular	<b>M:</b> die prematurely	<b>Function</b>

			<p>trafficking from TGN and recycling endosome to PM (exocytosis)</p> <p><b>Sc:</b> fusion of Golgi vesicles with PM, secretion, assembly of exocyst</p> <p><b>Dm:</b> synaptic growth responses in NMJ, regulates recycling endosome function, regulates furrow ingression, regulates exocytic trafficking</p>	<p>structures, PM, recycling endosomes, primary cilia</p> <p><b>Sc:</b> Golgi secretory vesicles, PM</p> <p><b>Dm:</b> PM, Golgi, recycling endosomes</p>	<p><b>Sc:</b> lethal</p> <p><b>Dm:</b> lethal</p>	<p><b>M:</b> (Ang et al., 2004; Huber et al., 1993; Yoshimura et al., 2007)</p> <p><b>Sc:</b> (Goud et al., 1988; Guo et al., 1999; Salminen and Novick, 1987)</p> <p><b>Dm:</b> (Mavor et al., 2016; West et al., 2015)</p> <p><b>Subcellular localization</b></p> <p><b>M:</b> (Ang et al., 2004; Chen et al., 2001; Huber et al., 1993; Sato et al., 2007; Yoshimura et al., 2007)</p> <p><b>Sc:</b> (Goud et al., 1988; Salminen and Novick, 1987)</p> <p><b>Dm:</b> (Mavor et al., 2016; West et al., 2015)</p> <p><b>Viability</b></p> <p><b>M:</b> (Sato et al., 2007)</p> <p><b>Sc:</b> (Giaever et al., 2002)</p> <p><b>Dm:</b> (Giagtzoglou et al., 2012)</p>
Rab8b			<p><b>M:</b> traffic from TGN to PM (exocytosis), ciliogenesis and apical transport</p>	<p><b>M:</b> Golgi, vesicular structures, PM, primary cilia</p>	<p><b>M:</b> viable</p>	<p><b>Function</b></p> <p><b>M:</b> (Huber et al., 1993; Sato et al., 2014)</p> <p><b>Subcellular localization</b></p> <p><b>M:</b> (Chen et al., 2001; Huber et al., 1993; Sato et al., 2014)</p> <p><b>Viability</b></p> <p><b>M:</b> (Sato et al., 2014)</p>
Rab8c (Rab13)			<p><b>M:</b> assembly epithelial tight junctions, endocytic recycling to PM, trafficking between recycling endosomes and TGN</p>	<p><b>M:</b> tight junctions, recycling endosomes, TGN</p>	<p><b>M:</b> viable</p>	<p><b>Function</b></p> <p><b>M:</b> (Kohler et al., 2004; Nokes et al., 2008)</p> <p><b>Subcellular localization</b></p> <p><b>M:</b> (Nokes et al., 2008; Zahraoui et al., 1994)</p> <p><b>Viability</b></p> <p><b>M:</b> International Mouse Phenotyping Consortium</p>
Rab9a	-	DmRab9	<p><b>M:</b> traffic between late endosomes and TGN</p>	<p><b>M:</b> late endosomes</p> <p><b>Dm:</b> early and late endosomes, TGN</p>	<p><b>M:</b> viable</p> <p><b>Dm:</b> viable</p>	<p><b>Function</b></p> <p><b>M:</b> (Lombardi et al., 1993)</p> <p><b>Dm:</b> (Dong et al., 2013)</p> <p><b>Subcellular localization</b></p> <p><b>M:</b> (Lombardi et al., 1993)</p>

			<b>Dm:</b> retrograde trafficking from endosomes to TGN			<b>Dm:</b> (Dong et al., 2013) <b>Viability</b> <b>M:</b> International Mouse Phenotyping Consortium
Rab9b	-		<b>M:</b> traffic between late endosomes and TGN	<b>M:</b> late endosomes	<b>M:</b> no KO model <b>Dm:</b> viable	<b>Function and subcellular localization</b> <b>M:</b> (Lombardi et al., 1993)
Rab10	-	DmRab10	<b>M:</b> transport from basolateral sorting endosomes to common endosomes, exocytosis of GLUT4 vesicles  <b>Dm:</b> regulation of basement membrane secretion/ organization	<b>M:</b> basolateral sorting endosome, GLUT4 vesicles  <b>Dm:</b> cytoplasm, basal follicle cell surface, lateral PM	<b>M:</b> lethal <b>Dm:</b> viable	<b>Function</b> <b>M:</b> (Babbey et al., 2006; Sano et al., 2007) <b>Dm:</b> (Isabella and Horne-Badovinac, 2016; Lerner et al., 2013) <b>Subcellular localization</b> <b>M:</b> (Babbey et al., 2006; Larance et al., 2005; Sano et al., 2007) <b>Dm:</b> (Isabella and Horne-Badovinac, 2016; Lerner et al., 2013) <b>Viability</b> <b>M:</b> (Lv et al., 2015)
Rab11a	Ypt31, 32	DmRab11	<b>M:</b> recycling from endosome to PM, traffic from TGN to PM  <b>Sc:</b> exit from trans Golgi, Golgi-PM transport, endosome-Golgi recycling  <b>Dm:</b> endocytic recycling	<b>M:</b> recycling endosomes, Golgi  <b>Sc:</b> transitional and late Golgi, endosomes  <b>Dm:</b> recycling endosomes	<b>M:</b> lethal <b>Sc:</b> viable, double mutant lethal <b>Dm:</b> lethal	<b>Function</b> <b>M:</b> (Ullrich et al., 1996; Urbe et al., 1993) <b>Sc:</b> (Benli et al., 1996; Chen et al., 2005; Jedd et al., 1997) <b>Dm:</b> (Dollar et al., 2002) <b>Subcellular localization</b> <b>M:</b> (Ullrich et al., 1996; Urbe et al., 1993) <b>Sc:</b> (Chen et al., 2005; Jedd et al., 1997) <b>Dm:</b> (Dollar et al., 2002) <b>Viability</b> <b>M:</b> (Yu et al., 2014) <b>Sc:</b> (Benli et al., 1996) <b>Dm:</b> (Bellen et al., 2004)
Rab11b			<b>M:</b> recycling from endosome to PM, traffic from TGN to PM	<b>M:</b> recycling endosomes, Golgi	<b>M:</b> viable	<b>Function and subcellular localization</b> <b>M:</b> (Ullrich et al., 1996; Urbe et al., 1993) <b>Viability</b> <b>M:</b> (D'Agostino et al., 2019)

Rab11c (Rab25)			<b>M:</b> apical recycling pathway	<b>M:</b> recycling endosomes	<b>M:</b> viable	<b>Function and subcellular localization</b> <b>M:</b> (Casanova et al., 1999) <b>Viability</b> <b>M:</b> (Nam et al., 2010)
Rab12	-	-	<b>M:</b> degradation of Transferrin receptor from recycling endosome to lysosome	<b>M:</b> recycling endosome	<b>M:</b> viable	<b>Function and subcellular localization</b> <b>M:</b> (Matsui et al., 2011) <b>Viability</b> <b>M:</b> International Mouse Phenotyping Consortium
Rab13 (Rab8c)	Sec4	DmRab8	<b>M:</b> assembly epithelial tight junctions, endocytic recycling to PM, trafficking between recycling endosomes and TGN  <b>Sc:</b> fusion of Golgi vesicles with PM, secretion, assembly of exocyst  <b>Dm:</b> synaptic growth responses in NMJ, regulates recycling endosome function, regulates furrow ingression, regulates exocytic trafficking	<b>M:</b> tight junctions, recycling endosomes, TGN  <b>Sc:</b> Golgi secretory vesicles, PM  <b>Dm:</b> PM, Golgi, recycling endosomes	<b>M:</b> viable <b>Sc:</b> lethal <b>Dm:</b> lethal	<b>Function</b> <b>M:</b> (Kohler et al., 2004; Nokes et al., 2008) <b>Sc:</b> (Goud et al., 1988; Guo et al., 1999; Salminen and Novick, 1987) <b>Dm:</b> (Mavor et al., 2016; West et al., 2015) <b>Subcellular localization</b> <b>M:</b> (Nokes et al., 2008; Zahraoui et al., 1994) <b>Sc:</b> (Goud et al., 1988; Salminen and Novick, 1987) <b>Dm:</b> (Mavor et al., 2016; West et al., 2015) <b>Viability</b> <b>M:</b> International Mouse Phenotyping Consortium <b>Sc:</b> (Giaever et al., 2002) <b>Dm:</b> (Giagtzoglou et al., 2012)
Rab14	-	DmRab14	<b>M:</b> regulation of carrier membranes between ER/Golgi and endosomes  <b>Dm:</b> phagosome maturation /acidification, fusion of	<b>M:</b> ER, TGN, early endosomes, GLUT4 vesicles  <b>Dm:</b> phagosomes, early and late endosomes	<b>M:</b> no KO model <b>Dm:</b> viable	<b>Function</b> <b>M:</b> (Junutula et al., 2004) <b>Dm:</b> (Garg and Wu, 2014) <b>Subcellular localization</b> <b>M:</b> (Junutula et al., 2004; Larance et al., 2005) <b>Dm:</b> (Garg and Wu, 2014)

			phagosomes with late endosomes and lysosomes			
Rab15	-	-	<b>M:</b> traffic from early/sorting endosome to recycling endosome	<b>M:</b> early/sorting endosomes, pericentriolar recycling endosomes	<b>M:</b> viable	<b>Function</b> <b>M:</b> (Zuk and Elferink, 2000) <b>Subcellular localization</b> <b>M:</b> (Zuk and Elferink, 1999, 2000) <b>Viability</b> <b>M:</b> International Mouse Phenotyping Consortium
Rab16 (Rab3d)	-	DmRab3	<b>M:</b> exocytosis <b>Dm:</b> regulation and maintenance of presynaptic active zone structure	<b>M:</b> secretory granules (in mast cells) <b>Dm:</b> presynaptic active zone, synapse	<b>M:</b> viable <b>Dm:</b> viable	<b>Function</b> <b>M:</b> (Tuvim et al., 1999) <b>Dm:</b> (Ehmann et al., 2014; Graf et al., 2009) <b>Subcellular localization</b> <b>M:</b> (Tuvim et al., 1999) <b>Dm:</b> (Chan et al., 2011; Graf et al., 2009) <b>Viability</b> <b>M:</b> (Riedel et al., 2002) <b>Dm:</b> (Graf et al., 2009)
Rab17	-	-	<b>M:</b> Transcytosis	<b>M:</b> recycling endosomes, basolateral PM, apical tubules	<b>M:</b> viable	<b>Function</b> <b>M:</b> (Zacchi et al., 1998) <b>Subcellular localization</b> <b>M:</b> (Hunziker and Peters, 1998; Lutcke et al., 1993; Zacchi et al., 1998) <b>Viability</b> <b>M:</b> International Mouse Phenotyping Consortium
Rab18	-	DmRab18	<b>M:</b> lipid droplet formation <b>Dm:</b> unknown	<b>M:</b> ER, Golgi, lipid droplets <b>Dm:</b> ER, early Golgi, early endosomes	<b>M:</b> viable <b>Dm:</b> viable	<b>Function</b> <b>M:</b> (Ozeki et al., 2005) <b>Subcellular localization</b> <b>M:</b> (Dejgaard et al., 2008; Ozeki et al., 2005) <b>Dm:</b> (Chan et al., 2011; Gillingham et al., 2014) <b>Viability</b> <b>M:</b> (Carpanini et al., 2014)

Rab19a	-	DmRab19	<b>M:</b> unknown <b>Dm:</b> promotes enteroendocrine cell differentiation (in cooperation with Atg16)	<b>M:</b> Golgi <b>Dm:</b> Golgi, recycling endosomes	<b>M:</b> viable <b>Dm:</b> viable	<b>Function</b> <b>Dm:</b> (Nagy et al., 2017) <b>Subcellular localization</b> <b>M:</b> (Sinka et al., 2008) <b>Dm:</b> (Chan et al., 2011; Gillingham et al., 2014; Sinka et al., 2008) <b>Viability</b> <b>M:</b> (Dickinson et al., 2016)
Rab19b (Rab43)	-		<b>M:</b> retrograde trafficking from endosomes to TGN, biogenesis and maintenance of Golgi structure, anterograde trafficking between ER-to-Golgi, through medial Golgi	<b>M:</b> ER, medial Golgi, TGN	<b>M:</b> viable <b>Dm:</b> viable	<b>Function</b> <b>M:</b> (Cox et al., 2016; Dejgaard et al., 2008; Fuchs et al., 2007; Haas et al., 2007) <b>Subcellular localization</b> <b>M:</b> (Cox et al., 2016; Dejgaard et al., 2008; Fuchs et al., 2007) <b>Viability</b> <b>M:</b> (Dickinson et al., 2016; Kretzer et al., 2016)
Rab20	-	-	<b>M:</b> early to late macropinosome maturation	<b>M:</b> macropinosomes	<b>M:</b> viable	<b>Function</b> <b>M:</b> (Egami and Araki, 2012a, b) <b>Subcellular localization</b> <b>M:</b> (Egami and Araki, 2012b) <b>Viability</b> <b>M:</b> (Dickinson et al., 2016)
Rab21	-	DmRab21	<b>M:</b> integrin endocytosis to regulate cell adhesion and cytokinesis <b>Dm:</b> fusion of autophagosomes with lysosomes, autophagosome maturation	<b>M:</b> early endosomes <b>Dm:</b> early and late endosomes	<b>M:</b> lethal <b>Dm:</b> viable	<b>Function</b> <b>M:</b> (Pellinen et al., 2006; Pellinen et al., 2008) <b>Dm:</b> (Jean et al., 2015) <b>Subcellular localization</b> <b>M:</b> (Simpson et al., 2004) <b>Dm:</b> (Jean et al., 2015; Jean et al., 2012) <b>Viability</b> <b>M:</b> International Mouse Phenotyping Consortium
Rab22a	-	-	<b>M:</b> endosomal trafficking to Golgi	<b>M:</b> early endosomes, TGN	<b>M:</b> viable	<b>Function and subcellular localization</b> <b>M:</b> (Kauppi et al., 2002) <b>Viability</b>

						<b>M:</b> International Mouse Phenotyping Consortium
Rab22b (Rab31)	-	-	<b>M:</b> transport of mannose 6-phosphate receptors from TGN to endosomes, TGN organization	<b>M:</b> early and late endosomes, TGN	<b>M:</b> viable	<b>Function</b> <b>M:</b> (Rodriguez-Gabin et al., 2009) <b>Subcellular localization</b> <b>M:</b> (Ng et al., 2007; Rodriguez-Gabin et al., 2001) <b>Viability</b> <b>M:</b> International Mouse Phenotyping Consortium
Rab23	-	DmRab23	<b>M:</b> negative regulator of mouse Sonic Hedgehog signaling pathway, left-right patterning in mouse embryo  <b>Dm:</b> restriction of actin accumulation in wing cells, localization of core PCP proteins, regulates PCP, regulates hedgehog ligand trafficking in germline stem cell niche	<b>M:</b> PM, early sorting endosomes  <b>Dm:</b> cytoplasm, PM	<b>M:</b> lethal <b>Dm:</b> viable	<b>Function</b> <b>M:</b> (Eggenschwiler et al., 2006; Eggenschwiler et al., 2001; Fuller et al., 2014) <b>Dm:</b> (Cicek et al., 2016; Pataki et al., 2010) <b>Subcellular localization</b> <b>M:</b> (Evans et al., 2003) <b>Dm:</b> (Pataki et al., 2010) <b>Viability</b> <b>M:</b> (Dickinson et al., 2016)
Rab24	-	-	<b>M:</b> maturation and/or clearance of autophagic compartments	<b>M:</b> ER, cis-Golgi, late endosomes	<b>M:</b> viable	<b>Function</b> <b>M:</b> (Yla-Anttila et al., 2015) <b>Subcellular localization</b> <b>M:</b> (Olkkonen et al., 1993) <b>Viability</b> <b>M:</b> (Dickinson et al., 2016)
Rab25 (Rab11c)	-	DmRab11	<b>M:</b> apical recycling pathway  <b>Sc:</b> exit from trans Golgi, Golgi-PM transport,	<b>M:</b> recycling endosomes  <b>Sc:</b> transitional and late Golgi, endosomes	<b>M:</b> viable <b>Sc:</b> viable, double mutant lethal <b>Dm:</b> lethal	<b>Function</b> <b>M:</b> (Casanova et al., 1999) <b>Sc:</b> (Benli et al., 1996; Chen et al., 2005; Jedd et al., 1997) <b>Dm:</b> (Dollar et al., 2002) <b>Subcellular localization</b>

			endosome-Golgi recycling  <b>Dm:</b> endocytic recycling	<b>Dm:</b> recycling endosomes		<b>M:</b> (Casanova et al., 1999) <b>Sc:</b> (Chen et al., 2005; Jedd et al., 1997) <b>Dm:</b> (Dollar et al., 2002) <b>Viability</b> <b>M:</b> (Nam et al., 2010) <b>Sc:</b> (Benli et al., 1996) <b>Dm:</b> (Bellen et al., 2004)
Rab26a	-	DmRab26	<b>M:</b> lysosomal traffic, secretion/exocytosis  <b>Dm:</b> stimulus-dependent membrane receptor turnover	<b>M:</b> secretory granules, lysosomes  <b>Dm:</b> synapse	<b>M:</b> viable <b>Dm:</b> viable	<b>Function</b> <b>M:</b> (Jin and Mills, 2014; Yoshie et al., 2000) <b>Dm:</b> This study <b>Subcellular localization</b> <b>M:</b> (Jin and Mills, 2014; Yoshie et al., 2000) <b>Dm:</b> (Chan et al., 2011) <b>Viability</b> <b>M:</b> (Dong et al., 2018)
Rab26b (Rab37)	-		<b>M:</b> mast cell degranulation/exocytosis of mast cell dense core granules, insulin exocytosis	<b>M:</b> (insulin-containing) secretory granules	<b>M:</b> no KO model <b>Dm:</b> viable	<b>Function</b> <b>M:</b> (Higashio et al., 2016; Ljubcic et al., 2013; Masuda et al., 2000) <b>Subcellular localization</b> <b>M:</b> (Ljubcic et al., 2013; Masuda et al., 2000)
Rab27a	-	DmRab27	<b>M:</b> transport of melanosomes to PM/mast cell degranulation, exosome secretion  <b>Dm:</b> exosomal secretion	<b>M:</b> multivesicular endosomes, melanosomes, melanosome-resident proteins  <b>Dm:</b> synapses, synaptic vesicles	<b>M:</b> viable <b>Dm:</b> viable	<b>Function</b> <b>M:</b> (Hume et al., 2001; Ostrowski et al., 2010) <b>Dm:</b> (Corrigan et al., 2014) <b>Subcellular localization</b> <b>M:</b> (Bahadoran et al., 2001; Hume et al., 2001; Ostrowski et al., 2010) <b>Dm:</b> (Chan et al., 2011) <b>Viability</b> <b>M:</b> (Wilson et al., 2000) <b>Dm:</b> (Chan et al., 2011)
Rab27b	-		<b>M:</b> transport of melanosomes, formation/maintenance of dendritic extensions in melanocytes, exosome	<b>M:</b> melanosomes, Golgi, TGN and multivesicular endosomes	<b>M:</b> viable	<b>Function</b> <b>M:</b> (Chen et al., 2002; Ostrowski et al., 2010; Tolmachova et al., 2007) <b>Subcellular localization</b> <b>M:</b> (Chen et al., 2002; Ostrowski et al., 2010)

			secretion, platelet dense granule secretion			<b>Viability</b> <b>M:</b> (Tolmachova et al., 2007)
Rab28	-	-	<b>M:</b> phagocytosis of outer cone segment (in murine retinal pigmented epithelium)	<b>M:</b> basal body and ciliary rootlet of photoreceptors	<b>M:</b> viable	<b>Function</b> <b>M:</b> (Ying et al., 2018) <b>Subcellular localization</b> <b>M:</b> (Roosing et al., 2013) <b>Viability</b> <b>M:</b> (Ying et al., 2018)
Rab29	-	-	<b>M:</b> maintenance of TGN, integrity retrograde traffic of Mannose-6-Phosphate receptor, lysosomal trafficking (Golgi-to-lysosome), master regulator of LRRK2	<b>M:</b> TGN	<b>M:</b> viable	<b>Function</b> <b>M:</b> (MacLeod et al., 2013; Purlyte et al., 2018; Wang et al., 2014) <b>Subcellular localization</b> <b>M:</b> (Wang et al., 2014) <b>Viability</b> <b>M:</b> (Kuwahara et al., 2016)
Rab30	-	DmRab30	<b>M:</b> structural integrity of Golgi apparatus  <b>Dm:</b> embryonic and adult morphogenesis (JNK-dependent dorsal closure, embryonic head involution, thorax closure)	<b>M:</b> Golgi  <b>Dm:</b> Golgi, endosomes, trans-Golgi	<b>M:</b> no KO model <b>Dm:</b> viable	<b>Function</b> <b>M:</b> (Kelly et al., 2012) <b>Dm:</b> (Thomas et al., 2009) <b>Subcellular localization</b> <b>M:</b> (Kelly et al., 2012) <b>Dm:</b> (Gillingham et al., 2014; Sinka et al., 2008; Thomas et al., 2009)
Rab31 (Rab22b)	-	-	<b>M:</b> transport of mannose 6-phosphate receptors from TGN to endosomes, TGN organization	<b>M:</b> early and late endosomes, TGN	<b>M:</b> viable	<b>Function</b> <b>M:</b> (Rodriguez-Gabin et al., 2009) <b>Subcellular localization</b> <b>M:</b> (Ng et al., 2007; Rodriguez-Gabin et al., 2001) <b>Viability</b> <b>M:</b> International Mouse Phenotyping Consortium
Rab32a	-		<b>M:</b> intracellular sorting of Tyrp-1 and tyrosinase,	<b>M:</b> mature melanosomes,	<b>M:</b> (sub)viable <b>Dm:</b> viable	<b>Function</b> <b>M:</b> (Alto et al., 2002; Wasmeier et al., 2006)

		DmRab32 (lightoid)	<p>sorting of melanogenic enzymes from TGN to melanosomes, synchronization of mitochondrial fission</p> <p><b>Dm:</b> eye pigment granule biosynthesis, maintenance of lipid droplet size, regulation of lipid storage, regulation of autophagy</p>	<p>perinuclear (Tyrp-1 containing) vesicles, mitochondria</p> <p><b>Dm:</b> lysosomes and autophagosomes</p>		<p><b>Dm:</b> (Ma et al., 2004; Wang et al., 2012)</p> <p><b>Subcellular localization</b></p> <p><b>M:</b> (Alto et al., 2002; Cohen-Solal et al., 2003; Wasmeier et al., 2006)</p> <p><b>Dm:</b> (Wang et al., 2012)</p> <p><b>Viability</b></p> <p><b>M:</b> (Aguilar et al., 2019; Dickinson et al., 2016)</p> <p><b>Dm:</b> (Ma et al., 2004)</p>
Rab32b (Rab38)	-		<p><b>M:</b> melanosome maturation, intracellular sorting of Tyrp-1 and tyrosinase, sorting of melanogenic enzymes from TGN to melanosomes</p>	<p><b>M:</b> mature melanosomes, perinuclear (Tyrp-1 containing) vesicles, mitochondria</p>	<p><b>M:</b> viable</p>	<p><b>Function and subcellular localization</b></p> <p><b>M:</b> (Wasmeier et al., 2006)</p> <p><b>Viability</b></p> <p><b>M:</b> (Aguilar et al., 2019)</p>
Rab33a	-	-	<p><b>M:</b> anterograde axonal transport of post-Golgi synaptophysin-pos. vesicles</p>	<p><b>M:</b> Golgi, synaptophysin-pos. vesicles</p>	<p><b>M:</b> no KO model</p>	<p><b>Function and subcellular localization</b></p> <p><b>M:</b> (Nakazawa et al., 2012)</p>
Rab33b	-	-	<p><b>M:</b> modulation of autophagosome formation, retrograde transport Golgi-to-ER</p>	<p><b>M:</b> Golgi apparatus (esp. medial Golgi cisternae)</p>	<p><b>M:</b> viable</p>	<p><b>Function</b></p> <p><b>M:</b> (Itoh et al., 2008; Valsdottir et al., 2001)</p> <p><b>Subcellular localization</b></p> <p><b>M:</b> (Zheng et al., 1998)</p> <p><b>Viability</b></p> <p><b>M:</b> International Mouse Phenotyping Consortium</p>
Rab34	-	-	<p><b>M:</b> intracellular lysosomal positioning, macropinosome formation, ciliary vesicle formation</p>	<p><b>M:</b> Golgi, macropinosomes,</p>	<p><b>M:</b> lethal</p>	<p><b>Function</b></p> <p><b>M:</b> (Sun et al., 2003; Wang and Hong, 2002; Xu et al., 2018)</p> <p><b>Subcellular localization</b></p>

						<p><b>M:</b> (Speight and Silverman, 2005; Sun et al., 2003; Wang and Hong, 2002)</p> <p><b>Viability</b></p> <p><b>M:</b> (Dickinson et al., 2016; Xu et al., 2018)</p>
Rab35	-	DmRab35	<p><b>M:</b> formation of phagosomes (phagocytosis), remodeling of actin cytoskeleton, cadherin-dependent adherens junction formation, controls fast endocytotic recycling pathway, cytokinesis</p> <p><b>Dm:</b> actin filament assembly during bristle development, vesicle transport during phagocytosis, trafficking from PM to early endosome, cytoskeletal remodeling at PM, endosomal trafficking to synaptic vesicles</p>	<p><b>M:</b> PM, endocytic compartments, near to actin filaments</p> <p><b>Dm:</b> PM, NMJ boutons, synapses of VNC</p>	<p><b>M:</b> lethal</p> <p><b>Dm:</b> semi-lethal</p>	<p><b>Function</b></p> <p><b>M:</b> (Charrasse et al., 2013; Chevallier et al., 2009; Egami et al., 2011; Kouranti et al., 2006)</p> <p><b>Dm:</b> (Jewett et al., 2017; Shim et al., 2010; Uytterhoeven et al., 2011; Zhang et al., 2009)</p> <p><b>Subcellular localization</b></p> <p><b>M:</b> (Chevallier et al., 2009; Kouranti et al., 2006)</p> <p><b>Dm:</b> (Chan et al., 2011; Jewett et al., 2017; Shim et al., 2010; Uytterhoeven et al., 2011)</p> <p><b>Viability</b></p> <p><b>M:</b> (Dickinson et al., 2016)</p>
Rab36	-	-	<p><b>M:</b> regulates spatial distribution of late endosomes and lysosomes, retrograde transport of melanosomes</p>	<p><b>M:</b> Golgi</p>	<p><b>M:</b> viable</p>	<p><b>Function</b></p> <p><b>M:</b> (Chen et al., 2010; Matsui et al., 2012)</p> <p><b>Subcellular localization</b></p> <p><b>M:</b> (Chen et al., 2010)</p> <p><b>Viability</b></p> <p><b>M:</b> (Dickinson et al., 2016)</p>
Rab37 (Rab26b)	-	DmRab26	<p><b>M:</b> mast cell degranulation/exocytosis of mast cell dense core</p>	<p><b>M:</b> (insulin-containing) secretory granules</p> <p><b>Dm:</b> synapse</p>	<p><b>M:</b> no KO model</p> <p><b>Dm:</b> viable</p>	<p><b>Function</b></p> <p><b>M:</b> (Higashio et al., 2016; Ljubicic et al., 2013; Masuda et al., 2000)</p> <p><b>Dm:</b> This study</p>

			granules, insulin exocytosis  <b>Dm:</b> stimulus-dependent membrane receptor turnover			<b>Subcellular localization</b> <b>M:</b> (Ljubicic et al., 2013; Masuda et al., 2000) <b>Dm:</b> (Chan et al., 2011)
Rab38 (Rab32b)	-	DmRab32	<b>M:</b> melanosome maturation, intracellular sorting of Tyrp-1 and tyrosinase, sorting of melanogenic enzymes from TGN to melanosomes  <b>Dm:</b> eye pigment granule biosynthesis, maintenance of lipid droplet size, regulation of lipid storage, regulation of autophagy	<b>M:</b> mature melanosomes, perinuclear (Tyrp-1 containing) vesicles, mitochondria  <b>Dm:</b> lysosomes and autophagosomes	<b>M:</b> viable <b>Dm:</b> viable	<b>Function</b> <b>M:</b> (Wasmeier et al., 2006) <b>Dm:</b> (Ma et al., 2004; Wang et al., 2012) <b>Subcellular localization</b> <b>M:</b> (Wasmeier et al., 2006) <b>Dm:</b> (Wang et al., 2012) <b>Viability</b> <b>M:</b> (Aguilar et al., 2019) <b>Dm:</b> (Ma et al., 2004)
Rab39a	-	DmRab39	<b>M:</b> secretion of pro-inflammatory cytokine, phagosome acidification, autophagosome formation  <b>Dm:</b> unknown	<b>M:</b> late endosomes, lysosomes  <b>Dm:</b> Golgi, late endosomes, synapse	<b>M:</b> viable <b>Dm:</b> viable	<b>Function</b> <b>M:</b> (Becker et al., 2009; Seto et al., 2013; Seto et al., 2011) <b>Subcellular localization</b> <b>M:</b> (Seto et al., 2013) <b>Dm:</b> (Chan et al., 2011; Gillingham et al., 2014; Jin et al., 2012) <b>Viability</b> <b>M:</b> (Cruz et al., 2020)
Rab39b	-		<b>M:</b> function in synaptic activity/transmission, regulates traffic of glutamate receptor subunits to synaptic terminals	<b>M:</b> Golgi	<b>M:</b> viable	<b>Function</b> <b>M:</b> (Mignogna et al., 2015) <b>Subcellular localization:</b> <b>M:</b> (Giannandrea et al., 2010) <b>Viability</b> <b>M:</b> (Gao et al., 2020)

Rab39c (Rab42)	-		<b>M:</b> unknown	<b>M:</b> unknown	<b>M:</b> no KO model	
Rab40a**	-	DmRab40	<b>M:</b> unknown <b>Dm:</b> unknown	<b>M:</b> unknown <b>Dm:</b> synapse and neuronal cell body	<b>M:</b> no KO model <b>Dm:</b> viable	<b>Subcellular localization</b> <b>Dm:</b> (Jin et al., 2012)
Rab40b	-		<b>M:</b> transport of MMP2/9 secretory vesicles during invadopodia formation, regulation of MMP secretion	<b>M:</b> TGN-derived secretory vesicles	<b>M:</b> viable	<b>Function and subcellular localization</b> <b>M:</b> (Jacob et al., 2013) <b>Viability</b> <b>M:</b> International Mouse Phenotyping Consortium
Rab40c	-		<b>M:</b> modulates biogenesis of lipid droplets, receptor recycling in oligodendrocytes	<b>M:</b> lipid droplets, recycling endosomes	<b>M:</b> subviable	<b>Function and subcellular localization</b> <b>M:</b> (Rodriguez-Gabin et al., 2004; Tan et al., 2013) <b>Viability</b> <b>M:</b> (Dickinson et al., 2016)
Rab40aL (RLGP)**	-		<b>M:</b> unknown	<b>M:</b> mitochondria	<b>M:</b> no KO model	<b>Subcellular localization</b> <b>M:</b> (Bedoyan et al., 2012; Saito-Ohara et al., 2002)
Rab41 (Rab6d)***	Ypt6	DmRab6	<b>M:</b> Golgi ribbon formation, ER-to-Golgi trafficking <b>Sc:</b> Endosome-Golgi, intra Golgi and retrograde Golgi-ER transport, delivery of Atg9 to phagophore assembly site <b>Dm:</b> regulates autophagy and insulin-TOR signaling, regulation of autolysosomal	<b>M:</b> Golgi <b>Sc:</b> Golgi <b>Dm:</b> Golgi, cytoplasmic vesicles, lysosomes and autophagosomes	<b>M:</b> no KO model <b>Sc:</b> viable <b>Dm:</b> lethal	<b>Function</b> <b>M:</b> (Liu et al., 2013; Liu et al., 2016) <b>Sc:</b> (Kawamura et al., 2014; Luo and Gallwitz, 2003; Suda et al., 2013; Yang and Rosenwald, 2016) <b>Dm:</b> (Ayala et al., 2018; Iwanami et al., 2016; Tong et al., 2011) <b>Subcellular localization</b> <b>M:</b> (Liu et al., 2013) <b>Sc:</b> (Kawamura et al., 2014) <b>Dm:</b> (Ayala et al., 2018; Tong et al., 2011) <b>Viability</b> <b>Sc:</b> (Giaever et al., 2002) <b>Dm:</b> (Purcell and Artavanis-Tsakonas, 1999)

			homeostasis, insulin signaling, axon guidance in R7 photoreceptors, apical transport pathway in photoreceptors			
Rab42 (Rab39c)	-	DmRab39	<b>M:</b> unknown <b>Dm:</b> unknown	<b>M:</b> unknown <b>Dm:</b> Golgi, late endosomes, synapse	<b>M:</b> no KO model <b>Dm:</b> viable	<b>Subcellular localization</b> <b>Dm:</b> (Chan et al., 2011; Gillingham et al., 2014; Jin et al., 2012)
Rab43 (Rab19b)	-	DmRab19	<b>M:</b> retrograde trafficking from endosomes to TGN, biogenesis and maintenance of Golgi structure, anterograde trafficking between ER-to-Golgi, through medial Golgi <b>Dm:</b> promotes enteroendocrine cell differentiation (in cooperation with Atg16)	<b>M:</b> ER, medial Golgi, TGN <b>Dm:</b> Golgi, recycling endosomes	<b>M:</b> viable <b>Dm:</b> viable	<b>Function</b> <b>M:</b> (Cox et al., 2016; Dejgaard et al., 2008; Fuchs et al., 2007; Haas et al., 2007) <b>Dm:</b> (Nagy et al., 2017) <b>Subcellular localization</b> <b>M:</b> (Cox et al., 2016; Dejgaard et al., 2008; Fuchs et al., 2007) <b>Dm:</b> (Chan et al., 2011; Gillingham et al., 2014; Sinka et al., 2008) <b>Viability</b> <b>M:</b> (Dickinson et al., 2016; Kretzer et al., 2016)
Rab44a	-	-	<b>M:</b> regulation of osteoclast differentiation, granule exocytosis in mast cells	<b>M:</b> Golgi, lysosomes	<b>M:</b> viable	<b>Function</b> <b>M:</b> (Kadowaki et al., 2020; Yamaguchi et al., 2018) <b>Subcellular localization</b> <b>M:</b> (Tokuhisa et al., 2020; Yamaguchi et al., 2018) <b>Viability</b> <b>M:</b> (Kadowaki et al., 2020)
Rab44b	-	-	<b>M:</b> regulation of osteoclast differentiation, granule exocytosis in mast cells	<b>M:</b> Golgi, lysosomes	<b>M:</b> viable	<b>Function</b> <b>M:</b> (Kadowaki et al., 2020; Yamaguchi et al., 2018) <b>Subcellular localization</b>

						<b>M:</b> (Tokuhisu et al., 2020; Yamaguchi et al., 2018) <b>Viability</b> <b>M:</b> (Kadowaki et al., 2020)
Rab45	-	-	<b>M:</b> induction of apoptosis in CML progenitor cells	<b>M:</b> perinuclear region	<b>M:</b> no KO model	<b>Function</b> <b>M:</b> (Nakamura et al., 2011) <b>Subcellular localization</b> <b>M:</b> (Shintani et al., 2007)
-	-	RabX1 (crowded)	<b>Dm:</b> trafficking between early and late endosomes, formation of endolysosomes	<b>Dm:</b> recycling endosomes, late endosomes	<b>Dm:</b> viable	<b>Function</b> <b>Dm:</b> (Laiouar et al., 2020; Woichansky et al., 2016) <b>Subcellular localization</b> <b>Dm:</b> (Chan et al., 2011; Laiouar et al., 2020)
-	-	RabX4	<b>Dm:</b> unknown	<b>Dm:</b> synapses, recycling endosomes	<b>Dm:</b> viable	<b>Subcellular localization</b> <b>Dm:</b> (Chan et al., 2011)
-	-	RabX6	<b>Dm:</b> unknown	<b>Dm:</b> neuronal cell body	<b>Dm:</b> viable	<b>Subcellular localization</b> <b>Dm:</b> (Jin et al., 2012)

\* = Rab6c is specific to Hominidae; \*\* = Rab40a and Rab40aL are specific to primates; \*\*\* = Rab41 (Rab6d) is specific to primates and dolphins (Klopper et al., 2012)

### References – Supplementary Table 3

- Aguilar, A., Weber, J., Boscher, J., Freund, M., Ziesel, C., Eckly, A., Magnenat, S., Bourdon, C., Hechler, B., Mangin, P.H., *et al.* (2019). Combined deficiency of RAB32 and RAB38 in the mouse mimics Hermansky-Pudlak syndrome and critically impairs thrombosis. *Blood Adv* 3, 2368-2380.
- Alto, N.M., Soderling, J., and Scott, J.D. (2002). Rab32 is an A-kinase anchoring protein and participates in mitochondrial dynamics. *J Cell Biol* 158, 659-668.
- Ang, A.L., Taguchi, T., Francis, S., Folsch, H., Murrells, L.J., Pypaert, M., Warren, G., and Mellman, I. (2004). Recycling endosomes can serve as intermediates during transport from the Golgi to the plasma membrane of MDCK cells. *J Cell Biol* 167, 531-543.
- Antony, C., Cibert, C., Geraud, G., Santa Maria, A., Maro, B., Mayau, V., and Goud, B. (1992). The small GTP-binding protein rab6p is distributed from medial Golgi to the trans-Golgi network as determined by a confocal microscopic approach. *J Cell Sci* 103 ( Pt 3), 785-796.
- Ayala, C.I., Kim, J., and Neufeld, T.P. (2018). Rab6 promotes insulin receptor and cathepsin trafficking to regulate autophagy induction and activity in *Drosophila*. *J Cell Sci* 131.
- Babbey, C.M., Ahktar, N., Wang, E., Chen, C.C., Grant, B.D., and Dunn, K.W. (2006). Rab10 regulates membrane transport through early endosomes of polarized Madin-Darby canine kidney cells. *Mol Biol Cell* 17, 3156-3175.
- Bahadoran, P., Aberdam, E., Mantoux, F., Busca, R., Bille, K., Yalman, N., de Saint-Basile, G., Casaroli-Marano, R., Ortonne, J.P., and Ballotti, R. (2001). Rab27a: A key to melanosome transport in human melanocytes. *J Cell Biol* 152, 843-850.
- Baker, K.P., Schaniel, A., Vestweber, D., and Schatz, G. (1990). A yeast mitochondrial outer membrane protein essential for protein import and cell viability. *Nature* 348, 605-609.
- Bardin, S., Miserey-Lenkei, S., Hurbain, I., Garcia-Castillo, D., Raposo, G., and Goud, B. (2015). Phenotypic characterisation of RAB6A knockout mouse embryonic fibroblasts. *Biol Cell* 107, 427-439.
- Becker, C.E., Creagh, E.M., and O'Neill, L.A. (2009). Rab39a binds caspase-1 and is required for caspase-1-dependent interleukin-1beta secretion. *J Biol Chem* 284, 34531-34537.
- Bedoyan, J.K., Schaibley, V.M., Peng, W., Bai, Y., Mondal, K., Shetty, A.C., Durham, M., Micucci, J.A., Dhiraaj, A., Skidmore, J.M., *et al.* (2012). Disruption of RAB40AL function leads to Martin--Probst syndrome, a rare X-linked multisystem neurodevelopmental human disorder. *J Med Genet* 49, 332-340.
- Bellen, H.J., Levis, R.W., Liao, G., He, Y., Carlson, J.W., Tsang, G., Evans-Holm, M., Hiesinger, P.R., Schulze, K.L., Rubin, G.M., *et al.* (2004). The BDGP gene disruption project: single transposon insertions associated with 40% of *Drosophila* genes. *Genetics* 167, 761-781.
- Benli, M., Doring, F., Robinson, D.G., Yang, X., and Gallwitz, D. (1996). Two GTPase isoforms, Ypt31p and Ypt32p, are essential for Golgi function in yeast. *EMBO J* 15, 6460-6475.
- Bucci, C., Parton, R.G., Mather, I.H., Stunnenberg, H., Simons, K., Hoflack, B., and Zerial, M. (1992). The small GTPase rab5 functions as a regulatory factor in the early endocytic pathway. *Cell* 70, 715-728.
- Cao, J., Ni, J., Ma, W., Shiu, V., Milla, L.A., Park, S., Spletter, M.L., Tang, S., Zhang, J., Wei, X., *et al.* (2014). Insight into insulin secretion from transcriptome and genetic analysis of insulin-producing cells of *Drosophila*. *Genetics* 197, 175-192.

Carpanini, S.M., McKie, L., Thomson, D., Wright, A.K., Gordon, S.L., Roche, S.L., Handley, M.T., Morrison, H., Brownstein, D., Wishart, T.M., *et al.* (2014). A novel mouse model of Warburg Micro syndrome reveals roles for RAB18 in eye development and organisation of the neuronal cytoskeleton. *Dis Model Mech* 7, 711-722.

Casanova, J.E., Wang, X., Kumar, R., Bhartur, S.G., Navarre, J., Woodrum, J.E., Altschuler, Y., Ray, G.S., and Goldenring, J.R. (1999). Association of Rab25 and Rab11a with the apical recycling system of polarized Madin-Darby canine kidney cells. *Mol Biol Cell* 10, 47-61.

Chan, C.C., Scoggin, S., Wang, D., Cherry, S., Dembo, T., Greenberg, B., Jin, E.J., Kuey, C., Lopez, A., Mehta, S.Q., *et al.* (2011). Systematic discovery of Rab GTPases with synaptic functions in *Drosophila*. *Curr Biol* 21, 1704-1715.

Charrasse, S., Comunale, F., De Rossi, S., Echard, A., and Gauthier-Rouviere, C. (2013). Rab35 regulates cadherin-mediated adherens junction formation and myoblast fusion. *Mol Biol Cell* 24, 234-245.

Chen, L., Hu, J., Yun, Y., and Wang, T. (2010). Rab36 regulates the spatial distribution of late endosomes and lysosomes through a similar mechanism to Rab34. *Mol Membr Biol* 27, 23-30.

Chen, S., Liang, M.C., Chia, J.N., Ngsee, J.K., and Ting, A.E. (2001). Rab8b and its interacting partner TRIP8b are involved in regulated secretion in AtT20 cells. *J Biol Chem* 276, 13209-13216.

Chen, S.H., Chen, S., Tokarev, A.A., Liu, F., Jedd, G., and Segev, N. (2005). Ypt31/32 GTPases and their novel F-box effector protein Rcy1 regulate protein recycling. *Mol Biol Cell* 16, 178-192.

Chen, Y., Samaraweera, P., Sun, T.T., Kreibich, G., and Orlow, S.J. (2002). Rab27b association with melanosomes: dominant negative mutants disrupt melanosomal movement. *J Invest Dermatol* 118, 933-940.

Cherry, S., Jin, E.J., Ozel, M.N., Lu, Z., Agi, E., Wang, D., Jung, W.H., Epstein, D., Meinertzhagen, I.A., Chan, C.C., *et al.* (2013). Charcot-Marie-Tooth 2B mutations in rab7 cause dosage-dependent neurodegeneration due to partial loss of function. *Elife* 2, e01064.

Chevallier, J., Koop, C., Srivastava, A., Petrie, R.J., Lamarche-Vane, N., and Presley, J.F. (2009). Rab35 regulates neurite outgrowth and cell shape. *FEBS Lett* 583, 1096-1101.

Cicek, I.O., Karaca, S., Brankatschk, M., Eaton, S., Urlaub, H., and Shcherbata, H.R. (2016). Hedgehog Signaling Strength Is Orchestrated by the mir-310 Cluster of MicroRNAs in Response to Diet. *Genetics* 202, 1167-1183.

Cohen-Solal, K.A., Sood, R., Marin, Y., Crespo-Carbone, S.M., Sinsimer, D., Martino, J.J., Robbins, C., Makalowska, I., Trent, J., and Chen, S. (2003). Identification and characterization of mouse Rab32 by mRNA and protein expression analysis. *Biochim Biophys Acta* 1651, 68-75.

Compagnon, J., Gervais, L., Roman, M.S., Chamot-Boeuf, S., and Guichet, A. (2009). Interplay between Rab5 and PtdIns(4,5)P2 controls early endocytosis in the *Drosophila* germline. *J Cell Sci* 122, 25-35.

Corrigan, L., Redhai, S., Leiblich, A., Fan, S.J., Perera, S.M., Patel, R., Gandy, C., Wainwright, S.M., Morris, J.F., Hamdy, F., *et al.* (2014). BMP-regulated exosomes from *Drosophila* male reproductive glands reprogram female behavior. *J Cell Biol* 206, 671-688.

Cox, J.V., Kansal, R., and Whitt, M.A. (2016). Rab43 regulates the sorting of a subset of membrane protein cargo through the medial Golgi. *Mol Biol Cell* 27, 1834-1844.

Cruz, F.M., Colbert, J.D., and Rock, K.L. (2020). The GTPase Rab39a promotes phagosome maturation into MHC-I antigen-presenting compartments. *EMBO J* 39, e102020.

D'Agostino, L., Nie, Y., Goswami, S., Tong, K., Yu, S., Bandyopadhyay, S., Flores, J., Zhang, X., Balasubramanian, I., Joseph, I., *et al.* (2019). Recycling Endosomes in Mature Epithelia Restrain Tumorigenic Signaling. *Cancer Res* 79, 4099-4112.

Darchen, F., Zahraoui, A., Hammel, F., Monteils, M.P., Tavitian, A., and Scherman, D. (1990). Association of the GTP-binding protein Rab3A with bovine adrenal chromaffin granules. *Proc Natl Acad Sci U S A* 87, 5692-5696.

de Madrid, B.H., Greenberg, L., and Hatini, V. (2015). RhoGAP68F controls transport of adhesion proteins in Rab4 endosomes to modulate epithelial morphogenesis of *Drosophila* leg discs. *Dev Biol* 399, 283-295.

Dejgaard, S.Y., Murshid, A., Erman, A., Kizilay, O., Verbich, D., Lodge, R., Dejgaard, K., Ly-Hartig, T.B., Pepperkok, R., Simpson, J.C., *et al.* (2008). Rab18 and Rab43 have key roles in ER-Golgi trafficking. *J Cell Sci* 121, 2768-2781.

Dey, S., Banker, G., and Ray, K. (2017). Anterograde Transport of Rab4-Associated Vesicles Regulates Synapse Organization in *Drosophila*. *Cell Rep* 18, 2452-2463.

Dickinson, M.E., Flenniken, A.M., Ji, X., Teboul, L., Wong, M.D., White, J.K., Meehan, T.F., Weninger, W.J., Westerberg, H., Adissu, H., *et al.* (2016). High-throughput discovery of novel developmental phenotypes. *Nature* 537, 508-514.

Dollar, G., Struckhoff, E., Michaud, J., and Cohen, R.S. (2002). Rab11 polarization of the *Drosophila* oocyte: a novel link between membrane trafficking, microtubule organization, and oskar mRNA localization and translation. *Development* 129, 517-526.

Dong, B., Kakiyama, K., Otani, T., Wada, H., and Hayashi, S. (2013). Rab9 and retromer regulate retrograde trafficking of luminal protein required for epithelial tube length control. *Nat Commun* 4, 1358.

Dong, W., He, B., Qian, H., Liu, Q., Wang, D., Li, J., Wei, Z., Wang, Z., Xu, Z., Wu, G., *et al.* (2018). RAB26-dependent autophagy protects adherens junctional integrity in acute lung injury. *Autophagy* 14, 1677-1692.

Egami, Y., and Araki, N. (2012a). Rab20 regulates phagosome maturation in RAW264 macrophages during Fc gamma receptor-mediated phagocytosis. *PLoS One* 7, e35663.

Egami, Y., and Araki, N. (2012b). Spatiotemporal Localization of Rab20 in Live RAW264 Macrophages during Macropinocytosis. *Acta Histochem Cytochem* 45, 317-323.

Egami, Y., Fukuda, M., and Araki, N. (2011). Rab35 regulates phagosome formation through recruitment of ACAP2 in macrophages during Fc gamma R-mediated phagocytosis. *J Cell Sci* 124, 3557-3567.

Eggenschwiler, J.T., Bulgakov, O.V., Qin, J., Li, T., and Anderson, K.V. (2006). Mouse Rab23 regulates hedgehog signaling from smoothed to Gli proteins. *Dev Biol* 290, 1-12.

Eggenschwiler, J.T., Espinoza, E., and Anderson, K.V. (2001). Rab23 is an essential negative regulator of the mouse Sonic hedgehog signalling pathway. *Nature* 412, 194-198.

Ehmann, N., van de Linde, S., Alon, A., Ljaschenko, D., Keung, X.Z., Holm, T., Rings, A., DiAntonio, A., Hallermann, S., Ashery, U., *et al.* (2014). Quantitative super-resolution imaging of Bruchpilot distinguishes active zone states. *Nat Commun* 5, 4650.

Entchev, E.V., Schwabedissen, A., and Gonzalez-Gaitan, M. (2000). Gradient formation of the TGF-beta homolog Dpp. *Cell* *103*, 981-991.

Evans, T.M., Ferguson, C., Wainwright, B.J., Parton, R.G., and Wicking, C. (2003). Rab23, a negative regulator of hedgehog signaling, localizes to the plasma membrane and the endocytic pathway. *Traffic* *4*, 869-884.

Fischer von Mollard, G., Mignery, G.A., Baumert, M., Perin, M.S., Hanson, T.J., Burger, P.M., Jahn, R., and Sudhof, T.C. (1990). rab3 is a small GTP-binding protein exclusively localized to synaptic vesicles. *Proc Natl Acad Sci U S A* *87*, 1988-1992.

Fischer von Mollard, G., Sudhof, T.C., and Jahn, R. (1991). A small GTP-binding protein dissociates from synaptic vesicles during exocytosis. *Nature* *349*, 79-81.

Fuchs, E., Haas, A.K., Spooner, R.A., Yoshimura, S., Lord, J.M., and Barr, F.A. (2007). Specific Rab GTPase-activating proteins define the Shiga toxin and epidermal growth factor uptake pathways. *J Cell Biol* *177*, 1133-1143.

Fuller, K., O'Connell, J.T., Gordon, J., Mauti, O., and Eggenschwiler, J. (2014). Rab23 regulates Nodal signaling in vertebrate left-right patterning independently of the Hedgehog pathway. *Dev Biol* *391*, 182-195.

Gao, Y., Wilson, G.R., Stephenson, S.E.M., Oulad-Abdelghani, M., Charlet-Berguerand, N., Bozaoglu, K., McLean, C.A., Thomas, P.Q., Finkelstein, D.I., and Lockhart, P.J. (2020). Distribution of Parkinson's disease associated RAB39B in mouse brain tissue. *Mol Brain* *13*, 52.

Garg, A., and Wu, L.P. (2014). Drosophila Rab14 mediates phagocytosis in the immune response to Staphylococcus aureus. *Cell Microbiol* *16*, 296-310.

Geppert, M., Bolshakov, V.Y., Siegelbaum, S.A., Takei, K., De Camilli, P., Hammer, R.E., and Sudhof, T.C. (1994). The role of Rab3A in neurotransmitter release. *Nature* *369*, 493-497.

Giaever, G., Chu, A.M., Ni, L., Connelly, C., Riles, L., Veronneau, S., Dow, S., Lucau-Danila, A., Anderson, K., Andre, B., *et al.* (2002). Functional profiling of the *Saccharomyces cerevisiae* genome. *Nature* *418*, 387-391.

Giagtzoglou, N., Yamamoto, S., Zitserman, D., Graves, H.K., Schulze, K.L., Wang, H., Klein, H., Roegiers, F., and Bellen, H.J. (2012). dEHBP1 controls exocytosis and recycling of Delta during asymmetric divisions. *J Cell Biol* *196*, 65-83.

Giannandrea, M., Bianchi, V., Mignogna, M.L., Sirri, A., Carrabino, S., D'Elia, E., Vecellio, M., Russo, S., Cogliati, F., Larizza, L., *et al.* (2010). Mutations in the small GTPase gene RAB39B are responsible for X-linked mental retardation associated with autism, epilepsy, and macrocephaly. *Am J Hum Genet* *86*, 185-195.

Gillingham, A.K., Sinka, R., Torres, I.L., Lilley, K.S., and Munro, S. (2014). Toward a comprehensive map of the effectors of rab GTPases. *Dev Cell* *31*, 358-373.

Gorvel, J.P., Chavrier, P., Zerial, M., and Gruenberg, J. (1991). rab5 controls early endosome fusion in vitro. *Cell* *64*, 915-925.

Goud, B., Salminen, A., Walworth, N.C., and Novick, P.J. (1988). A GTP-binding protein required for secretion rapidly associates with secretory vesicles and the plasma membrane in yeast. *Cell* *53*, 753-768.

Goud, B., Zahraoui, A., Tavitian, A., and Saraste, J. (1990). Small GTP-binding protein associated with Golgi cisternae. *Nature* *345*, 553-556.

Graf, E.R., Daniels, R.W., Burgess, R.W., Schwarz, T.L., and DiAntonio, A. (2009). Rab3 dynamically controls protein composition at active zones. *Neuron* *64*, 663-677.

Guerra, F., and Bucci, C. (2016). Multiple Roles of the Small GTPase Rab7. *Cells* *5*.

Guo, W., Roth, D., Walch-Solimena, C., and Novick, P. (1999). The exocyst is an effector for Sec4p, targeting secretory vesicles to sites of exocytosis. *EMBO J* *18*, 1071-1080.

Haas, A.K., Yoshimura, S., Stephens, D.J., Preisinger, C., Fuchs, E., and Barr, F.A. (2007). Analysis of GTPase-activating proteins: Rab1 and Rab43 are key Rabs required to maintain a functional Golgi complex in human cells. *J Cell Sci* *120*, 2997-3010.

Higashio, H., Satoh, Y., and Saino, T. (2016). Mast cell degranulation is negatively regulated by the Munc13-4-binding small-guanosine triphosphatase Rab37. *Sci Rep* *6*, 22539.

Huber, L.A., Pimplikar, S., Parton, R.G., Virta, H., Zerial, M., and Simons, K. (1993). Rab8, a small GTPase involved in vesicular traffic between the TGN and the basolateral plasma membrane. *J Cell Biol* *123*, 35-45.

Hume, A.N., Collinson, L.M., Rapak, A., Gomes, A.Q., Hopkins, C.R., and Seabra, M.C. (2001). Rab27a regulates the peripheral distribution of melanosomes in melanocytes. *J Cell Biol* *152*, 795-808.

Hunziker, W., and Peters, P.J. (1998). Rab17 localizes to recycling endosomes and regulates receptor-mediated transcytosis in epithelial cells. *J Biol Chem* *273*, 15734-15741.

Isabella, A.J., and Horne-Badovinac, S. (2016). Rab10-Mediated Secretion Synergizes with Tissue Movement to Build a Polarized Basement Membrane Architecture for Organ Morphogenesis. *Dev Cell* *38*, 47-60.

Ishida, M., Ohbayashi, N., Maruta, Y., Ebata, Y., and Fukuda, M. (2012). Functional involvement of Rab1A in microtubule-dependent anterograde melanosome transport in melanocytes. *J Cell Sci* *125*, 5177-5187.

Itoh, T., Fujita, N., Kanno, E., Yamamoto, A., Yoshimori, T., and Fukuda, M. (2008). Golgi-resident small GTPase Rab33B interacts with Atg16L and modulates autophagosome formation. *Mol Biol Cell* *19*, 2916-2925.

Iwanami, N., Nakamura, Y., Satoh, T., Liu, Z., and Satoh, A.K. (2016). Rab6 Is Required for Multiple Apical Transport Pathways but Not the Basolateral Transport Pathway in *Drosophila* Photoreceptors. *PLoS Genet* *12*, e1005828.

Jacob, A., Jing, J., Lee, J., Schedin, P., Gilbert, S.M., Peden, A.A., Junutula, J.R., and Prekeris, R. (2013). Rab40b regulates trafficking of MMP2 and MMP9 during invadopodia formation and invasion of breast cancer cells. *J Cell Sci* *126*, 4647-4658.

Jean, S., Cox, S., Nassari, S., and Kiger, A.A. (2015). Starvation-induced MTMR13 and RAB21 activity regulates VAMP8 to promote autophagosome-lysosome fusion. *EMBO Rep* *16*, 297-311.

Jean, S., Cox, S., Schmidt, E.J., Robinson, F.L., and Kiger, A. (2012). Sbf/MTMR13 coordinates PI(3)P and Rab21 regulation in endocytic control of cellular remodeling. *Mol Biol Cell* *23*, 2723-2740.

Jedd, G., Mulholland, J., and Segev, N. (1997). Two new Ypt GTPases are required for exit from the yeast trans-Golgi compartment. *J Cell Biol* *137*, 563-580.

Jedd, G., Richardson, C., Litt, R., and Segev, N. (1995). The Ypt1 GTPase is essential for the first two steps of the yeast secretory pathway. *J Cell Biol* *131*, 583-590.

Jewett, C.E., Vanderleest, T.E., Miao, H., Xie, Y., Madhu, R., Loerke, D., and Blankenship, J.T. (2017). Planar polarized Rab35 functions as an oscillatory ratchet during cell intercalation in the *Drosophila* epithelium. *Nat Commun* *8*, 476.

Jin, E.J., Chan, C.C., Agi, E., Cherry, S., Hanacik, E., Buszczak, M., and Hiesinger, P.R. (2012). Similarities of *Drosophila* rab GTPases based on expression profiling: completion and analysis of the rab-Gal4 kit. *PLoS One* 7, e40912.

Jin, R.U., and Mills, J.C. (2014). RAB26 coordinates lysosome traffic and mitochondrial localization. *J Cell Sci* 127, 1018-1032.

Junutula, J.R., De Maziere, A.M., Peden, A.A., Ervin, K.E., Advani, R.J., van Dijk, S.M., Klumperman, J., and Scheller, R.H. (2004). Rab14 is involved in membrane trafficking between the Golgi complex and endosomes. *Mol Biol Cell* 15, 2218-2229.

Kadowaki, T., Yamaguchi, Y., Kido, M.A., Abe, T., Ogawa, K., Tokuhisa, M., Gao, W., Okamoto, K., Kiyonari, H., and Tsukuba, T. (2020). The large GTPase Rab44 regulates granule exocytosis in mast cells and IgE-mediated anaphylaxis. *Cell Mol Immunol* 17, 1287-1289.

Kauppi, M., Simonsen, A., Bremnes, B., Vieira, A., Callaghan, J., Stenmark, H., and Olkkonen, V.M. (2002). The small GTPase Rab22 interacts with EEA1 and controls endosomal membrane trafficking. *J Cell Sci* 115, 899-911.

Kawamura, N., Sun-Wada, G.H., Aoyama, M., Harada, A., Takasuga, S., Sasaki, T., and Wada, Y. (2012). Delivery of endosomes to lysosomes via microautophagy in the visceral endoderm of mouse embryos. *Nat Commun* 3, 1071.

Kawamura, S., Nagano, M., Toshima, J.Y., and Toshima, J. (2014). Analysis of subcellular localization and function of the yeast Rab6 homologue, Ypt6p, using a novel amino-terminal tagging strategy. *Biochem Biophys Res Commun* 450, 519-525.

Ke, H., Feng, Z., Liu, M., Sun, T., Dai, J., Ma, M., Liu, L.P., Ni, J.Q., and Pastor-Pareja, J.C. (2018). Collagen secretion screening in *Drosophila* supports a common secretory machinery and multiple Rab requirements. *J Genet Genomics*.

Kelly, E.E., Giordano, F., Horgan, C.P., Jollivet, F., Raposo, G., and McCaffrey, M.W. (2012). Rab30 is required for the morphological integrity of the Golgi apparatus. *Biol Cell* 104, 84-101.

Kirisako, T., Baba, M., Ishihara, N., Miyazawa, K., Ohsumi, M., Yoshimori, T., Noda, T., and Ohsumi, Y. (1999). Formation process of autophagosome is traced with Apg8/Aut7p in yeast. *J Cell Biol* 147, 435-446.

Kohler, K., Louvard, D., and Zahraoui, A. (2004). Rab13 regulates PKA signaling during tight junction assembly. *J Cell Biol* 165, 175-180.

Kouranti, I., Sachse, M., Arouche, N., Goud, B., and Echard, A. (2006). Rab35 regulates an endocytic recycling pathway essential for the terminal steps of cytokinesis. *Curr Biol* 16, 1719-1725.

Kretzer, N.M., Theisen, D.J., Tussiwand, R., Briseno, C.G., Grajales-Reyes, G.E., Wu, X., Durai, V., Albring, J., Bagadia, P., Murphy, T.L., *et al.* (2016). RAB43 facilitates cross-presentation of cell-associated antigens by CD8alpha+ dendritic cells. *J Exp Med* 213, 2871-2883.

Kuwahara, T., Inoue, K., D'Agati, V.D., Fujimoto, T., Eguchi, T., Saha, S., Wolozin, B., Iwatsubo, T., and Abeliovich, A. (2016). LRRK2 and RAB7L1 coordinately regulate axonal morphology and lysosome integrity in diverse cellular contexts. *Sci Rep* 6, 29945.

Laiouar, S., Berns, N., Brech, A., and Riechmann, V. (2020). RabX1 Organizes a Late Endosomal Compartment that Forms Tubular Connections to Lysosomes Consistent with a "Kiss and Run" Mechanism. *Curr Biol* 30, 1177-1188 e1175.

Larance, M., Ramm, G., Stockli, J., van Dam, E.M., Winata, S., Wasinger, V., Simpson, F., Graham, M., Junutula, J.R., Guilhaus, M., *et al.* (2005). Characterization of the role of the Rab GTPase-activating protein AS160 in insulin-regulated GLUT4 trafficking. *J Biol Chem* 280, 37803-37813.

Lerner, D.W., McCoy, D., Isabella, A.J., Mahowald, A.P., Gerlach, G.F., Chaudhry, T.A., and Horne-Badovinac, S. (2013). A Rab10-dependent mechanism for polarized basement membrane secretion during organ morphogenesis. *Dev Cell* 24, 159-168.

Lipatova, Z., Belogortseva, N., Zhang, X.Q., Kim, J., Taussig, D., and Segev, N. (2012). Regulation of selective autophagy onset by a Ypt/Rab GTPase module. *Proc Natl Acad Sci U S A* *109*, 6981-6986.

Liu, S., Hunt, L., and Storrie, B. (2013). Rab41 is a novel regulator of Golgi apparatus organization that is needed for ER-to-Golgi trafficking and cell growth. *PLoS One* *8*, e71886.

Liu, S., Majeed, W., Kudlyk, T., Lupashin, V., and Storrie, B. (2016). Identification of Rab41/6d Effectors Provides an Explanation for the Differential Effects of Rab41/6d and Rab6a/a' on Golgi Organization. *Front Cell Dev Biol* *4*, 13.

Ljubicic, S., Bezzi, P., Brajkovic, S., Nesca, V., Guay, C., Ohbayashi, N., Fukuda, M., Abderrhamani, A., and Regazzi, R. (2013). The GTPase Rab37 Participates in the Control of Insulin Exocytosis. *PLoS One* *8*, e68255.

Lombardi, D., Soldati, T., Riederer, M.A., Goda, Y., Zerial, M., and Pfeffer, S.R. (1993). Rab9 functions in transport between late endosomes and the trans Golgi network. *EMBO J* *12*, 677-682.

Lorincz, P., Toth, S., Benko, P., Lakatos, Z., Boda, A., Glatz, G., Zobel, M., Bisi, S., Hegedus, K., Takats, S., *et al.* (2017). Rab2 promotes autophagic and endocytic lysosomal degradation. *J Cell Biol* *216*, 1937-1947.

Lund, V.K., Madsen, K.L., and Kjaerulff, O. (2018). *Drosophila* Rab2 controls endosome-lysosome fusion and LAMP delivery to late endosomes. *Autophagy* *14*, 1520-1542.

Luo, Z., and Gallwitz, D. (2003). Biochemical and genetic evidence for the involvement of yeast Ypt6-GTPase in protein retrieval to different Golgi compartments. *J Biol Chem* *278*, 791-799.

Lutcke, A., Jansson, S., Parton, R.G., Chavrier, P., Valencia, A., Huber, L.A., Lehtonen, E., and Zerial, M. (1993). Rab17, a novel small GTPase, is specific for epithelial cells and is induced during cell polarization. *J Cell Biol* *121*, 553-564.

Lv, P., Sheng, Y., Zhao, Z., Zhao, W., Gu, L., Xu, T., and Song, E. (2015). Targeted disruption of Rab10 causes early embryonic lethality. *Protein Cell* *6*, 463-467.

Ma, J., Plesken, H., Treisman, J.E., Edelman-Novemsky, I., and Ren, M. (2004). Lightoid and Claret: a rab GTPase and its putative guanine nucleotide exchange factor in biogenesis of *Drosophila* eye pigment granules. *Proc Natl Acad Sci U S A* *101*, 11652-11657.

MacLeod, D.A., Rhinn, H., Kuwahara, T., Zolin, A., Di Paolo, G., McCabe, B.D., Marder, K.S., Honig, L.S., Clark, L.N., Small, S.A., *et al.* (2013). RAB7L1 interacts with LRRK2 to modify intraneuronal protein sorting and Parkinson's disease risk. *Neuron* *77*, 425-439.

Mallard, F., Tang, B.L., Galli, T., Tenza, D., Saint-Pol, A., Yue, X., Antony, C., Hong, W., Goud, B., and Johannes, L. (2002). Early/recycling endosomes-to-TGN transport involves two SNARE complexes and a Rab6 isoform. *J Cell Biol* *156*, 653-664.

Masuda, E.S., Luo, Y., Young, C., Shen, M., Rossi, A.B., Huang, B.C., Yu, S., Bennett, M.K., Payan, D.G., and Scheller, R.H. (2000). Rab37 is a novel mast cell specific GTPase localized to secretory granules. *FEBS Lett* *470*, 61-64.

Matsui, T., Itoh, T., and Fukuda, M. (2011). Small GTPase Rab12 regulates constitutive degradation of transferrin receptor. *Traffic* *12*, 1432-1443.

Matsui, T., Ohbayashi, N., and Fukuda, M. (2012). The Rab interacting lysosomal protein (RILP) homology domain functions as a novel effector domain for small GTPase Rab36: Rab36 regulates retrograde melanosome transport in melanocytes. *J Biol Chem* *287*, 28619-28631.

Mavor, L.M., Miao, H., Zuo, Z., Holly, R.M., Xie, Y., Loerke, D., and Blankenship, J.T. (2016). Rab8 directs furrow ingression and membrane addition during epithelial formation in *Drosophila melanogaster*. *Development* *143*, 892-903.

Meresse, S., Gorvel, J.P., and Chavrier, P. (1995). The rab7 GTPase resides on a vesicular compartment connected to lysosomes. *J Cell Sci* *108 ( Pt 11)*, 3349-3358.

Mignogna, M.L., Giannandrea, M., Gurgone, A., Fanelli, F., Raimondi, F., Mapelli, L., Bassani, S., Fang, H., Van Anken, E., Alessio, M., *et al.* (2015). The intellectual disability protein RAB39B selectively regulates GluA2 trafficking to determine synaptic AMPAR composition. *Nat Commun* *6*, 6504.

Nagy, P., Szatmari, Z., Sandor, G.O., Lippai, M., Hegedus, K., and Juhasz, G. (2017). *Drosophila* Atg16 promotes enteroendocrine cell differentiation via regulation of intestinal Slit/Robo signaling. *Development* *144*, 3990-4001.

Nakamura, S., Takemura, T., Tan, L., Nagata, Y., Yokota, D., Hirano, I., Shigeno, K., Shibata, K., Fujie, M., Fujisawa, S., *et al.* (2011). Small GTPase RAB45-mediated p38 activation in apoptosis of chronic myeloid leukemia progenitor cells. *Carcinogenesis* *32*, 1758-1772.

Nakazawa, H., Sada, T., Toriyama, M., Tago, K., Sugiura, T., Fukuda, M., and Inagaki, N. (2012). Rab33a mediates anterograde vesicular transport for membrane exocytosis and axon outgrowth. *J Neurosci* *32*, 12712-12725.

Nam, K.T., Lee, H.J., Smith, J.J., Lapierre, L.A., Kamath, V.P., Chen, X., Aronow, B.J., Yeatman, T.J., Bhartur, S.G., Calhoun, B.C., *et al.* (2010). Loss of Rab25 promotes the development of intestinal neoplasia in mice and is associated with human colorectal adenocarcinomas. *J Clin Invest* *120*, 840-849.

Ng, E.L., Wang, Y., and Tang, B.L. (2007). Rab22B's role in trans-Golgi network membrane dynamics. *Biochem Biophys Res Commun* *361*, 751-757.

Nickerson, D.P., Russell, M.R.G., Lo, S.Y., Chapin, H.C., Milnes, J., and Merz, A.J. (2012). Termination of isoform-selective Vps21/Rab5 signaling at endolysosomal organelles by Msb3/Gyp3. *Traffic* *13*, 1411-1428.

Nokes, R.L., Fields, I.C., Collins, R.N., and Folsch, H. (2008). Rab13 regulates membrane trafficking between TGN and recycling endosomes in polarized epithelial cells. *J Cell Biol* *182*, 845-853.

Nyitrai, H., Wang, S.S.H., and Kaeser, P.S. (2020). ELKS1 Captures Rab6-Marked Vesicular Cargo in Presynaptic Nerve Terminals. *Cell Rep* *31*, 107712.

Olkkonen, V.M., Dupree, P., Killisch, I., Lutcke, A., Zerial, M., and Simons, K. (1993). Molecular cloning and subcellular localization of three GTP-binding proteins of the rab subfamily. *J Cell Sci* *106 ( Pt 4)*, 1249-1261.

Opdam, F.J., Echard, A., Croes, H.J., van den Hurk, J.A., van de Vorstenbosch, R.A., Ginsel, L.A., Goud, B., and Fransen, J.A. (2000). The small GTPase Rab6B, a novel Rab6 subfamily member, is cell-type specifically expressed and localised to the Golgi apparatus. *J Cell Sci* *113 ( Pt 15)*, 2725-2735.

Ostrowski, M., Carmo, N.B., Krumeich, S., Fanget, I., Raposo, G., Savina, A., Moita, C.F., Schauer, K., Hume, A.N., Freitas, R.P., *et al.* (2010). Rab27a and Rab27b control different steps of the exosome secretion pathway. *Nat Cell Biol* *12*, 19-30; sup pp 11-13.

Ozeki, S., Cheng, J., Tauchi-Sato, K., Hatano, N., Taniguchi, H., and Fujimoto, T. (2005). Rab18 localizes to lipid droplets and induces their close apposition to the endoplasmic reticulum-derived membrane. *J Cell Sci* *118*, 2601-2611.

Pataki, C., Matusek, T., Kurucz, E., Ando, I., Jenny, A., and Mihaly, J. (2010). *Drosophila* Rab23 is involved in the regulation of the number and planar polarization of the adult cuticular hairs. *Genetics* *184*, 1051-1065.

Pellinen, T., Arjonen, A., Vuoriluoto, K., Kallio, K., Fransen, J.A., and Ivaska, J. (2006). Small GTPase Rab21 regulates cell adhesion and controls endosomal traffic of beta1-integrins. *J Cell Biol* *173*, 767-780.

Pellinen, T., Tuomi, S., Arjonen, A., Wolf, M., Edgren, H., Meyer, H., Grosse, R., Kitzing, T., Rantala, J.K., Kallioniemi, O., *et al.* (2008). Integrin trafficking regulated by Rab21 is necessary for cytokinesis. *Dev Cell* *15*, 371-385.

Plutner, H., Cox, A.D., Pind, S., Khosravi-Far, R., Bourne, J.R., Schwaninger, R., Der, C.J., and Balch, W.E. (1991). Rab1b regulates vesicular transport between the endoplasmic reticulum and successive Golgi compartments. *J Cell Biol* 115, 31-43.

Purcell, K., and Artavanis-Tsakonas, S. (1999). The developmental role of warthog, the notch modifier encoding Drab6. *J Cell Biol* 146, 731-740.

Purlyte, E., Dhekne, H.S., Sarhan, A.R., Gomez, R., Lis, P., Wightman, M., Martinez, T.N., Tonelli, F., Pfeffer, S.R., and Alessi, D.R. (2018). Rab29 activation of the Parkinson's disease-associated LRRK2 kinase. *EMBO J* 37, 1-18.

Riedel, D., Antonin, W., Fernandez-Chacon, R., Alvarez de Toledo, G., Jo, T., Geppert, M., Valentijn, J.A., Valentijn, K., Jamieson, J.D., Sudhof, T.C., *et al.* (2002). Rab3D is not required for exocrine exocytosis but for maintenance of normally sized secretory granules. *Mol Cell Biol* 22, 6487-6497.

Rodriguez-Gabin, A.G., Almazan, G., and Larocca, J.N. (2004). Vesicle transport in oligodendrocytes: probable role of Rab40c protein. *J Neurosci Res* 76, 758-770.

Rodriguez-Gabin, A.G., Cammer, M., Almazan, G., Charron, M., and Larocca, J.N. (2001). Role of rRAB22b, an oligodendrocyte protein, in regulation of transport of vesicles from trans Golgi to endocytic compartments. *J Neurosci Res* 66, 1149-1160.

Rodriguez-Gabin, A.G., Yin, X., Si, Q., and Larocca, J.N. (2009). Transport of mannose-6-phosphate receptors from the trans-Golgi network to endosomes requires Rab31. *Exp Cell Res* 315, 2215-2230.

Roosing, S., Rohrschneider, K., Beryozkin, A., Sharon, D., Weisschuh, N., Staller, J., Kohl, S., Zelinger, L., Peters, T.A., Neveling, K., *et al.* (2013). Mutations in RAB28, encoding a farnesylated small GTPase, are associated with autosomal-recessive cone-rod dystrophy. *Am J Hum Genet* 93, 110-117.

Saito-Ohara, F., Fukuda, Y., Ito, M., Agarwala, K.L., Hayashi, M., Matsuo, M., Imoto, I., Yamakawa, K., Nakamura, Y., and Inazawa, J. (2002). The Xq22 inversion breakpoint interrupted a novel Ras-like GTPase gene in a patient with Duchenne muscular dystrophy and profound mental retardation. *Am J Hum Genet* 71, 637-645.

Salminen, A., and Novick, P.J. (1987). A ras-like protein is required for a post-Golgi event in yeast secretion. *Cell* 49, 527-538.

Sano, H., Eguez, L., Teruel, M.N., Fukuda, M., Chuang, T.D., Chavez, J.A., Lienhard, G.E., and McGraw, T.E. (2007). Rab10, a target of the AS160 Rab GAP, is required for insulin-stimulated translocation of GLUT4 to the adipocyte plasma membrane. *Cell Metab* 5, 293-303.

Sato, T., Iwano, T., Kunii, M., Matsuda, S., Mizuguchi, R., Jung, Y., Hagiwara, H., Yoshihara, Y., Yuzaki, M., Harada, R., *et al.* (2014). Rab8a and Rab8b are essential for several apical transport pathways but insufficient for ciliogenesis. *J Cell Sci* 127, 422-431.

Sato, T., Mushiake, S., Kato, Y., Sato, K., Sato, M., Takeda, N., Ozono, K., Miki, K., Kubo, Y., Tsuji, A., *et al.* (2007). The Rab8 GTPase regulates apical protein localization in intestinal cells. *Nature* 448, 366-369.

Schimmoller, F., and Riezman, H. (1993). Involvement of Ypt7p, a small GTPase, in traffic from late endosome to the vacuole in yeast. *J Cell Sci* 106 ( Pt 3), 823-830.

Schluter, O.M., Khvotchev, M., Jahn, R., and Sudhof, T.C. (2002). Localization versus function of Rab3 proteins. Evidence for a common regulatory role in controlling fusion. *J Biol Chem* 277, 40919-40929.

Schluter, O.M., Schmitz, F., Jahn, R., Rosenmund, C., and Sudhof, T.C. (2004). A complete genetic analysis of neuronal Rab3 function. *J Neurosci* 24, 6629-6637.

Seachrist, J.L., Anborgh, P.H., and Ferguson, S.S. (2000). beta 2-adrenergic receptor internalization, endosomal sorting, and plasma membrane recycling are regulated by rab GTPases. *J Biol Chem* *275*, 27221-27228.

Sechi, S., Frappaolo, A., Frascini, R., Capalbo, L., Gottardo, M., Belloni, G., Glover, D.M., Wainman, A., and Giansanti, M.G. (2017). Rab1 interacts with GOLPH3 and controls Golgi structure and contractile ring constriction during cytokinesis in *Drosophila melanogaster*. *Open Biol* *7*.

Segev, N., Mulholland, J., and Botstein, D. (1988). The yeast GTP-binding YPT1 protein and a mammalian counterpart are associated with the secretion machinery. *Cell* *52*, 915-924.

Seto, S., Sugaya, K., Tsujimura, K., Nagata, T., Horii, T., and Koide, Y. (2013). Rab39a interacts with phosphatidylinositol 3-kinase and negatively regulates autophagy induced by lipopolysaccharide stimulation in macrophages. *PLoS One* *8*, e83324.

Seto, S., Tsujimura, K., and Koide, Y. (2011). Rab GTPases regulating phagosome maturation are differentially recruited to mycobacterial phagosomes. *Traffic* *12*, 407-420.

Shim, J., Lee, S.M., Lee, M.S., Yoon, J., Kweon, H.S., and Kim, Y.J. (2010). Rab35 mediates transport of Cdc42 and Rac1 to the plasma membrane during phagocytosis. *Mol Cell Biol* *30*, 1421-1433.

Shintani, M., Tada, M., Kobayashi, T., Kajihio, H., Kontani, K., and Katada, T. (2007). Characterization of Rab45/RASEF containing EF-hand domain and a coiled-coil motif as a self-associating GTPase. *Biochem Biophys Res Commun* *357*, 661-667.

Simpson, J.C., Griffiths, G., Wessling-Resnick, M., Fransen, J.A., Bennett, H., and Jones, A.T. (2004). A role for the small GTPase Rab21 in the early endocytic pathway. *J Cell Sci* *117*, 6297-6311.

Singer-Kruger, B., Stenmark, H., Dusterhoft, A., Philippsen, P., Yoo, J.S., Gallwitz, D., and Zerial, M. (1994). Role of three rab5-like GTPases, Ypt51p, Ypt52p, and Ypt53p, in the endocytic and vacuolar protein sorting pathways of yeast. *J Cell Biol* *125*, 283-298.

Sinka, R., Gillingham, A.K., Kondylis, V., and Munro, S. (2008). Golgi coiled-coil proteins contain multiple binding sites for Rab family G proteins. *J Cell Biol* *183*, 607-615.

Speight, P., and Silverman, M. (2005). Diacylglycerol-activated Hmunc13 serves as an effector of the GTPase Rab34. *Traffic* *6*, 858-865.

Suda, Y., Kurokawa, K., Hirata, R., and Nakano, A. (2013). Rab GAP cascade regulates dynamics of Ypt6 in the Golgi traffic. *Proc Natl Acad Sci U S A* *110*, 18976-18981.

Sun, P., Yamamoto, H., Suetsugu, S., Miki, H., Takenawa, T., and Endo, T. (2003). Small GTPase Rah/Rab34 is associated with membrane ruffles and macropinosomes and promotes macropinosome formation. *J Biol Chem* *278*, 4063-4071.

Sun, Y., Shestakova, A., Hunt, L., Sehgal, S., Lupashin, V., and Storrie, B. (2007). Rab6 regulates both ZW10/RINT-1 and conserved oligomeric Golgi complex-dependent Golgi trafficking and homeostasis. *Mol Biol Cell* *18*, 4129-4142.

Tan, R., Wang, W., Wang, S., Wang, Z., Sun, L., He, W., Fan, R., Zhou, Y., Xu, X., Hong, W., *et al.* (2013). Small GTPase Rab40c associates with lipid droplets and modulates the biogenesis of lipid droplets. *PLoS One* *8*, e63213.

Thibault, S.T., Singer, M.A., Miyazaki, W.Y., Milash, B., Dompe, N.A., Singh, C.M., Buchholz, R., Demsky, M., Fawcett, R., Francis-Lang, H.L., *et al.* (2004). A complementary transposon tool kit for *Drosophila melanogaster* using P and piggyBac. *Nat Genet* *36*, 283-287.

Thomas, C., Rousset, R., and Noselli, S. (2009). JNK signalling influences intracellular trafficking during *Drosophila* morphogenesis through regulation of the novel target gene Rab30. *Dev Biol* *331*, 250-260.

Tisdale, E.J., and Balch, W.E. (1996). Rab2 is essential for the maturation of pre-Golgi intermediates. *J Biol Chem* *271*, 29372-29379.

Tisdale, E.J., Bourne, J.R., Khosravi-Far, R., Der, C.J., and Balch, W.E. (1992). GTP-binding mutants of rab1 and rab2 are potent inhibitors of vesicular transport from the endoplasmic reticulum to the Golgi complex. *J Cell Biol* *119*, 749-761.

Tokuhisa, M., Kadowaki, T., Ogawa, K., Yamaguchi, Y., Kido, M.A., Gao, W., Umeda, M., and Tsukuba, T. (2020). Expression and localisation of Rab44 in immune-related cells change during cell differentiation and stimulation. *Sci Rep* *10*, 10728.

Tolmachova, T., Abrink, M., Futter, C.E., Authi, K.S., and Seabra, M.C. (2007). Rab27b regulates number and secretion of platelet dense granules. *Proc Natl Acad Sci U S A* *104*, 5872-5877.

Tong, C., Ohyama, T., Tien, A.C., Rajan, A., Haueter, C.M., and Bellen, H.J. (2011). Rich regulates target specificity of photoreceptor cells and N-cadherin trafficking in the *Drosophila* visual system via Rab6. *Neuron* *71*, 447-459.

Trischler, M., Stoorvogel, W., and Ullrich, O. (1999). Biochemical analysis of distinct Rab5- and Rab11-positive endosomes along the transferrin pathway. *J Cell Sci* *112* ( Pt 24), 4773-4783.

Tuvim, M.J., Adachi, R., Chocano, J.F., Moore, R.H., Lampert, R.M., Zera, E., Romero, E., Knoll, B.J., and Dickey, B.F. (1999). Rab3D, a small GTPase, is localized on mast cell secretory granules and translocates to the plasma membrane upon exocytosis. *Am J Respir Cell Mol Biol* *20*, 79-89.

Ullrich, O., Reinsch, S., Urbe, S., Zerial, M., and Parton, R.G. (1996). Rab11 regulates recycling through the pericentriolar recycling endosome. *J Cell Biol* *135*, 913-924.

Urbe, S., Huber, L.A., Zerial, M., Tooze, S.A., and Parton, R.G. (1993). Rab11, a small GTPase associated with both constitutive and regulated secretory pathways in PC12 cells. *FEBS Lett* *334*, 175-182.

Uytterhoeven, V., Kuenen, S., Kasproiwicz, J., Miskiewicz, K., and Verstreken, P. (2011). Loss of skywalker reveals synaptic endosomes as sorting stations for synaptic vesicle proteins. *Cell* *145*, 117-132.

Valsdottir, R., Hashimoto, H., Ashman, K., Koda, T., Storrie, B., and Nilsson, T. (2001). Identification of rabaptin-5, rabex-5, and GM130 as putative effectors of rab33b, a regulator of retrograde traffic between the Golgi apparatus and ER. *FEBS Lett* *508*, 201-209.

van der Sluijs, P., Hull, M., Webster, P., Male, P., Goud, B., and Mellman, I. (1992). The small GTP-binding protein rab4 controls an early sorting event on the endocytic pathway. *Cell* *70*, 729-740.

Vitelli, R., Santillo, M., Lattero, D., Chiariello, M., Bifulco, M., Bruni, C.B., and Bucci, C. (1997). Role of the small GTPase Rab7 in the late endocytic pathway. *J Biol Chem* *272*, 4391-4397.

Wang, C., Liu, Z., and Huang, X. (2012). Rab32 is important for autophagy and lipid storage in *Drosophila*. *PLoS One* *7*, e32086.

Wang, S., Ma, Z., Xu, X., Wang, Z., Sun, L., Zhou, Y., Lin, X., Hong, W., and Wang, T. (2014). A role of Rab29 in the integrity of the trans-Golgi network and retrograde trafficking of mannose-6-phosphate receptor. *PLoS One* *9*, e96242.

Wang, T., and Hong, W. (2002). Interorganellar regulation of lysosome positioning by the Golgi apparatus through Rab34 interaction with Rab-interacting lysosomal protein. *Mol Biol Cell* *13*, 4317-4332.

Wasmeier, C., Romao, M., Plowright, L., Bennett, D.C., Raposo, G., and Seabra, M.C. (2006). Rab38 and Rab32 control post-Golgi trafficking of melanogenic enzymes. *J Cell Biol* 175, 271-281.

West, R.J., Lu, Y., Marie, B., Gao, F.B., and Sweeney, S.T. (2015). Rab8, POSH, and TAK1 regulate synaptic growth in a *Drosophila* model of frontotemporal dementia. *J Cell Biol* 208, 931-947.

Wilson, S.M., Yip, R., Swing, D.A., O'Sullivan, T.N., Zhang, Y., Novak, E.K., Swank, R.T., Russell, L.B., Copeland, N.G., and Jenkins, N.A. (2000). A mutation in Rab27a causes the vesicle transport defects observed in ashen mice. *Proc Natl Acad Sci U S A* 97, 7933-7938.

Woichansky, I., Beretta, C.A., Berns, N., and Riechmann, V. (2016). Three mechanisms control E-cadherin localization to the zonula adherens. *Nat Commun* 7, 10834.

Wucherpennig, T., Wilsch-Brauninger, M., and Gonzalez-Gaitan, M. (2003). Role of *Drosophila* Rab5 during endosomal trafficking at the synapse and evoked neurotransmitter release. *J Cell Biol* 161, 609-624.

Xu, S., Liu, Y., Meng, Q., and Wang, B. (2018). Rab34 small GTPase is required for Hedgehog signaling and an early step of ciliary vesicle formation in mouse. *J Cell Sci* 131.

Yamaguchi, Y., Sakai, E., Okamoto, K., Kajiya, H., Okabe, K., Naito, M., Kadowaki, T., and Tsukuba, T. (2018). Rab44, a novel large Rab GTPase, negatively regulates osteoclast differentiation by modulating intracellular calcium levels followed by NFATc1 activation. *Cell Mol Life Sci* 75, 33-48.

Yang, S., and Rosenwald, A.G. (2016). Autophagy in *Saccharomyces cerevisiae* requires the monomeric GTP-binding proteins, Arl1 and Ypt6. *Autophagy* 12, 1721-1737.

Ying, G., Boldt, K., Ueffing, M., Gerstner, C.D., Frederick, J.M., and Baehr, W. (2018). The small GTPase RAB28 is required for phagocytosis of cone outer segments by the murine retinal pigmented epithelium. *J Biol Chem* 293, 17546-17558.

Yla-Anttila, P., Mikkonen, E., Happonen, K.E., Holland, P., Ueno, T., Simonsen, A., and Eskelinen, E.L. (2015). RAB24 facilitates clearance of autophagic compartments during basal conditions. *Autophagy* 11, 1833-1848.

Yoshie, S., Imai, A., Nashida, T., and Shimomura, H. (2000). Expression, characterization, and localization of Rab26, a low molecular weight GTP-binding protein, in the rat parotid gland. *Histochem Cell Biol* 113, 259-263.

Yoshimura, S., Egerer, J., Fuchs, E., Haas, A.K., and Barr, F.A. (2007). Functional dissection of Rab GTPases involved in primary cilium formation. *J Cell Biol* 178, 363-369.

Young, J., Menetrey, J., and Goud, B. (2010). RAB6C is a retrogene that encodes a centrosomal protein involved in cell cycle progression. *J Mol Biol* 397, 69-88.

Young, J., Stauber, T., del Nery, E., Vernos, I., Pepperkok, R., and Nilsson, T. (2005). Regulation of microtubule-dependent recycling at the trans-Golgi network by Rab6A and Rab6A'. *Mol Biol Cell* 16, 162-177.

Yousefian, J., Troost, T., Grawe, F., Sasamura, T., Fortini, M., and Klein, T. (2013). Dmon1 controls recruitment of Rab7 to maturing endosomes in *Drosophila*. *J Cell Sci* 126, 1583-1594.

Yu, S., Yehia, G., Wang, J., Stypulkowski, E., Sakamori, R., Jiang, P., Hernandez-Enriquez, B., Tran, T.S., Bonder, E.M., Guo, W., *et al.* (2014). Global ablation of the mouse Rab11a gene impairs early embryogenesis and matrix metalloproteinase secretion. *J Biol Chem* 289, 32030-32043.

Zacchi, P., Stenmark, H., Parton, R.G., Orioli, D., Lim, F., Giner, A., Mellman, I., Zerial, M., and Murphy, C. (1998). Rab17 regulates membrane trafficking through apical recycling endosomes in polarized epithelial cells. *J Cell Biol* *140*, 1039-1053.

Zahraoui, A., Joberty, G., Arpin, M., Fontaine, J.J., Hellio, R., Tavitian, A., and Louvard, D. (1994). A small rab GTPase is distributed in cytoplasmic vesicles in non polarized cells but colocalizes with the tight junction marker ZO-1 in polarized epithelial cells. *J Cell Biol* *124*, 101-115.

Zhang, J., Fonovic, M., Suyama, K., Bogyo, M., and Scott, M.P. (2009). Rab35 controls actin bundling by recruiting fascin as an effector protein. *Science* *325*, 1250-1254.

Zheng, J.Y., Koda, T., Fujiwara, T., Kishi, M., Ikehara, Y., and Kakinuma, M. (1998). A novel Rab GTPase, Rab33B, is ubiquitously expressed and localized to the medial Golgi cisternae. *J Cell Sci* *111 ( Pt 8)*, 1061-1069.

Zuk, P.A., and Elferink, L.A. (1999). Rab15 mediates an early endocytic event in Chinese hamster ovary cells. *J Biol Chem* *274*, 22303-22312.

Zuk, P.A., and Elferink, L.A. (2000). Rab15 differentially regulates early endocytic trafficking. *J Biol Chem* *275*, 26754-26764.

## Supplementary Table / Supplementary File 4

### A: Homozygous mutants

18 degree	days until... (after egg collection)			number of adults in total	Ø number of adults per vial
	first instar larva	pupa	adult		
control	0	8.43 ± 0.13	16.8 ± 0.14	170	8.1 ± 1.82
<i>rab3</i>	0.4 ± 0.13	9.29 ± 0.18	18.1 ± 0.24	159	7.57 ± 1.02
<i>rab4</i>	0.1 ± 0.07	9.19 ± 0.09	17.38 ± 0.11	516	24.57 ± 2.1
<i>rab9</i>	0.29 ± 0.1	7.86 ± 0.08	16.71 ± 0.12	344	16.38 ± 1.41
<i>rab14</i>	0.1 ± 0.07	7.57 ± 0.11	15.76 ± 0.1	473	22.52 ± 1.82
<i>rab18</i>	0.33 ± 0.13	9.05 ± 0.21	17.62 ± 0.25	203	9.67 ± 1.17
<i>rab19</i>	0.1 ± 0.07	8.76 ± 0.14	18.1 ± 0.17	275	13.1 ± 1.44
<i>rab21</i>	0.29 ± 0.12	8.29 ± 0.1	16.95 ± 0.16	368	17.52 ± 0.98
<i>rab23</i>	0.24 ± 0.1	8.62 ± 0.11	17.19 ± 0.11	239	11.38 ± 1.01
<i>rab26</i>	0.24 ± 0.1	8.71 ± 0.1	17 ± 0.1	442	21.05 ± 1.91
<i>rab27</i>	0.1 ± 0.07	8.86 ± 0.1	17.1 ± 0.07	368	17.52 ± 1.16
<i>rab32</i>	0.1 ± 0.07	9.38 ± 0.11	18 ± 0.17	316	15.05 ± 0.87
<i>rab39</i>	0	9.05 ± 0.13	17.76 ± 0.1	523	24.9 ± 1.75
<i>rab40</i>	0.33 ± 0.16	10.19 ± 0.09	18.67 ± 0.14	261	12.42 ± 0.98
<i>rabX1</i>	1.71 ± 0.46	10.56 ± 0.26	19.24 ± 0.2	37	1.76 ± 0.32
<i>rabX4</i>	0.9 ± 0.14	12 ± 0.3	21.4 ± 0.53	8	0.38 ± 0.13
<i>rabX6</i>	0	9.14 ± 0.14	17.8 ± 0.13	446	21.24 ± 2.64

25 degree	days until... (after egg collection)			number of adults in total	Ø number of adults per vial
	first instar larva	pupa	adult		
control	0.15 ± 0.08	4.86 ± 0.08	8.95 ± 0.05	230	10.95 ± 2.01
<i>rab3</i>	0.2 ± 0.09	5 ± 0.12	9.2 ± 0.12	197	9.85 ± 1.45
<i>rab4</i>	0.1 ± 0.07	5.29 ± 0.1	9.25 ± 0.16	634	30.19 ± 2.06
<i>rab9</i>	0.14 ± 0.08	5	9	411	19.57 ± 1.63
<i>rab14</i>	0.1 ± 0.07	4.62 ± 0.11	8.67 ± 0.14	499	23.76 ± 1.75
<i>rab18</i>	0.05 ± 0.05	4.86 ± 0.08	8.9 ± 0.07	345	16.43 ± 1.34
<i>rab19</i>	0.24 ± 0.1	4.95 ± 0.08	9.71 ± 0.1	379	18.04 ± 1.51
<i>rab21</i>	0.19 ± 0.09	5	8.95 ± 0.05	412	19.62 ± 1.74
<i>rab23</i>	0.1 ± 0.07	4.86 ± 0.08	9	305	14.52 ± 1.71
<i>rab26</i>	0.2 ± 0.09	4.95 ± 0.05	9.1 ± 0.07	480	22.86 ± 2.1
<i>rab27</i>	0.14 ± 0.08	5	9	382	18.19 ± 1.12
<i>rab32</i>	0.29 ± 0.1	5.24 ± 0.1	9.19 ± 0.11	459	21.86 ± 1.62
<i>rab39</i>	0.24 ± 0.1	5.14 ± 0.08	9.43 ± 0.11	627	29.86 ± 2.69
<i>rab40</i>	0.24 ± 0.1	5.7 ± 0.13	9.95 ± 0.15	241	11.48 ± 1.14
<i>rabX1</i>	0.56 ± 0.15	5.29 ± 0.14	9.67 ± 0.14	40	1.9 ± 0.35
<i>rabX4</i>	0.89 ± 0.08	7.14 ± 0.7	12	2	0.1 ± 0.1
<i>rabX6</i>	0.05 ± 0.05	5.05 ± 0.05	9.23 ± 0.1	459	21.86 ± 2.62

29 degree	days until... (after egg collection)			# number of adults in total	Ø number of adults per vial
	first instar larva	pupa	adult		
control	0.15 ± 0.09	4	7.67 ± 0.11	112	5.33 ± 1.21
<i>rab3</i>	0.1 ± 0.07	4.19 ± 0.09	7.57 ± 0.11	168	8 ± 0.81
<i>rab4</i>	0	4.52 ± 0.11	8	572	27 ± 2.14
<i>rab9</i>	0.14 ± 0.08	3.95 ± 0.05	7.57 ± 0.11	369	17.57 ± 1.73
<i>rab14</i>	0	4.05 ± 0.05	7.43 ± 0.11	516	24.57 ± 1.66
<i>rab18</i>	0.1 ± 0.07	4.19 ± 0.09	7.35 ± 0.11	291	13.86 ± 1.68
<i>rab19</i>	0.19 ± 0.09	4.05 ± 0.05	8.94 ± 0.18	132	7.33 ± 1.4
<i>rab21</i>	0.05 ± 0.05	4.19 ± 0.09	8 ± 0.2	378	18.9 ± 1.72
<i>rab23</i>	0.29 ± 0.1	4	7.95 ± 0.05	288	13.71 ± 0.92
<i>rab26</i>	0.29 ± 0.1	4.14 ± 0.08	7.81 ± 0.09	378	18 ± 1.76
<i>rab27</i>	0.05 ± 0.05	4	7.43 ± 0.11	444	21.14 ± 0.95

<i>rab32</i>	0.24 ± 0.1	4.33 ± 0.11	8	307	14.62 ± 1.01
<i>rab39</i>	0.19 ± 0.09	4.1 ± 0.07	7.81 ± 0.09	572	27.24 ± 2.3
<i>rab40</i>	0.33 ± 0.11	4 ± 0.12	7.31 ± 0.1	280	13.33 ± 0.74
<i>rabX1</i>	0.81 ± 0.16	4.75 ± 0.11	8.19 ± 0.1	38	1.81 ± 0.38
<i>rabX4</i>	0.75 ± 0.1	6.38 ± 0.56	13.5 ± 3.5	2	0.1 ± 0.1
<i>rabX6</i>	0.19 ± 0.09	4.05 ± 0.05	7.76 ± 0.1	445	21.19 ± 2.75

## B: Validation in backcrossed backgrounds

18 degree	days until... (after egg collection)			number of adults in total	Ø number of adults per vial
	first instar larva	pupa	adult		
control	0.05 ± 0.05	8.5 ± 0.1	16.7 ± 0.14	290	13.81 ± 1.25
<i>rab3</i>	0.52 ± 0.19	10 ± 0.41	18 ± 0.41	23	5.75 ± 0.48
<i>rab4</i>	0.05 ± 0.05	9.38 ± 0.18	18.52 ± 0.15	190	9.05 ± 0.79
<i>rab9</i>	0.14 ± 0.08	8.33 ± 0.13	17 ± 0.18	284	13.52 ± 0.99
<i>rab14</i>	0.1 ± 0.07	8.38 ± 0.11	16.95 ± 0.19	176	8.38 ± 0.93
<i>rab19</i>	0.05 ± 0.05	8.86 ± 0.2	18.29 ± 0.22	224	10.67 ± 1.52
<i>rab32</i>	0.33 ± 0.11	10.32 ± 0.17	18.74 ± 0.2	136	7.16 ± 1
<i>rab39</i>	0	8.71 ± 0.27	17.8 ± 0.24	327	15.57 ± 1.32
<i>rab40</i>	0.19 ± 0.09	9.33 ± 0.22	17.86 ± 0.19	207	9.86 ± 0.67
<i>rabX1</i>	0.67 ± 0.16	10.1 ± 0.21	18.38 ± 0.27	33	2.54 ± 0.37
<i>rabX4</i>	1.88 ± 0.4	-	-	-	-
<i>rabX6</i>	0	9.29 ± 0.14	18.29 ± 0.22	378	18 ± 1.62

25 degree	days until... (after egg collection)			number of adults in total	Ø number of adults per vial
	first instar larva	pupa	adult		
control	0.05 ± 0.05	5.24 ± 0.1	9.19 ± 0.09	317	15.1 ± 1.07
<i>rab19</i>	0.05 ± 0.05	4.86 ± 0.08	9.95 ± 0.11	309	14.7 ± 1.51
<i>rab40</i>	0.43 ± 0.11	5.71 ± 0.14	9.9 ± 0.14	131	6.24 ± 0.67
<i>rabX1</i>	0.7 ± 0.22	5.35 ± 0.13	9.6 ± 0.15	36	1.8 ± 0.24
<i>rabX4</i>	0.88 ± 0.18	7	13	1	0.05 ± 0.05

29 degree	days until... (after egg collection)			# number of adults in total	Ø number of adults per vial
	first instar larva	pupa	adult		
control	0	4.19 ± 0.09	7.95 ± 0.05	265	12.62 ± 1.5
<i>rab4</i>	0	4.1 ± 0.07	7.81 ± 0.09	255	12.14 ± 0.95
<i>rab18</i>	0.05 ± 0.05	4	6.86 ± 0.1	332	15.81 ± 1.86
<i>rab19</i>	0	4.05 ± 0.05	8.48 ± 0.11	194	9.24 ± 1.32
<i>rabX1</i>	0.5 ± 0.11	5.13 ± 0.17	8.9 ± 0.28	30	2.31 ± 0.36
<i>rabX4</i>	1.07 ± 0.07	7 ± 0.58	13	1	0.05 ± 0.05

### C: Validation of mutants over deficiencies

18 degree	days until... (after egg collection)			number of adults in total	Ø number of adults per vial
	first instar larva	pupa	adult		
control	0.05 ± 0.05	8.5 ± 0.1	16.7 ± 0.14	290	13.81 ± 1.25
<i>rab3/rab3</i> Df	0.29 ± 0.1	8.52 ± 0.15	16.24 ± 0.17	96	4.57 ± 0.8
<i>rab4/rab4</i> Df	0.24 ± 0.1	9.19 ± 0.16	16.9 ± 0.23	233	11.1 ± 0.89
<i>rab9/rab9</i> Df	0.19 ± 0.09	7.57 ± 0.11	15.24 ± 0.15	168	8 ± 0.48
<i>rab14/rab14</i> Df	0.1 ± 0.07	7.62 ± 0.11	15.48 ± 0.15	192	9.14 ± 1.04
<i>rab19/rab19</i> Df	0.48 ± 0.11	8.24 ± 0.1	17.71 ± 0.3	142	6.76 ± 0.74
<i>rab32/rab32</i> Df	0.1 ± 0.07	9.67 ± 0.17	17.48 ± 0.13	192	9.14 ± 0.57
<i>rab39/rab39</i> Df	0.38 ± 0.13	8.62 ± 0.15	16.05 ± 0.11	124	5.9 ± 0.65
<i>rab40/rab40</i> Df	0.19 ± 0.09	9.9 ± 0.17	17.25 ± 0.3	116	5.52 ± 0.72
<i>rabX1/rabX1</i> Df	1.61 ± 0.14	9.67 ± 0.2	17.37 ± 0.35	85	4.25 ± 0.6
<i>rabX4/rabX4</i> Df	1.1 ± 0.18	11.11 ± 0.34	20.26 ± 0.49	57	2.85 ± 0.51
<i>rabX6/rabX6</i> Df	0.29 ± 0.1	9.45 ± 0.18	17.65 ± 0.13	153	7.65 ± 0.95

25 degree	days until... (after egg collection)			number of adults in total	Ø number of adults per vial
	first instar larva	pupa	adult		
control	0.05 ± 0.05	5.24 ± 0.1	9.19 ± 0.09	317	15.1 ± 1.07
<i>rab19/rab19</i> Df	0.29 ± 0.1	5.24 ± 0.1	10.1 ± 0.12	151	7.19 ± 0.69
<i>rab40/rab40</i> Df	0.33 ± 0.11	5.67 ± 0.14	9.38 ± 0.11	110	5.24 ± 0.1
<i>rabX1/rabX1</i> Df	0.76 ± 0.17	5.48 ± 0.13	9.35 ± 0.11	65	3.1 ± 0.34
<i>rabX4/rabX4</i> Df	1.36 ± 0.2	7.38 ± 0.18	12 ± 0.2	23	3.29 ± 0.52

29 degree	days until... (after egg collection)			# number of adults in total	Ø number of adults per vial
	first instar larva	pupa	adult		
control	0	4.19 ± 0.09	7.95 ± 0.05	265	12.62 ± 1.5
<i>rab4/rab4</i> Df	0.2 ± 0.09	4.3 ± 0.11	7.7 ± 0.11	236	11.8 ± 0.78
<i>rab19/rab19</i> Df	0.14 ± 0.08	4.1 ± 0.1	8.7 ± 0.1	117	5.57 ± 0.88
<i>rabX1/rabX1</i> Df	0.84 ± 0.14	4.75 ± 0.11	8.69 ± 0.12	24	1.2 ± 0.22
<i>rabX4/rabX4</i> Df	1 ± 0.12	5.71 ± 0.13	10.36 ± 0.2	26	1.86 ± 0.23

## 5. Manuscript 3

### **The RUSH System in *Drosophila* – A transgenic toolbox to study intracellular localization dynamics of Rab GTPases**

**Kohrs, F. E.**, Pavlović, B., Kiral, F. R., Wolfenberger, H., Daumann, I.-M., Port, F., Boutros, M., Hiesinger, P. R.

Parts of the experimental data presented and discussed in this manuscript have already been published in a Biorxiv preprint: **“Systematic functional analysis of Rab GTPases reveals limits of neuronal robustness in *Drosophila*”**

**Kohrs, F. E.**, Daumann, I.-M., Pavlović, B., Jin, E. J., Lin, S.-C., Port, F., Kiral, F. R., Wolfenberger, H., Mathejczyk, T. F., Chan, C.-C., Boutros, M., Hiesinger, P. R.

bioRxiv 2020.02.21.959452

DOI: <https://doi.org/10.1101/2020.02.21.959452>

#### **Author contributions**

Proof-of-principle experiments with RUSH-Rab7, as well as retention and release experiments using nervous system-enriched RUSH-Rabs in developing pupal eye-brain complexes were designed and performed by myself under the supervision of Prof. Dr. P. Robin Hiesinger. Heike Wolfenberger helped with the retention and release experiments. Ferdi Ridvan Kiral originally designed the SBP-tagged Rab GTPases as well as the hook strains for *Drosophila* analysis and contributed to the generation of the RUSH flies. Proof-of-principle experiments in larval wing imaginal discs and salivary glands were performed by Bojana Pavlović under the supervision of Dr. Filip Port and Prof. Dr. Michael Boutros. The comparison between YFP-tagged and SBP-YFP-tagged Rab GTPases was done by myself and Ilsa-Maria Daumann. Quantification and data analysis were performed by me and Prof. Dr. P. Robin Hiesinger. This thesis chapter was written by me under the supervision of Prof. Dr. P. Robin Hiesinger.

## The RUSH System in *Drosophila* – A transgenic toolbox to study intracellular localization dynamics of Rab GTPases

Kohrs, F. E., Pavlović, B., Kiral, F. R., Wolfenberger, H., Daumann, I.-M., Port, F., Boutros, M., Hiesinger, P. R.

### SUMMARY

Coordinated signaling and membrane trafficking is crucial for the development of multicellular tissues in all eukaryotic organisms. The members of the evolutionary conserved family of small Rab GTPases act as key regulators of intracellular vesicle trafficking in the endomembrane system. Their expression patterns and subcellular localizations have been previously analyzed. While half of all *Drosophila* Rabs are specifically expressed or enriched in the nervous system, roughly one-third are localized ubiquitously in the organism. However, the complete functional repertoire of all Rabs is still unknown. In this study, we report the generation and application of the complete transgenic fly collection for the acute and synchronous release of all 26 Rab GTPases in different developing tissues using the RUSH system. This two-state assay is based on the retention and acute release of a tagged protein from a ‘hook compartment’, from where the synchronized trafficking of the protein of interest can be subsequently followed. Although originally established for mammalian cell culture, we could identify conditions to study intracellular trafficking dynamics and re-localization behaviors for the nervous system-enriched Rab proteins in developing photoreceptor neurons. While ‘fast-releasing’ Rabs mostly targeted distinct compartments, ‘slow-releasing’ ones localize diffusely in the cytoplasm of photoreceptor cell bodies. Two Rab GTPases actively re-localize to axon terminals within the first 60 minutes after release. The transgenic RUSH library generated here, provides a toolbox to further investigate Rab-mediated signaling and trafficking processes during multicellular tissue development *in vivo*.

## INTRODUCTION

Multicellular tissue development in all eukaryotic organisms depends greatly on membrane trafficking, which is necessary for the transport of materials between various membrane-bound compartments. As such, coordinated intracellular trafficking is crucial for pattern formation and cellular differentiation during development. It underlies developmental signaling pathways, correct sorting and transport of membrane-bound receptors, and delivery and insertion of plasma membrane components for its expansion, among other things. *Drosophila* is a widely used model organism to study specific gene functions and membrane trafficking machineries during multicellular tissue development (Chan et al., 2011a; Hales et al., 2015; Mirzoyan et al., 2019; Schlacht et al., 2014; Stewart, 2002; Winkle and Gupton, 2016).

Therefore, one way to gain more knowledge about the intracellular signaling and trafficking mechanisms underlying complex tissue development is to examine master regulators of membrane trafficking in *Drosophila*. The highly evolutionary conserved family of small Rab GTPases constitute the largest branch of the Ras superfamily and the first mammalian family members were initially identified from a rat brain cDNA library, hence their name Rab GTPases (*ras* gene from rat *brain*) (Rojas et al., 2012; Touchot et al., 1987). In their capacity as key regulators of membrane trafficking, Rab GTPases mediate fundamental processes of transport such as vesicle formation, vesicle movement, and fusion of vesicles with their target membranes. They can be found in all eukaryotic cells albeit with varying compositions and have been generally used as compartment identifiers of the endocytic and secretory pathway in the past. Some of them have even become 'gold-standard markers' such as Rab5 (early endosomes) and Rab7 (late endosomes and multivesicular bodies) (Behnia and Munro, 2005; Pfeffer, 2013; Zerial and McBride, 2001; Zhen and Stenmark, 2015). In *Drosophila*, 26 protein-encoding *rab* genes have been identified (Chan et al., 2011b; Jin et al., 2012), while 66 *rab* genes are present in the human genome (Gillingham et al., 2014), and 11 Rab-related *ypt* genes in budding yeast (Grosshans et al., 2006; Pfeffer, 2013). Previously, large-scale profiling efforts have revealed that, while roughly one-third of all *Drosophila* Rab GTPases are ubiquitously expressed, half of all are neuron-specific or enriched in the nervous system with a predominant synaptic localization (Chan et al., 2011b; Dunst et al., 2015; Jin et al., 2012). Yet, the roles of many Rab GTPases in signaling and membrane trafficking during multicellular tissue development have remained mostly unknown.

So far, techniques to acutely manipulate individual Rab GTPase functions have not been established for any multicellular model organism *in vivo*. An assay which would allow for the acute and synchronizable trafficking of proteins of interest would facilitate the analysis of their intracellular localization and trafficking dynamics (Depaoli et al., 2019). For instance, the retention

using selective hooks (RUSH) system is a two-state assay originally designed to investigate secretory protein traffic in mammalian cells *in vitro* (Boncompain et al., 2012). It is based on the retention and acute synchronized release of tagged proteins from a hook compartment allowing for the (in)activation of protein function. So far, the RUSH system has been successfully used for other proteins in mammalian cell culture but not in living tissues of *Drosophila* (Lisse et al., 2017; Moti et al., 2019; Niu et al., 2019; Pacheco-Fernandez et al., 2020; Pawar et al., 2017; Petkovic et al., 2014).

Here, we provide the first transgenic *Drosophila* collection for the acute and synchronized release of tagged Rab proteins in intact multicellular tissues using the RUSH system. We find that the applicability of the system is limited to some extent. However, conditions for the synchronized release could be identified in developing photoreceptor neurons and salivary glands. Focusing on nervous system-enriched Rab GTPases in photoreceptors, the RUSH system reveals different intracellular trafficking dynamics with ‘fast’ or ‘slow’ release properties as well as re-localization of two Rab proteins from the cell body to the axon terminal. Our transgenic fly collection provides a basis to systematically analyze intracellular localization dynamics, by that yielding valuable information on acutely Rab-regulated membrane trafficking during tissue development in a multicellular organism.

## RESULTS

### **Generation of the transgenic *Drosophila* collection for the acute and synchronized release of Rab GTPases using the RUSH system**

In order to closely examine the intracellular signaling and localization dynamics of Rab GTPases during the development of multicellular tissues in *Drosophila*, we established the RUSH system for Rabs using our newly generated transgenic fly collection. Briefly, this synchronized trafficking assay is based on the removal of a protein of interest from its place of action by retaining it at stably expressed hook compartments. The hook itself contains Streptavidin and RUSH Rab proteins bind to them through their Streptavidin-binding peptide (SBP) tag. Addition of Biotin allows for the acute and synchronous release of the tagged proteins from the hook compartments as Biotin has a higher binding affinity toward Streptavidin, outcompeting the SBP-tag (Boncompain et al., 2012). The rationale behind the RUSH experiments is to follow the acutely released Rab proteins, via an additional YFP-tag, as they change their subcellular localization in a synchronous manner (Fig. 1A). This provides us with an opportunity to determine which Rab GTPases mark distinct compartments, are diffusely localized in the cytoplasm, and re-localize to axon terminals.

## **Limitations to the applicability of the RUSH system exist in developing multicellular tissues in *Drosophila***

Here, we have generated a collection of transgenic fly strains, including 26 UAS-SBP-YFP-Rab lines, based on the previously published collection of YFP-tagged wild type Rab variants, which were used to systematically analyze the subcellular localization of Rab proteins in neurons (Suppl. Fig. 1A) (Chan et al., 2011b; Jin et al., 2012; Zhang et al., 2007). Testing the newly generated SBP-YFP-Rab fusion proteins in comparison to the respective YFP-Rab fusion proteins revealed identical subcellular localization patterns in developing photoreceptor neurons (nervous system-enriched Rab GTPases shown in Suppl. Fig. 1C). Further, the collection contains four different Streptavidin-hooks, three with their retention site at the endoplasmic reticulum (ER) and one at the Golgi, all of them based on the original publication of the RUSH system (Suppl. Fig. 1B) (Boncompain et al., 2012). An initial screen revealed that the ER-hook caused more adverse effects than the hook located at the Golgi apparatus. Thus, we chose to use the cytoplasmic Golgi-hook, UAS-Streptavidin-Golgin-84, for the establishment of the RUSH system in *Drosophila* as it did not obviously affect photoreceptor development. However, the general applicability of the system was somewhat limited as the expression of the Streptavidin-hook affected the development of different complex tissues to varying degrees, as discussed below. Additionally, flies need to be raised on egg white-enriched food rendering the food 'Biotin-free' as the presence of Biotin leads to the release from the RUSH-hook. Chicken egg white contains high amounts of Avidin, which binds to the Biotin present in the normal fly food, thus making it unavailable for absorption by the flies (Landenberger et al., 2004). However, we observed prolonged developmental timing especially during larval stages as well as a reduction in number and viability of the progeny raised on egg white-enriched, Biotin-free food. Of all tissues tested, developing wing imaginal discs proved to be most challenging for RUSH experiments. In particular, the individual expression SBP-YFP-Rabs and Golgi-hook in flies raised on normal fly food is tolerated by the tissue and no toxicity was noticeable (Suppl. Fig. 2A-B). While combination of both constructs led to an abnormal morphology with cell toxicity (Suppl. Fig. 2C). Moreover, expression of combined RUSH constructs in wing imaginal discs of flies raised on egg white-enriched food, led to cell toxicity and massive morphological deformities in the discs as well as lethality during larval and early pupal stages (Suppl. Fig. 2D). These adverse effects on morphology and viability were observed for multiple RUSH Rab-hook combinations, including Rab proteins which are not endogenously localized in the epithelial cells of developing wings. Thus, the general expression of RUSH constructs causes these detriments and no conditions to study the synchronized release of Rab GTPases could be identified. However, we were able to identify conditions for the application of the RUSH assay in photoreceptor neurons of *ex vivo* cultures of pupal eye-brain complexes (Ozel et al., 2015) and 3<sup>rd</sup> larval instar salivary glands (Suppl. Fig. 2E-H).

# Figure 1

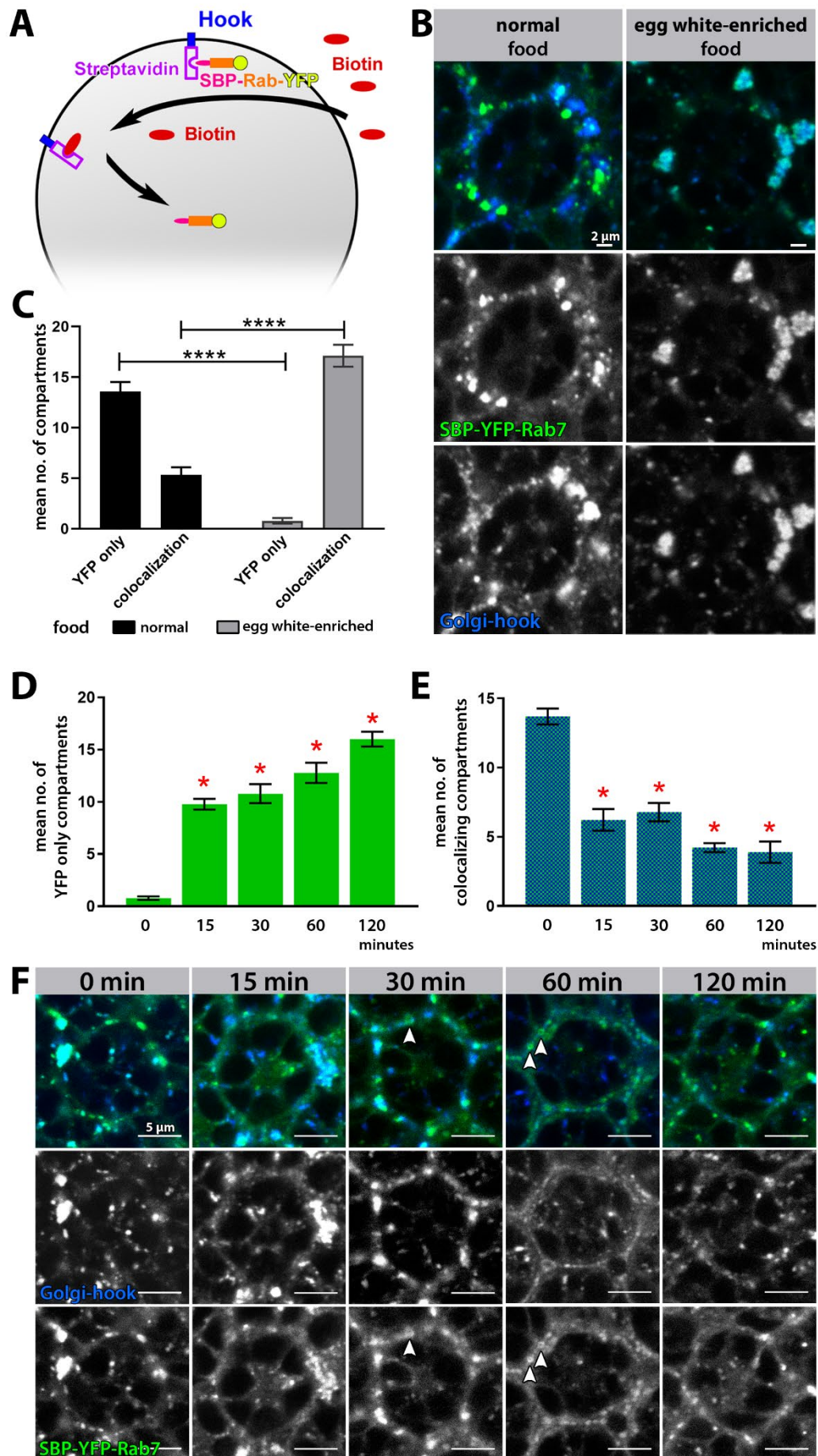


**Figure 1: Establishment of a release-protocol for the RUSH system in developing photoreceptors in *Drosophila* using Rab7** (A) Schematic diagram of the RUSH system. (B) Visual comparison of the retention rate of Rab7 (green) to the Golgi-hook (blue) in developing photoreceptor cell bodies of flies raised on normal fly food compared to egg white-enriched, Biotin-deficient fly food. Shown are single ommatidia from retinas of ~P+40% pupae. Immunolabeling of the Golgi-hook with Streptavidin (blue). Scale bar = 2  $\mu$ m. (C) Raising flies on egg white-enriched fly food increases the retention rate (colocalization) of Rab7 (green) to the Golgi-hook (blue) significantly compared to raising them on normal food. The amount of 'free', un-retained Rab7 (YFP-only) is significantly higher when flies are raised on normal fly food compared to egg white-enriched food. Mean  $\pm$  SEM; \*\*\*\*  $p \leq 0.0001$ ; number of ommatidia  $n = 9$  for each food condition (normal vs. egg white-enriched) from 3-5 animals; Ordinary one-way ANOVA with pair-wise comparison, Holm Šidák test. (D) Quantification of proof-of-principle experiments show a significant release of Rab7 from the Golgi-hook within the first 15 minutes of Biotin incubation. The amount of YFP-only Rab7 compartments increases further with time of incubation. Mean  $\pm$  SEM; red \*  $p \leq 0.0001$  compared to control (0 minutes, no Biotin incubation); number of ommatidia  $n = 9$  from 3-5 animals for each Biotin incubation time point; Ordinary one-way ANOVA with pair-wise comparison, Holm Šidák test. (E) Quantification of proof-of-principle experiments show a significant decrease in colocalization of Golgi-hook compartments with Rab7 within the first 15 minutes of Biotin incubation. The amounts of Golgi-hook compartments colocalizing with Rab7 decreases further with time of incubation. Mean  $\pm$  SEM; red \*  $p \leq 0.0001$  compared to control (0 minutes, no Biotin incubation); number of ommatidia  $n = 9$  from 3-5 animals for each Biotin incubation time point; Ordinary one-way ANOVA with pair-wise comparison, Holm Šidák test. (F) Visual representation of the Biotin-release timeline of Rab7 (green) from the Golgi-hook (blue). With Biotin incubation, Rab7 is released from the Golgi-hook. Formation of Rab7-positive ring-like structures (white arrowheads) can be observed after 30-60 minutes. Immunolabeling of Golgi-hook with Streptavidin. Scale bar = 5  $\mu$ m.

---

### **A Biotin-release protocol could be successfully established in *ex vivo* cultures of developing photoreceptor neurons**

Initially, proof-of-principle experiments, using the well-characterized late endosomal Rab7, were performed. We first carried out a rescue experiment to verify the functionality of the SBP-tagged Rab7, the RUSH version of this small GTPase. The null mutant of the ubiquitously expressed Rab is lethal under homozygosity, while expression of the SBP-fusion protein by the *rab7*-Gal4 knock-in in the mutant background yielded viable progeny. Thus, the RUSH version of Rab7 proved to be a functional Rab GTPase. The presence of trace amounts of Biotin in the normal fly food necessitates the use of egg white-enriched, Biotin-free food to raise flies (Landenberger et al., 2004). This is substantiated by the significant differences in retention rates observed between the two food types in both developing photoreceptors and salivary glands (Fig. 1B-C; Suppl. Fig. 2E-F). In photoreceptor neurons, only about 25% of the quantifiable Rab7-positive compartments colocalize with the Golgi-hook compartments when flies were raised on normal molasses formulation food. While a retention rate of approximately 96% was achieved by feeding egg white-enriched fly food to the RUSH flies (Fig. 1B-C). Even though retention is leaky to a small extent, we were able to establish a Biotin release-protocol for *ex vivo* cultures of pupal eye-brain complexes observing an increasing separation of RUSH Rab7 from the Golgi-hook with the duration of Biotin incubation (Fig. 1D-F).

Within minutes, the number of released Rab7-only compartments grew significantly (Fig. 1D), while in turn a reduction in the amount of colocalizing compartments was observed (Fig. 1E). After 30-60 minutes of Biotin incubation characteristic Rab7-positive transient rings appeared indicating the maturation of late endosomal compartments (white arrowheads in Fig. 1F) (Cherry et al., 2013). Another confirmation that the SBP-Rab7 fusion protein is a functional Rab GTPase.

### **Nervous system-enriched Rab GTPases exhibit distinct release dynamics in photoreceptor cell bodies**

Already prior to the addition of Biotin to the *ex vivo* culture, Rab7 forms large, artificial aggregates together with the Golgi hook in photoreceptor neurons, which resolve after incubation with Biotin (Fig. 1F). We observed similar aggregates for several Rab GTPases with high expression in the nervous system, particularly Rab3, RabX4, Rab27, Rab26, Rab19, Rab32, and RabX1 (Rabs sorted by their expression pattern in Suppl. Fig. 3; Suppl. Fig. 4). After addition of Biotin, these aggregates dissipate to different degrees and are mostly gone after 60 minutes for Rab3, Rab26, and Rab19, though considerable aggregates at the hook remained for the other Rab proteins (Suppl. Fig. 4). Further, performing release experiments for all nervous system Rabs allowed us to identify different trafficking dynamics within the first 15 minutes of Biotin incubation (Fig. 2; Suppl. Fig. 5). Four Rab GTPases, RabX4, RabX1, RabX6, and Rab21, can be classified as ‘fast-releasing’, as 50% or more of the hook compartments had released these specific Rab proteins (Fig. 2A-E). In contrast to this, Rab27, Rab26, and Rab19 were identified as ‘slow-releasing’. Here, only about 20% of Golgi-hook compartments lost their colocalization (Fig. 2A, F-H). In case of the ‘fast’ Rabs, most of these immediately marked distinct compartments in the cytoplasm of the photoreceptor cell bodies (marked in green in Fig. 2A; Suppl. Fig. 5A, B, D; Suppl. Fig. 3), while the three ‘slow-releasing’ Rab GTPases localize diffusely after addition of Biotin (Suppl. Fig. 3). The specific release dynamics for three Rab proteins, Rab23, Rab9, and Rab4, could not be determined, as these exhibit an almost exclusive membranous localization in the photoreceptor cell bodies already prior to Biotin application (Suppl. Fig. 5K-M). Furthermore, a high number of compartments are present in interommatidial cells for Rab21, leading to morphological disruptions which we did not detect for other Rab GTPases (Suppl. Fig. 3; Suppl. Fig. 4).

## Figure 2

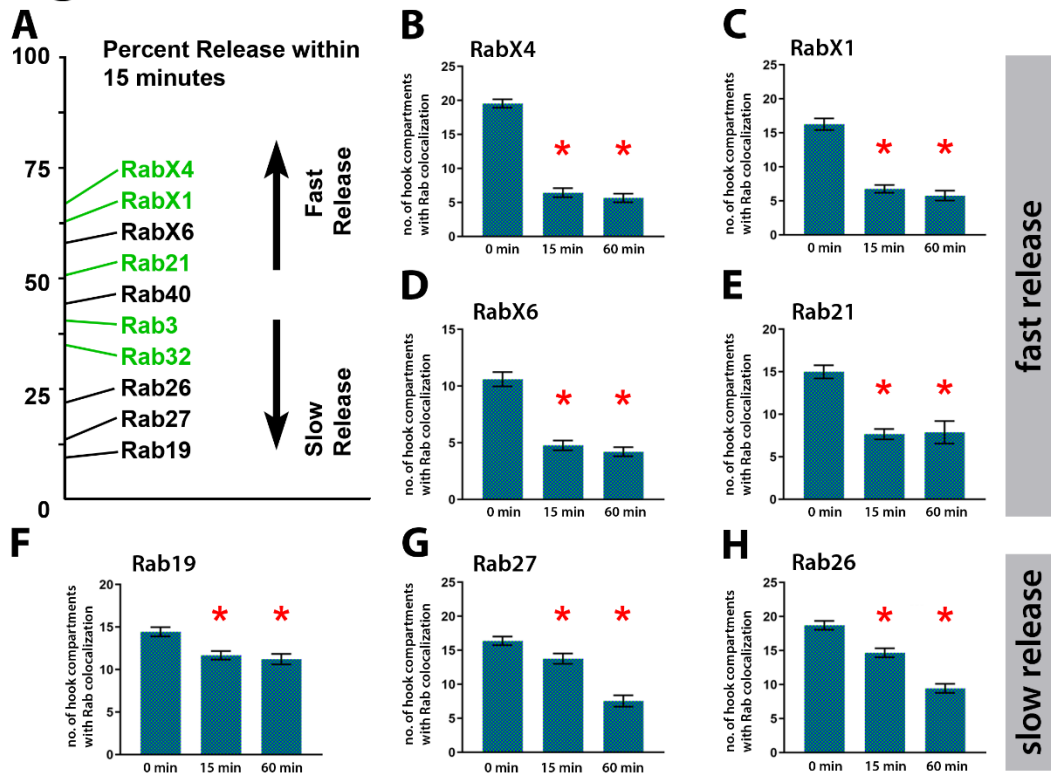


**Figure 2: Identification of release dynamics of nervous system-enriched Rab GTPases in developing photoreceptors** (A) Graphical representation of percent release of 10 nervous system-enriched Rab GTPases within 15 minutes of Biotin incubation. The majority of ‘fast-releasing’ Rab GTPases display distinct compartments in the cell body (marked in green), while most of the ‘slow-releasing’ Rab GTPases localize diffusely in the photoreceptor cytoplasm after being released from the Golgi-hook. (B-E) RabX4, RabX1, RabX6, and Rab21 were identified as a ‘fast-releasing’ Rabs, within the first 15 minutes of Biotin incubation 50% of the Golgi-hook lost colocalization with the respective RUSH-Rab. Mean  $\pm$  SEM; red \*  $p \leq 0.0001$ ; number of ommatidia  $n = 9$  from 3-5 animals for each Biotin incubation time point; Ordinary one-way ANOVA with pair-wise comparison, Holm-Šidák test. (F-H) Rab19, Rab27, and Rab26 were identified as ‘slow-releasing’ Rabs, within the first 15 minutes of Biotin incubation less than 25% of the Golgi-hook lost colocalization with the respective RUSH-Rab. Mean  $\pm$  SEM; (Rab19 and Rab26), red \*  $p < 0.05$  (Rab27); number of ommatidia  $n = 9$  from 3-5 animals for each Biotin incubation time point; Ordinary one-way ANOVA with pair-wise comparison, Holm-Šidák test.

### Two nervous system-enriched Rab GTPases re-localize to axon terminals after release from the hook compartments

Besides systematically analyzing release dynamics, we examined the re-localization behavior of all nervous system-enriched Rabs after 60 minutes of Biotin incubation. For this, we measured the fluorescence ratio between axon terminals and cell bodies (Fig. 3; Suppl. Fig. 6). Significant increases in the fluorescence ratio were detected for Rab26, Rab23, and Rab4 (Fig. 3A). But while the increase for Rab4 was entirely due to the loss of Golgi-hook localization in the cell bodies, Rab26

and Rab23 show a distinct re-localization to the axon terminals (Fig. 3B-C; Suppl. Fig. 6). No evidence for the trafficking of membrane compartments from cell body to axon terminal could be provided, as all three Rab proteins are either mostly membrane-bound (Rab23 and Rab4) or diffusely localized in the cytoplasm (Rab26). It is noteworthy, that very low levels of Golgi-hook fluorescence can be observed in axon terminals, just as all nervous system-enriched Rab GTPases are present in the terminals to varying low degrees already prior to the addition of Biotin and their subsequent release.

### Figure 3

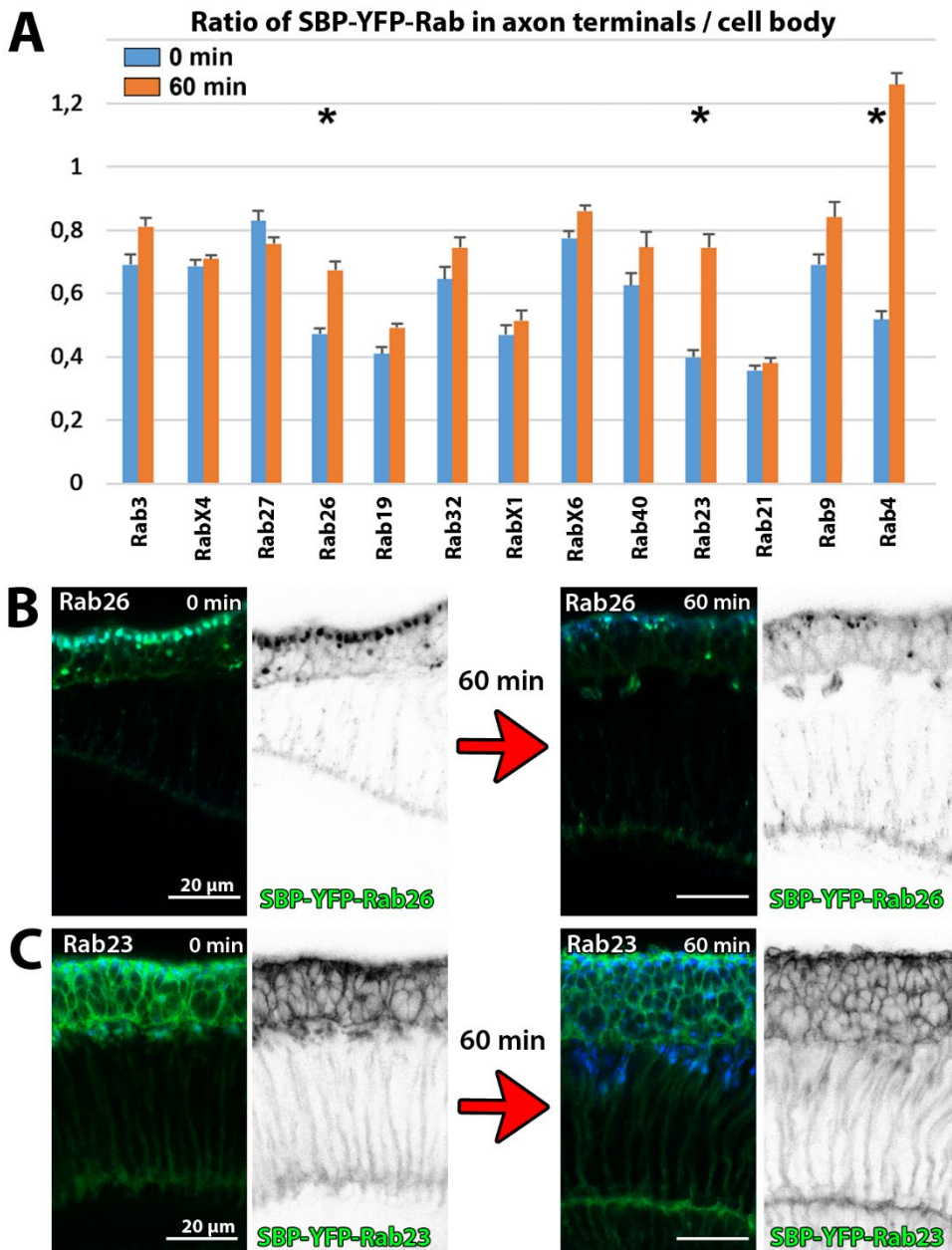


Figure 3: Identification of re-localization dynamics of nervous system-enriched Rab GTPases from cell bodies to axon terminals (A) Quantification of the fluorescence ratio between axon terminals to cell

Figure 3 continued

bodies before (0 minutes) and after (60 minutes) Biotin incubation shows an increase in axon terminal localization for Rab23 and Rab26. The increase in fluorescence ratio for Rab4 is solely based on the loss of hook localization. Mean  $\pm$  SEM; \*  $p < 0.05$ ; Ordinary one-way ANOVA with pair-wise comparison, Holm-Šidák test. **(B)** Cross-section showing retina to lamina axon terminals reveal a significant re-localization of Rab26 (green, single channel) away from the Golgi-hook (blue) in the retina after 60 minutes of Biotin incubation. Immunolabeling of Golgi-hook with Streptavidin. Scale bar = 20  $\mu$ m. **(C)** Cross-section showing retina to lamina axon terminals reveal a significant re-localization of Rab23 (green, single channel) away from the Golgi-hook (blue) in the retina after 60 minutes of incubation with Biotin. Immunolabeling of Golgi-hook with Streptavidin. Scale bar = 20  $\mu$ m.

All in all, we could identify different trafficking dynamics for the nervous system Rab GTPases, with ‘fast-releasing’ Rabs that mark distinct compartments after their release from the Golgi-hook in cell bodies (RabX4, RabX1, and Rab21) and ‘slow-releasing’ Rabs that diffusely localize in the cytoplasm (Rab27, Rab26, and Rab19). In addition, two Rab GTPases (Rab26 and Rab23) are actively re-localizing to the photoreceptor axon terminals (Table 1).

**Table 1**

Rab GTPases	Expression pattern	(Re-) Localization		
		RUSH rel	RUSH cb	RUSH axon
1 Rab3	nervous system high			
2 RabX4	nervous system high			
3 Rab27	nervous system high			
4 Rab26	nervous system high			
5 Rab19	nervous system high			
6 Rab32	nervous system high			
7 RabX1	nervous system high			
8 RabX6	nervous system high			
9 Rab40	nervous system high			
10 Rab23	nervous system high			
11 Rab21	nervous system high			
12 Rab9	nervous system high			
13 Rab4	nervous system high			
14 Rab14	widespread			
15 Rab18	widespread			
16 Rab39	widespread			
17 Rab10	widespread			
18 Rab30	ubiquitous			
19 Rab7	ubiquitous			
20 Rab8	ubiquitous			
21 Rab2	ubiquitous			
22 Rab1	ubiquitous			
23 Rab6	ubiquitous			
24 Rab35	ubiquitous			
25 Rab5	ubiquitous			
26 Rab11	ubiquitous			

**Table 1: Summary of the RUSH analyses performed in developing *Drosophila* photoreceptors**

Overview of RUSH analyses performed for the nervous system-enriched Rab GTPases. Rabs are listed according to their expression pattern, going from ‘nervous system high’ (blue) at the top to ‘widespread’ (grey) to the ‘ubiquitous’ (white) Rabs at the bottom. Color code: Rab proteins used for RUSH analyses are highlighted in dark green. Darker red to lighter red denotes higher to lower (re-)localization of examined Rab GTPases.

## DISCUSSION

In this study, we generated the first complete transgenic fly collection for the acute and synchronous RUSH release assay for all 26 Rab GTPases along with four different hook compartment lines, which are based on the original RUSH publication (Boncompain et al., 2012). Here, intracellular localization dynamics of nervous system-enriched Rabs in photoreceptor neurons were examined more closely. Initial proof-of-principle experiments revealed that the SBP-YFP-tagged nervous system Rab GTPases exhibit comparable subcellular localization patterns to the YFP-tagged Rab proteins (Zhang et al., 2007). As such the SBP-tag does not perturb protein localization in developing photoreceptor neurons *per se*. Furthermore, the RUSH version of ubiquitous Rab7 acts as functional Rab GTPase rescuing the lethality observed for the homozygous *rab7* null mutant (Cherry et al., 2013). Ultimately, we could identify several ‘fast-’ and ‘slow-releasing’ Rab proteins which mostly localize to distinct compartments or diffusely in the cytoplasm, respectively. Mapping possible ‘target compartments’ after Rab release, by techniques such as antibody labeling, might facilitate the further analysis of novel cellular trafficking functions. As many of the roles of nervous system-enriched Rab GTPases during development as well as function are still relatively unknown (Kohrs et al., 2021). Closely examining the re-localization behavior of all nervous system Rab GTPases we identified Rab26 and Rab23 as two Rab proteins which actively re-locate to synapses within 60 minutes of release. Recently, a synaptic function of Rab26 was revealed during a more in-depth functional characterization. More specifically, it has a role in the transport of the acetylcholine-receptor subunit  $D\alpha 4$  specifically at cholinergic synapses of outer photoreceptors in *Drosophila* (Kohrs et al., 2021). Generally, the complete collection of transgenic RUSH lines established here can be used as a toolbox for further comprehensive analyses of Rab-regulated trafficking.

In this study, we also included a critical assessment of the limitations of the acute RUSH release system in developing multicellular tissues in *Drosophila*. Ultimately, two criteria have to be fulfilled for the successful application of the RUSH assay to release and activate proteins in an acute and synchronized manner. First, to achieve high retention at the hook compartments, the tissue needs to be in a Biotin-free environment as the acute addition of Biotin is needed for protein release. Second, SBP-tagged proteins have to be functionally inactive when bound to the hook compartments prior to release as they are sequestered away from their endogenous place of action. These two conditions are most easily met on a shorter timescale. Especially as both, the prolonged expression of the combined RUSH constructs (hook and Rab) as well as the raising of flies on egg white-enriched food, has detrimental effects on tissue development and *Drosophila* viability. Further, different tissues were differentially affected and especially wing imaginal discs

were the most sensitive in contrast to developing photoreceptors as well as salivary glands, which both proved to be more resistant regarding the experimental conditions. One possible explanation might be that toxicity, induced by the transgenic constructs, is alleviated in bigger cells such as the epithelial cells, which form the salivary glands. These cells are significantly larger than those present in the wing disc epithelium and the local concentration of transgenic constructs might be reduced (Andrew et al., 2000). Also, this may account for the more resistant nature of developing photoreceptors here. Photoreceptor neurons represent larger cells with long axons where the local concentration of the transgenic constructs in cell bodies might be reduced by an additional, aberrant subcellular localization (Kanca et al., 2017). Thus, it might explain the presence of the Golgi-hook in axons and their terminals as, endogenously, the Golgi apparatus and its outposts are absent from these neuronal domains (Gonzalez et al., 2018; Hanus and Ehlers, 2008; Ye et al., 2007). Further, the nervous system-enriched Rab GTPases exhibited varying aggregation and localization behaviors in the cell bodies of developing photoreceptors already prior to Biotin incubation. This indicates an incomplete inactivation of protein functions of these Rabs to varying degrees.

Overall, our systematic analysis of small Rab GTPases revealed several limitations of the RUSH system in developing multicellular tissues in *Drosophila*. In particular, sensitivities towards individual SBP-Rab fusion protein properties, localization of the hook compartment, type of investigated tissue, and Biotin content of the food. Especially considering the adverse effects caused by Biotin-free conditions over longer periods of time, the here established *Drosophila* RUSH collection is more applicable on a shorter timescale during early development.

## **MATERIALS AND METHODS**

### **Fly husbandry and genetics**

For retention and release experiments using the RUSH system, flies were raised on egg white-enriched molasses formulation food. For this, 20 g spray-dried, powdered chicken egg white were dissolved in 20 ml de-ionized water and added to 230 ml liquid molasses formulation food after the regular cooking process. To prevent coagulation of the dissolved egg white, the temperature of the liquid food needs to be below 42°C. In addition, RUSH-Rab7 flies were raised on normal molasses formulation food to compare the retention rate between flies raised on the two different types of food. Stocks were kept at room temperature (22-23°C) on normal molasses formulation food, while crosses were kept at 25°C on egg white-enriched food.

For all RUSH-experiments in developing photoreceptors, following lines were used: ;shortGMR-Gal4/CyO; (Bloomington stock #1104) as a driver line and ;;UAS-Streptavidin-Golgin-84 for the retention at the Golgi. For the proof-of-principle experiments of the RUSH system in developing photoreceptors, the following transgenic *Drosophila* line was used: ;UAS-SBP-YFP-Rab7;. For the Biotin-release experiments of the nervous system-enriched Rab GTPases, the following *Drosophila* lines were used: ;UAS-SBP-YFP-Rab3/CyO;, ;UAS-SBP-YFP-Rab4/CyO;, ;UAS-SBP-YFP-Rab9/CyO;, ;UAS-SBP-YFP-Rab19/CyO;, ;UAS-SBP-YFP-Rab21/CyO;, ;UAS-SBP-YFP-Rab23/CyO;, ;UAS-SBP-YFP-Rab26/CyO;, ;UAS-SBP-YFP-Rab27/CyO;, ;UAS-SBP-YFP-Rab32/CyO;, ;UAS-SBP-YFP-Rab40/CyO;, ;UAS-SBP-YFP-RabX1/CyO;, UAS-SBP-YFP-RabX4/CyO;, and ;UAS-SBP-YFP-RabX6/CyO;. For the RUSH-release experiments in the pouch of larval imaginal wing discs and 3<sup>rd</sup> instar larval salivary glands, the following transgenic lines were used: ; nubbin-Gal4; as a driver line in the wing disc, ;; sgs3-Gal4 as a driver line in the salivary glands, ;;UAS-Streptavidin-Golgin-84 for the retention at the Golgi and ; UAS-SBP-YFP-Rab7/CyO;.

To compare the expression pattern in developing pupal P+40% eye-brain complexes of YFP- and SBP-YFP-tagged flies, the following *Drosophila* lines were used: ;shortGMR-Gal4/CyO; (Bloomington stock #1104) as a driver line and ;;GMR-myr-tdTomato/Tm6B to mark the photoreceptor projections. The following YFP-tagged lines were used: ;UAS-YFP-Rab3WT; (Bloomington stock #9762), ;UAS-YFP-Rab4WT; (Bloomington stock #23269), ;UAS-YFP-Rab9WT; (Bloomington stock #9783), ;UAS-YFP-Rab19WT; (Bloomington stock #24150), ;UAS-YFP-Rab21WT; (Bloomington stock #23242), ;UAS-YFP-Rab23WT/CyO; (Bloomington stock #9803), ;UAS-YFP-Rab26WT/CyO; (Bloomington stock #23245), ;UAS-YFP-Rab27WT; (Bloomington stock #9810), ;UAS-YFP-Rab32WT; (Bloomington stock #9821), ;UAS-YFP-Rab40WT; (Bloomington stock #23248), ;UAS-YFP-RabX1WT; (Bloomington stock #9840), ;;UAS-YFP-RabX4WT (Bloomington stock #9851), ;UAS-YFP-RabX6WT; (Bloomington stock #23279). The following SBP-YFP-tagged lines were used: ;UAS-SBP-YFP-Rab3/CyO;, ;UAS-SBP-YFP-Rab4/CyO;, ;UAS-SBP-YFP-Rab9/CyO;, ;UAS-SBP-YFP-Rab19/CyO;, ;UAS-SBP-YFP-Rab21/CyO;, ;UAS-SBP-YFP-Rab23/CyO;, ;UAS-SBP-YFP-Rab26/CyO;, ;UAS-SBP-YFP-Rab27/CyO;, ;UAS-SBP-YFP-Rab32/CyO;, ;UAS-SBP-YFP-Rab40/CyO;, ;UAS-SBP-YFP-RabX1/CyO;, UAS-SBP-YFP-RabX4/CyO;, and ;UAS-SBP-YFP-RabX6/CyO;.

### **Generation of the transgenic RUSH toolbox**

Conventional cloning and phiC31 integrase-mediated transgenesis were used to generate all RUSH-system flies. This was performed by WellGenetics Inc. (Taipei, Taiwan). To generate the RUSH-Rab GTPases (UAS-SBP-YFP-tagged), the genomic DNA of the respective wild type variant (Zhang et al.,

2007) was used to get the YFP-Rab fragment, while the SBP fragment was provided by Addgene (plasmid #65305, donated by Franck Perez). Using XhoI/XbaI cutting sites, both fragments were cloned into a pUAST-attB vector and integrated into the *Drosophila* genome with the same landing site  $\gamma^1w^{1118}$ ; PBac ( $\gamma^+$ -attP-3B) VK00002 (Bloomington stock #9723). RUSH transgenic *Drosophila* lines were generated for all 26 protein-encoding Rab GTPases. Four different hook lines, tagged with Streptavidin, were generated. One is located at the Golgi, UAS-Streptavidin-Golgin-84 (Addgene, plasmid #65305), facing the cytoplasmic site, while three are located at the Endoplasmic Reticulum, UAS-Streptavidin-KDEL (Addgene, plasmid #65306), UAS-Streptavidin-STIM1-NN (Addgene, plasmid #65311), UAS-Streptavidin-li (Addgene, plasmid #65312), facing the luminal domain (KDEL, STIM1-NN) or the cytoplasmic site (li). All plasmids were donated by Franck Perez. Hook fragments were first amplified by PCR and, using XhoI/XbaI sites as enzyme cutting sites, cloned into a pUAST-attB vector. For the integration of the constructs into the *Drosophila* genome, two different landing sites were used, which are  $\gamma^1 w^{1118}$ ; PBac ( $\gamma^+$ -attP-9A) VK00018 (Bloomington stock #9736) for the second chromosome and  $\gamma^1 M$  (vas-int.Dm) ZH-2A w\*; PBac ( $\gamma^+$ -attP-3B) VK00033 (Bloomington stock #24871) for the third chromosome.

### **Immunohistochemistry**

Tissues were dissected in ice-cold Gibco™ Schneider's *Drosophila* Medium (Thermo Fisher Scientific) and collected in ice-cold culture medium (Ozel et al., 2015). For incubation with Biotin, 2 mg powdered D-Biotin was dissolved in 1 ml culture medium. Experimental tissues were incubated with Biotin-containing culture medium, while control tissues were incubated with Biotin-free culture medium for the same amount of time (proof-of-principle experiments in pupal photoreceptors: 15, 30, 60, and 120 minutes, proof-of-principle experiments in salivary glands: 15 and 30 minutes, release experiments: 15 and 60 minutes; fluorescence ratio experiments: 60 minutes). After incubation, both control and experimental tissues were shortly washed with Gibco™ Schneider's *Drosophila* Medium (Thermo Fisher Scientific) and fixated in PBS with 4% paraformaldehyde for 30 minutes at room temperature. After fixation, tissues were washed several times with PBST (PBS + 0.4% Triton X-100). The following primary antibody was used: mouse anti-Streptavidin (1:100, Novus Biologicals). Pupal eye-brain complexes and wing discs were incubated overnight, while salivary glands were incubated for three days. The following secondary antibodies were used: Goat anti-mouse Alexa647 (1:500; Jackson ImmunoResearch Laboratories) or Goat anti-rabbit Alexa 594 (1:800, Thermo Fisher Scientific) and tissues were incubated overnight. DNA in salivary glands was labeled using Hoechst dye (1:2000, Thermo Fisher Scientific). All samples were

mounted in Vectashield mounting medium (Vector Laboratories), while pupal eye-brain complexes were mounted with their dorsal side up, to fully expose photoreceptor terminals in the lamina.

### **Confocal Microscopy, Image Processing and Quantification**

All microscopic data acquisition was performed using a white laser Leica SP8 X with 20x and 63x Glycerol objectives (NA = 1.3). Leica image files were processed with Imaris (Bitplane) and ImageJ (National Institute of Health). Postprocessing was performed using Photoshop (CS6, Adobe Inc.), Illustrator (CS6, Adobe Inc.), Photoshop (CS6, Adobe Inc.) and GraphPad Prism 8.3.0 (GraphPad Software Inc.) were used to plot the data.

The fluorescence intensity ratio between axon terminals in the lamina region and cell bodies were quantified by measuring 8 bit pixel intensities in several different regions of interest. This was followed up by statistical analyses. For the colocalization experiments, single slices were manually quantified, whereby only individually discernable compartments were counted and analyzed. GraphPad Prism 8.3.0 (GraphPad Software Inc.) was used for statistical analyses and all specific statistical tests as well as sample numbers are indicated for each experiment in the respective figure legend.

### **Author contributions**

Friederike E. Kohrs: Methodology, Investigation, Formal analysis, Visualization, Writing - original draft. Bojana Pavlović: Methodology, Investigation, Formal analysis, Visualization. F. Ridvan Kiral: Methodology. Heike Wolfenber: Investigation. Ilsa-Maria Daumann: Investigation, Formal analysis, Visualization. Filip Port: Methodology, Investigation, Supervision. Michael Boutros: Conceptualization, Supervision, Funding acquisition, Project administration. P. Robin Hiesinger: Conceptualization, Formal analysis, Supervision, Funding acquisition, Project administration, Writing - original draft.

## REFERENCES

- Andrew, D.J., Henderson, K.D., and Seshiah, P. (2000). Salivary gland development in *Drosophila melanogaster*. *Mech Dev* 92, 5-17.
- Behnia, R., and Munro, S. (2005). Organelle identity and the signposts for membrane traffic. *Nature* 438, 597-604.
- Boncompain, G., Divoux, S., Gareil, N., de Forges, H., Lescure, A., Latreche, L., Mercanti, V., Jollivet, F., Raposo, G., and Perez, F. (2012). Synchronization of secretory protein traffic in populations of cells. *Nat Methods* 9, 493-498.
- Chan, C.C., Epstein, D., and Hiesinger, P.R. (2011a). Intracellular trafficking in *Drosophila* visual system development: a basis for pattern formation through simple mechanisms. *Dev Neurobiol* 71, 1227-1245.
- Chan, C.C., Scoggin, S., Wang, D., Cherry, S., Dembo, T., Greenberg, B., Jin, E.J., Kuey, C., Lopez, A., Mehta, S.Q., *et al.* (2011b). Systematic discovery of Rab GTPases with synaptic functions in *Drosophila*. *Curr Biol* 21, 1704-1715.
- Cherry, S., Jin, E.J., Ozel, M.N., Lu, Z., Agi, E., Wang, D., Jung, W.H., Epstein, D., Meinertzhagen, I.A., Chan, C.C., *et al.* (2013). Charcot-Marie-Tooth 2B mutations in rab7 cause dosage-dependent neurodegeneration due to partial loss of function. *Elife* 2, e01064.
- Depaoli, M.R., Bischof, H., Eroglu, E., Burgstaller, S., Ramadani-Muja, J., Rauter, T., Schinagl, M., Waldeck-Weiermair, M., Hay, J.C., Graier, W.F., *et al.* (2019). Live cell imaging of signaling and metabolic activities. *Pharmacol Ther* 202, 98-119.
- Dunst, S., Kazimiers, T., von Zadow, F., Jambor, H., Sagner, A., Brankatschk, B., Mahmoud, A., Spann, S., Tomancak, P., Eaton, S., *et al.* (2015). Endogenously tagged rab proteins: a resource to study membrane trafficking in *Drosophila*. *Dev Cell* 33, 351-365.
- Gillingham, A.K., Sinka, R., Torres, I.L., Lilley, K.S., and Munro, S. (2014). Toward a comprehensive map of the effectors of rab GTPases. *Dev Cell* 31, 358-373.
- Gonzalez, C., Cornejo, V.H., and Couve, A. (2018). Golgi bypass for local delivery of axonal proteins, fact or fiction? *Curr Opin Cell Biol* 53, 9-14.
- Grosshans, B.L., Ortiz, D., and Novick, P. (2006). Rabs and their effectors: achieving specificity in membrane traffic. *Proc Natl Acad Sci U S A* 103, 11821-11827.
- Hales, K.G., Korey, C.A., Larracuente, A.M., and Roberts, D.M. (2015). Genetics on the Fly: A Primer on the *Drosophila* Model System. *Genetics* 201, 815-842.
- Hanus, C., and Ehlers, M.D. (2008). Secretory outposts for the local processing of membrane cargo in neuronal dendrites. *Traffic* 9, 1437-1445.
- Jin, E.J., Chan, C.C., Agi, E., Cherry, S., Hanacik, E., Buszczak, M., and Hiesinger, P.R. (2012). Similarities of *Drosophila* rab GTPases based on expression profiling: completion and analysis of the rab-Gal4 kit. *PLoS One* 7, e40912.
- Kanca, O., Bellen, H.J., and Schnorrer, F. (2017). Gene Tagging Strategies To Assess Protein Expression, Localization, and Function in *Drosophila*. *Genetics* 207, 389-412.
- Kohrs, F.E., Daumann, I.M., Pavlovic, B., Jin, E.J., Kiral, F.R., Lin, S.C., Port, F., Wolfenberger, H., Mathejczyk, T.F., Linneweber, G.A., *et al.* (2021). Systematic functional analysis of rab GTPases reveals limits of neuronal robustness to environmental challenges in flies. *Elife* 10.
- Landenberger, A., Kabil, H., Harshman, L.G., and Zemleni, J. (2004). Biotin deficiency decreases life span and fertility but increases stress resistance in *Drosophila melanogaster*. *J Nutr Biochem* 15, 591-600.
- Lisse, D., Monzel, C., Vicario, C., Manzi, J., Maurin, I., Coppey, M., Piehler, J., and Dahan, M. (2017). Engineered Ferritin for Magnetogenetic Manipulation of Proteins and Organelles Inside Living Cells. *Adv Mater* 29.
- Mirzoyan, Z., Sollazzo, M., Allocca, M., Valenza, A.M., Grifoni, D., and Bellosta, P. (2019). *Drosophila melanogaster*: A Model Organism to Study Cancer. *Front Genet* 10, 51.

Moti, N., Yu, J., Boncompain, G., Perez, F., and Virshup, D.M. (2019). Wnt traffic from endoplasmic reticulum to filopodia. *PLoS One* *14*, e0212711.

Niu, L.L., Ma, T.J., Yang, F., Yan, B., Tang, X., Yin, H.D., Wu, Q., Huang, Y., Yao, Z.P., Wang, J.F., *et al.* (2019). Atlastin-mediated membrane tethering is critical for cargo mobility and exit from the endoplasmic reticulum. *PNAS* *116*, 14029-14038.

Ozel, M.N., Langen, M., Hassan, B.A., and Hiesinger, P.R. (2015). Filopodial dynamics and growth cone stabilization in *Drosophila* visual circuit development. *Elife* *4*.

Pacheco-Fernandez, N., Pakdel, M., Blank, B., Sanchez-Gonzalez, I., Weber, K., Tran, M.L., Hecht, T.K., Gautsch, R., Beck, G., Perez, F., *et al.* (2020). Nucleobindin-1 regulates ECM degradation by promoting intra-Golgi trafficking of MMPs. *J Cell Biol* *219*.

Pawar, S., Ungricht, R., Tiefenboeck, P., Leroux, J.C., and Kutay, U. (2017). Efficient protein targeting to the inner nuclear membrane requires Atlastin-dependent maintenance of ER topology. *Elife* *6*.

Petkovic, M., Jemaiel, A., Daste, F., Specht, C.G., Izeddin, I., Vorkel, D., Verbavatz, J.M., Darzacq, X., Triller, A., Pfenninger, K.H., *et al.* (2014). The SNARE Sec22b has a non-fusogenic function in plasma membrane expansion. *Nat Cell Biol* *16*, 434-444.

Pfeffer, S.R. (2013). Rab GTPase regulation of membrane identity. *Curr Opin Cell Biol* *25*, 414-419.

Rojas, A.M., Fuentes, G., Rausell, A., and Valencia, A. (2012). The Ras protein superfamily: evolutionary tree and role of conserved amino acids. *J Cell Biol* *196*, 189-201.

Schlacht, A., Herman, E.K., Klute, M.J., Field, M.C., and Dacks, J.B. (2014). Missing pieces of an ancient puzzle: evolution of the eukaryotic membrane-trafficking system. *Cold Spring Harb Perspect Biol* *6*, a016048.

Stewart, B.A. (2002). Membrane trafficking in *Drosophila* wing and eye development. *Semin Cell Dev Biol* *13*, 91-97.

Touchot, N., Chardin, P., and Tavitian, A. (1987). Four additional members of the ras gene superfamily isolated by an oligonucleotide strategy: molecular cloning of YPT-related cDNAs from a rat brain library. *Proc Natl Acad Sci U S A* *84*, 8210-8214.

Winkle, C.C., and Gupton, S.L. (2016). Membrane Trafficking in Neuronal Development: Ins and Outs of Neural Connectivity. *Int Rev Cell Mol Biol* *322*, 247-280.

Ye, B., Zhang, Y., Song, W., Younger, S.H., Jan, L.Y., and Jan, Y.N. (2007). Growing dendrites and axons differ in their reliance on the secretory pathway. *Cell* *130*, 717-729.

Zerial, M., and McBride, H. (2001). Rab proteins as membrane organizers. *Nat Rev Mol Cell Biol* *2*, 107-117.

Zhang, J., Schulze, K.L., Hiesinger, P.R., Suyama, K., Wang, S., Fish, M., Acar, M., Hoskins, R.A., Bellen, H.J., and Scott, M.P. (2007). Thirty-one flavors of *Drosophila* rab proteins. *Genetics* *176*, 1307-1322.

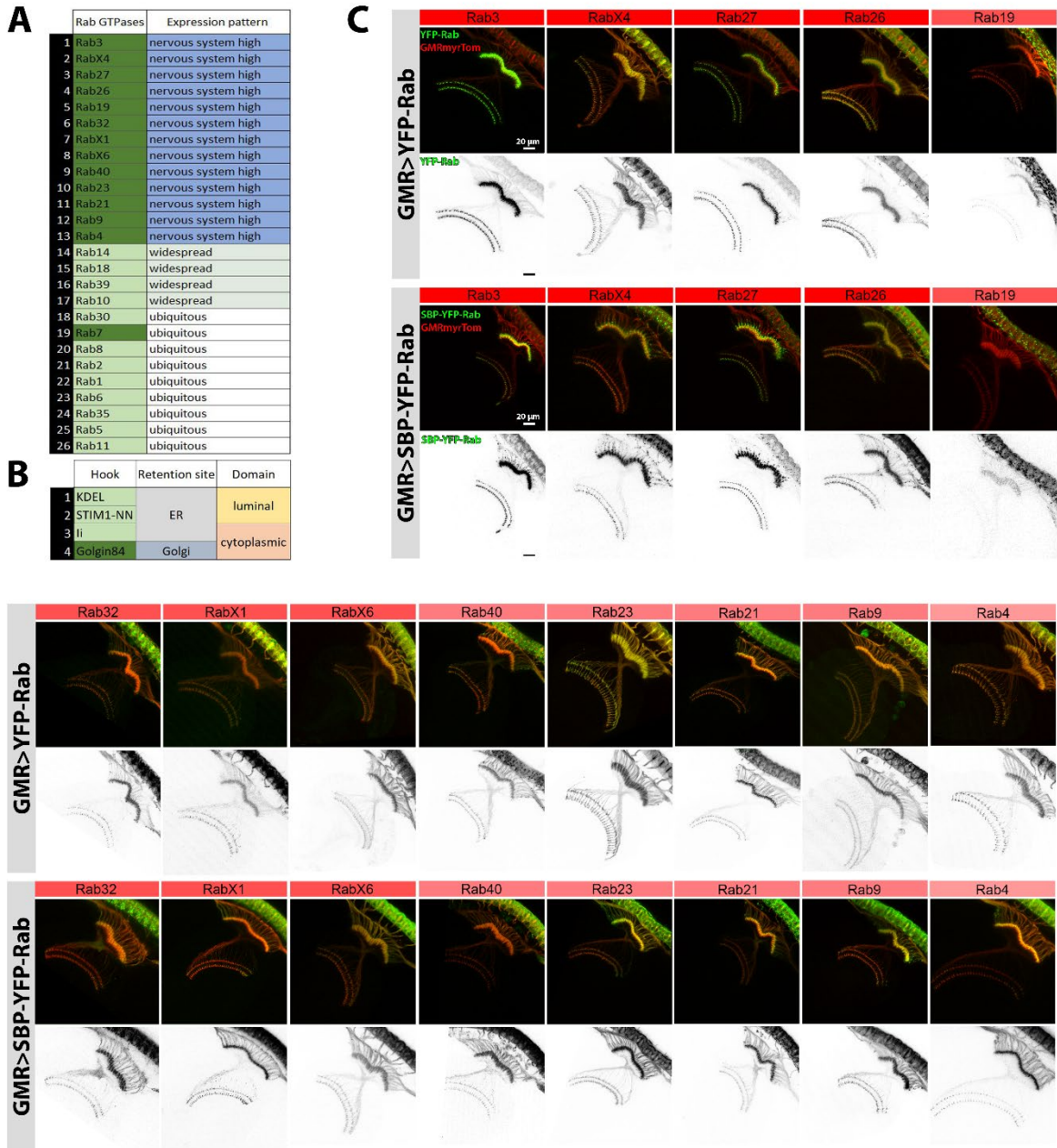
Zhen, Y., and Stenmark, H. (2015). Cellular functions of Rab GTPases at a glance. *J Cell Sci* *128*, 3171-3176.

## SUPPLEMENTARY INFORMATION

### **The RUSH System in *Drosophila* – A transgenic toolbox to study intracellular localization dynamics of Rab GTPases**

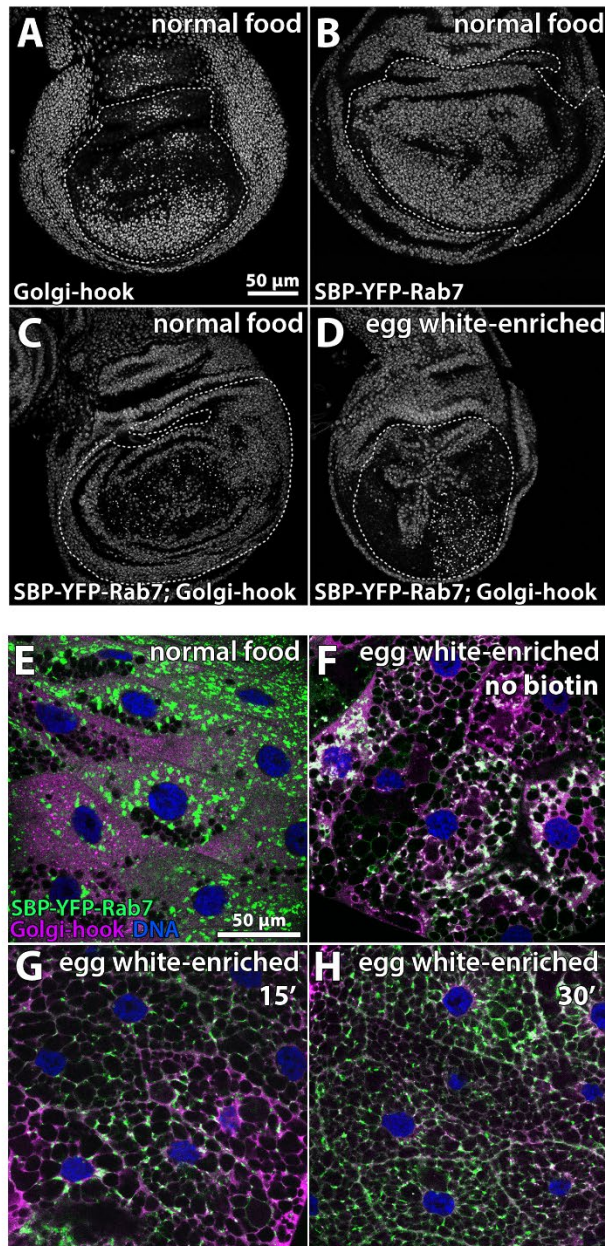
Kohrs et al.

# Supplementary Figure 1



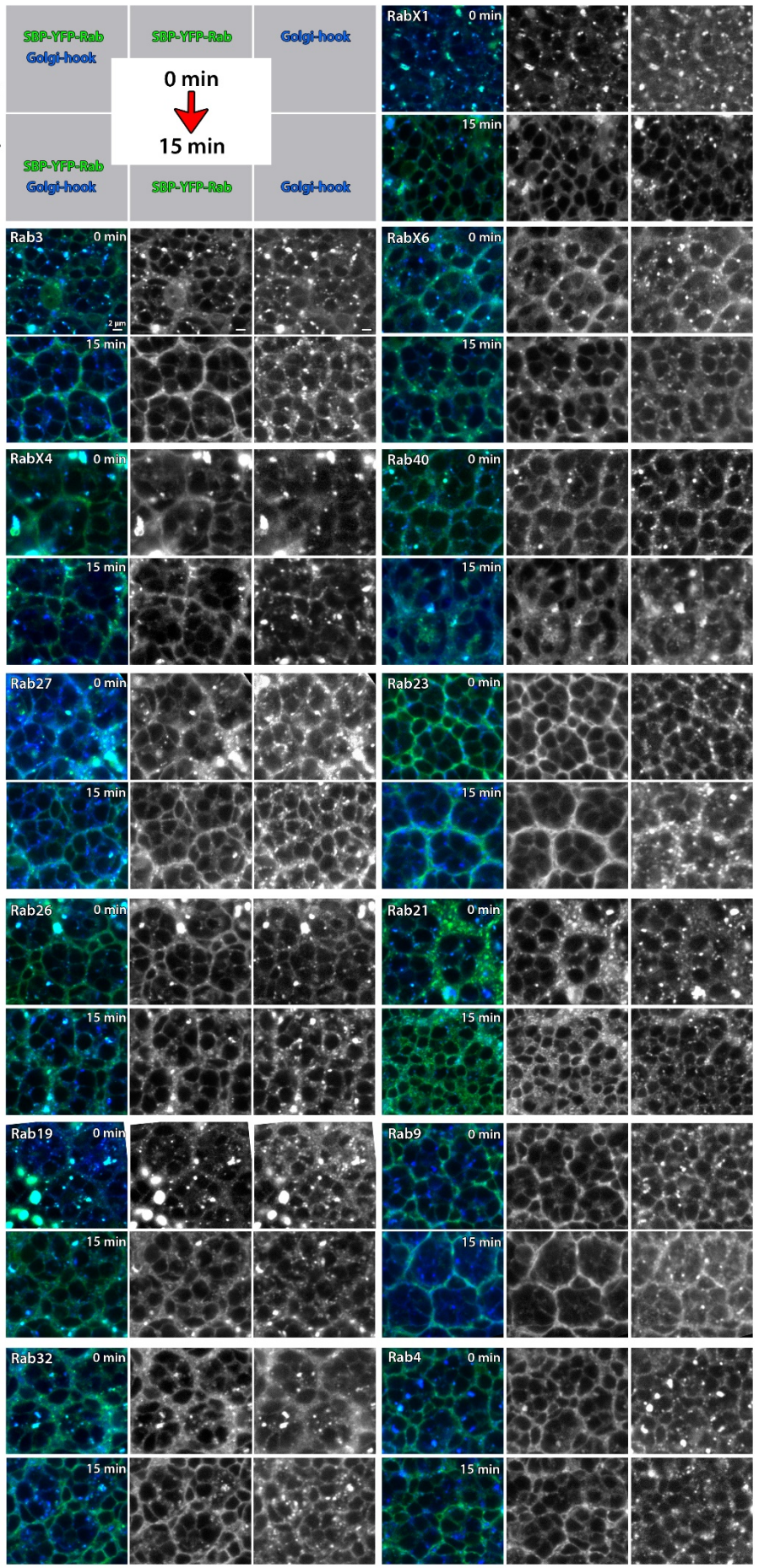
**Supplementary Figure 1: Overview of transgenic RUSH lines and comparison between nervous system-enriched YFP-Rab and SBP-YFP-Rab fusion proteins expressed in developing photoreceptors (A)** List of 26 transgenic RUSH-Rabs, sorted according to their expression pattern, going from ‘nervous system high’ (blue) at the top to ‘widespread’ (grey) to the ‘ubiquitous’ (white) Rabs at the bottom. Rab proteins used for RUSH analyses are highlighted in dark green. **(B)** List of four transgenic hook lines, sorted by their retention site (ER or Golgi) and domain (luminal or cytoplasmic). **(C)** Comparison of the expression patterns of YFP-tagged Rab GTPases with newly generated SBP-YFP-tagged Rabs reveals no significant differences in their subcellular localization in ~P+40% pupal eye-brain complexes. Labeling of developing photoreceptors by GMR-myrtTomato (red). YFP- and SBP-YFP-tag shown in green and in the single channels (grey scale). Scale bar = 20 μm; number of eye-brain complexes n = 3-6.

## Supplementary Figure 2



**Supplementary Figure 2: Proof-of-principle experiments with RUSH-Rab7 performed in larval wing discs and third instar salivary glands (A-D)** Expression of transgenic RUSH lines in larval wing imaginal discs. Expression of the Golgi-hook (A) or RUSH-Rab7 (B) under nubbin-Gal4 does not affect normal wing disc development when flies are raised on normal food. Expression of both constructs leads to apoptosis and dead cell shedding, even if raised on normal food (C). Expression of both constructed leads to highly deformed imaginal wing discs and larval lethality prior to pupation, when flies are raised on egg white-enriched food (D). Scale bar = 50  $\mu$ m. (E-H) Expression of transgenic RUSH lines in third instar salivary glands. Expression of the Golgi-hook (magenta) and RUSH-Rab7 (green) under sgs3-Gal4 does not affect salivary gland development, neither when flies were raised on normal food (E), nor when raised on egg white-enriched food (F). RUSH-Rab7 was released from the Golgi-hook after Biotin incubation for 15 (G) or 30 minutes (H). Immunolabeling of the Golgi-hook with Streptavidin. DNA (blue) was labeled with Hoechst dye. Scale bar = 50  $\mu$ m.

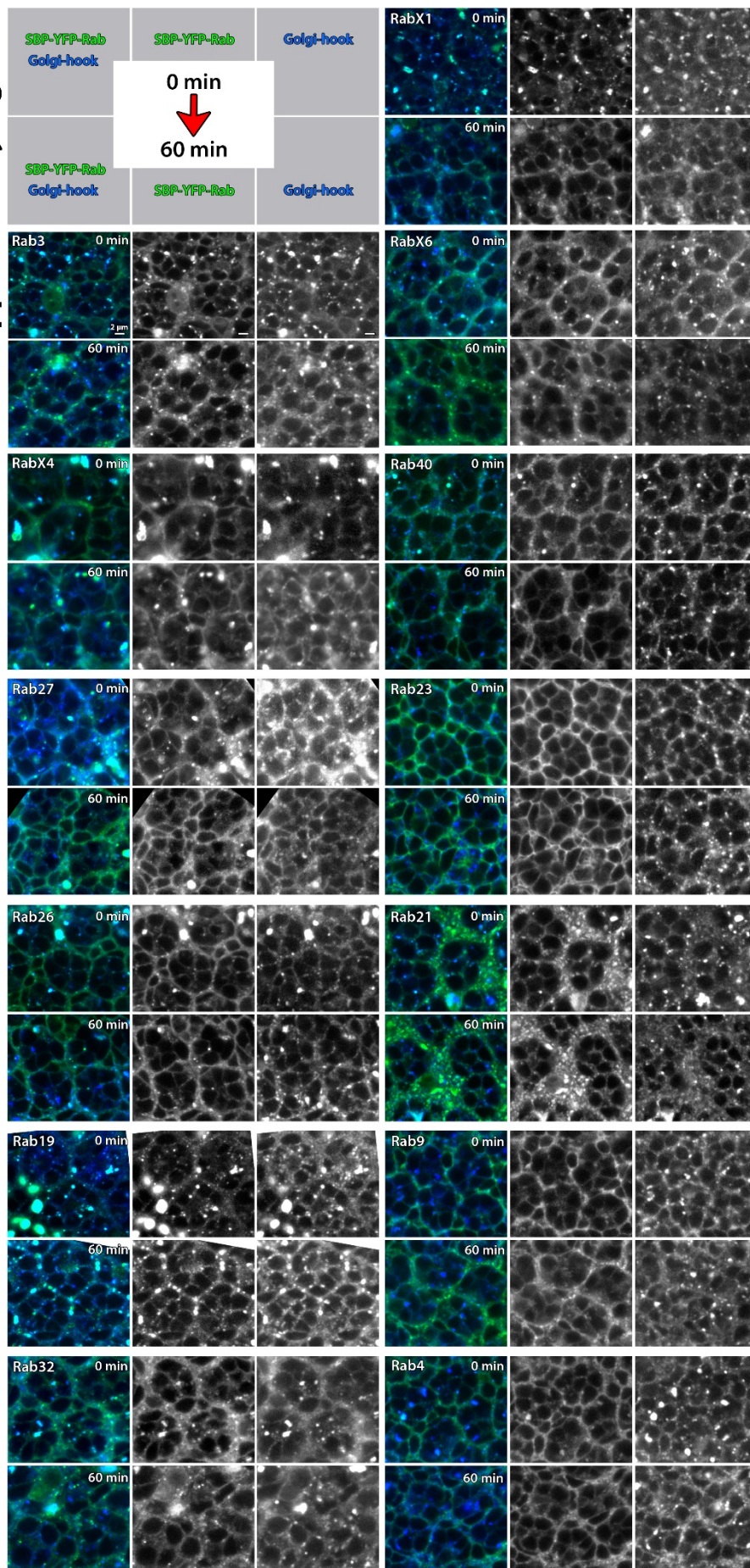
**Supplementary Figure 3**



**Supplementary Figure 3: RUSH release experiments for all nervous system-enriched Rab GTPases with 15 minutes of Biotin incubation**

Rab GTPases are sorted according to their expression pattern (see Suppl. Fig. 1 as reference). Retention (0 minutes, no Biotin) and release (15 minutes of Biotin incubation) of all nervous system-enriched Rab GTPases (green, single channel grey scale) from the Golgi hook (blue, single channel grey scale). Shown are images of ommatidia of retina from ~P+40% pupae. Immunolabeling of the Golgi-hook with Streptavidin. Scale bar = 2  $\mu$ m; number of retinas n = 3-5 for each incubation time point.

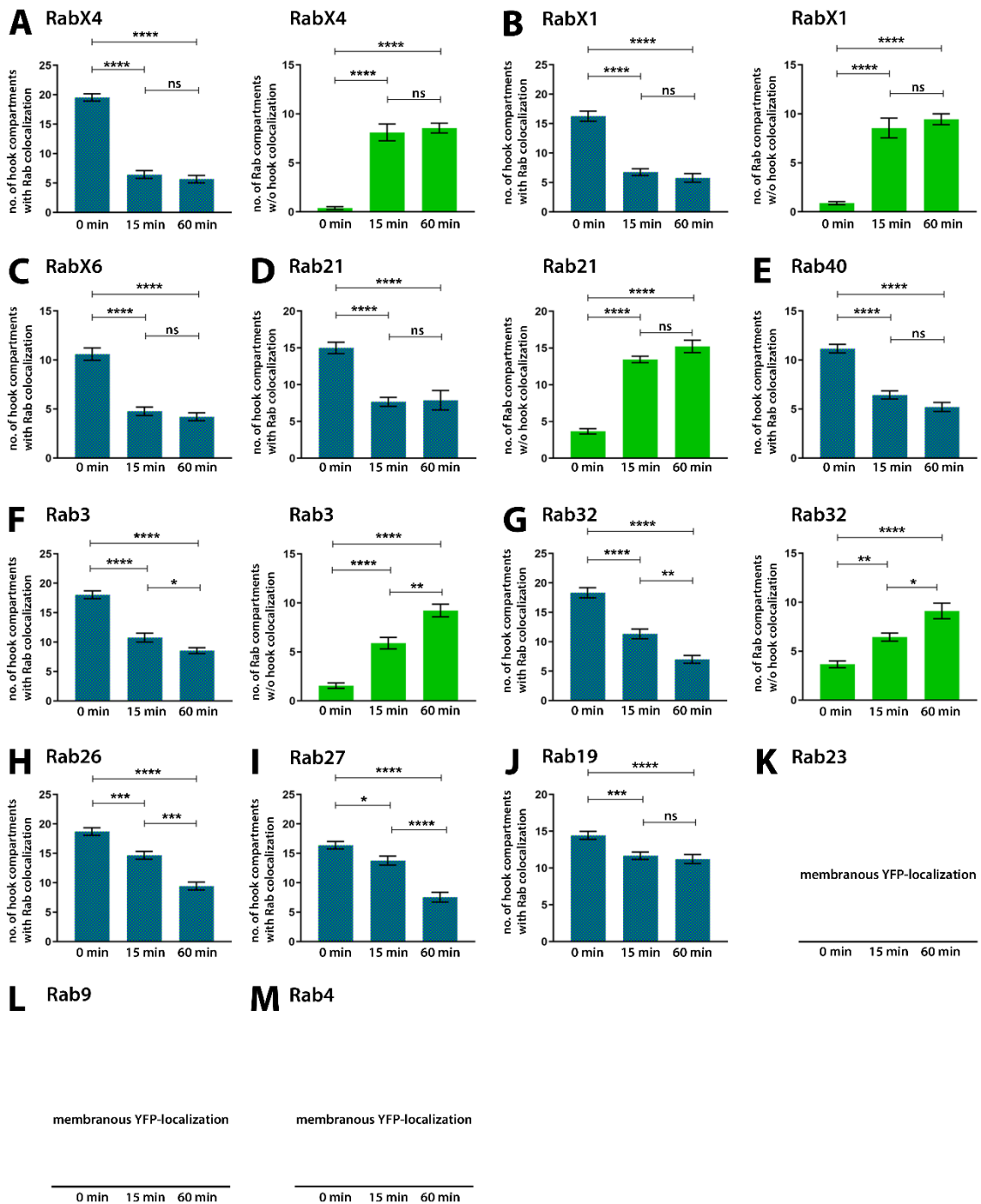
**Supplementary Figure 4**



**Supplementary Figure 4: RUSH release experiments for all nervous system-enriched Rab GTPases with 60 minutes of Biotin incubation**

Rab GTPases are sorted according to their expression pattern (see Supplementary Figure 1 as reference). Retention (0 minutes, no Biotin) and release (60 minutes Biotin incubation) of all nervous system-enriched Rab GTPases (green, single channel grey scale) from the Golgi hook (blue, single channel grey scale). Shown are images of ommatidia of retina from ~P+40% pupae. Immunolabeling of the Golgi-hook with Streptavidin. Scale bar = 2  $\mu$ m; number of retinas n = 3-5 for each incubation time point.

# Supplementary Figure 5

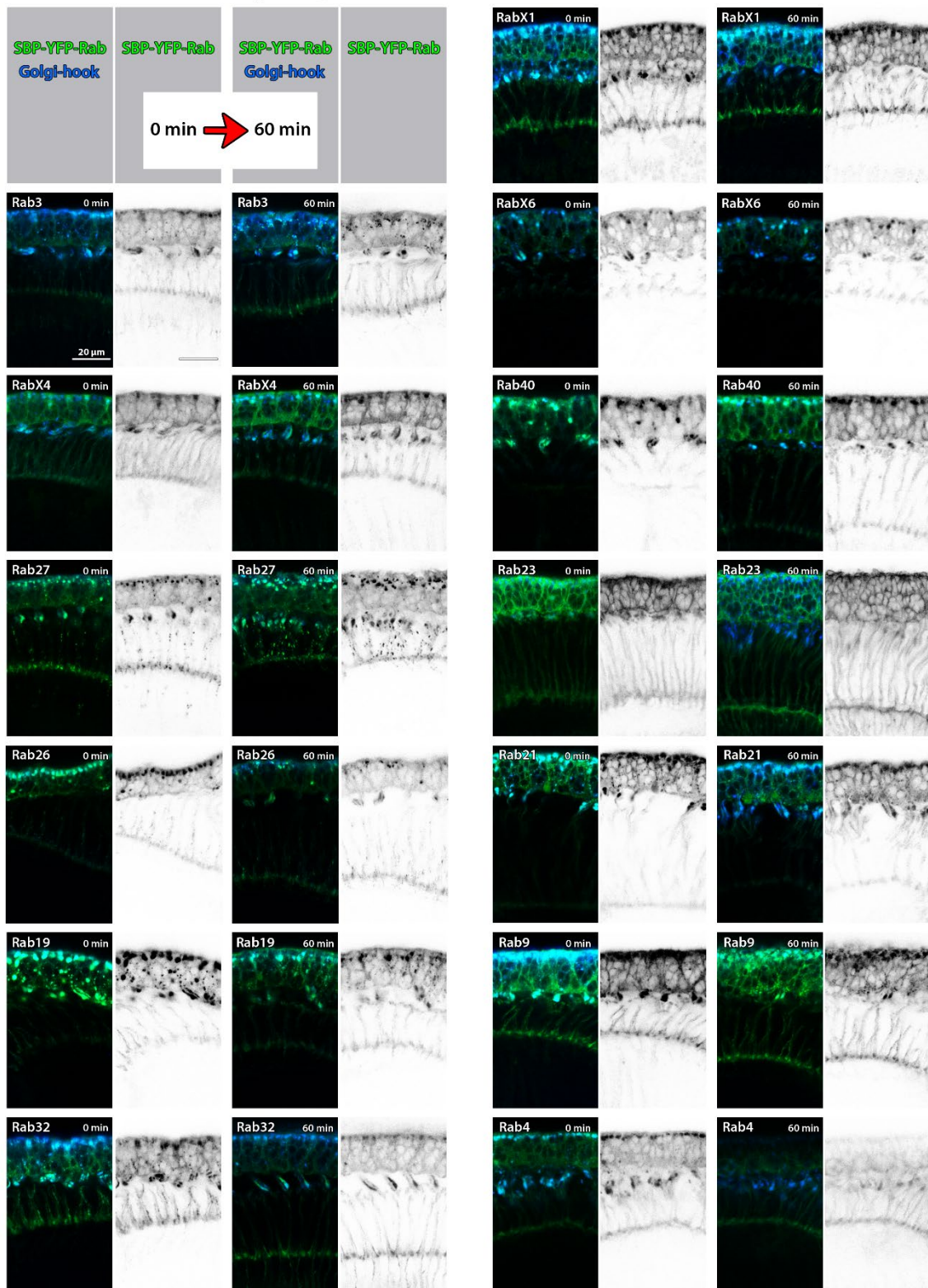


**Supplementary Figure 5: Quantification of retention and release rates of all nervous system-enriched Rab GTPases from the Golgi-hook (A-J)** Diagrams are sorted according to their release properties within in the first 15 minutes after the addition of Biotin. **(A)** RabX4 was identified as a ‘fast-releasing’ Rab. Within the first 15 minutes of Biotin incubation 50% of the Golgi-hook lost colocalization with RUSH-RabX4 (patterned bar chart), while the amount of RUSH-RabX4 (YFP-only) compartments increased significantly (green bar chart). RUSH-RabX4 compartments are distinctly localized in the cytoplasm of the photoreceptor cell bodies. Mean  $\pm$  SEM; \*\*\*\*  $p < 0.0001$ ; number of ommatidia  $n = 9$  from 3-5 animals for each Biotin incubation time point; Ordinary one-way ANOVA with pair-wise comparison, Holm-Šidák test. **(B)** RabX1 was identified as a ‘fast-releasing’ Rab. Within the first 15 minutes of Biotin incubation 50% of the

*Supplementary Figure 5 continued*

Golgi-hook lost colocalization with RUSH-RabX1 (patterned bar chart), while the amount of RUSH-RabX1 (YFP-only) compartments increased significantly (green bar chart). RUSH-RabX1 compartments are distinctly localized in the cytoplasm of the photoreceptor cell bodies. Mean  $\pm$  SEM; ns = non-significant, \*\*\*\*  $p \leq 0.0001$ ; number of ommatidia  $n = 9$  from 3-5 animals for each Biotin incubation time point; Ordinary one-way ANOVA with pair-wise comparison, Holm-Šidák test. **(C)** RabX6 was identified as a ‘fast-releasing’ Rab, within the first 15 minutes of Biotin incubation 50% of the Golgi-hook lost colocalization with RUSH-RabX6. Mean  $\pm$  SEM; ns = non-significant, \*\*\*\*  $p \leq 0.0001$ ; number of ommatidia  $n = 9$  from 3-5 animals for each Biotin incubation time point; Ordinary one-way ANOVA with pair-wise comparison, Holm-Šidák test. **(D)** Rab21 was identified as a ‘fast-releasing’ Rab. Within the first 15 minutes of Biotin incubation 50% of the Golgi-hook lost colocalization with RUSH-Rab21 (patterned bar chart), while the amount of RUSH-Rab21 (YFP-only) compartments increased significantly (green bar chart). RUSH-Rab21 compartments are distinctly localized in the cytoplasm of the photoreceptor cell bodies. Mean  $\pm$  SEM; ns = non-significant, \*\*\*\*  $p \leq 0.0001$ ; number of ommatidia  $n = 9$  from 3-5 animals for each Biotin incubation time point; Ordinary one-way ANOVA with pair-wise comparison, Holm-Šidák test. **(E)** Rab40 was identified as a ‘intermediate releasing’ Rab, within the first 15 minutes of Biotin incubation Golgi-hook lost significant colocalization with RUSH-Rab32. Mean  $\pm$  SEM; ns = non-significant, \*\*\*\*  $p \leq 0.0001$ ; number of ommatidia  $n = 9$  from 3-5 animals for each Biotin incubation time point; Ordinary one-way ANOVA with pair-wise comparison, Holm-Šidák test. **(F)** Rab3 was identified as a ‘intermediate releasing’ Rab. Within the first 15 minutes of Biotin incubation Golgi-hook lost significant colocalization with RUSH-Rab3 (patterned bar chart), while the amount of RUSH-Rab3 (YFP-only) compartments increased significantly (green bar chart). RUSH-Rab3 compartments are distinctly localized in the cytoplasm of the photoreceptor cell bodies. Mean  $\pm$  SEM; ns = non-significant, \*  $p < 0.05$ , \*\*  $p \leq 0.01$ , \*\*\*\*  $p \leq 0.0001$ ; number of ommatidia  $n = 9$  from 3-5 animals for each Biotin incubation time point; Ordinary one-way ANOVA with pair-wise comparison, Holm-Šidák test. **(G)** Rab32 was identified as a ‘intermediate releasing’ Rab. Within the first 15 minutes of Biotin incubation Golgi-hook lost significant colocalization with RUSH-Rab32 (patterned bar chart), while the amount of RUSH-Rab32 (YFP-only) compartments increased significantly (green bar chart). RUSH-Rab32 compartments are distinctly localized in the cytoplasm of the photoreceptor cell bodies. Mean  $\pm$  SEM; \*\*  $p \leq 0.01$ , \*\*\*\*  $p \leq 0.0001$ ; number of ommatidia  $n = 9$  from 3-5 animals for each Biotin incubation time point; Ordinary one-way ANOVA with pair-wise comparison, Holm-Šidák test. **(H)** Rab26 was identified as a ‘slow-releasing’ Rab, within the first 15 minutes of Biotin incubation less than 25% of the Golgi-hook lost colocalization with RUSH-Rab26. Mean  $\pm$  SEM; \*\*\*  $p \leq 0.001$ , \*\*\*\*  $p \leq 0.0001$ ; number of ommatidia  $n = 9$  from 3-5 animals for each Biotin incubation time point; Ordinary one-way ANOVA with pair-wise comparison, Holm-Šidák test. **(I)** Rab27 was identified as a ‘slow-releasing’ Rab, within the first 15 minutes of Biotin incubation less than 25% of the Golgi-hook lost colocalization with RUSH-Rab27. Mean  $\pm$  SEM; \*  $p < 0.05$ , \*\*\*\*  $p \leq 0.0001$ ; number of ommatidia  $n = 9$  from 3-5 animals for each Biotin incubation time point; Ordinary one-way ANOVA with pair-wise comparison, Holm-Šidák test. **(J)** Rab19 was identified as a ‘slow-releasing’ Rab, within the first 15 minutes of Biotin incubation less than 25% of the Golgi-hook lost colocalization with RUSH-Rab19. Mean  $\pm$  SEM; ns = non-significant, \*\*\*  $p \leq 0.001$ , \*\*\*\*  $p \leq 0.0001$ ; number of ommatidia  $n = 9$  from 3-5 animals for each Biotin incubation time point; Ordinary one-way ANOVA with pair-wise comparison, Holm-Šidák test. **(K-M)** Retention or release rates could not be quantified, as the RUSH versions of Rab23, Rab9, and Rab4 show a membranous localization in the photoreceptor cell bodies.

## Supplementary Figure 6



### Supplementary Figure 6: RUSH re-localization experiments for all nervous system-enriched Rab GTPases with 60 minutes of Biotin incubation

Rab GTPases are sorted according to their expression pattern (see Supplementary Figure 1 as reference). Retention (0 minutes, no Biotin) and release (60 minutes Biotin incubation) of all nervous system-enriched Rab GTPases (green, single channel grey scale) from the Golgi hook (blue) in photoreceptor cell bodies. For some Rab GTPases a re-localization of the protein to the photoreceptor axon terminals can be observed after

*Supplementary Figure 6 continued*

60 minutes of Biotin incubation. Shown are cross-sections of retinas and photoreceptor axon projections in the lamina region of ~P+40% pupae. Immunolabeling of the Golgi-hook with Streptavidin. Scale bar = 20  $\mu\text{m}$ ; number of retinas  $n = 3-5$  for each incubation time point.

## 6. General discussion

Neurons are long-lived, post-mitotic cells with a highly polarized and often complex morphology (Bentley and Banker, 2016). As such, they require specialized membrane trafficking and degradation pathways during neurodevelopment, including transport of needed building materials and regulated plasma membrane expansion (Kiral et al., 2020; Winkle and Gupton, 2016), during synaptic function (Sudhof, 2004), as well as during functional homeostasis and maintenance (Wang et al., 2013). Rab GTPases, in their function as master regulators of intracellular membrane trafficking between membranous compartments, are involved in all of these processes. However, only a limited number of them have been analyzed for their specific roles in neurons (Chan et al., 2011; Pfeffer, 2017; Zhen and Stenmark, 2015).

At the core of my doctoral studies was the first systematic functional characterization of nervous system-enriched Rab GTPases in *Drosophila*. With this, I want to contribute to answer questions in the field of (Rab-mediated) endomembrane trafficking, including, what are the roles of Rab GTPases with high expression in the nervous system during development, as well as neuronal function and maintenance in the multicellular organism *Drosophila*? Further, in a greater context, how do individual Rab GTPases contribute to the robustness of membrane trafficking events and therefore to the health as well as neuronal and synaptic homeostasis of neurons? To approach these questions experimentally in an unbiased way, we used a collection of molecularly defined *rab* null mutants to check for evolutionary selected roles during robust development and function (Manuscript 2; Kohrs et al., 2021), as well as a transgenic toolbox based on the published RUSH system to identify intracellular localization and trafficking dynamics of Rab GTPases (Manuscript 3; Kohrs et al., unpublished) (Boncompain et al., 2012). Additionally, the experimental work was corroborated by extensive literature research on Rab-mediated membrane trafficking events and neurodegenerative diseases, establishing possible ‘cause and effect’ relations in Manuscript 1 (Kiral et al., 2018). In the following sections of this chapter, I will discuss the major results of my doctoral studies and set them in relation to previously published work.

## 6.1 The associations between Rab GTPases and neurodegenerative diseases are more correlative than causative

Coordinated membrane trafficking is essential for neurons, not only during their development and function. They also rely on it to maintain neuronal and synaptic homeostasis, as well as their health over extended periods of time. Especially synapses, sites of extensive membrane turnover, depend on functional maintenance mechanisms. Hence, it is not surprising, that the loss of synaptic integrity has been identified as an early hallmark of numerous neurodegenerative diseases (Bezprozvanny and Hiesinger, 2013; Henstridge et al., 2019; Wang et al., 2013). As reviewed in detail in Manuscript 1 (Kiral et al., 2018), several Rab GTPases and the intracellular membrane trafficking pathways these mediate in the nervous system, have been both directly and indirectly linked to the onset and progression of neurodegenerative diseases, such as Alzheimer's (AD) and Parkinson's disease (PD).

Impairment of certain trafficking pathways, especially of the early endosomal and endolysosomal degradation pathway, have been identified as so called 'drivers of pathology' in diseases like PD, AD, and the rare sensory neuropathy Charcot-Marie-Tooth (CMT). However, the relationship between specific Rab GTPases and neurodegeneration has been mostly correlative rather than causative. So far, no other *rab* mutant was causatively linked to neurodegenerative disease pathology, apart from Rab7 and Rab39b, where a clear causal link between mutations in the *rab* loci and CMT2B and familial PD, respectively, could be identified (Guadagno and Progida, 2019; Kiral et al., 2018; Kuwahara and Iwatsubo, 2020; Singh and Muqit, 2020). Often the defects or changes in the levels of Rabs are not the primary cause, but rather are secondary or downstream of disease pathology.

Therefore, it is crucial to first identify the individual requirements of neurons to stay healthy as well as functional and second to establish the specific roles of Rab proteins in intracellular membrane trafficking. This needs to happen prior to investigating the intricate relations between Rab GTPases, Rab-mediated trafficking events, and neurodegenerative disease pathology.

## 6.2 Nervous system-enriched Rab GTPases serve modulatory roles in membrane trafficking, differentially affecting robust development and function

Previously, a systematic expression profiling effort revealed that all 26 *Drosophila* Rab GTPases are expressed in the nervous system, albeit with different localization patterns. Surprisingly, half of these are enriched or strongly enriched in the nervous system and predominantly located in the synaptic neuropil in the developing and adult brain (Chan et al., 2011; Jin et al., 2012). However, the majority of these nervous system-enriched Rab proteins have remained largely uncharacterized so far, which motivated the experimental work presented in Manuscript 2 (Kohrs et al., 2021). We posed the following questions: With so many Rab GTPases being nervous system-enriched, do they have specific roles in development as well as in the function and maintenance of neurons? Are these neuronal roles essential or rather more specialized and modulatory? And can varying environmental conditions reveal context-dependent Rab functions?

To address these questions, 17 molecularly defined null mutants (*rab 2, 4, 9, 10, 14, 18, 19, 21, 23, 26, 30, 35, 39, 40, X1, X4, and X6*) were generated to complete the *rab* null mutant collection. 9 *rab* mutants already existed before this study (*rab 1, 3, 5, 6, 7, 8, 11, 27, and 32*). Over the years, the family of small Rab GTPases has been analyzed multiple times to gain insight into the membrane trafficking networks they regulate. For instance, effector analyses (Gillingham et al., 2014), expression profiling efforts with endogenously tagged or wild type Rab variants (Chan et al., 2011; Dunst et al., 2015; Jin et al., 2012), and cell type-specific systematic RNAi knockdown analyses (Best and Leptin, 2020) have been performed. Further, the gene family has been reviewed in their capacity as compartment identifiers, trafficking coordinators, and intracellular membrane organizers (Gurkan et al., 2005; Pfeffer, 1994; Stenmark, 2009; Zerial and McBride, 2001). However, so far, no systematic functional analysis in a multicellular organism has been performed to elucidate Rab functions.

While loss of ubiquitously expressed *rab* genes leads to lethality under homozygosity, null mutants for all 13 nervous system-enriched *rabs* are viable and fertile under laboratory conditions. Although, some mutant chromosomes show a competitive disadvantage. Yet, laboratory conditions exert only minimal selection pressure, food and water are provided *ad libitum*, and flies are reared in non-crowded conditions under room temperature. Therefore, we hypothesized that these 13 nervous system-enriched Rab

GTPases have likely non-essential, more specialized functions in the organism and that these only reveal themselves in a context-specific manner, under non-laboratory and more stimulating conditions. Previously, modulatory roles for nervous system-enriched Rab proteins have already been proposed and discussed, based on the findings that expression of dominant negative variants did not affect neuronal survival in flies, nor did the expression of the constitutively active and dominant negative variants cause any obvious defects during development and function (Chan et al., 2011; Harris and Littleton, 2011). However, phenotypic differences have already been described between several loss-of-function mutants and the corresponding dominant negative variants, not only in *Drosophila* but also for mammalian Rabs. Examples include Rab7, where functional loss of *rab7* leads to a stimulus-dependent degeneration of *Drosophila* photoreceptors, starting at the synapses. Contrary to this, expression of the dominant negative variant does not lead to any morphological or functional defects. More importantly, dominant negative Rab7 could partially rescue the null mutant phenotype, indicating retained wild type function to some degree (Chan et al., 2011; Cherry et al., 2013). Another example is mammalian Rab18. Here, the silencing of *rab18* function strongly impairs the radial migration of developing primary cortical neurons in mice. While neuronal migration is only very mildly affected when the dominant negative variant is expressed in the same cell-type (Wu et al., 2016). Therefore, the careful analysis of single *rab* mutant phenotypes can provide reliable evidence for their modulatory, specialized roles.

Correctly operating membrane trafficking machineries are essential during development and function of the nervous system. Given the Rabs' proposed modulatory role, we devised a series of assays to systematically analyze the developmental and functional robustness of the nervous system in the homozygous viable and fertile *rab* mutant flies. Here in this context, robustness is defined as the ability of a given system to tolerate variations in a prevalent environmental condition to a certain extent (Hiesinger and Hassan, 2018). For instance, *Drosophila*, amongst other animals, has evolved to robustly develop a functional brain under a variety of developmental temperatures (Kiral et al., 2021). As such, *rab* mutant development was specifically challenged with different temperatures, while continuous light stimulation was used to challenge neuronal function as well as maintenance in a controlled manner. The systematic analysis revealed context-specific roles, where every individual *rab* mutants affected different aspects of development or neuronal function and

might contribute to a deeper understanding of functional requirements of neurons under evolutionary selection.

In more detail, environmental temperature has a strong effect on developmental processes, physiology and overall fitness of ectotherms, like flies, which have only very limited abilities to regulate their own body temperature (Cheung and Ma, 2015; Dillon et al., 2009; Gillooly et al., 2002). The physiological permissive temperature range for wild type *Drosophila* is roughly between 18°C - 29°C, with its thermal preference being 25°C for optimal growth (Economos and Lints, 1986; Hamada et al., 2008; Siddiqui and Barlow, 1972). In general, robust development will result in a ‘normal’ outcome (here a functioning adult fly), even under more variable conditions as long as these are inside a certain tolerable range. Interestingly, the majority of viable and fertile *rab* null mutants, developed at one of the three tested temperatures (18°C, 25°C, and 29°C), differentially affected the developmental timing and robustness of the flies. While some mutants (*rabX1* and *rabX4*) exhibited specific developmental phenotypes, independent of the environmental temperature, other mutants exhibited a stronger sensitivity towards higher (*rab18*, *rab19*, and *rab32*) or lower temperatures (*rab4* and *rab40*) during their development. This indicates that the majority of homozygous viable and fertile *rab* mutants represent, to varying extents, sensitized genetic backgrounds during development under more variable temperatures.

To specifically test the function and maintenance of neurons under challenging conditions, we used white light to continuously stimulate mature photoreceptor neurons. In invertebrates, like *Drosophila*, as well as in vertebrates, already continuous light stimulation of wild type photoreceptors can cause a reduction in photoresponse, eventually affecting neuronal maintenance, leading to retinal blindness and degeneration (Lee and Montell, 2004; Noell et al., 1966). With our light stimulation paradigm, the tested populations of white-eyed wild type flies showed a gradual decrease in synaptic transmission as well as depolarization over a period of seven days, with two days of light stimulation representing a highly sensitized time window. Testing inside this dynamic range allows for the identification of changes in the neuronal function of mutant photoreceptors. The systematic screen of all homozygous viable *rab* null mutants, using ERG recordings, revealed four nervous system-enriched *rab* mutants (*rab 3*, *19*, *26*, and *X6*), which showed a stimulus-dependent functional transmission defect without any pre-existing functional or morphological defects of the eye. Furthermore, these four Rab GTPases exhibited a strong protein localization to the synaptic neuropil in the adult fly brain, highlighting a correlation

between adult neuronal expression with synaptic localization and robust synaptic function under challenging, continuous stimulation. Analyzing the morphology of outer rhabdomeres and photoreceptor axon projections before and after light stimulation revealed 10 *rab* mutants with possible roles in activity-dependent membrane turnover in rhabdomeres, two of them (*rab19* and *rab26*) showing an additional phenotype, in form of membrane protein accumulations in axon terminals in the lamina.

The different stimulation assays revealed a range of context-specific phenotypes for all nervous system-enriched *rab* mutants which would have remained phenotypically sub-threshold if kept under non-stimulating laboratory conditions (Hiesinger, 2021). The fact that all nervous system-enriched *rab* mutants are viable and differentially affect development or function when challenged, supports the hypothesis of evolutionarily selected, specialized Rab functions involved in the modulation of membrane trafficking in order to maintain robust development and function under varying conditions. Here, variable environmental conditions revealed context-dependent Rab functions, where many of the viable mutants did not display obvious developmental or functional phenotypes under laboratory conditions. Different Rab GTPases might have more or less context-dependency. In our functional analysis we used varying environmental conditions as a form of context. However, examining Rabs with respect to different contexts, which also include subcellular localization, availability of downstream binding effectors, as well as cell type, might reveal new or conserved regulatory roles during membrane trafficking. An integrative analysis of contextual roles of individual Rab proteins across species could be the next step in understanding why there are so many Rab GTPases.

Finally, the generation of the *rab* mutant collection, its systematic mutant characterization in combination with the expression pattern analysis, provides the basis for more in-depth analyses of single nervous system-enriched *rab* mutants, of which many still have unclear or unknown functions. Interestingly, an overwhelming amount of known Rab functions is inferred from analyses of constitutively active and dominant negative Rab variants (see Supplementary Tables of Kohrs et al., 2021). However, the amino acid substitutions, which are used to stabilize the different variants in their active or inactive state, might affect the molecular properties of Rabs in unpredicted and more complex ways. Previously, it has been shown that two mammalian Rab proteins, which were assumed to be constitutively active, could actually not be activated by the respective GEFs. However, only four Rab-GEF combinations in total were examined in this study, suggesting that more Rabs

could be misidentified as constitutively active, given the high number of Rab GTPases and interacting GEFs (Langemeyer et al., 2014; Nottingham and Pfeffer, 2014). Further, phenotypic differences between null mutants and dominant negative Rab variants have already been described, as discussed earlier in this section. And dominant negative variants might retain some wild type function, as is the case of Rab7 (Cherry et al., 2013). Thus, findings based on Rab variants may be ambiguous to some extent and need to be interpreted with caution. Loss-of-function analyses are a well-established way to elucidate wild type gene functions. Yet, for the majority of *Drosophila* Rab GTPases no molecularly defined null mutant was even available until now and for the mammalian Rabs, still not all mouse models exist (see Supplementary Tables of Kohrs et al., 2021). The functional characterization of the nervous system-enriched *Drosophila* Rab26 highlights the importance and necessity of a careful mutant analysis, as discussed in the next section.

### **6.3 The nervous system-enriched Rab26 functions in stimulus-dependent, synapse-specific receptor trafficking in *Drosophila***

Although many Rab GTPases, across different species, are enriched in or specific to the nervous system, only few of those, including Rab3, Rab27, as well as Rab26, have been examined for their neuronal roles (Chan et al., 2011; D'Adamo et al., 2014; Jin et al., 2012; Kiral et al., 2018). Rab3 and Rab27 regulate, somewhat redundantly, synaptic vesicle exocytosis and neurotransmitter release at the presynapse (Binotti et al., 2016; Fischer von Mollard et al., 1991; Guadagno and Progida, 2019; Schluter et al., 2004), while in *Drosophila*, additional roles were identified. Rab3 functions in the localization of crucial active zone proteins in the larval NMJ (Chen et al., 2015; Graf et al., 2009), while Rab27 has been shown to modulate *Drosophila* lifespan and mutant flies exhibit circadian rhythm defects (Chan et al., 2011; Lien et al., 2020). Nervous system-enriched Rab26 has been proposed to link synaptic vesicle recycling to the autophagic pathway in both mammals and *Drosophila* (Binotti et al., 2015). However, in this study, which was primarily based on the overexpression of Rab26 variants, no direct connection between the Rab protein, synaptic vesicles, and autophagy was established in *Drosophila*. During our systematic functional mutant analysis, we could observe several phenotypes in the *rab26* mutant flies, which would indicate a possible role of Rab26 at synaptic terminals: Displaying no defects prior to stimulation, *rab26* mutant flies show a stimulus-dependent synaptic transmission defect after two days. Furthermore, after continuous light stimulation, membrane proteins, such as

Chaoptin, accumulate specifically in the proximal region of the lamina, where outer R1-R6 photoreceptor axon projections terminate. Photoreceptor-specific knockdown of Rab26 using a RNAi approach mimics the whole-body mutant phenotype. In addition, this accumulation phenotype can be rescued by photoreceptor-specific expression of Rab26 in the mutant background, indicative of a cell-autonomous phenotype. Moreover, endogenous Rab26 shows a predominant localization to the synaptic neuropil.

To pinpoint the role of Rab26 at synaptic terminals, we first performed similar experiments as Binotti and colleagues, using our newly generated null mutant in addition to Rab26 variants expressed in larval NMJs as well as in adult fly photoreceptors. While we observed partial colocalization of Rab26 variants and endogenous Rab26 with several endosomal markers, no colocalization with the autophagosomal marker Atg8 and only a partial overlap with a synaptic vesicle marker in NMJs was discernable. Additionally, no level changes for autophagosomal and synaptic vesicle markers were observed in the *rab26* mutant. Our findings suggest that *Drosophila* Rab26 is not directly linked to synaptic vesicles and autophagy in NMJs during development or in functional neurons of the visual system. Moreover, until now no other study has demonstrated a direct or indirect link between *Drosophila* Rab26 and autophagy, irrespective of cell type. Besides Binotti and colleagues (2015), others have examined the role of mammalian Rab26 in connection to autophagy, mainly using Rab26 variants in non-neuronal cell lines for their analyses (Dong et al., 2018; Luningschror et al., 2017; Siadous et al., 2021; Witte et al., 2020). However, a functional analysis of mammalian *rab26* in neurons has not been performed so far and it would be interesting to see if the link to autophagy will be corroborated by the mutant.

Yet, endogenous Rab26 localizes to a subset of synapses marked by the synaptic scaffold protein Bruchpilot in the proximal region of the adult *Drosophila* lamina. The same region where continuous light stimulation leads to characteristic accumulations of the photoreceptor membrane protein Chaoptin, as well as of the choline acetyltransferase (ChAT) in the *rab26* mutant. Based on a recent transcriptome study, outer photoreceptors R1-R6, which terminate in the lamina, are not known to be cholinergic themselves but are predicted to express a single acetylcholine receptor subunit nAChRalpha4 ( $D\alpha 4$ , rye) (Davis et al., 2020). Cholinergic L4 neurons, so far known for their role in progressive motion detection, exhibit the distinct stimulus-dependent upregulation of ChAT in the *rab26* mutant. Furthermore, they are the only lamina neurons that specifically form connections to the proximal end of axon terminals of outer photoreceptors, providing synaptic input most likely

via D $\alpha$ 4 (Davis et al., 2020; Fischbach and Dittrich, 1989; Kolodziejczyk et al., 2008; Luthy et al., 2014; Rivera-Alba et al., 2011; Tuthill et al., 2013). Using a D $\alpha$ 4 RNAi approach, established in Amita Sehgal's lab (Shi et al., 2014), we could mimic the *rab26* mutant phenotype, by specifically knocking down D $\alpha$ 4 in photoreceptors, highlighting a function for Rab26 in the stimulus-dependent receptor trafficking at specific cholinergic synapses in the fly visual system. Yet, it is still unknown at which exact step in the postsynaptic trafficking process Rab26 plays a role and this would need further investigation.

The postsynaptic identity of outer photoreceptors, which are mostly known as the main presynaptic input source of the fly visual system, is quite interesting. It has been shown that direct synaptic feedback onto photoreceptors comes from local excitatory interneurons, namely L4 neurons with their collaterals from directly neighboring cartridges and lamina wide-field neurons type 1 and 2 (Lawf, cholinergic), as well as from amacrine cells (glutamatergic) (Dau et al., 2016; Davis et al., 2020; Kolodziejczyk et al., 2008; Rivera-Alba et al., 2011). The exact role of these feedback connections is unknown, but previously, it has been proposed that local interneurons can function as fine-tuning regulators of photoreceptor function (Dau et al., 2016). In Manuscript 2 we could show that Rab26 is overall strongly associated with the cholinergic system in the fly visual system, showing an expression pattern similar to that of the cholinergic marker ChAT in the optic lobe. As such, Rab26 localizes to the presynaptic terminals of Lawf type 2 neurons in the distal region of the lamina. It would be interesting to expand on possible postsynaptic roles of Rab26 in other cholinergic neuron types and examine if the role in receptor-subunit trafficking is conserved in these neurons. Furthermore, *Drosophila* Rab26 likely exerts a so far unknown presynaptic function in membrane trafficking as well, as this nervous system Rab endogenously localizes to larval NMJs, which form glutamatergic synapses (Chou et al., 2020; Kohrs et al., 2021). Ultimately, determining the specific, context-dependent wild type functions of individual Rab proteins and the membrane trafficking events these regulate, will be critical for causative disease analyses and help expand our understanding of what keeps neurons alive and functional in the first place.

## **6.4 Localization dynamics of Rab GTPases revealed by the RUSH system**

Analysis of acute Rab functions in a spatiotemporally controlled manner in differentially specialized cells of intact tissues would further increase our knowledge of Rab-mediated

endomembrane trafficking. However, experimental approaches in *Drosophila* have been limited so far, and therefore, my collaborator Bojaná Pavlovic, a member of Prof. Dr. Michael Boutros' lab (DKFZ, Heidelberg) and I tried to establish the 'retention using selective hooks' (RUSH) system in several developing multicellular tissues in *Drosophila* to facilitate studies on intracellular localization and trafficking dynamics of Rab GTPases (Manuscript 3). First generated and published by the lab of Frank Perez, the assay is based on the selective retention and acute synchronous release of a tagged protein of interest from a 'hook compartment' by the addition of the small molecule Biotin and was originally designed for mammalian cell culture (Boncompain et al., 2012). So far, published findings on synchronized trafficking kinetics of various proteins based on the RUSH assay have solely been made in mammalian cell lines and not in intact tissues of any multicellular organism (Lisse et al., 2017; Moti et al., 2019; Niu et al., 2019; Pacheco-Fernandez et al., 2020; Pawar et al., 2017; Petkovic et al., 2014). In developing photoreceptors, we could identify conditions that allowed for the release of tagged Rab proteins from our selected 'hook compartment' the Golgi within minutes, based on proof-of-principle experiments using the well-characterized late endosomal marker Rab7. This release protocol was further corroborated by proof-of-principle experiments performed in 3<sup>rd</sup> instar salivary glands by Bojaná Pavlovic. Retention and acute, synchronous release from the hook allowed for the identification of 'fast-releasing' Rabs most of them being recruited to distinct membrane compartments inside the photoreceptor cell body, 'slow-releasing' Rabs which show a diffuse cytoplasmic localization in the cell body, as well as two Rab GTPases that re-localize to the photoreceptor axon terminals in the lamina within one hour of release from the Golgi-hook in photoreceptor cell bodies. Interestingly, one of these two was the nervous system-enriched Rab26, for which we could already show a predominant synaptic localization using our Rab26 antibody, as well as the endogenously tagged protein (Dunst et al., 2015). Moreover, in our mutant analysis, we could identify a role of this Rab protein in receptor subunit trafficking in outer R1-R6 photoreceptor terminals in the lamina (see Manuscript 2). Additionally, future analyses of localization and trafficking dynamics of the Rab proteins should include the mapping of 'target compartments'. That is to say, to which compartments the Rab proteins traffic first after release from the hook, would play a part in the identification of their regulatory roles in membrane trafficking. Yet, this might be more feasible in a Biotin-independent assay which shows less detrimental effects, as discussed below. In general, studying the intracellular localization dynamics of single neuronal Rab

GTPases in combination with the functional *rab* mutant analyses more closely will surely reveal new details on Rab-mediated trafficking pathways specifically required in neurons.

However, the applicability of the RUSH assay was limited to some extent depending on the tested tissue. Already the expression of different RUSH hooks alone, localized to ER or Golgi, had varying detrimental effects on the development, where the wing disc proved to be the most sensitive. Additionally, Biotin-deficient fly food, necessary for successful retention to the hook compartment, caused developmental delays especially during larval stages as well as a reduction in offspring number and viability. Several Rab proteins formed aggregates at the Golgi-hook in the developing photoreceptor cell bodies, prior to Biotin stimulation. Unfortunately, in the wing imaginal discs, no conditions to use the RUSH system could be established, as the discussed detrimental effects were too extensive.

Targeting the hook to a different intracellular location like the plasma membrane or mitochondria might prove to be beneficial for the applicability of the RUSH system in *ex vivo* cultures of developing multicellular tissues in *Drosophila*. Tissue defects, which can already be observed under the constant expression of the Golgi-hook, might in part be due to disruptions of the secretory pathway. The Golgi apparatus is an essential organelle in the eukaryotic cell and part of the intracellular secretory pathway, regulating post-translational modifications, such as glycosylation, of newly synthesized proteins and lipids, as well as the sorting of secretory cargoes to their final destination (Boncompain and Perez, 2013; Rothman, 2010). Further, high levels of overexpressed Golgin-84, functioning here as Golgi-hook protein, have been shown to cause Golgi ribbon fragmentation in HeLa cells (Diao et al., 2003). Additionally, when selecting the localization of the hook, it is important to consider the possibility that the tested Rab protein or in general the protein of interest might have a previously unknown function at this organelle. The rationale of the RUSH system is to sequester the tagged protein away from its place of action and follow its acute, synchronized release. Consequently, release dynamics from the hook compartments would not be as informative and might even be misinterpreted as a lack of release from the hook if the Rab protein endogenously functions at the hook compartment. In the case of the Golgi-hook, several predominantly ubiquitous Rab GTPases are known to associate with the Golgi apparatus membrane. Further, Golgins, coiled-coil proteins which form a cytomatrix around the Golgi complex, are known to have multiple Rab binding sites (Goud et al., 2018; Muschalik and Munro, 2018; Sinka et al., 2008). Thus, a set of experiments using different hooks might be needed here to accurately examine individual Rab dynamics.

Another possibility for the examination of the intracellular localization dynamics of Rab GTPases would be to use a different molecular tool based on ligand-modulated antibody fragments (LAMAs). This system allows for the selective retention and acute, synchronized release of proteins upon addition of small molecules and was recently published by the lab of Kai Johnsson (Farrants et al., 2020). Briefly, this method uses a chimeric protein consisting of a nanobody selectively binding to GFP or GFP-based proteins and a circular permuted form of bacterial dihydrofolate reductase (cpDHFR). Instead of Biotin as an external stimulus, two small non-toxic, cell-permeable molecules are administered: nicotinamide adenine dinucleotide phosphate (NADPH), a cofactor of DHFR, and trimethoprim (TMP), an anti-bacterial drug and DHFR inhibitor. Upon binding, cpDHFR changes into its folded form, sterically blocking the binding to the fluorescently-tagged protein and thereby releasing it. Here, the major advantage compared to the RUSH system is that no Biotin-free conditions are necessary to achieve retention, thus avoiding detrimental effects on developmental timing and robustness. So far, proof-of-principle experiments with Rab7 and the chimeric LAMA protein stably expressed either at the Golgi or on the outer mitochondrial membrane have been successfully conducted in the *Drosophila* wing imaginal disc by my collaborator Bojana Pavlović. The expression of the Golgi-hook needs to be temporally restricted, by using the temperature-sensitive Gal80 mutant (Gal80ts), to avoid cell toxicity resulting in massively deformed wing discs. However, the newly generated Mitochondria-hook allows for its constant expression without causing toxicity or death of cells. This indicates that mitochondria are more robust compartments for protein retention. Perspectively, an efficient LAMA assay could be used to sequester endogenously-tagged Rab proteins away from their place of action, thereby creating conditional *rab* mutants. Previously, a RNAi approach was used to systematically knockdown endogenously-tagged Rabs by targeting the fluorescent tag (Best and Leptin, 2020; Dunst et al., 2015). However, the advantage here would be to be able to initiate an acute ‘rescue’ of the Rab depleted cells and examine phenotypic consequences before and after release from the hook compartments. However, further proof-of-principle analyses will be needed to investigate the exact retention rates of Rab proteins and to show the system’s applicability in other developing tissues in *Drosophila* such as pupal eye-brain complexes.

## 7. Concluding remarks and future directions

The primary goal of my doctoral thesis was to provide a first systematic and comparative functional analysis of the nervous system-enriched Rab GTPases in *Drosophila*. Previously available comparative studies were often based on the expression profiling of endogenously tagged Rab proteins and Rab variants, or on cell type-specific knockdown/knockout approaches (Best and Leptin, 2020; Chan et al., 2011; Dunst et al., 2015; Harris and Littleton, 2011; Homma et al., 2019; Jin et al., 2012; Udayar et al., 2013). Until now, no systematic and comparative *rab* null mutant analysis for any multicellular organism was available to further investigate evolutionary selected functions of Rab GTPases and the membrane trafficking events these regulate in neurons. During our systematic mutant analysis, we observed that, although a high number of nervous system-enriched Rab GTPases exist in *Drosophila* these are not individually required for the viability of neurons or the survival of the organism under laboratory conditions. However, we identified context-dependent roles where every single viable *rab* mutant affected a different aspect of development or neuronal function. These roles only became apparent under more challenging environmental conditions, as mutant phenotypes were sub-threshold under laboratory rearing conditions. Nervous system-enriched Rab GTPases seem to be involved in the modulation of membrane trafficking in order to maintain the robustness of development and function under variable environmental conditions. It would be interesting to reveal additional contextual roles of individual Rab GTPases. For example, by using other environmental stimuli, such as nutrient availability, or by examining different (neuronal) cell types. An integrative analysis of context-dependent Rab functions will surely contribute to a better understanding of why there are so many Rab GTPases.

Building on our systematic null mutant analyses, which revealed a range of context-dependent phenotypes, in-depth characterizations of individual Rab GTPases could now be performed. For many of them, especially the nervous system-enriched Rabs, their complete functionality is still unknown. Using a multi-method approach combining detailed, cell type-specific functional analyses with other approaches, such as subcellular localization profiling or live-imaging of intracellular compartment dynamics, will surely lead to the identification of specific functions. In our comparative study, we could establish a so far unknown role of *Drosophila* Rab26 in receptor-subunit trafficking at cholinergic synapses of outer photoreceptors. Moreover, intracellular trafficking pathways have been described

in neurons where up to now no regulatory Rabs have been identified. For instance, it was recently demonstrated that autophagosomes selectively form at tips of synaptogenic filopodia in developing R7 photoreceptors, leading to their destabilization through degradation of synaptic building materials. Thereby, the bulk degradation mechanism autophagy contributes to the restriction of synapse formation and synaptic partner choice by regulating axonal filopodial dynamics during synaptogenesis (Kiral et al., 2020). It will be exciting to discover if Rab GTPases are involved in the regulation of autophagy during neuronal wiring in *Drosophila*, and if they are, which ones exactly.

Further, the complete null mutant collection provides a valuable tool to experimentally establish functional redundancies between individual Rab proteins using double mutant combinations. Small Rab GTPases constitute a highly conserved protein family with great evolutionary plasticity, exhibiting individual losses as well as diversification and expansion of paralogues (Klopper et al., 2012). Closely related paralogous with high sequence conservation or Rab proteins exhibiting identical subcellular localization profiles may share redundant or similar functions (Chan et al., 2011; Jin et al., 2012; Zhang et al., 2007). Thus, the absence of a phenotype in a single mutant background does not necessarily mean that the Rab protein is not functional in the tested context, but that another Rab GTPase might act redundantly. A careful double mutant analysis can provide more insight into functional properties of individual Rab GTPases.

Additionally, integrative analyses of null mutant observations and intracellular protein localization dynamics are useful to gain more insight into the role of Rab GTPases and the membrane trafficking pathways they regulate during neuronal development and function. Two-state assays, based on the selective retention and acute, synchronous release of proteins of interest, have the potential to reveal the trafficking dynamics of tagged Rab proteins. However, while the RUSH system exhibits several disadvantages in developing multicellular tissues in *Drosophila* and would need additional improvements, the LAMA system might prove to be a more reliable choice to study the intracellular localization dynamics of single Rab GTPases and initial proof-of-principle experiments conducted by my collaborator Bojana Pavlovic seem promising.

Identifying more of the different, context-dependent functions of Rab GTPases and the trafficking events these mediate, will not only expand our understanding of how they contribute to the development, function, and maintenance of a robust nervous system, but

also if and how their impairment is causally linked to the onset and progression of various neurodegenerative diseases, such as AD or PD. Finally, while I could answer many of the more ‘Rab-centric’ questions, the bigger more ‘neuron-centric’ questions still await clarification. For example, what are the molecular machineries behind neuron-specific membrane trafficking networks? And ultimately, what keeps neurons and their synaptic connections healthy and functional over extensive periods of time? The small Rab GTPases and the intracellular membrane trafficking events these mediate will play a key role answering those queries.

## 8. Summary

One common feature of all eukaryotic cells is the presence of various specialized organelles, separated by membranes, which necessitates a coordinated trafficking of materials between these subcellular membrane-bound compartments. Especially neurons, with their long lifespan, polarized and often complex morphology, as well as their specialized functions, have particular requirements for membrane trafficking. Not surprisingly, membrane trafficking is involved in all aspects of neuronal development, function, and long-term maintenance. The evolutionary conserved family of small Rab GTPases functions as key regulator of coordinated vesicular trafficking in the endomembrane system. Expression profiling efforts revealed that in *Drosophila* half of all Rab GTPases are enriched in or specific to the nervous system, in humans it is one-third. However, the exact functions of the majority of nervous system-enriched Rab proteins are still unknown. Thus, studying the individual roles of those Rab GTPases more closely provides a great opportunity to gain more insight into the membrane trafficking networks in neurons. Ultimately, this will surely contribute to the understanding of what keeps neurons and in particular synapses healthy and functional over extended periods of time. In the nervous system, Rab GTPases and the membrane trafficking events these mediate have been widely associated with many neurodegenerative diseases. However, the established relations are often more correlatively than causatively linked, as discussed in Manuscript 1.

Regarding the importance of an intact intracellular trafficking machinery for the development as well as neuronal function and maintenance, I primarily focused on the systematic functional analysis of nervous system-enriched Rab GTPases in *Drosophila* during my doctoral work. Previously, no systematic *rab* mutant characterization in any multicellular organism had been performed. The analysis, presented in Manuscript 2, revealed that the homozygous mutants of all nervous system-enriched Rab GTPases, raised under laboratory conditions, are viable and fertile, whereas, null mutants of ubiquitously expressed Rabs are all lethal under homozygosity. Thus, suggesting that Rab proteins, with high expression in the nervous system, serve more modulatory, specialized functions which are not essential for the survival of the organism. Further, we could show that all viable *rab* mutants differentially affect the development or neuronal function under variable, more challenging environmental conditions, such as temperature and light. This highlights the evolved robustness of developmental processes and nervous system function towards varying conditions. Additionally, during the in-depth functional analysis of nervous system-

enriched Rab26, we revealed a stimulus-dependent role in the trafficking of the single acetylcholine receptor subunit  $D\alpha 4$  at cholinergic synapses of outer photoreceptors. However, we could not verify a role for Rab26 in the autophagic turnover of synaptic vesicles in neurons.

Additional assays, such as the RUSH system, can be useful to support functional analyses. While this acute, synchronous release system could be established for Rabs in developing photoreceptors and salivary glands, wing imaginal discs proved to be more sensitive and no working conditions could be established. Using the RUSH assay, different release dynamics with ‘fast’ as well as ‘slow’ releasing Rab GTPases could be identified as shown in Manuscript 3. Further, two nervous system-enriched Rab proteins, namely Rab23 and Rab26, show a clear re-localization from the cell body to the axon terminals, which is in agreement with their predominant synaptic neuropil localization revealed by expression profiling.

In conclusion, the findings made during my doctoral work will contribute to a better understanding of the functional requirements of neurons regarding Rab-mediated membrane trafficking. The complete *rab* null mutant collection as well as the RUSH and LAMA transgenic toolbox provide a strong basis for further investigations of individual Rab functions during development and homeostasis.

## 9. Zusammenfassung

Ein gemeinsames Merkmal von allen eukaryotischen Zellen ist das Vorhandensein von verschiedenen spezialisierten Organellen, welche durch Membranen voneinander getrennt sind. Daher müssen die Zellen den koordinierten Transport von Materialien zwischen diesen subzellulären membrangebundenen Kompartimenten sicherstellen. Besonders die langlebigen Nervenzellen, mit ihrer polarisierten und oftmals komplexen Morphologie, sowie spezialisierten Funktionen, stellen besondere Anforderungen an den Membrantransport. Es ist nicht weiter überraschend, dass der Membrantransport in allen Aspekten der neuronalen Entwicklung, Funktion und langfristigen Erhaltung involviert ist. Die evolutionär konservierte Familie von kleinen Rab GTPasen fungiert als zentraler Regulator des koordinierten Vesikeltransports im Endomembransystem. Expressionsanalysen zeigen, dass in *Drosophila* die Hälfte aller Rab GTPasen im Nervensystem angereichert oder spezifisch vorhanden ist, wohingegen es im Menschen ein Drittel sind. Jedoch sind die genauen Funktionen für die Mehrzahl der im Nervensystem angereicherten Rab Proteine noch unbekannt. Daher bietet die genauere Untersuchung der individuellen Rollen dieser Rab GTPasen die großartige Möglichkeit einen besseren Einblick in die Netzwerke des Membrantransports innerhalb von Neuronen zu erhalten. Letztendlich wird dies sicherlich zum Verständnis beitragen, was Nervenzellen und insbesondere deren Synapsen gesund und funktionell über längere Zeit hält. Rab GTPasen und die von ihnen im Nervensystem regulierten Membrantransportwege wurden schon oftmals mit verschiedenen neurodegenerativen Erkrankungen in Verbindung gebracht. Allerdings stehen diese gefundenen Verbindungen oftmals eher korrelativ als kausativ miteinander im Zusammenhang, wie in Manuskript 1 näher erläutert.

Hinsichtlich der Bedeutung einer intakten Membrantransportmaschinerie für die Entwicklung als auch für die Funktion und den Erhalt von Nervenzellen, habe ich mich während meiner Doktorarbeit hauptsächlich auf die systematische funktionelle Analyse von Rab GTPasen fokussiert, die im Nervensystem von *Drosophila* angereichert sind. Bislang ist keine systematische Charakterisierung von *rab* Mutanten, in multizellulären Organismen, durchgeführt worden. Die Analyse, wie dargestellt in Manuskript 2, ergab, dass die homozygoten Mutanten, der im Nervensystem angereicherten Rab GTPasen, lebensfähig und fruchtbar sind, wenn diese unter Laborbedingungen aufwachsen. Wohingegen die Nullmutanten von ubiquitär exprimierten Rab GTPasen homozygot letal sind. Folglich liegt

es nahe, dass Rab Proteine, mit einer hohen Expression im Nervensystem, vermehrt modulatorische, spezialisierte Funktionen ausüben, welche nicht essentiell für das Überleben des Organismus sind. Weiter konnten wir zeigen, dass alle lebensfähigen *rab* Mutanten die Entwicklung oder neuronale Funktion bei variablen, schwierigen Umweltbedingungen, wie zum Beispiel Temperatur und Licht, unterschiedlich beeinflussen. Dies unterstreicht die evolutionär entstandene Robustheit des Nervensystems, im Hinblick auf dessen Entwicklung und Funktion, gegenüber veränderlichen Bedingungen. Zusätzlich identifizierten wir während der eingehenden Funktionsanalyse des im Nervensystem angereicherten Rab26, bei diesem eine stimulusabhängige Rolle im Transport der Acetylcholinrezeptor-Untereinheit  $\text{D}\alpha 4$  in cholinergen Synapsen der äußeren Photorezeptoren. Jedoch konnte eine Rolle für Rab26 in der autophagischen Degradation synaptischer Vesikel in Neuronen nicht verifiziert werden.

Zusätzliche Assays, wie etwa das RUSH System, sind nützlich, um Funktionsanalysen weiter zu untermauern. Während dieses auf einer akuten und synchronen Proteinfreisetzung basierende System, für Rabs in sich entwickelnden Photorezeptoren und Speicheldrüsen etabliert werden konnte, stellten sich die Imaginalscheiben der Flügel als weitaus empfindlicher heraus und es konnten keine funktionierenden Versuchsbedingungen ermittelt werden. Mittels des RUSH Assays konnten verschiedene Freisetzungsdynamiken mit ‘schnell’ sowie ‘langsam’ freigesetzten Rab GTPasen identifiziert werden, wie wir in Manuskript 3 aufzeigen. Weiterhin weisen zwei im Nervensystem angereicherte Rab Proteine, namentlich Rab23 und Rab26, eine deutliche Re-lokalisierung vom Zellkörper zu den präsynaptischen Endigungen auf. Dies stimmt mit ihrer überwiegenden Lokalisierung im synaptischen Neuropil überein, was mittels Expressionsanalysen gezeigt wurde.

Abschließend möchte ich feststellen, dass die während meiner Doktorarbeit erzielten Ergebnisse zu einem besseren Verständnis der funktionellen Ansprüche von Neuronen bezüglich des von Rab Proteinen vermittelten Membrantransports beitragen werden. Die komplette Kollektion an *rab* Nullmutanten sowie die transgenen RUSH und LAMA Toolboxen bilden eine solide Basis für weitere Untersuchungen von individuellen Rab Funktionen während der Entwicklung und Homöostase.

## 10. References

- Ang, A.L., Taguchi, T., Francis, S., Folsch, H., Murrells, L.J., Pypaert, M., Warren, G., and Mellman, I. (2004). Recycling endosomes can serve as intermediates during transport from the Golgi to the plasma membrane of MDCK cells. *J Cell Biol* 167, 531-543.
- Apitz, H., and Salecker, I. (2014). A challenge of numbers and diversity: neurogenesis in the *Drosophila* optic lobe. *J Neurogenet* 28, 233-249.
- Arimura, N., Kimura, T., Nakamuta, S., Taya, S., Funahashi, Y., Hattori, A., Shimada, A., Menager, C., Kawabata, S., Fujii, K., *et al.* (2009). Anterograde transport of TrkB in axons is mediated by direct interaction with Slp1 and Rab27. *Dev Cell* 16, 675-686.
- Bains, M., Zaegel, V., Mize-Berge, J., and Heidenreich, K.A. (2011). IGF-I stimulates Rab7-RILP interaction during neuronal autophagy. *Neurosci Lett* 488, 112-117.
- Barr, F., and Lambright, D.G. (2010). Rab GEFs and GAPs. *Curr Opin Cell Biol* 22, 461-470.
- Barr, F.A. (2013). Review series: Rab GTPases and membrane identity: causal or inconsequential? *J Cell Biol* 202, 191-199.
- Behnia, R., and Munro, S. (2005). Organelle identity and the signposts for membrane traffic. *Nature* 438, 597-604.
- Belusic, G. (2011). ERG in *Drosophila*. In *Electroretinograms*, D.G. Belusic, ed. (InTech).
- Bentley, M., and Banker, G. (2016). The cellular mechanisms that maintain neuronal polarity. *Nat Rev Neurosci* 17, 611-622.
- Best, B.T., and Leptin, M. (2020). Multiple Requirements for Rab GTPases in the Development of *Drosophila* Tracheal Dorsal Branches and Terminal Cells. *G3 (Bethesda)* 10, 1099-1112.
- Bezprozvanny, I., and Hiesinger, P.R. (2013). The synaptic maintenance problem: membrane recycling, Ca<sup>2+</sup> homeostasis and late onset degeneration. *Mol Neurodegener* 8, 23.
- Binotti, B., Jahn, R., and Chua, J.J. (2016). Functions of Rab Proteins at Presynaptic Sites. *Cells* 5.
- Binotti, B., Pavlos, N.J., Riedel, D., Wenzel, D., Vorbruggen, G., Schalk, A.M., Kuhnel, K., Boyken, J., Erck, C., Martens, H., *et al.* (2015). The GTPase Rab26 links synaptic vesicles to the autophagy pathway. *Elife* 4, e05597.
- Boncompain, G., Divoux, S., Gareil, N., de Forges, H., Lescure, A., Latreche, L., Mercanti, V., Jollivet, F., Raposo, G., and Perez, F. (2012). Synchronization of secretory protein traffic in populations of cells. *Nat Methods* 9, 493-498.
- Boncompain, G., and Perez, F. (2013). The many routes of Golgi-dependent trafficking. *Histochem Cell Biol* 140, 251-260.
- Bonifacino, J.S., and Glick, B.S. (2004). The mechanisms of vesicle budding and fusion. *Cell* 116, 153-166.
- Brighthouse, A., Dacks, J.B., and Field, M.C. (2010). Rab protein evolution and the history of the eukaryotic endomembrane system. *Cell Mol Life Sci* 67, 3449-3465.
- Brown, T.C., Correia, S.S., Petrok, C.N., and Esteban, J.A. (2007). Functional compartmentalization of endosomal trafficking for the synaptic delivery of AMPA receptors during long-term potentiation. *J Neurosci* 27, 13311-13315.
- Cai, H., Reinisch, K., and Ferro-Novick, S. (2007). Coats, tethers, Rabs, and SNAREs work together to mediate the intracellular destination of a transport vesicle. *Dev Cell* 12, 671-682.
- Chan, C.C., Scoggin, S., Wang, D., Cherry, S., Dembo, T., Greenberg, B., Jin, E.J., Kuey, C., Lopez, A., Mehta, S.Q., *et al.* (2011). Systematic discovery of Rab GTPases with synaptic functions in *Drosophila*. *Curr Biol* 21, 1704-1715.
- Chen, S., Gendelman, H.K., Roche, J.P., Alsharif, P., and Graf, E.R. (2015). Mutational Analysis of Rab3 Function for Controlling Active Zone Protein Composition at the *Drosophila* Neuromuscular Junction. *PLoS One* 10, e0136938.
- Cheng, P.L., and Poo, M.M. (2012). Early events in axon/dendrite polarization. *Annu Rev Neurosci* 35, 181-201.
- Cherry, S., Jin, E.J., Ozel, M.N., Lu, Z., Agi, E., Wang, D., Jung, W.H., Epstein, D., Meinertzhagen, I.A., Chan, C.C., *et al.* (2013). Charcot-Marie-Tooth 2B mutations in rab7 cause dosage-dependent neurodegeneration due to partial loss of function. *Elife* 2, e01064.

Cheung, D., and Ma, J. (2015). Probing the impact of temperature on molecular events in a developmental system. *Sci Rep* 5, 13124.

Chinchore, Y., Mitra, A., and Dolph, P.J. (2009). Accumulation of rhodopsin in late endosomes triggers photoreceptor cell degeneration. *PLoS Genet* 5, e1000377.

Chou, V.T., Johnson, S.A., and Van Vactor, D. (2020). Synapse development and maturation at the drosophila neuromuscular junction. *Neural Dev* 15, 11.

Colley, N.J. (2012). Retinal degeneration in the fly. *Adv Exp Med Biol* 723, 407-414.

D'Adamo, P., Masetti, M., Bianchi, V., More, L., Mignogna, M.L., Giannandrea, M., and Gatti, S. (2014). RAB GTPases and RAB-interacting proteins and their role in the control of cognitive functions. *Neurosci Biobehav Rev* 46 Pt 2, 302-314.

Dacks, J.B., and Field, M.C. (2007). Evolution of the eukaryotic membrane-trafficking system: origin, tempo and mode. *J Cell Sci* 120, 2977-2985.

Dau, A., Friederich, U., Dongre, S., Li, X., Bollepalli, M.K., Hardie, R.C., and Juusola, M. (2016). Evidence for Dynamic Network Regulation of Drosophila Photoreceptor Function from Mutants Lacking the Neurotransmitter Histamine. *Front Neural Circuits* 10, 19.

Davis, F.P., Nern, A., Picard, S., Reiser, M.B., Rubin, G.M., Eddy, S.R., and Henry, G.L. (2020). A genetic, genomic, and computational resource for exploring neural circuit function. *Elife* 9.

de Wit, H., Lichtenstein, Y., Kelly, R.B., Geuze, H.J., Klumperman, J., and van der Sluijs, P. (2001). Rab4 regulates formation of synaptic-like microvesicles from early endosomes in PC12 cells. *Mol Biol Cell* 12, 3703-3715.

Deinhardt, K., Salinas, S., Verastegui, C., Watson, R., Worth, D., Hanrahan, S., Bucci, C., and Schiavo, G. (2006). Rab5 and Rab7 control endocytic sorting along the axonal retrograde transport pathway. *Neuron* 52, 293-305.

Diao, A., Rahman, D., Pappin, D.J., Lucocq, J., and Lowe, M. (2003). The coiled-coil membrane protein golgin-84 is a novel rab effector required for Golgi ribbon formation. *J Cell Biol* 160, 201-212.

Diekmann, Y., Seixas, E., Gouw, M., Tavares-Cadete, F., Seabra, M.C., and Pereira-Leal, J.B. (2011). Thousands of rab GTPases for the cell biologist. *PLoS Comput Biol* 7, e1002217.

Dillon, M.E., Wang, G., Garrity, P.A., and Huey, R.B. (2009). Review: Thermal preference in Drosophila. *J Therm Biol* 34, 109-119.

Dong, W., He, B., Qian, H., Liu, Q., Wang, D., Li, J., Wei, Z., Wang, Z., Xu, Z., Wu, G., *et al.* (2018). RAB26-dependent autophagy protects adherens junctional integrity in acute lung injury. *Autophagy* 14, 1677-1692.

Dulubova, I., Lou, X., Lu, J., Huryeva, I., Alam, A., Schneggenburger, R., Sudhof, T.C., and Rizo, J. (2005). A Munc13/RIM/Rab3 tripartite complex: from priming to plasticity? *EMBO J* 24, 2839-2850.

Dunst, S., Kazimiers, T., von Zadow, F., Jambor, H., Sagner, A., Brankatschk, B., Mahmoud, A., Spann, S., Tomancak, P., Eaton, S., *et al.* (2015). Endogenously tagged rab proteins: a resource to study membrane trafficking in Drosophila. *Dev Cell* 33, 351-365.

Economos, A.C., and Lints, F.A. (1986). Developmental temperature and life span in Drosophila melanogaster. I. Constant developmental temperature: evidence for physiological adaptation in a wide temperature range. *Gerontology* 32, 18-27.

Elias, M., Brighouse, A., Gabernet-Castello, C., Field, M.C., and Dacks, J.B. (2012). Sculpting the endomembrane system in deep time: high resolution phylogenetics of Rab GTPases. *J Cell Sci* 125, 2500-2508.

Eva, R., Dassie, E., Caswell, P.T., Dick, G., French-Constant, C., Norman, J.C., and Fawcett, J.W. (2010). Rab11 and its effector Rab coupling protein contribute to the trafficking of beta 1 integrins during axon growth in adult dorsal root ganglion neurons and PC12 cells. *J Neurosci* 30, 11654-11669.

Farrants, H., Tarnawski, M., Muller, T.G., Otsuka, S., Hiblot, J., Koch, B., Kueblbeck, M., Krausslich, H.G., Ellenberg, J., and Johnsson, K. (2020). Chemogenetic Control of Nanobodies. *Nat Methods* 17, 279-282.

Fernandes, A.C., Uytterhoeven, V., Kuenen, S., Wang, Y.C., Slabbaert, J.R., Swerts, J., Kasprovicz, J., Aerts, S., and Verstreken, P. (2014). Reduced synaptic vesicle protein degradation at lysosomes curbs TBC1D24/sky-induced neurodegeneration. *J Cell Biol* 207, 453-462.

Fischbach, K.F., and Dittrich, A.P.M. (1989). The optic lobe of *Drosophila melanogaster*. I. A Golgi analysis of wild-type structure. *Cell and Tissue Research* 258, 441-475.

Fischer von Mollard, G., Sudhof, T.C., and Jahn, R. (1991). A small GTP-binding protein dissociates from synaptic vesicles during exocytosis. *Nature* 349, 79-81.

Futerman, A.H., and Banker, G.A. (1996). The economics of neurite outgrowth--the addition of new membrane to growing axons. *Trends Neurosci* 19, 144-149.

Gallwitz, D., Donath, C., and Sander, C. (1983). A yeast gene encoding a protein homologous to the human c-has/bas proto-oncogene product. *Nature* 306, 704-707.

Gerges, N.Z., Backos, D.S., and Esteban, J.A. (2004). Local control of AMPA receptor trafficking at the postsynaptic terminal by a small GTPase of the Rab family. *J Biol Chem* 279, 43870-43878.

Gillingham, A.K., Sinka, R., Torres, I.L., Lilley, K.S., and Munro, S. (2014). Toward a comprehensive map of the effectors of rab GTPases. *Dev Cell* 31, 358-373.

Gillooly, J.F., Charnov, E.L., West, G.B., Savage, V.M., and Brown, J.H. (2002). Effects of size and temperature on developmental time. *Nature* 417, 70-73.

Gotz, T.W.B., Puchkov, D., Lysiuk, V., Lutzkendorf, J., Nikonenko, A.G., Quentin, C., Lehmann, M., Sigrist, S.J., and Petzoldt, A.G. (2021). Rab2 regulates presynaptic precursor vesicle biogenesis at the trans-Golgi. *J Cell Biol* 220.

Goud, B., Liu, S., and Storrie, B. (2018). Rab proteins as major determinants of the Golgi complex structure. *Small GTPases* 9, 66-75.

Graf, E.R., Daniels, R.W., Burgess, R.W., Schwarz, T.L., and DiAntonio, A. (2009). Rab3 dynamically controls protein composition at active zones. *Neuron* 64, 663-677.

Grosshans, B.L., Ortiz, D., and Novick, P. (2006). Rabs and their effectors: achieving specificity in membrane traffic. *Proc Natl Acad Sci U S A* 103, 11821-11827.

Guadagno, N.A., and Progidia, C. (2019). Rab GTPases: Switching to Human Diseases. *Cells* 8.

Guerra, F., and Bucci, C. (2016). Multiple Roles of the Small GTPase Rab7. *Cells* 5.

Gurkan, C., Lapp, H., Alory, C., Su, A.I., Hogenesch, J.B., and Balch, W.E. (2005). Large-scale profiling of Rab GTPase trafficking networks: the membrome. *Mol Biol Cell* 16, 3847-3864.

Haberman, A., Williamson, W.R., Epstein, D., Wang, D., Rina, S., Meinertzhagen, I.A., and Hiesinger, P.R. (2012). The synaptic vesicle SNARE neuronal Synaptobrevin promotes endolysosomal degradation and prevents neurodegeneration. *J Cell Biol* 196, 261-276.

Hamada, F.N., Rosenzweig, M., Kang, K., Pulver, S.R., Ghezzi, A., Jegla, T.J., and Garrity, P.A. (2008). An internal thermal sensor controlling temperature preference in *Drosophila*. *Nature* 454, 217-220.

Hanus, C., and Ehlers, M.D. (2008). Secretory outposts for the local processing of membrane cargo in neuronal dendrites. *Traffic* 9, 1437-1445.

Hara, T., Nakamura, K., Matsui, M., Yamamoto, A., Nakahara, Y., Suzuki-Migishima, R., Yokoyama, M., Mishima, K., Saito, I., Okano, H., *et al.* (2006). Suppression of basal autophagy in neural cells causes neurodegenerative disease in mice. *Nature* 441, 885-889.

Hardie, R.C. (2012). Phototransduction mechanisms in *Drosophila* microvillar photoreceptors. *Wiley Interdisciplinary Reviews: Membrane Transport and Signaling* 1, 162-187.

Harris, K.P., and Littleton, J.T. (2011). Vesicle trafficking: a Rab family profile. *Curr Biol* 21, R841-843.

Henstridge, C.M., Tzioras, M., and Paolicelli, R.C. (2019). Glial Contribution to Excitatory and Inhibitory Synapse Loss in Neurodegeneration. *Front Cell Neurosci* 13, 63.

Hiesinger, P.R. (2021). Brain wiring with composite instructions. *Bioessays* 43, e2000166.

Hiesinger, P.R., and Hassan, B.A. (2018). The Evolution of Variability and Robustness in Neural Development. *Trends Neurosci* 41, 577-586.

Homma, Y., and Fukuda, M. (2016). Rabin8 regulates neurite outgrowth in both GEF activity-dependent and -independent manners. *Mol Biol Cell* 27, 2107-2118.

Homma, Y., Kinoshita, R., Kuchitsu, Y., Wawro, P.S., Marubashi, S., Oguchi, M.E., Ishida, M., Fujita, N., and Fukuda, M. (2019). Comprehensive knockout analysis of the Rab family GTPases in epithelial cells. *J Cell Biol* 218, 2035-2050.

Huber, L.A., Dupree, P., and Dotti, C.G. (1995). A deficiency of the small GTPase rab8 inhibits membrane traffic in developing neurons. *Mol Cell Biol* 15, 918-924.

Huber, L.A., Pimplikar, S., Parton, R.G., Virta, H., Zerial, M., and Simons, K. (1993). Rab8, a small GTPase involved in vesicular traffic between the TGN and the basolateral plasma membrane. *J Cell Biol* *123*, 35-45.

Hutagalung, A.H., and Novick, P.J. (2011). Role of Rab GTPases in membrane traffic and cell physiology. *Physiol Rev* *91*, 119-149.

Iwanami, N., Nakamura, Y., Satoh, T., Liu, Z., and Satoh, A.K. (2016). Rab6 Is Required for Multiple Apical Transport Pathways but Not the Basolateral Transport Pathway in Drosophila Photoreceptors. *PLoS Genet* *12*, e1005828.

Jackson, G.R. (2008). Guide to understanding Drosophila models of neurodegenerative diseases. *PLoS Biol* *6*, e53.

Jain, N., and Ganesh, S. (2016). Emerging nexus between RAB GTPases, autophagy and neurodegeneration. *Autophagy* *12*, 900-904.

Jaiswal, M., Haelterman, N.A., Sandoval, H., Xiong, B., Donti, T., Kalsotra, A., Yamamoto, S., Cooper, T.A., Graham, B.H., and Bellen, H.J. (2015). Impaired Mitochondrial Energy Production Causes Light-Induced Photoreceptor Degeneration Independent of Oxidative Stress. *PLoS Biol* *13*, e1002197.

Jaiswal, M., Sandoval, H., Zhang, K., Bayat, V., and Bellen, H.J. (2012). Probing mechanisms that underlie human neurodegenerative diseases in Drosophila. *Annu Rev Genet* *46*, 371-396.

Jean, S., and Kiger, A.A. (2012). Coordination between RAB GTPase and phosphoinositide regulation and functions. *Nat Rev Mol Cell Biol* *13*, 463-470.

Jennings, B.H. (2011). Drosophila – a versatile model in biology & medicine. *Materials Today* *14*, 190-195.

Jin, E.J., Chan, C.C., Agi, E., Cherry, S., Hanacik, E., Buszczak, M., and Hiesinger, P.R. (2012). Similarities of Drosophila rab GTPases based on expression profiling: completion and analysis of the rab-Gal4 kit. *PLoS One* *7*, e40912.

Jin, E.J., Kiral, F.R., and Hiesinger, P.R. (2018a). The where, what, and when of membrane protein degradation in neurons. *Dev Neurobiol* *78*, 283-297.

Jin, E.J., Kiral, F.R., Ozel, M.N., Burchardt, L.S., Osterland, M., Epstein, D., Wolfenberger, H., Prohaska, S., and Hiesinger, P.R. (2018b). Live Observation of Two Parallel Membrane Degradation Pathways at Axon Terminals. *Curr Biol* *28*, 1027-1038 e1024.

Katz, B., and Minke, B. (2009). Drosophila photoreceptors and signaling mechanisms. *Front Cell Neurosci* *3*, 2.

Kiral, F.R., Dutta, S.B., Linneweber, G.A., Poppa, C., von Kleist, M., Hassan, B.A., and Hiesinger, P.R. (2021). Variable brain wiring through scalable and relative synapse formation in *Drosophila*. [bioRxiv, 2021.2005.2012.443860](https://doi.org/10.1101/2021.05.2012.443860).

Kiral, F.R., Kohrs, F.E., Jin, E.J., and Hiesinger, P.R. (2018). Rab GTPases and Membrane Trafficking in Neurodegeneration. *Curr Biol* *28*, R471-R486.

Kiral, F.R., Linneweber, G.A., Mathejczyk, T., Georgiev, S.V., Wernet, M.F., Hassan, B.A., von Kleist, M., and Hiesinger, P.R. (2020). Autophagy-dependent filopodial kinetics restrict synaptic partner choice during Drosophila brain wiring. *Nat Commun* *11*, 1325.

Kjos, I., Vestre, K., Guadagno, N.A., Borg Distefano, M., and Progidia, C. (2018). Rab and Arf proteins at the crossroad between membrane transport and cytoskeleton dynamics. *Biochim Biophys Acta Mol Cell Res* *1865*, 1397-1409.

Klopper, T.H., Kienle, N., Fasshauer, D., and Munro, S. (2012). Untangling the evolution of Rab G proteins: implications of a comprehensive genomic analysis. *BMC Biol* *10*, 71.

Kohrs, F.E., Daumann, I.M., Pavlovic, B., Jin, E.J., Kiral, F.R., Lin, S.C., Port, F., Wolfenberger, H., Mathejczyk, T.F., Linneweber, G.A., *et al.* (2021). Systematic functional analysis of rab GTPases reveals limits of neuronal robustness to environmental challenges in flies. *Elife* *10*.

Kolodziejczyk, A., Sun, X., Meinertzhagen, I.A., and Nassel, D.R. (2008). Glutamate, GABA and acetylcholine signaling components in the lamina of the Drosophila visual system. *PLoS One* *3*, e2110.

Komatsu, M., Waguri, S., Chiba, T., Murata, S., Iwata, J., Tanida, I., Ueno, T., Koike, M., Uchiyama, Y., Kominami, E., *et al.* (2006). Loss of autophagy in the central nervous system causes neurodegeneration in mice. *Nature* *441*, 880-884.

Kramer, R., Rode, S., and Rumpf, S. (2019). Rab11 is required for neurite pruning and developmental membrane protein degradation in *Drosophila* sensory neurons. *Dev Biol* 451, 68-78.

Kumar, J.P. (2012). Building an ommatidium one cell at a time. *Dev Dyn* 241, 136-149.

Kuwahara, T., and Iwatsubo, T. (2020). The Emerging Functions of LRRK2 and Rab GTPases in the Endolysosomal System. *Front Neurosci* 14, 227.

Langemeyer, L., Nunes Bastos, R., Cai, Y., Itzen, A., Reinisch, K.M., and Barr, F.A. (2014). Diversity and plasticity in Rab GTPase nucleotide release mechanism has consequences for Rab activation and inactivation. *Elife* 3, e01623.

Lasiecka, Z.M., and Winckler, B. (2011). Mechanisms of polarized membrane trafficking in neurons -- focusing in on endosomes. *Mol Cell Neurosci* 48, 278-287.

Lee, S.J., and Montell, C. (2004). Suppression of constant-light-induced blindness but not retinal degeneration by inhibition of the rhodopsin degradation pathway. *Curr Biol* 14, 2076-2085.

Lien, W.Y., Chen, Y.T., Li, Y.J., Wu, J.K., Huang, K.L., Lin, J.R., Lin, S.C., Hou, C.C., Wang, H.D., Wu, C.L., *et al.* (2020). Lifespan regulation in alpha/beta posterior neurons of the fly mushroom bodies by Rab27. *Aging Cell* 19, e13179.

Lisse, D., Monzel, C., Vicario, C., Manzi, J., Maurin, I., Coppey, M., Piehler, J., and Dahan, M. (2017). Engineered Ferritin for Magnetogenetic Manipulation of Proteins and Organelles Inside Living Cells. *Adv Mater* 29.

Lu, Q., Wang, P.S., and Yang, L. (2021). Golgi-associated Rab GTPases implicated in autophagy. *Cell Biosci* 11, 35.

Luningschror, P., Binotti, B., Dombert, B., Heimann, P., Perez-Lara, A., Slotta, C., Thau-Habermann, N., C, R.v.C., Karl, F., Damme, M., *et al.* (2017). Plekhhg5-regulated autophagy of synaptic vesicles reveals a pathogenic mechanism in motoneuron disease. *Nat Commun* 8, 678.

Luthy, K., Ahrens, B., Rawal, S., Lu, Z., Tarnogorska, D., Meinertzhagen, I.A., and Fischbach, K.F. (2014). The irre cell recognition module (IRM) protein Kirre is required to form the reciprocal synaptic network of L4 neurons in the *Drosophila* lamina. *J Neurogenet* 28, 291-301.

Luzio, J.P., Pryor, P.R., and Bright, N.A. (2007). Lysosomes: fusion and function. *Nat Rev Mol Cell Biol* 8, 622-632.

Maday, S., and Holzbaur, E.L. (2014). Autophagosome biogenesis in primary neurons follows an ordered and spatially regulated pathway. *Dev Cell* 30, 71-85.

Maday, S., Wallace, K.E., and Holzbaur, E.L. (2012). Autophagosomes initiate distally and mature during transport toward the cell soma in primary neurons. *J Cell Biol* 196, 407-417.

McLauchlan, H., Newell, J., Morrice, N., Osborne, A., West, M., and Smythe, E. (1998). A novel role for Rab5-GDI in ligand sequestration into clathrin-coated pits. *Curr Biol* 8, 34-45.

Meinertzhagen, I.A., and O'Neil, S.D. (1991). Synaptic organization of columnar elements in the lamina of the wild type in *Drosophila melanogaster*. *J Comp Neurol* 305, 232-263.

Mignogna, M.L., and D'Adamo, P. (2018). Critical importance of RAB proteins for synaptic function. *Small GTPases* 9, 145-157.

Mignogna, M.L., Giannandrea, M., Gurgone, A., Fanelli, F., Raimondi, F., Mapelli, L., Bassani, S., Fang, H., Van Anken, E., Alessio, M., *et al.* (2015). The intellectual disability protein RAB39B selectively regulates GluA2 trafficking to determine synaptic AMPAR composition. *Nat Commun* 6, 6504.

Milligan, S.C., Alb, J.G., Jr., Elagina, R.B., Bankaitis, V.A., and Hyde, D.R. (1997). The phosphatidylinositol transfer protein domain of *Drosophila* retinal degeneration B protein is essential for photoreceptor cell survival and recovery from light stimulation. *J Cell Biol* 139, 351-363.

Mizushima, N. (2007). Autophagy: process and function. *Genes Dev* 21, 2861-2873.

Montell, C. (2012). *Drosophila* visual transduction. *Trends Neurosci* 35, 356-363.

Morante, J., and Desplan, C. (2008). The color-vision circuit in the medulla of *Drosophila*. *Curr Biol* 18, 553-565.

Mori, Y., Fukuda, M., and Henley, J.M. (2014). Small GTPase Rab17 regulates the surface expression of kainate receptors but not alpha-amino-3-hydroxy-5-methyl-4-isoxazolepropionic acid (AMPA) receptors in hippocampal neurons via dendritic trafficking of Syntaxin-4 protein. *J Biol Chem* 289, 20773-20787.

Moti, N., Yu, J., Boncompain, G., Perez, F., and Virshup, D.M. (2019). Wnt traffic from endoplasmic reticulum to filopodia. *PLoS One* 14, e0212711.

Muller, M.P., and Goody, R.S. (2018). Molecular control of Rab activity by GEFs, GAPs and GDI. *Small GTPases* 9, 5-21.

Muschalik, N., and Munro, S. (2018). Golgins. *Curr Biol* 28, R374-R376.

Nakazawa, H., Sada, T., Toriyama, M., Tago, K., Sugiura, T., Fukuda, M., and Inagaki, N. (2012). Rab33a mediates anterograde vesicular transport for membrane exocytosis and axon outgrowth. *J Neurosci* 32, 12712-12725.

Neriec, N., and Desplan, C. (2016). From the Eye to the Brain: Development of the Drosophila Visual System. *Curr Top Dev Biol* 116, 247-271.

Ng, E.L., and Tang, B.L. (2008). Rab GTPases and their roles in brain neurons and glia. *Brain Res Rev* 58, 236-246.

Niu, L.L., Ma, T.J., Yang, F., Yan, B., Tang, X., Yin, H.D., Wu, Q., Huang, Y., Yao, Z.P., Wang, J.F., *et al.* (2019). Atlastin-mediated membrane tethering is critical for cargo mobility and exit from the endoplasmic reticulum. *P Natl Acad Sci USA* 116, 14029-14038.

Niu, M., Zheng, N., Wang, Z., Gao, Y., Luo, X., Chen, Z., Fu, X., Wang, Y., Wang, T., Liu, M., *et al.* (2020). RAB39B Deficiency Impairs Learning and Memory Partially Through Compromising Autophagy. *Front Cell Dev Biol* 8, 598622.

Noell, W.K., Walker, V.S., Kang, B.S., and Berman, S. (1966). Retinal damage by light in rats. *Invest Ophthalmol* 5, 450-473.

Nottingham, R.M., and Pfeffer, S.R. (2014). Mutant enzymes challenge all assumptions. *Elife* 3, e02171.

Oberegelsbacher, C., Schneider, C., Voolstra, O., Cerny, A., and Huber, A. (2011). The Drosophila TRPL ion channel shares a Rab-dependent translocation pathway with rhodopsin. *Eur J Cell Biol* 90, 620-630.

Pacheco-Fernandez, N., Pakdel, M., Blank, B., Sanchez-Gonzalez, I., Weber, K., Tran, M.L., Hecht, T.K., Gautsch, R., Beck, G., Perez, F., *et al.* (2020). Nucleobindin-1 regulates ECM degradation by promoting intra-Golgi trafficking of MMPs. *J Cell Biol* 219.

Parker, S.S., Cox, C., and Wilson, J.M. (2018). Rabs set the stage for polarity. *Small GTPases* 9, 116-129.

Pavlos, N.J., Gronborg, M., Riedel, D., Chua, J.J., Boyken, J., Kloepper, T.H., Urlaub, H., Rizzoli, S.O., and Jahn, R. (2010). Quantitative analysis of synaptic vesicle Rabs uncovers distinct yet overlapping roles for Rab3a and Rab27b in Ca<sup>2+</sup>-triggered exocytosis. *J Neurosci* 30, 13441-13453.

Pavlos, N.J., and Jahn, R. (2011). Distinct yet overlapping roles of Rab GTPases on synaptic vesicles. *Small GTPases* 2, 77-81.

Pawar, S., Ungricht, R., Tiefenboeck, P., Leroux, J.C., and Kutay, U. (2017). Efficient protein targeting to the inner nuclear membrane requires Atlastin-dependent maintenance of ER topology. *Elife* 6.

Petkovic, M., Jemaiel, A., Daste, F., Specht, C.G., Izeddin, I., Vorkel, D., Verbavatz, J.M., Darzacq, X., Triller, A., Pfenninger, K.H., *et al.* (2014). The SNARE Sec22b has a non-fusogenic function in plasma membrane expansion. *Nat Cell Biol* 16, 434-444.

Pfeffer, S.R. (1994). Rab GTPases: master regulators of membrane trafficking. *Curr Opin Cell Biol* 6, 522-526.

Pfeffer, S.R. (2001). Rab GTPases: specifying and deciphering organelle identity and function. *Trends Cell Biol* 11, 487-491.

Pfeffer, S.R. (2013). Rab GTPase regulation of membrane identity. *Curr Opin Cell Biol* 25, 414-419.

Pfeffer, S.R. (2017). Rab GTPases: master regulators that establish the secretory and endocytic pathways. *Mol Biol Cell* 28, 712-715.

Piper, R.C., and Katzmann, D.J. (2007). Biogenesis and function of multivesicular bodies. *Annu Rev Cell Dev Biol* 23, 519-547.

Raiborg, C., Wenzel, E.M., Pedersen, N.M., Olsvik, H., Schink, K.O., Schultz, S.W., Vietri, M., Nisi, V., Bucci, C., Brech, A., *et al.* (2015). Repeated ER-endosome contacts promote endosome translocation and neurite outgrowth. *Nature* 520, 234-238.

Rivera-Alba, M., Vitaladevuni, S.N., Mishchenko, Y., Lu, Z., Takemura, S.Y., Scheffer, L., Meinertzhagen, I.A., Chklovskii, D.B., and de Polavieja, G.G. (2011). Wiring economy and volume exclusion determine neuronal placement in the Drosophila brain. *Curr Biol* 21, 2000-2005.

Rojas, A.M., Fuentes, G., Rausell, A., and Valencia, A. (2012). The Ras protein superfamily: evolutionary tree and role of conserved amino acids. *J Cell Biol* 196, 189-201.

Rothman, J.E. (2010). The future of Golgi research. *Mol Biol Cell* 21, 3776-3780.

Sanes, J.R., and Zipursky, S.L. (2010). Design principles of insect and vertebrate visual systems. *Neuron* 66, 15-36.

Saxena, S., Bucci, C., Weis, J., and Kruttgen, A. (2005). The small GTPase Rab7 controls the endosomal trafficking and neuritogenic signaling of the nerve growth factor receptor TrkA. *J Neurosci* 25, 10930-10940.

Schlacht, A., Herman, E.K., Klute, M.J., Field, M.C., and Dacks, J.B. (2014). Missing pieces of an ancient puzzle: evolution of the eukaryotic membrane-trafficking system. *Cold Spring Harb Perspect Biol* 6, a016048.

Schluter, O.M., Khvotchev, M., Jahn, R., and Sudhof, T.C. (2002). Localization versus function of Rab3 proteins. Evidence for a common regulatory role in controlling fusion. *J Biol Chem* 277, 40919-40929.

Schluter, O.M., Schmitz, F., Jahn, R., Rosenmund, C., and Sudhof, T.C. (2004). A complete genetic analysis of neuronal Rab3 function. *J Neurosci* 24, 6629-6637.

Schopf, K., and Huber, A. (2017). Membrane protein trafficking in *Drosophila* photoreceptor cells. *Eur J Cell Biol* 96, 391-401.

Semerdjieva, S., Shortt, B., Maxwell, E., Singh, S., Fonarev, P., Hansen, J., Schiavo, G., Grant, B.D., and Smythe, E. (2008). Coordinated regulation of AP2 uncoating from clathrin-coated vesicles by rab5 and hRME-6. *J Cell Biol* 183, 499-511.

Sender, R., and Milo, R. (2021). The distribution of cellular turnover in the human body. *Nat Med* 27, 45-48.

Shi, M., Yue, Z., Kuryatov, A., Lindstrom, J.M., and Sehgal, A. (2014). Identification of Redeye, a new sleep-regulating protein whose expression is modulated by sleep amount. *Elife* 3, e01473.

Shieh, B.H. (2011). Molecular genetics of retinal degeneration: A *Drosophila* perspective. *Fly* 5, 356-368.

Siadous, F.A., Cantet, F., Van Schaik, E., Burette, M., Allombert, J., Lakhani, A., Bonaventure, B., Goujon, C., Samuel, J., Bonazzi, M., *et al.* (2021). Coxiella effector protein CvpF subverts RAB26-dependent autophagy to promote vacuole biogenesis and virulence. *Autophagy* 17, 706-722.

Siddiqui, W.H., and Barlow, C.A. (1972). Population Growth of *Drosophila melanogaster* (Diptera: Drosophilidae) at Constant and Alternating Temperatures<sup>1</sup>. *Annals of the Entomological Society of America* 65, 993-1001.

Singh, P.K., and Muqit, M.M.K. (2020). Parkinson's: A Disease of Aberrant Vesicle Trafficking. *Annu Rev Cell Dev Biol* 36, 237-264.

Sinka, R., Gillingham, A.K., Kondylis, V., and Munro, S. (2008). Golgi coiled-coil proteins contain multiple binding sites for Rab family G proteins. *J Cell Biol* 183, 607-615.

Spinosa, M.R., Progida, C., De Luca, A., Colucci, A.M., Alifano, P., and Bucci, C. (2008). Functional characterization of Rab7 mutant proteins associated with Charcot-Marie-Tooth type 2B disease. *J Neurosci* 28, 1640-1648.

Stavoe, A.K.H., and Holzbaur, E.L.F. (2019). Autophagy in Neurons. *Annu Rev Cell Dev Biol* 35, 477-500.

Stenmark, H. (2009). Rab GTPases as coordinators of vesicle traffic. *Nat Rev Mol Cell Biol* 10, 513-525.

Sudhof, T.C. (2004). The synaptic vesicle cycle. *Annu Rev Neurosci* 27, 509-547.

Takano, T., Xu, C., Funahashi, Y., Namba, T., and Kaibuchi, K. (2015). Neuronal polarization. *Development* 142, 2088-2093.

Takemura, S.Y., Xu, C.S., Lu, Z., Rivlin, P.K., Parag, T., Olbris, D.J., Plaza, S., Zhao, T., Katz, W.T., Umayam, L., *et al.* (2015). Synaptic circuits and their variations within different columns in the visual system of *Drosophila*. *Proc Natl Acad Sci U S A* 112, 13711-13716.

Tokarev, A.A.A., A, Segev, N (2000-2013). Overview of Intracellular Compartments and Trafficking Pathways.

Touchot, N., Chardin, P., and Tavitian, A. (1987). Four additional members of the ras gene superfamily isolated by an oligonucleotide strategy: molecular cloning of YPT-related cDNAs from a rat brain library. *Proc Natl Acad Sci U S A* 84, 8210-8214.

Tuthill, J.C., Nern, A., Holtz, S.L., Rubin, G.M., and Reiser, M.B. (2013). Contributions of the 12 neuron classes in the fly lamina to motion vision. *Neuron* 79, 128-140.

Udayar, V., Buggia-Prevot, V., Guerreiro, R.L., Siegel, G., Rambabu, N., Soohoo, A.L., Ponnusamy, M., Siegenthaler, B., Bali, J., Aesg, *et al.* (2013). A paired RNAi and RabGAP overexpression screen identifies Rab11 as a regulator of beta-amyloid production. *Cell Rep* 5, 1536-1551.

Ugur, B., Chen, K., and Bellen, H.J. (2016). Drosophila tools and assays for the study of human diseases. *Dis Model Mech* 9, 235-244.

Uytterhoeven, V., Kuenen, S., Kasprowitz, J., Miskiewicz, K., and Verstreken, P. (2011). Loss of skywalker reveals synaptic endosomes as sorting stations for synaptic vesicle proteins. *Cell* 145, 117-132.

Verhoeven, K., De Jonghe, P., Coen, K., Verpoorten, N., Auer-Grumbach, M., Kwon, J.M., FitzPatrick, D., Schmedding, E., De Vriendt, E., Jacobs, A., *et al.* (2003). Mutations in the small GTP-ase late endosomal protein RAB7 cause Charcot-Marie-Tooth type 2B neuropathy. *Am J Hum Genet* 72, 722-727.

Villarroel-Campos, D., Bronfman, F.C., and Gonzalez-Billault, C. (2016). Rab GTPase signaling in neurite outgrowth and axon specification. *Cytoskeleton (Hoboken)* 73, 498-507.

Wang, D., Chan, C.C., Cherry, S., and Hiesinger, P.R. (2013). Membrane trafficking in neuronal maintenance and degeneration. *Cell Mol Life Sci* 70, 2919-2934.

Wang, S., Hu, C., Wu, F., and He, S. (2017). Rab25 GTPase: Functional roles in cancer. *Oncotarget* 8, 64591-64599.

Wang, T., and Montell, C. (2007). Phototransduction and retinal degeneration in Drosophila. *Pflugers Arch* 454, 821-847.

Wernet, M.F., Mazzoni, E.O., Celik, A., Duncan, D.M., Duncan, I., and Desplan, C. (2006). Stochastic spineless expression creates the retinal mosaic for colour vision. *Nature* 440, 174-180.

Williamson, W.R., Wang, D., Haberman, A.S., and Hiesinger, P.R. (2010). A dual function of V0-ATPase a1 provides an endolysosomal degradation mechanism in Drosophila melanogaster photoreceptors. *J Cell Biol* 189, 885-899.

Winkle, C.C., and Gupton, S.L. (2016). Membrane Trafficking in Neuronal Development: Ins and Outs of Neural Connectivity. *Int Rev Cell Mol Biol* 322, 247-280.

Witte, K.E., Slotta, C., Lutkemeyer, M., Kitke, A., Coras, R., Simon, M., Kaltschmidt, C., and Kaltschmidt, B. (2020). PLEKHG5 regulates autophagy, survival and MGMT expression in U251-MG glioblastoma cells. *Sci Rep* 10, 21858.

Wong, Y.C., and Holzbaur, E.L. (2015). Autophagosome dynamics in neurodegeneration at a glance. *J Cell Sci* 128, 1259-1267.

Wu, Q., Sun, X., Yue, W., Lu, T., Ruan, Y., Chen, T., and Zhang, D. (2016). RAB18, a protein associated with Warburg Micro syndrome, controls neuronal migration in the developing cerebral cortex. *Mol Brain* 9, 19.

Wucherpennig, T., Wilsch-Brauninger, M., and Gonzalez-Gaitan, M. (2003). Role of Drosophila Rab5 during endosomal trafficking at the synapse and evoked neurotransmitter release. *J Cell Biol* 161, 609-624.

Xiong, B., Bayat, V., Jaiswal, M., Zhang, K., Sandoval, H., Charnig, W.L., Li, T., David, G., Duraine, L., Lin, Y.Q., *et al.* (2012). Crag is a GEF for Rab11 required for rhodopsin trafficking and maintenance of adult photoreceptor cells. *PLoS Biol* 10, e1001438.

Xiong, B., and Bellen, H.J. (2013). Rhodopsin homeostasis and retinal degeneration: lessons from the fly. *Trends Neurosci* 36, 652-660.

Yamaguchi, S., Desplan, C., and Heisenberg, M. (2010). Contribution of photoreceptor subtypes to spectral wavelength preference in Drosophila. *Proc Natl Acad Sci U S A* 107, 5634-5639.

Ye, B., Zhang, Y., Song, W., Younger, S.H., Jan, L.Y., and Jan, Y.N. (2007). Growing dendrites and axons differ in their reliance on the secretory pathway. *Cell* 130, 717-729.

Zerial, M., and McBride, H. (2001). Rab proteins as membrane organizers. *Nat Rev Mol Cell Biol* 2, 107-117.

Zhang, J., Schulze, K.L., Hiesinger, P.R., Suyama, K., Wang, S., Fish, M., Acar, M., Hoskins, R.A., Bellen, H.J., and Scott, M.P. (2007). Thirty-one flavors of Drosophila rab proteins. *Genetics* 176, 1307-1322.

- Zhen, Y., and Stenmark, H. (2015). Cellular functions of Rab GTPases at a glance. *J Cell Sci* 128, 3171-3176.
- Zhu, Y. (2013). The *Drosophila* visual system: From neural circuits to behavior. *Cell Adh Migr* 7, 333-344.

## **11. Declaration of independence**

I declare that I have authored this thesis independently and that all experiments within this thesis were conducted by myself or that contributors have been acknowledged by name, and that all references used have been cited accordingly.